INVESTIGATING SODIUM HEXAMETAPHOSPHATE AS A TOPICAL TREATMENT FOR CALCIFIC BAND KERATOPATHY

by

NAOMI BENNETT

A thesis submitted to the University of Birmingham for the degree of
DOCTOR OF PHILOSOPHY

Healthcare Technologies Institute
School of Chemical Engineering
College of Engineering and Physical Sciences
University of Birmingham
8th April 2022

Abstract

Calcific Band Keratopathy is a condition affecting the cornea, leading to the deposition of hydroxyapatite mineral in the Bowman's membrane, sub-epithelium and anterior stroma. This condition reduces visual acuity and causes discomfort. Band keratopathy is most commonly treated with a superficial keratectomy and ethylenediaminetetraacetic acid (EDTA) chelation, however, patients may not be offered this treatment if they have other ocular co-morbidities, or the condition is not advanced. Therefore alternative, less invasive treatment options are required. In this investigation, it was found that sodium hexametaphosphate (HMP) could form the basis of an alternative topical treatment for the condition, with HMP significantly reducing the mineral present in a hydroxyapatite sol *in vitro.* Both cellular monolayer assays of corneal cells and tissue biopsy assays of corneal tissue provided evidence of HMP affecting cellular metabolism and reducing intra-cellular adherence. Gellan, alginate and chitosan gels each responded differently to the addition of HMP. Alginate showed a reduction in shear viscosity when assessed using rheometry, whereas both gellan and chitosan crosslinked with HMP addition and increased in viscosity. The increase in crosslink density exhibited in the gellan fluid gel and chitosan gel rendered both unsuitable for use as an eye drop. Chitosan films were developed, however, only alginate was found to release a suitable therapeutic dose of HMP. An *ex vivo* porcine model of band keratopathy was developed, and assessment of 0.5M HMP, 1M HMP, alginate and 0.5M HMP and 2% EDTA showed that each was successful in significantly reducing mineralisation, with 1M HMP as the most effective.

Acknowledgements

With huge thanks to my supervisors, Dr Lisa Hill and Professor Liam Grover for not only giving me the opportunity to do this work but all the support, advice and encouragement they have given me along the way. My advice to anyone who has asked me about doing a PhD has been to prioritise the supervisors over everything else – I feel unbelievably fortunate to have had you as mine.

Lisa, thank you for always keeping me on track, supplying biscuits and of course – attempting to shape me into a biologist. Liam, thank you for your undying enthusiasm for good science, it has kept me both motivated and entertained and taught me more than I can easily quantify. Both of you are brilliant, both in your own right and as a team.

To the people in both the NoScar team and the HTI – thank you for all your help and advice. Thank you, Chloe Thomas, for your never-ending patience and generally being the most amazing lab-mate, and Hannah Lamont for always having helpful advice to give or being a shoulder to cry on. You are both fantastic scientists and I can't wait to see what you get up to in future.

To my wife, Lizzie, for putting up with me whilst I try and get this thing done and putting me first when it's come down to it. To my parents, for pretending to understand what I'm talking about, and to Nanny, for being the only person who actually does. To Ellie, for forgiving me for being an absentee housemate, and Sophie, for the memes.

With thanks to the Engineering and Physical Sciences Research Council (UKRI) for funding this research project.

Table of Contents

List of Figures

List of Tables

Abbreviations and Key terms

ADP	Adenosine Diphosphate
AMD	Age-related Macular Degeneration
AMP	Adenosine Monophosphate
AMT	Amniotic membrane transplantation
ATP	Adenosine Triphosphate
BAK, BAC	Benzalkonium Chloride
BCVA	Best corrected visual acuity
BK, CBK	Band Keratopathy, Calcific Band Keratopathy
CMC	Carboxymethylcellulose
EDTA	Ethylenediaminetetraacetic acid
GDP	Guanosine Diphosphate
GTP	Guanosine Triphosphate
H&E	Haemoxylin and Eosin
HA	Hydroxyapatite
HA	Hyaluronic acid
HBSS	Hanks Balanced Salt Solution
HMP, S-HMP	Sodium hexametaphosphate
HPMC	Hydroxypropyl methylcellulose
LPHN	Lipid Polymer Hybrid Nanoparticles
MHC	Major Histocompatibility Complex
mPTP	Mitochondrial permeability transition pore

MTT	3-(4,5-dimethylthiazol-2-yl)-2,5-diphenyl tetrazolium bromide)
MUC1	Mucin 1
MUC5AC	Mucin 5AC
MW	Molecular Weight
NHSBT	National Health Service Blood and Transplant
OCT	Optical Coherence Tomography
OCT medium	Optimal Cutting Temperature medium
PAA	Poly Acrylic Acid
PBS	Phosphate Buffered Saline
PEG	Polyethylene Glycol
PolyP	PolyPhosphate
PPG	Polypropylene Glycol
PPK1	PolyPhosphate Kinase 1
PPK2	PolyPhosphate Kinase 2
PPX	Exopolyphosphotase
PTK	Phototherapeutic keratectomy
PVA	Polyvinyl Alcohol
SBF	Simulated Bodily Fluid
SEM	Standard Error of the Mean
sIgA	Secretory Immunoblogulin A
SLN	Solid Lipid Nanoparticle
TFBUT	Tear Film Break-up Time
TGF-β	Transforming Growth Factor Beta
TPP	Tri-PolyPhosphate

1.

INTRODUCTION AND LITERATURE REVIEW

1. Introduction and Literature Review

Sections 1.2 to 1.7 were published as part of a progress report in Advanced Functional Materials (Material, Immunological, and Practical Perspectives on Eye Drop Formulation, N. H. Bennett, H. R. Chinnery, L. E. Downie, L. J. Hill and L. M. Grover, Advanced Functional Materials 2020 Vol. 30 Issue 14 DOI: 10.1002/adfm.201908476).

1.1 Band keratopathy

Mineralization processes are an important part of the normal functioning of bodily systems, necessary for maintaining a balance of calcium, creating bone and preserving bone density. However, ectopic mineralization - calcification of soft tissues - can be serious and life-limiting. This is particularly dangerous in the heart and vasculature, where stiffening of the tissue or blockages can lead to critical cardiac damage [2]. Ectopic calcification can be broadly categorized as either dystrophic – a result of diseased or damaged tissue, or metastatic – a result of a serum calcium/phosphate imbalance [3]. It is suggested that in most tissues there is a continuous action of both calcification-inducing and calcification-inhibiting molecules to maintain a balance that prevents ectopic calcification [3, 4]. Dysregulation can lead to mineral build-up, typically taking the form of calcium oxalate or a calcium-phosphate salt such as hydroxyapatite [5].

It is widely accepted, although not uncontested, that mineral formation under biological conditions requires the presence of a nucleator and nucleation site. It is thought that osteoblasts can produce their own nucleators to allow the mineralization of bone and teeth, creating a dense collagen network in which hydroxyapatite crystals become embedded [5, 6]. Much of the debate around the processes of both pathological and

healthy mineralisation focuses on the role of matrix vesicles (MVs) which are suggested to regulate the phosphate ratio in the matrix [7]. It is still unclear as to how much parity exists between the mechanisms of bone formation and the development of ectopic calcification.

In the eye, mineralisation in the retina - in the form of drusen - can be a symptom of sight-threatening dry age-related macular degeneration (dry-AMD) [8]. In the anterior (front) eye, mineralisation is most commonly a secondary effect of another underlying systemic condition, but can also occur due to local injury or loss of tissue homeostasis. Calcific Band keratopathy (BK) is a corneal condition which presents as the accumulation of calcium-hydroxyapatite mineral in the bowman's layer of the cornea (Figure 1.1). In severe cases, this mineral can span to the stroma, or can breach the epithelial layer leading to significant discomfort [9]. This mineralisation leads to obstruction of the light passing through the cornea and reduced visual acuity. Patients also describe dryness and a 'grainy' feeling – known as foreign body sensation. If the condition progresses uncontrolled, the mineral can compromise the structure of the cornea, increasing the risk of ulceration [10]. This condition most commonly presents in patients on long-term topical glaucoma therapy or with chronic corneal oedema, parahyperthyroidism, renal failure or juvenile idiopathic arthritis [10-15]. It has also been associated with the use of silicone oil in lens replacements and phosphate preservatives in eyedrops [9]. The global prevalence of BK is not well recorded, however recent studies in different countries have provided some suggestion of the rate of occurrence. In India, a study of over 2.5 million electronic health records of people who visited various ophthalmic hospitals revealed a prevalence of BK of 0.33% [16]. In Taiwan, a study of patients with end stage renal disease found an increased

risk of band keratopathy compared to controls, with 230/94039 ESRD patients having a diagnosis of BK compared to 26/94039 matched controls (giving a prevalence of 0.24% and 0.028% respectively) [15]. The rate of band keratopathy appears to be very low in the general population, predominantly affecting those with other, linked conditions.

The exact mechanism through which the calcium deposits form in cases of BK remains under question, however evidence can be gained from other conditions in which metallic compounds build up in the cornea, for example, the build-up of copper in Wilson's disease [17, 18]. In the eye, Wilson's disease presents as a green/brown ring near the limbus called a Kayser-Fleischer (K-F) ring. This appears on anterior ocular coherence tomography (OCT) scans as a hyperreflective band [17]. The ring is formed by the deposition of copper in the Descemet's membrane [17, 18]. Wilson's disease is a recessive genetic condition which causes the dysregulation of copper metabolism and the accumulation of copper in various tissues [17]. It is therefore reasonable to assume that the formation of calcium-phosphate deposits in Band Keratopathy is likely due to the metabolic dysregulation of calcium and phosphate in the corneal tissue or elsewhere. As in other conditions in which ectopic calcification takes place, the process through which band keratopathy develops can be considered as either dystrophic, a result of chronic inflammation and damage to the ocular tissues, or metastatic, due to an imbalance of calcium and phosphate ions - either due to systemic dysregulation or the introduction of high concentrations of these ions from external sources [9]. In the case of dystrophic mechanisms of BK, it is suggested that changes in the pH of the tissue environment facilitate the formation of the mineral. It is common in tissues for calcium and phosphate ions to exist at concentrations close to the limit of their solubility

in solution. When the pH of these tissues changes rapidly, the calcium-phosphate mineral precipitates and is deposited in the extra-cellular space [19]. These pH changes can be attributed to changes in the tissue metabolism or the tear osmolarity due to conditions such as dry eye syndrome. It is also most common for deposits to form in areas of the cornea that have the most exposure to the outside air [9]. A previous study which examined the potential role of vitamin D overdoses in the development of band keratopathy in rabbits found that only the subjects with exposed corneal surfaces formed calcium-phosphate deposits, and those with closed eyelids did not [20]. The characteristic hydroxyapatite deposits formed in cases of Band Keratopathy are therefore thought to form in the central cornea due, in part, to the action of tear evaporation and gaseous exchange of the tear film, which allows for greater exposure to oxygen and greater loss of acidifying carbon dioxide than elsewhere in the eye [19].

In the early stages of the BK, the foreign body sensation can be managed with lubricating artificial tears or a soft bandage contact lens. If the condition worsens, or the risks associated with treatment are mitigated, the usual treatment for BK involves performing a superficial keratectomy. This involves the removal of the primary epithelial layer through abrasion or with ethanol, and then the application of Ethylenediaminetetraacetic acid (EDTA) to the ocular surface either on a soaked paper disc or into a well. EDTA chelates the calcium in the hydroxyapatite, breaking up the deposit [10]. This process is most commonly administered with the patient awake and their eye anaesthetised by a local anaesthetic injection. EDTA chelation is not the only treatment available, with mechanical debridement (without a chelating agent) or phototherapeutic keratectomy (PTK; laser ablation) also used to treat the condition in

some cases [9]. However, both have significant disadvantages, with mechanical debridement leaving a rough corneal surface once the mineral deposit has been removed, and PTK being linked with hyperopic or myopic shifts – changes in the refractive properties of the cornea which have a significant impact on vision [9]. Mechanical debridement is therefore most commonly used in combination with chemical chelation, and PTK is used where the chemical chelation procedure is ill-advised due to ocular comorbidities. The PTK procedure is much more costly than the EDTA chelation procedure due to the nature of the specialist equipment required [9]. As an additional recovery aid to each of these procedures, amniotic membrane transplantation (AMT) is sometimes deployed to improve the healing of the epithelium post-operatively, improving both the healing (re-epithelialisation) rate and the smoothness of the corneal surface [9, 21].

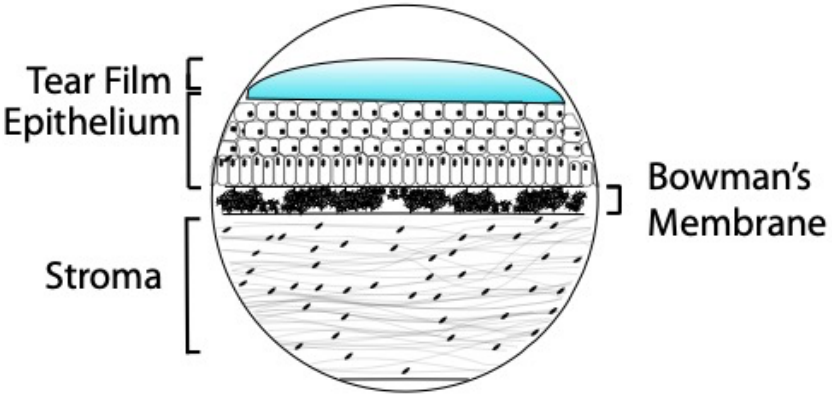

Figure 1.1: a representation of the mineral deposits that characterise BK, showing the structures of the cornea affected. The tear film and epithelium represent the very front of the eye – the ocular surface. The hydroxyapatite mineral most commonly forms in the Bowman's membrane, occasionally breaching the epithelial layer or becoming embedded in the stroma as the condition progresses.

In order to develop a novel topical treatment for band keratopathy, it is necessary to develop an understanding of the current methods deployed in topical ocular drug delivery, the opportunities for innovation and the limitations of topical formulations.

1.2 The ocular structure and environment

The modern world is designed to be navigated through sight, and as a result, ocular conditions can be extremely limiting. There is both a fascination and a general sensitivity around the eyes. The NHSBT transplant activity report 2020/21 states that as of 31 March 2021, 10.0% of people who joined the organ donation register chose not to donate their corneas [22]. Globally, the number of people who would classify as blind or partially sighted is set to increase by 200-300% by 2050, due to the general ageing of the global population [23]. In the United Kingdom, AMD poses the greatest threat to the average person's sight, followed by cataracts, diabetic retinopathy, and glaucoma, respectively. A 2018 review into the economic impact in the UK of blindness – defined as best corrected visual acuity (BCVA) of < 6/60 in the better-seeing eye - and sight loss - defined as BCVA of < 6/12 to 6/60 in the better-seeing eye - found that associated healthcare costs were around £2.99 billion in 2013 [24]. This growing burden of disease highlights the need for the development of both better management techniques and more effective treatment options for those experiencing sight loss or blindness.

Our eyes develop *in utero* from extensions of the brain's neural tissue. This neural tissue forms the retina – the light-sensitive part of the eye [25]. Humans have two types of photoreceptor cells in the retina — rods for low light, and cones for colour. These cells hold 'opsin' pigments which change conformation when they are hit by a photon

[26]. This change in conformation creates an electrical current which is transmitted to the brain. The anterior tissues – the cornea, lens and iris - function to direct light towards the fovea, the part of the retina that has the highest density of cone cells and offers the highest visual acuity [27]. The first tissue the light passes through in an open eye is the cornea, which focuses the light. The iris, the smooth muscle ring which gives eyes their colour, contracts or expands to control how much light passes through to the lens and beyond. The lens acts as an additional focus, before the light passes through the vitreous and reaches the retina [27]. When the light reaches the retina it has been inverted by the curvature of the cornea and lens, meaning the image has to be re-inverted by the brain – a feature examined through the use of mirrored glasses in the classic experiments performed by George Stratton and Roberto Ardigò in the 1800s [28].

1.2.1 The anterior ocular immune system

Unlike most other organs the eye is relatively exposed to the outside environment. The eye is considered ‘immune privileged’, meaning that regulation of some immune responses occurs within and by the tissue, rather than *via* the systemic immune system [29]. So-called ‘immune privilege’ lends itself towards some ocular tissues developing tolerance to certain stimuli on exposure, rather than inducing the expected inflammatory response that would occur in other peripheral tissue sites such as the skin [30]. This allows for protection against infection, whilst also protecting the delicate ocular tissues against repeated inflammatory responses, which can result in the loss of transparency of key tissues and ultimately blindness [31, 32]. The bias towards tolerance is maintained through immuno-suppressive agents, such as transforming growth factor-beta (TGF-β) and α-melatonin stimulating hormone, which limit or direct

the activity of both the resident immune cells and infiltrating leukocytes. In addition to mechanisms that regulate the nature of the adaptive immune responses, the resilience of the ocular surface in avoiding infection - despite its exposed location - is due to a robust repertoire of anatomical features (including apical epithelial tight junctions, paucity of afferent lymphatics and blood vessels) and innate immune components such as tear lysozyme, anti-microbial defensins and secretory IgA. Most infections that occur in the eye are usually secondary to mechanical damage to the ocular surface, from injury or contact lens wear, or impaired barrier integrity, which compromises the innate ocular defence mechanisms [31]. When considering the immunological implications of topical ocular treatments, it is the anterior tissues that are of particular interest as these tissues are both in contact with and treated directly by these topical therapies.

The immune cells naturally present in the anterior tissues of the eye can change their phenotype and function depending on the inflammatory environment and the disease state [33]. It is also important to recognise the diverse functions of the tear film, especially if an eye drop is to be designed to aid/replicate those functions. However, the anterior eye has multiple structural barriers to invasion that form the front line of the ocular immune system, including the mucosal layer and tear film, before tissue-specific immune cells are recruited [29].

1.2.2 The tear film

The surface of the eye is lubricated and smoothed by the tear film. Components of the tear film work to trap debris (mucins), kill pathogens (lysozymes, phospholipids, etc), collect foreign bodies (sIgA) and assist with the removal of said bodies through blinking

[34, 35]. The tear film has traditionally been described as having a mucin layer, an aqueous phase and a lipid phase, however, these layers are not necessarily discreet.

Mucins act to promote an optimally lubricated ocular surface by supporting the spreading of the bulk of the tear film over the outer corneal and conjunctival tissues. Secreted, gel-forming MUC5AC and cell adhesive MUC1 additionally facilitate pathogen removal by trapping the pathogen and preventing its adhesion to the underlying epithelial tissue [35-38]. The longer, surface adhesive mucins also allow for the formation of reservoirs of oxidative enzymes, defensins, lysozymes and lactoferrin – proteins produced by scavenger cells (neutrophilic granulocytes) that are attracted to inflammation – which work to reduce the adhesion of bacteria and remove damaged host tissue [35, 39]. Mucins are of particular interest when considering ocular drug delivery routes, as these mucins can interact with polymers to facilitate the beneficial mucoadhesive properties of some eye drops [40-45]. Certain molecules within the tear film are also bactericidal. Gram-negative bacteria are killed by lysozymes, which split their muramic acid linkages [34, 46]. Secretory phospholipase A2 acts against gram-positive bacteria [16], alongside lactoferrin and transferrin which - as the names indicate - bind iron [34, 39]. Psoriasin, an antimicrobial agent found on the skin, has also been detected at the ocular surface [47].

The primary antibody present in tears is secretory immunoglobulin A (sIgA), which is produced in the lacrimal gland. sIgA works to prevent bacterial adhesion, aggregate neutralised pathogens and allow clearance of the pathogens from the ocular surface [48] [35]. It has also been associated with the increased chemotaxis of neutrophils and other immune cells during the prolonged period of eyelid closure during sleep [49].

Tear lipids can also augment the bactericidal properties of tears, as short-chain lipids affect the surface properties of the bacterial cell membrane, and long-chain lipids have a direct effect on bacterial metabolism [39, 50]. It has been shown that tear film lipids can induce cell lysis, distortion and cell wall damage in both gram-negative and gram-positive bacteria [50]. Additionally, the lipid phase of the tear film is thought to offer protection to the aqueous phase from evaporation, ensuring optimal lubrication of the ocular surface [51-53].

These processes maintained by the tear film all act as part of a wider complex mechanism of ocular surface protection. This system remains virtually impenetrable to pathogens unless there is a physical disruption to the barrier or injury to the tissue.

1.3 Ocular drug delivery

Ocular drug delivery is a challenging but rapidly evolving area of research. It is well documented that the biological systems that keep the eye free of debris and protect the vital posterior structures, also present a barrier to topical drug delivery [54, 55]. Eye drops are most commonly used for treating the anterior structures of the eye (Figure 1.2) – the cornea, conjunctiva, sclera, ciliary body and trabecular meshwork – as a passage to the posterior segment of the eye is restricted [56, 57]. The cornea comprises sublayers with different properties; the epithelial and endothelial layers are lipophilic, and the stroma is hydrophilic [57, 58]. These properties heavily influence which drugs and carriers are effective in passing across the cornea, with positively charged carriers showing higher penetration than neutral or negatively charged carriers [59]. Drugs that are both lipid- and water-soluble (amphiphilic) also show improved penetration [58, 60].

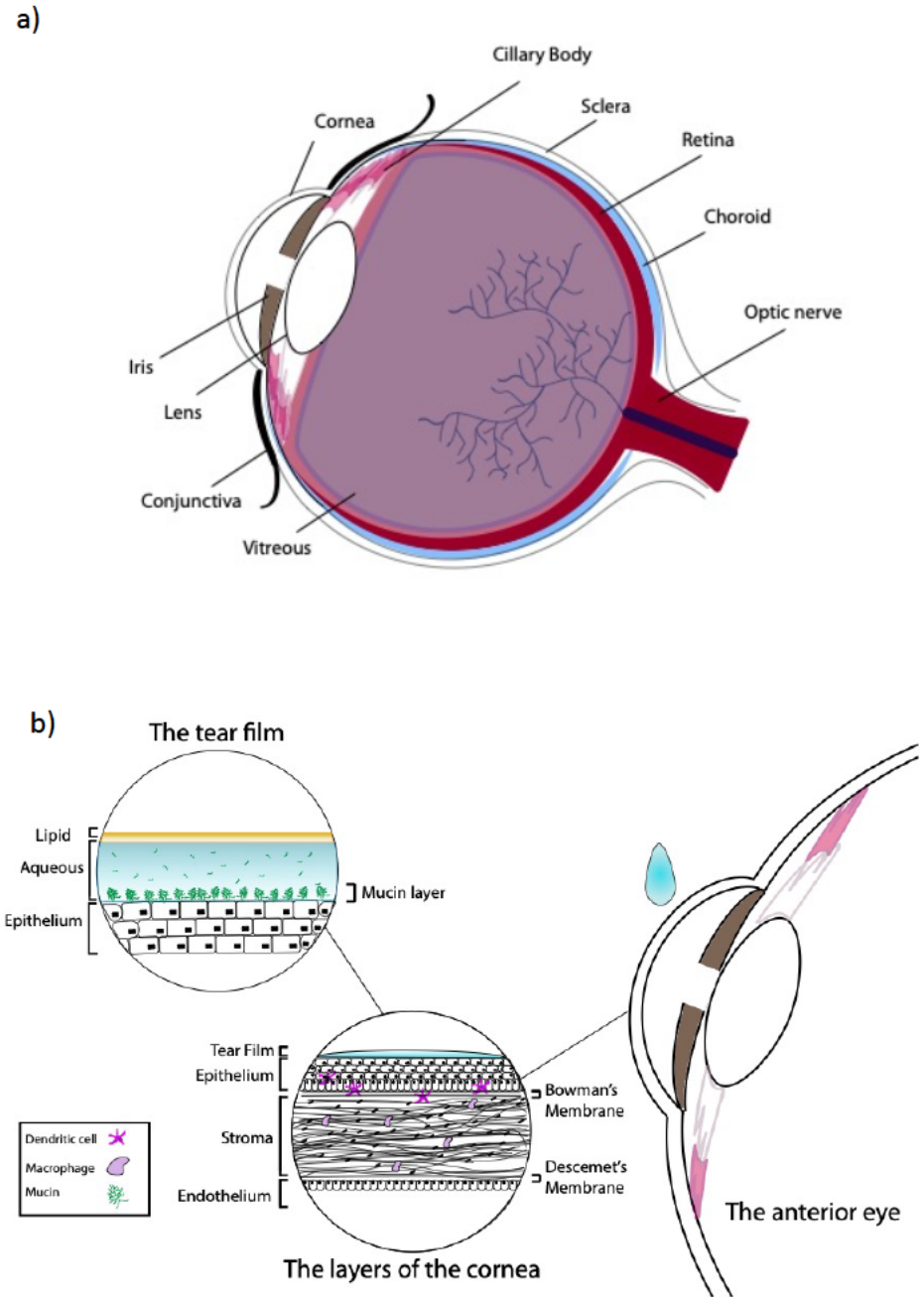

Figure 1.2: a) The structure of the whole eye, with the anterior (front-facing) tissues to the left of the diagram and the posterior tissues to the right. b) The transparent cornea and the tear film represent the anterior ocular surface. The cornea is made of layers of cells which perform different functions in both maintaining transparency and creating the ocular barrier. The cornea is home to resident immune cells such as macrophages and dendritic cells which form part of the defence from infection.

1.3.1 *Eye drops*

Eye drops are most commonly applied directly to the cornea or into the conjunctival sac. Eye drops can be used for therapeutic drug delivery (e.g., corticosteroids, antibiotics, etc.), or for symptom management (e.g., artificial tears for dry eye disease). Eye drops typically include a solvent, electrolytes, a thickening agent, an active agent/drug and in some cases a preservative (e.g., benzalkonium chloride). In addition, with the intent of mirroring natural tears, eye drops have an optimum pH of approximately 7.4 and a closely controlled osmolarity [29].

Polymers were first used within eye drops to take advantage of their mucoadhesive properties and improve the residence time and resistance to lacrimal clearance of the drops [56]. Conventional aqueous eye drops are rapidly cleared by blinking and lacrimal drainage, which creates severe limitations to the bioavailability of any therapeutic agent being delivered. Eye drops are said to provide a bioavailability of around 5% of the delivered drug [61]. Predictions of the average residence time of eye drops on the ocular surface vary greatly, with there being multiple methods of assessing this in both clinical and research settings. Optical coherence tomography (OCT) can be used for *in vivo* assessments in clinical and experimental settings and has shown retention times of up to 60 minutes for gel eye drops. This method has also highlighted significant differences in the clearance rates for gel and aqueous drop formulations [62, 63].

It is more common for residence time to be measured as a function of tear film break-up time (TFBUT) using fluorescein, which has provided values for drop retention ranging from 10 to 90 minutes [64-66]. The nature of the drug being delivered, the polymer additive, its concentration and the use of preservatives can be adapted to

create the best possible combination of properties for the desired treatment effect. These changes do however only have minimal impact on the objectively low efficacy of eye drops compared to more invasive treatments such as intraocular injections (for the diseases for which they are available) [67]. Despite this, eye drops still offer an attractive treatment option, due to their ease of administration, versatility and low cost.

1.3.2 Conventional polymer additives for eye drop formulations

Eye drops formulated for the management of dry eye disease - which involves chronic damage to the ocular surface and leads to discomfort and inflammation - typically use polymeric agents to provide ocular lubrication and/or stabilise the tear film [68, 69] (Table 1, Table 2). Polymers also increase the ocular retention time of the drops compared to purely aqueous solutions. Certain charged polymers (of which many are listed below) offer the advantage of mucoadhesion – adherence to the mucosal layer of the tear film, which further increases the residence time of the drops on the ocular surface [60, 70]. Currently, commercially available eye drop products (Table 1, Table 2) will often include one, or more, biocompatible polymeric agents.

Table 1. Examples of over-the-counter (United Kingdom) non-medicated artificial tear eye drops and their thickening agents

Type	Product name/*Brand*	Thickening agent	Concentration (%)
Artificial tears	Carmize 0.5% *Aspire Pharma* (PF), Cellusan 1% *Farmigea* (PF), Evolve Carmellose *Lumecare* 0.5% (PF), Melopthal, PF Drops Carmellose *Martindale*, Xailin Fresh *Nicox*	Carboxymethycellulose	0.5-1.0%
	Optive *Allergan*	Carboxymethycellulose	0.5%
	Optive Plus *Allergan*	Carboxymethycellulose	0.5%
		Castor Oil	0.25%
	Systane, Systane Gel Drops, Systane Ultra *Alcon (Novartis)*	Polypropylene Glycol	0.3%
		PEG 400	0.4%
	Systane Balance *Alcon (Novartis)*	Polypropylene Glycol	0.6%
	Evolve Hypromellose *Lumecare*, Hydromoor *Rayner*, Hypromellose *FDC*, Hypromol *Ennogen*, Lumecare Hypromellose, Lumecare Tear drops, Ocu-lube Sai-Med, PF Drops Hypromellose *Moorfields*, SoftDrops eye drops *Ajanta*, Vizulize Hypromellose, Xailin Hydrate *Nicox*	Hydroxypropylmethylcellulose	0.3-0.5%
	Liquifilm Tears *Allergan*, Sno tears *Chavvin*	Polyvinyl Alcohol	1.4%
	Refresh Opthalmic *Allergan*	Polyvinyl Alcohol	1.4%
		Povidone	0.6%
	Artelac Rebalance *Bausch + Lomb*, Clinitas, Evolve HA *Lumecare*, Hy-Opti *Alissa*, Hyabak *Thea pharmaceuticals*, Hylo-fresh *URSAPHARM*, Hylo-forte *URSAPHARM*	Sodium Hyaluronate	0.1-0.4%

	Blink Intensive Tears *Abbot*	Sodium Hyaluronate	0.2%
		PEG	0.25%
	HydraMed *Farmigea*	Sodium Hyaluronate	0.2%
		Tamarind Seed polysaccharide	0.2%
	Hylo-care *URSAPHARM*	Sodium Hyaluronate	0.1%
		Dexpanthanol	2%
	Hylo-Dual *URSAPHARM*	Sodium Hyaluronate	0.05%
		Ectoin	2%
	Lubristil Gel *Moorfields*	Sodium Hyaluronate	0.15%
		Xanthan Gum	1%
	Optive Fusion *Allergan*	Sodium Hyaluronate	0.1%
		Carboxymethylcellulose	0.5%
		Glycerol	0.9%
	Thealoz Duo *Thea*	Sodium Hyaluronate	0.15%
		Trehalose	3%
	Thealoz Duo Gel Thea	Sodium Hyaluronate	0.15%
		Trehalose	3%
		Carbomer	0.25%
	Emustil *Rayner*	Soy bean oil	7%
		Natural Phospholipids	3%
	Artelac Nighttime gel *Bausch + Lomb*, Clinitas Carbomer gel *Altacor*, Evolve carbomer 980 eyegel *Lumecare*, Lumecare carbomer eye gel, Xailin gel *VISU pharma*	Carbomer (Polyacryclic acid)	0.2%

Table 2: Active ingredients and main thickening agents of different types of medicated eye drops (United Kingdom)

Purpose	Product name/*Brand*	Active ingredient	Thickening agent
Artificial tear	Ilube *Rayner*	Acetlycysteine 5%	Hydroxypropylmethylcellulose
Antiviral treatment	Virgan *Thea pharmaceuticals*	ganciclovir 0.15%	Carbomer 974P
Allergy relief	Otrivine-Antistin *Thea pharmaceuticals*	Xylometazoline 0.05% Antazoline 0.5%	-
	Optilast *Mylan*	Azelastine hydrochloride 0.05%	Hydroxypropylmethylcellulose
	Emadine *Alcon*	emedastine 0.5 mg/ml	Hydroxypropylmethylcellulose
	Relestat *Allergan*	0.5 mg/ml epinastine hydrochloride	-
	Zaditen *Thea Pharmaceuticals*	0.345 mg/ml ketotifen fumarate	Glycerol
	Alomide *Novartis*	Lodoxamide 0.1%	Hydroxypropylmethylcellulose
Glaucoma treatment	Iopidine *Novartis*	Apraclonidine 5mg/ml	-
	Lumigan *Allergan*	0.3mg/ml bimatoprost	-
	Alphagan/ Brymont *Allergan*	2mg/ml Brimonidine	Polyvinyl Alcohol
	Azopt *Novartis*	10mg/ml Brinzolamide	Carbomer 974P
	Trusopt *Santen*	22.26 mg/ml dorzolamide hydrochloride	Hydroxyethyl cellulose
	Monopost *Thea Pharmaceuticals*	50 µg/ml latanoprost	Carbomer 974P PEG (macrogol 4000)
	Betagan *Allergan*	levobunolol hydrochloride 0.5%	Polyvinyl Alcohol
	Oftaquix *Santen*	5.12 mg/ml levofloxacin hemihydrate	-
	Saflutan *Santen*	15 micrograms/ml tafluprost	Glycerol
	Travatan *Novartis*	40 micrograms/ml travoprost	Polypropylene glycol
	Betoptic *Novartis*	Betaxolol 0.5%	Carbomer 974P
	Tiopex gel *Thea Pharmaceuticals*	1mg/g timolol	Polyvinyl alcohol
Bacterial eye infections	Azyter *Thea*	azithromycin dihydrate 15mg/g	Medium chain triglycerides
	Golden Eye	Chloramphenicol 0.5%	-
	Fucithalmic Viscous eye drops *Advanz pharma*	10mg/g Fusidic acid	Carbomer
	Gentamicin eye/ear *FDC International*	0.3% gentamicin	-
	Ciloxan *Novartis*	Ciprofloxacin 0.3%	-

Eye inflammation (e.g., post-cataract surgery)	Betnesol *RPH Pharmaceuticals AB*	Betamethasone 0.1% Neomycin 0.385%	PEG 300
	Vistamethasone *Martindale Pharma*	Betamethasone Sodium Phosphate 0.1%	-
	Yellox *Bausch + Lomb*	0.9mg/ml sodium sesquihydrate/Bromfenac	-
	Maxidex *Novartis*	Dexamethasone 0.1%	Hydroxypropylmethylcellulose
	FML *Allergan*	1 mg/ml Fluorometholone	Polyvinyl Alcohol
	Ocufen *Allergan*	Flurbiprofen sodium 0.03%	Polyvinyl Alcohol
	Acular *Allergan*	Ketorolac trometamol 5 mg/ml	-
	Lotemax *Bausch + Lomb*	0.5%w/v loteprednol etabonate	Glycerol
	Nevanac *Novartis*	3 mg/ml nepafenac	Polypropylene Glycol Carbomer Carboxymethylcellulose galactomannan polysaccharide
	Pred forte *Allergan*	1% prednisolone acetate	hydroxypropylmethylcellulose
	Vexol *Alcon*	1% Rimexolone	Carbomer
	Tobradex *Novartis*	Tobramycin 3mg/ml Dexamethasone 1mg/ml	Hydroxyethylcellulose
	Voltarol Optha *Thea Pharmaceuticals*	Diclofenac sodium 1mg/ml	Polypropylene glycol

1.3.3 Natural Polymers

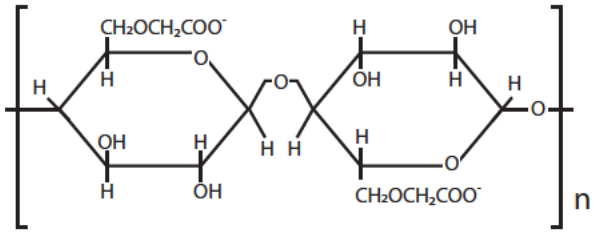

Figure 1.3.1: Carboxymethylcellulose structure.

Various ethers of different viscosities and solubilities can be harvested from cellulose, including carboxymethylcellulose (CMC) (Figure 1.3.1) and hydroxypropylmethylcellulose (HPMC) (Figure 1.3.2) [71]. These inexpensive polymers are found in many commercial eyedrops (Tables 1 and 2) as mucoadhesive thickening agents. Cellulose alone is poorly soluble, however, CMC as a cellulose ether overcomes this [72]. Their renewable source also qualifies cellulose and its derivatives as sustainable polymers [71].

The viscosities of eyedrops created with CMC are directly proportional to the molecular weight of the CMC chains, and CMC solutions can reach high viscosities without the presence of crosslinks [73]. Viscosity is also influenced by the pH and ions in the solvent/solution as this alters the conformation of the polymer chains [74]. CMC is polyanionic and the presence of multiple hydroxy groups provides CMC with mucoadhesive, hydrophilic properties [60, 75]. This also enhances swelling in CMC gels, branding them ‘superabsorbent’, and allows CMC to be pH-responsive *in situ* [71]. The mucoadhesive properties of CMC (and other polymers) are advantageous for drug delivery using eye drops. Compared to medicated non-polymeric (non-

viscous) drops, medicated CMC drops have been shown to improve the ocular concentration of the glaucoma drug timolol by 300-900% [76]. CMC is, however, most commonly used in artificial tear eye drops, which are used to provide relief of dry eye symptoms. Although CMC is efficacious for the symptomatic treatment of dry eye disease, there are now artificial tear formulations with more advanced components, such as sodium hyaluronate, which show additional benefits [73].

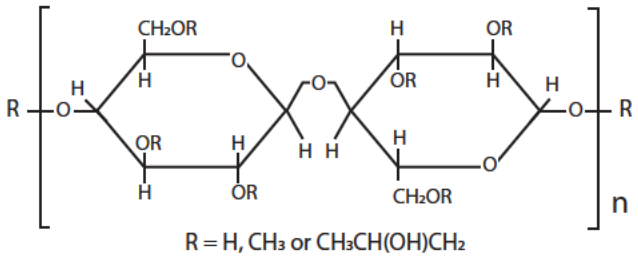

Figure 1.3.2: Hydroxypropylmethylcelllulose structure

HPMC (Figure 1.3.2) is less viscous than CMC but shows superior properties as an emollient – an important factor for treating dry eye disease and promoting epithelial health [73]. HPMC is used both as a thickening agent in medicated drops and as a mucoadhesive and treating agent in artificial tear drops. HPMC and HPMC-composite microspheres have also been created and tested for drug delivery applications and shown favourable drug delivery profiles in the gut [77-79].

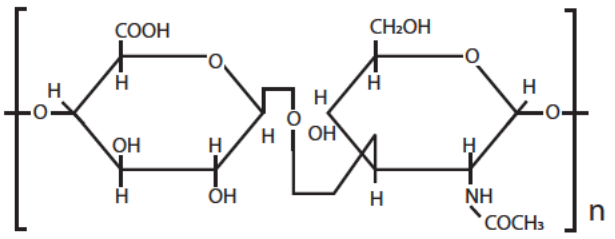

Figure 1.3.3: Hyaluronic Acid structure

Hyaluronic acid (HA) (Figure 1.3.3) is a naturally occurring polymer formed of linear polysaccharide chains, with sub-units of d-glucuronic acid and N-acetyl-d-glucosamine. These polysaccharide chains form with multiple hydrophilic anionic sites, which attract water molecules and allow HA solutions to become viscous and show beneficial rheological properties [72]. The molecular weight of the HA naturally present in the body elicits different immunological and cellular responses, with shorter chains appearing more conducive to cell growth and repair than long-chain forms [72, 80, 81]. This has potential repercussions for the systemic effects of HA use. Chain length has also been found to have a direct influence on the appropriate concentration of HA that should be incorporated into eye drops to allow for improved ocular retention and viscoelasticity. For a given concentration, it was found that in most cases commercially available eye drops only reach one-third of the optimum chain length value required [82].

HA is incorporated into eye drops to manage dry eye (artificial tears) but is not commonly used in medicated drops. HA has a higher ocular retention compared to CMC or HPMC and has also been shown to have effects on corneal epithelial cell healing in animal models [73] and to improve corneal recovery in patients with superficial punctate keratitis compared to CMC [83]. Larger studies have shown comparable results between CMC and HA with respect to the stabilisation of the tear film after cataract surgery [84], and clinical trials using HA eye drops demonstrate the efficacy of this therapy for improving symptoms and clinical signs in moderate-to-severe dry eye disease over three months [85]. Although HA shows the same, if not

improved, benefits for on-eye retention and epithelial health compared to CMC and HPMC in the treatment of dry eye disease, it is infrequently used in medicated drops for other eye conditions. HA does not show a significant detrimental drug binding effect [86]. The exclusion of HA from medicated drops could be due to cellulose-based polymers being of lower cost and simpler synthesis.

1.3.4 Synthetic polymers

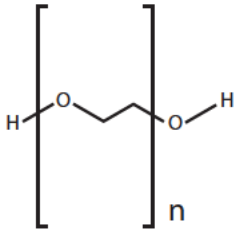

Figure 1.3.4: PEG structure

Polyethylene-glycol (PEG) (Figure 1.3.4) and polypropylene-glycol (PPG) are biocompatible synthetic polymers [87]. PEG and PPG are usually used as a backbone and then modified in various ways to create the desired properties. In comparison to CMC, PPG/PEG eye drops maintain a higher optical clarity after use, which can improve the patient experience and subsequently could improve compliance with treatment regimens [88]. When chain length exceeds a threshold of 200kDA, PEG exhibits mucoadhesive properties, but still shows limited adhesion in comparison to CMC [45]. Used either separately, or in conjunction as a mixture or co-block polymer, PEG and PPG polymers are relevant to a spectrum of medical and industrial applications. PPG and PEG have been used alongside hydroxymethyl-guar (a

naturally occurring gelling agent) to increase the viscosity of eye drops [88, 89]. This combination has been shown to be effective as a therapy for dry eye disease [89, 90].

PEG is amphiphilic and therefore very versatile and modifiable. These properties render PEG a common choice for testing hybrid lipid-polymer systems and for modifying the surface of difference carriers [91-94]. PEGylation is the name given to this process. As PEG does not elicit an immune response, it is used to dampen the potential response to an otherwise immunogenic carrier by modifying the surface charge or acting as a bridge for other molecules that elicit the desired immune response [92]. PEGylation can also modify the solubility of proteins – such modifications could make a significant difference to the penetrability of a carrier through the corneal barrier, for which charge is a vital factor.

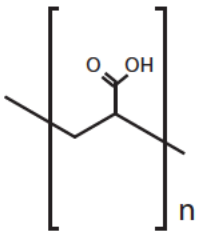

Figure 1.3.5: PAA monomer structure

Polyacrylic acid (PAA) (Figure 1.3.5) is another synthetic hydrophilic polymer used to create superabsorbent gels for children's nappies and cosmetics under the commercial name 'carbomer' [95]. Carbomers are traditionally synthesised in a benzene solvent, raising issues for medical applications. Other solvents, such as ethyl acetate and cyclohexane [96], can be used as an alternative. Most commercial drops which

describe themselves as ‘gel’ drops use carbomers. Carbomers do gel, however, the properties of the gels are heavily influenced by pH, solvents and surfactants [97-99].

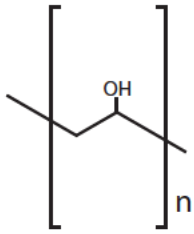

Figure 1.3.6: Polyvinyl alcohol monomer structure

Polyvinyl alcohol (Figure 1.3.6) is a common synthetic polymer used to enhance the viscosity of eye drops. Synthesis of polyvinyl alcohol involves hydrolysing polyvinyl acetate [100]. Thiolated PVA is mucoadhesive, and even short-chain PVA could enhance the viscosity of eye drops beyond the threshold for greater corneal retention [100, 101]. It is much more common for PVA to be used in gel form. PVA gels can be formed through physical crosslinking or irradiation, and show favourable degradation profiles for drug delivery [102].

1.4 Innovations in topical ocular drug delivery

The drawbacks of currently available eye drops are well documented, and it is worth noting that alternative forms of topical treatment are being investigated including ocular devices such as contact lenses and inserts [32, 61, 103-109]. However, eye drops remain a non-invasive and patient-friendly approach to ocular disease management and treatment.

Patients have previously reported limitations to their daily activities when eye drop application frequency is increased, as they must accommodate the additional applications and may not feel comfortable using eye drops outside of their home environment [110-116]. The simplest treatment regimens are shown to have better adherence and persistence from patients [110-116]. The increase in efficacy of drops with higher bioavailability may reduce the necessary frequency of administration and increase patient adherence to the regimes.

There is no one simple or 'best' answer as to how to most effectively improve the formulation of topical eye drops. The question of which material or structure will be most effective will ultimately depend on the nature of the disease being treated, its influence on the physiology and function of the eye's anterior tissues, and the chemistry of the therapeutic drug.

1.4.1 Innovations in ocular drug delivery: hydrogels and fluid gels

Hydrogels are now increasingly being investigated for use as biological scaffolds, drug delivery devices and as alternatives to plasters and sutures. Hydrogels show tuneable mechanical properties, drug release profiles and degradation rates [117-120]. Natural

polymers are generally non-toxic and biodegradable and have the added advantage of binding with cells and proteins. However, natural polymer-based hydrogels can have poor mechanical strength, and high variability, and can still provoke an immune response despite being non-toxic. Synthetic polymers are more consistent and tuneable in their properties but do not inherently interact with proteins or cells [119].

Several manufacturers advertise commercially available ‘gel’ eye drops. However, there is a disparity between the commercial and academic interpretation of what constitutes a ‘gel’, with many ‘gel’ drops simply incorporating viscous polymers to improve the rheological properties instead of creating a true hydrogel. True hydrogels, crosslinked polymer networks that entrap and hold water (Figure 1.4) [121], are yet to fully translate into commercial use. This is due to several practical factors, including the toxicity of some crosslinking agents to the ocular surface, the rate of lachrymal clearance limiting *in-situ* gelling, pre-formed gels being harder to administer, limitations in pH and temperature sensitivity and patient-focused outcomes (such as comfort and clarity of vision).

As an alternative to pre-formed gels, *in-situ* gels have been tested to allow for simple ocular administration [29, 118, 119, 122-124]. Harsh chemical gelation agents would be inappropriate for ocular use, so natural variables should be exploited, such as temperature, pH and the presence of electrolytes or proteins [125].

Other considerations for formulations include that the solvent and cross-linking agents that form the gel structure must not have a toxic or damaging effect on ocular cells and tissues. They must also be compatible with the drug being carried. That said, both

impact the final structure of the gel and therefore must also produce the desired characteristics within the gel [126]. Aqueous vs. anhydrous (alcohol) gel formation provides different structures and properties of gel, and these structural changes can inhibit the ability of certain polymer structures to deliver drugs effectively [127, 128].

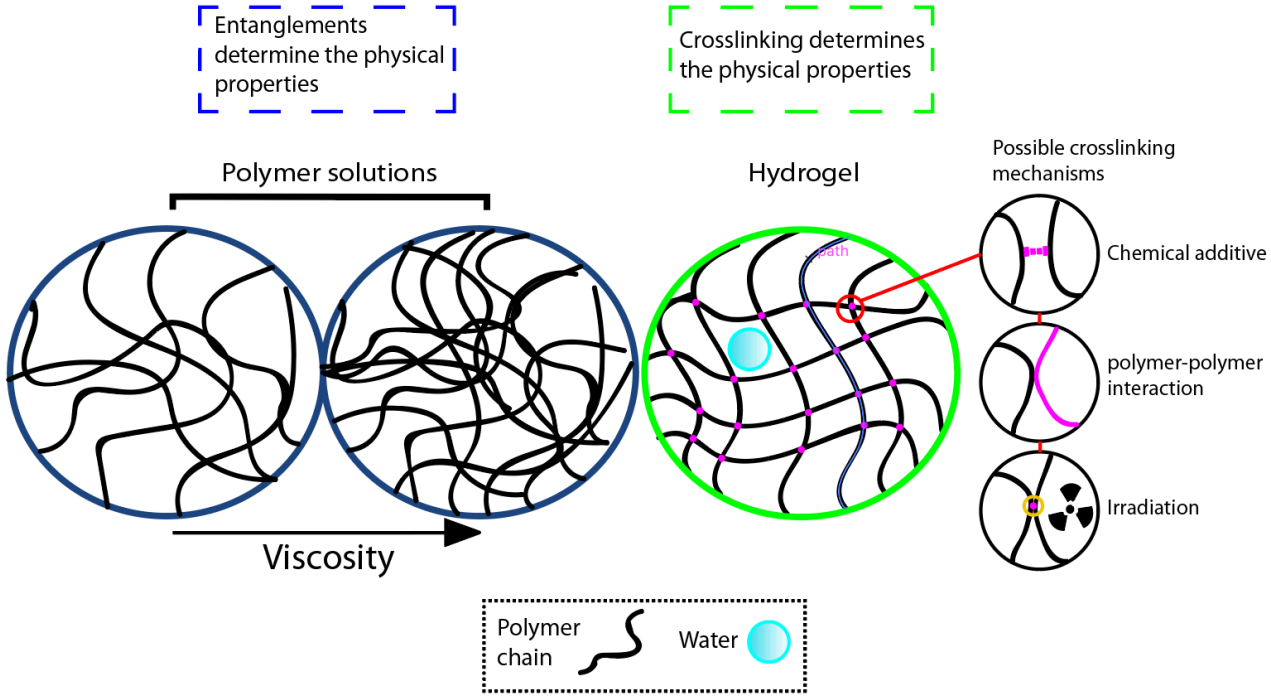

Figure 1.4: A comparison of the structure of polymer solutions and hydrogels. Polymer solutions form entanglements which determine the physical properties, and the number of entanglements tends to increase with concentration, increasing viscosity. Hydrogels entrap water through cross-linking.

The radiation-initiated cross-linking of some gels has the added benefit of sterilising the gel [71], however pre-formed gels pose a challenge for topical application.

Fluid gels may circumvent issues with administration, allowing for better control of rheological properties and the ability to administer consistent drops [95, 129, 130].

Fluid gels have been explored as a versatile deviation from the traditional hydrogel structure and are formed by shearing a hydrogel during manufacture to produce a complex hydrogel microstructure, formed from a bed of gel particles as opposed to a macrostructure [95]. Fluid gels, therefore, retain the viscosity and favourable drug delivery profile of a gel, whilst allowing for the necessary flow characteristics for spraying, pouring and drop formation, and they present a promising medium for eye drops [95, 129-137]. The level of shearing the gels is exposed to can also control the microstructure, which in turn can control the spreadability of the drop. The use of mucoadhesive gels which have been sheared to provide a fluid gel with the optimum balance of viscosity and wettability may circumvent some of the issues raised.

1.4.2 Lipid-based drug delivery systems

Although tailoring mucoadhesive polymers presents one option for improving the efficacy of eye drops, other avenues are also being explored, including emulsions and microemulsions, lipid-based carriers and permeation enhancers [99, 132, 138]. Lipid or emulsion-based eye drops show comparable results to conventional polymer-based drops with regard to retention and drug delivery [51, 138-140]. Emulsions also offer the added benefit of being able to carry hydrophobic/poorly water-soluble drugs [141]. However, there are concerns with regard to the methods of synthesis relying on a high proportion of surfactants (<10%) which interact with the ocular surface and increase the residence time of the drops but can be cytotoxic to the corneal cells. There are also concerns as to how well emulsions will last in prolonged storage – if the dispersion of the emulsion becomes uneven and separation occurs, the dosage of each eye drop will become uneven and the therapeutic threshold may not be reached [142].

As with simple polymeric drugs for dry eye disease, the drops do not have to carry a drug to have a therapeutic effect. Lipids themselves can treat a number of conditions including dry eye disease and meibomian gland disorder [138, 139, 143, 144]. In such cases, the addition of topical lipids or fatty acids can help rebuild the natural lipid film almost instantaneously, helping replenish the protective function of the lipid components of the tears [143]. Such as with the polymer choice in polymeric drops, the choice of oil in emulsion-based drops significantly changes the properties of the drop. Long-chain oils do not interact with the surfactants or emulsify as easily as short-chain oils, but show a higher drug solubility [145]. This means a balance has to be struck between drug compatibility and emulsion stability. The proportion of oil in the drop is also dependent upon the dose of drug which needs to be carried [142]. This means the properties of the resulting emulsion are largely dictated by the nature of the drug being delivered.

Liposomes – nanospheres with one or more phospholipid bi-layers – have also been investigated for use in drops with increased corneal penetration with considerable success [145-147]. However, the use of liposomes elsewhere in the body has been shown to elicit an inflammatory immune response. This response has even been harnessed as an adjuvant for vaccines [147, 148]. This raises questions for long-term ocular use, as prolonged inflammation can be extremely detrimental to eye health.

Solid lipid nanoparticles offer similar advantages to polymeric nanoparticles in terms of permeation of the natural barriers of the eye, whilst also presenting the option to carry drugs that may not be transportable in a polymeric system. SLNs can be

optimised to target specific pathologies as different combinations of lipid structures (triglycerides, fatty acids, waxes etc) can be used. Solid lipid nanoparticles are less likely to be made with harsh solvents, which may be beneficial for conditions where the ocular surface is already damaged or inflamed. However, they do normally incorporate surfactants to stabilise the emulsion, and despite these measures can still carry a lot of water and undergo structural changes during storage which can lead to a reduced drug-carrying capacity [149]. SLN drops do, however, typically contain proportionally less surfactant than emulsion drops [141]. Similarly, smaller liposomes can be designed and optimized to carry and deliver both hydrophilic and hydrophobic drugs by adjusting the lamellar structure [150, 151]. Both SLNs and liposomes can be designed as polymer-lipid composites to draw on the advantageous properties of both and allow for various synthesis methods [151].

Emulsion-based eye drops can incorporate polymers to allow for mucoadhesion, whilst using lipids to transport the hydrophobic drug [152]. This approach can be carried across into nano-carriers, with the synthesis of lipid-polymer hybrid nanoparticles (LPHN). These nano-carriers can deliver a hydrophobic drug in a polymer core, which is surrounded by a lipid layer. This lipid layer acts to ensure the hydrophobic drug remains encapsulated whilst also enhancing permeability through lipophilic tissues [151].

1.5 Immunological response to polymeric materials in the eye

The response of immune cells to the presence of biomaterials on the ocular surface will likely differ from examples of implantation elsewhere in the body, due to the plasticity and tolerance of ocular immune cells, and the consistent exposure of the ocular surface to the external environment. One example of regular, prolonged contact

of polymers to the ocular surface (as opposed to the current minimal contact of aqueous eye drops) is with contact lenses. An increase in dendritic cell numbers in the central cornea has been observed to occur in silicone-hydrogel contact lens wear [153, 154], as has an increase in tear inflammatory markers [155, 156]. Contact lens wearers can also experience a range of conditions linked to ocular surface inflammation, including dry eye disease [157, 158], contact lens associated red eye (CLARE) [159] and contact lens intolerance [160]. The use of polymeric eye drops is unlikely to elicit a similar response, as even with a prolonged residence time the overall contact time with the ocular surface and any mechanical disruption will be minimal in comparison.

There may be potential to harness the properties of the polymers to induce biomaterials-based immunomodulation in relation to ocular surface diseases. Immunomodulation, both intentional and unintentional (as a result of interaction between immune cells and drug delivery devices), needs to be considered when formulating eye drops. Concerns for the use of materials with longer residence times in the eye have arisen around the potential for an incomplete breakdown in devices designed to biodegrade to release their drug load and the uncertainty of responses to the by-products of the decomposition of different materials. In a repeated dosing situation, as with eye drops, there is a risk of material build-up and an associated inflammatory response [161]. Material may build in the conjunctival sac, which poses a potential risk as the conjunctiva is more prone to inflammatory responses than the cornea [39]. This could also lead to a foreign-object response and a feeling of discomfort, which will not aid adherence to a treatment regime.

1.5.1 The immune environment of the cornea, sclera and conjunctiva

When examining the use of topical ocular drug delivery methods, it is important to recognise the potential for undesirable inflammatory responses from the ocular tissues, as well as opportunities to use immune responses for the benefit of the treatment regime.

Research in both human and murine models has demonstrated, after substantial debate, that bone marrow-derived macrophages ($CD45^+$ $CD11b^+$ $CD11c$) and dendritic cells ($CD45^+$ $CD11b^+$ $CD11c^+$) reside in the healthy cornea, more specifically in the stroma (Figure 1.2b) [27, 162]. It has also been widely reported that dendritic cells and macrophages become more abundant in ocular tissues as disease severity and inflammation progress, as with elsewhere in the body [162-166]. It has been suggested that dendritic cells in particular are recruited to the cornea from the limbus [39, 167]. Not all macrophages and dendritic cells in the cornea are mature and ready to act as antigen-presenting cells, as approximately 70% of resident tissue macrophages are negative for the MHC class II complex, which is a molecule critical for activation of T lymphocytes [167, 168]. Epithelial tissues elsewhere in the body are associated with a much wider variety of leukocyte subsets, so it is suggested that resident corneal macrophages have the ability to adapt after exposure to certain stimuli (such as trauma) to impart wound-healing functions [162, 166, 169]. Previously, the idea was upheld that macrophages act as part of the innate immune system and dendritic cells as part of the adaptive immune system, however in the eye these lines are blurred due to the adaptability of both cell types, and their role in the tolerance and wound healing responses [166, 170]. Cytokines regulate the recruitment and function

of inflammatory cells that play critical roles in epithelial cell regeneration and stromal remodelling [162, 167].

The limbus, which defines the border between the transparent cornea and the non-transparent sclera, is home to the blood and lymphatic vessels that provide a pathway for the antigen-presenting macrophages and dendritic cells to engage with T-lymphocytes [167]. Gamma-delta (γδ) T-cells, which primarily reside in the limbus, have been shown to be pivotal in the regeneration of corneal epithelial tissue after injury [171]. In mice, specific T-helper cells have been shown to gather in the limbus and then spill into the conjunctiva during an inflammatory response, leading to conjunctiva-related allergy symptoms [172].

The activities of the immune cells and the limbal vasculature are influenced by the release of histamines and prostaglandins by immunocompetent cells residing in the conjunctival epithelium [27]. The conjunctiva is home to the same immune cell types that reside in the cornea (i.e., dendritic cells and macrophages) [39] but also has its own lymphatic drainage, allowing rapid trafficking by the antigen-presenting cells and the induction of a rapid response to pathogens and/or injury [48]. The conjunctiva also contains its own collection of immune cells such as T-cells, antibody-secreting B-cells and histamine-producing mast cells, which are arranged as so-called conjunctiva associated lymphoid tissue (CALT; [173, 174]). As a result, the conjunctiva is far more prone to inflammatory and allergic responses than tolerance responses compared with the cornea [39].

1.6 Tuning the properties of eye drops

Bioavailability considers the therapeutic efficacy of a treatment in terms of the amount of drug that becomes available to the tissue over the treatment window. When formulating an eye drop with greater bioavailability, there are multiple approaches to consider: i) ensuring the residence time of the drop is extended to create a larger delivery window (Figure 1.5.1), ii) ensuring the release profile of the delivery vehicle and the dose of the drug being carried allows for the optimum dose to be delivered across that window and iii) enhancing the permeation of the drug through the tissue.

The residence time of eye drops is increased when the drops can withstand the ocular surface's natural clearance mechanisms. Predictions of eye drop residence time are commonly calculated based on a combination of rheological testing and estimations of tear turnover rate and blinking mechanics. It is the general understanding that the natural tear film is shear thinning, a property which could be easily emulated in polymeric eye drops [175]. Assessment of tear film turnover is commonplace in clinical settings in the form of simple fluorescein clearance tests. In order to assess the residence of eye drops *in vivo*, this same test can be replicated with the fluorescein dye incorporated into the eye drop [176].

1.6.1 Mucoadhesion

The mucosa of the ocular surface plays an important role in the protection and function of the eye. The mucus on the ocular surface originates from the surrounding goblet cells. The glands which produce the other aqueous and lipid components in the tear film are based in the surrounding mucosal tissue also - the conjunctiva and superior and inferior tarsus (eyelids). Increases in the amount and the consistency of the mucus produced can be indicative of inflammation, or a reduction can lead to epithelial damage and dry eye disease [177, 178]. The majority of the ocular mucus is held to

the ocular surface in a glycocalyx layer (Figure 1.6); however, some secreted mucins float freely in the aqueous portion of the tear film [38, 177, 179]. The glycocalyx forms a protective barrier and an additional layer to penetrate for drug delivery purposes but also creates the possibility of extending the residence time of an eye drop if the correct properties are enhanced.

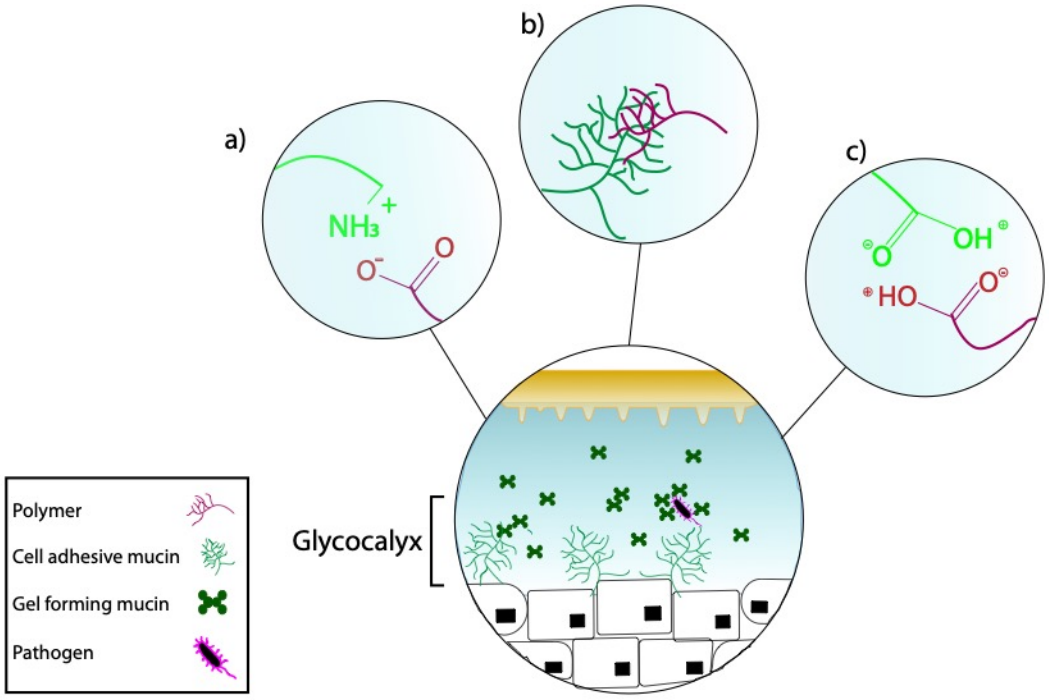

Figure 1.6: The anatomical elements of mucoadhesion and the mechanisms of adhesion including a) strong electrostatic attraction, b) physical entanglement and c) hydrostatic bonding

The mucins responsible for the improvement in retention time of mucoadhesive vehicles are the surface adhesive mucins in the glycocalyx [36, 38]. In order to stabilise the tear film, these mucins are hydrophilic, and the longest (MUC16) have a MW of around 2.5 million. Polymers exhibit mucoadhesion through a number of possible mucin-polymer interactions which can be electrostatic (hydrogen bonding or

electrostatic binding) or through physical entanglement (Figure 1.5.1) [38, 178]. As mucoadhesion, therefore, requires direct contact between the polymer and the mucosal layer, the wettability of the polymer matrix and the contact angle between the two layers are vitally important [180].

1.6.2 Viscosity

Another avenue investigated for overcoming the eye's natural barriers to drug delivery and improving the bioavailability of the carried drug is to increase the viscosity of the eye drop [29, 181-183]. Tests have shown that more viscous drops show a higher resistance to lachrymal clearance and stay resident on the surface of the eye longer [32, 61, 67, 82, 95, 184-187]. As with mucoadhesion, this increases the window available for drug delivery. Rheological assessments which determine viscosity are also frequently used to test the mucoadhesive properties of a polymer solution or gel [185, 188-191]. This links properties like viscosity and elastic strength to mucoadhesion. However, both cannot be increased indefinitely – as viscosity increases so does the surface tension of the drop. Various studies have examined the contact angle of drops *in vivo* and *in vitro* to assess how changes in viscosity, surface tension and surface chemistry affect the 'wetting' of the drop [192-194]. Viscosity appears to limit the spreadability of the drop, which in turn limits the mucoadhesion [180]. This is not necessarily a linear relationship as, for example, in viscous hydrogel drops, the crosslinking mechanism in the gel may change the surface chemistry which can also influence mucoadhesion - either positively or negatively [185]. The surface tension of an eye drop formulation has also been highlighted to have an important relationship with the drop size, and its consistency over multiple applications [195, 196]. It was also shown that drop bottle applications produce highly variable results

among patients, with drug type (flow characteristics), concentration and drop viscosity affecting drop size [195].

1.6.3 Rheology as a test for eye drops

Rheological techniques attributed to the specialism of viscometry are commonly deployed to assess the viscosity of gel-like materials. Rheology can be used to examine the properties of materials from Newtonian fluids to Hookean solids. Rheology compares the relationship between applied forces and the geometrical effects induced by these forces at a point. There is an assumed continuum – it is assumed that the measured behaviour is the same at any point other than at the boundaries [197].

There are two equations which describe the basic rheological state of materials, the Newton law of liquids:

$$\gamma = \frac{\sigma}{\eta}$$

Where γ – the rate of shear deformation, σ − shear stress, η – viscosity

and Hooke's law of solids:

$$\varepsilon = \frac{\sigma_{\mathrm{E}}}{\mathrm{E}}$$

where ε – deformation, σE − tensile stress and E − elastic (or Young's) modulus

However, there are limitations to these models. In solids, there are multiple time-dependent behaviours such as creep and relaxation which cannot be explained within Hooke's model. Additionally, both models require a linear relationship between stress (σ) and deformation (γ or ε) [197]. It is, however, possible for liquids to display non-

Newtonian behaviour, where shear stress is not proportional to shear rate and viscosity is not constant [197]. Non-Newtonian liquids can be viscous or viscoelastic. In viscous liquids, the work of deformation is lost (dissipates). Viscoelastic liquids, on the other hand, can store work energy as elastic energy and return it as elastic deformation [198].

These concepts are particularly relevant to the study of polymeric solutions. Generally, as the amount of polymer in a solution increases, so does the viscosity and in turn the non-Newtonian behaviour of the liquid. Most polymers exhibit a critical shear stress rate, above which the viscosity changes [198]. Polymeric solutions can be shear thickening – with viscosity increasing with increasing shear stress – or shear thinning – with viscosity decreasing with increasing shear stress [199]. Shear thickening is not to be mistaken for 'spurt', where a maximum shear stress is reached, and flow is no longer possible [198]. In this case, the material begins to slide along the walls of the measuring device.

Rheological assessments allow us to gain a better understanding of how polymeric solutions intended for eye drops behave under shear stress, such as blinking. Blinking creates a stress of 24.2 Pa in the downward phase and 12.1 Pa in the upward phase respectively on the corneal surface, creating a shear rate of up to 33,000s^{1} [200, 201]. Using physiologically relevant parameters in rheological assessments can therefore also provide an idea of the theoretically expected residence time for an eye drop [202].

When 18 commercially available HA-based eye drops were assessed, their viscosities were found to fall in the range of 2.5 to 2034.4 mPa·s [203]. There is a balance to be struck between ease of administration, blurring vision, patient comfort and eye drop residence time when formulating a viscous eye drop. Although most preparations

undergo some form of rheological testing *in vitro* as an assessment of their properties, this often does not take into account the complexity of blinking conditions. The natural curvature of the eye, and where the drop sits in relation to the eyelids must be considered and assessed when examining the behaviour of the drops [43, 81, 97, 126, 186, 202, 204, 205].

1.6.4 Controlled release

Each drug has an upper and lower limit of efficacy – a therapeutic threshold - which is directly associated with the concentration present in the target tissue (bioavailability). Drug delivery systems need to release their carried drug at a suitable rate to maintain a therapeutically effective dose across the treatment time window, otherwise, any improvements in residence time will not translate to improvements in treatment efficacy [184]. Different drug delivery vehicles offer different levels of tunability of the drug release profile [32, 87, 182, 206, 207]. Where the drug delivery relies on the disintegration of the carrier, drug release may be limited by slow disintegration. Many hydrogels are also responsive to ionic and pH changes [123, 182, 208]. Additionally, a strong interaction between the drug and the carrier may change the release profile of the delivery device, hindering delivery and preventing the drug from reaching or sustaining the therapeutic threshold [106]. The mechanism of drug loading is also important, as different methods create different release profiles but also involve different solvents [209]. The loading of nanoparticles is also limited by the fact that the encapsulated phase makes up a very small fraction of the overall mixture, and the loading is limited to the equilibrium point between the phases [210]. Relevant tests which take the temperature and pH of the destination tissue into account can give an idea of the expected *in vivo* delivery profile of a specific formulation.

1.6.5 Alternative mechanisms of ocular tissue penetration

Formulating eye drops which overcome the ocular barriers to drug delivery can involve facilitating easier passage of the drug through the ocular tissue. The main barrier to trans-corneal drug delivery is the epithelial layer, within which there are inter-cellular protein junctions and bindings which work to prevent penetration through the multiple cellular layers (Figure 1.5.3). Lipophilic drugs travel through the cornea by passing through the lipid bilayer of the cells themselves. Transport through the stroma is restricted to diffusion, so this is the rate-limiting step of the process [61]. Hydrophilic drugs must pass through the cellular tight junctions, which present the most significant barrier to penetration. It is also common for hydrophilic drugs to then accumulate in the stroma, which may limit passage to posterior tissues [61].

In order to reach the posterior structures of the eye, drugs must be able to pass through the cornea (this is also necessary for treating some corneal diseases). Due to the risks associated with increasing the permeability of the cornea itself, investigations have focused on how to surpass the cornea's natural barriers with amphiphilic molecules and carriers. However, even when a drug or carrier shows increased corneal permeation, this improvement is currently negligible when compared to the loss of the drug through the conjunctiva (~85%) and the limitations of residence on the corneal surface, and therefore efficacy of treatment is not yet significantly improved *in vivo* [211].

1.7 Chelating agents in topical ocular drug delivery

The first attempts at improving the penetration of drugs through the cornea involved incorporating pharmaceutical permeation enhancers such as EDTA to interfere with the epithelial tight junctions to allow for the passage of drugs into the stroma.

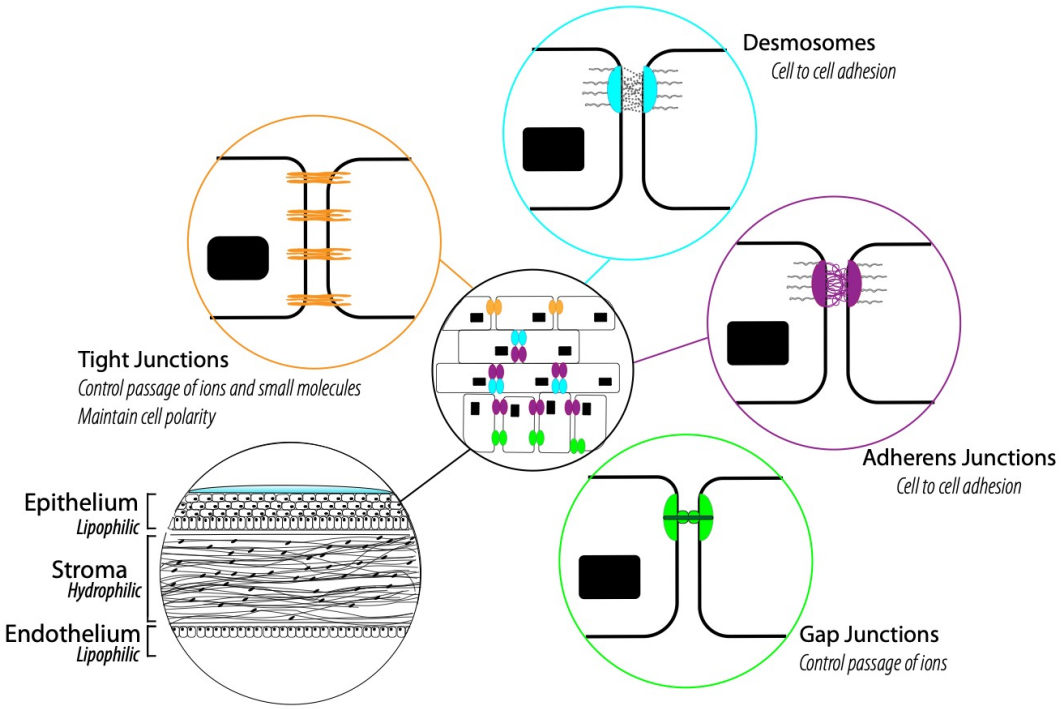

Figure 1.7: The wider structural and epithelial intra-cellular barriers to drug penetration in the cornea [1]

Both benzalkonium chloride (BAC/BAK) – a common preservative used in multi-dosage drops – and EDTA have been shown to improve the penetration of drugs through the cornea *in vitro* [60, 212]. Calcium plays a vital role in cell-to-cell and cell-to-substrate adhesion. Cadherin membrane glycoproteins have been highlighted as key players in cell-to-cell adhesion in most tissues, and depend on calcium ions for their function [213]. Cadherins can be subdivided into types E, P and N, with E and P cadherins expressed in the corneal epithelium and N cadherins expressed in the

corneal endothelium of mice [214]. Cadherins form trans-dimers with the cadherins on opposing membranes to create intra-cellular adhesion. In the corneal epithelium, this is reinforced with actin to produce adherens junctions (Figure 1.7) [215]. EDTA and similar compounds sequester calcium ions from the epithelial layer, impacting the function of the tight junctions and allowing for the delivery of molecules beyond [216]. Although this may appear positive for drug delivery, this process can affect the health of the corneal epithelium, leading to additional discomfort and secondary ocular conditions, such as superficial punctate keratitis and lower sensory nerve density [217]. The enhanced ocular penetrative effect has also not been replicated in *in vivo* studies, where the contact time of the eye drop preparation is much shorter [218].

There is also evidence to suggest that in drops that use a combination approach of pharmaceutical permeation enhancer and residence-prolonging polymers in solution, the polymer/drug/permeation enhancer interactions overall limit the bioavailability of the drug [219]. EDTA in particular has therefore been examined for both its influence on the penetrability of ocular tissue and its ability to remove calcium deposits from the ocular surface. However, in the cases of both EDTA and BAK, the use of chelating agents in the eye raises questions about ocular toxicity.

1.8 Inorganic Polyphosphates in cellular metabolism

Polyphosphates such as Adenosine Tri-, Di- and Monophosphate (ATP, ADP and AMP) are well known for the important role they play in cellular metabolism. In bacteria, studies have found evidence for the production of the enzymes polyphosphate kinase 1 (PPK1), which is suggested to allow the transfer of terminal phosphate units from ATP to inorganic polyphosphate chains, and polyphosphate kinase 2 (PPK2), which allows for the transfer of phosphate units from polyphosphate to guanosine

diphosphate (GDP), forming guanosine triphosphate (GTP) [220-223]. The potential importance of polyphosphate in bacterial cell metabolism and regulation has led to investigations which successfully used polyphosphate kinase depletion to tackle antibiotic resistance [224]. These same enzymes have been adapted for industrial use, and PPK from different sources can catalyse the synthesis of ATP from short-chain polyphosphates and AMP [225]. Exopolyphosphotase (PPX) is a third enzyme found in bacteria, which can hydrolyse polyphosphate chains into individual phosphate (Pi) units, potentially creating an energy reservoir from polyphosphate stores [224, 226, 227]. In starvation stress, PPX (which degrades polyphosphate) is inhibited [228]. Polyphosphate has therefore been found to play an important role in several key bacterial functions, including cell survival and stress response, motility, biofilm formation and heavy metals processing [224, 226, 228].

It has only recently been found that inorganic polyphosphates may play a role in this intracellular metabolism in mammalian cells. A specific hexokinase found in hepatic cells has been found to exclusively use inorganic phosphate, with a particular affinity to hexametaphosphate, and is inhibited by ATP [229]. Inorganic polyphosphates have also been found to be distributed in osteoblasts, and bone regeneration models in which rats were treated with polyphosphate have suggested that they may play a role in osteoblast growth and differentiation, and bone formation [230-232]. Both prokaryotes and eukaryotes have stores of polyphosphate, usually found in acidocalcisomes – acidic organelles similar to lysosomes which also store calcium [233, 234]. Human platelets have similar granular organelles, which are believed to be key to the release of polyphosphate which is triggered in the platelet activation [235-237]. It is a relatively recent discovery that polyphosphate plays a role in blood clotting

as a pro-coagulant [235]. Inorganic polyphosphate has been suggested to play a key role in calcium homeostasis within the mitochondria [238]. It has previously been known that orthophosphate acted as a buffer in calcium homeostasis within the cell, however, this mechanism alone would lead to the formation of insoluble calcium phosphate precipitates. It is now suggested that intracellular polyP may facilitate this process by inhibiting the formation of precipitates when free calcium levels remain elevated [238]. Additional investigations have discovered significant levels of inorganic polyphosphate ($polyP_{25}$) in cardiac muscle cells, and that the polyP levels are altered in metabolic stress conditions such as ischaemia and heart failure [239]. It is suggested that in these same cells, polyP activates the mitochondrial permeability transition pore (mPTP), and may facilitate the process through which calcium ions can accumulate in the mitochondria in heart disease [240].

Earlier studies have provided evidence that polyP regulates mTOR activation in animal cells, suggesting a role in the proliferation pathway [241]. The list of proteins with which inorganic polyphosphates have been found to interact and possibly allosterically control is growing, so much so that work has begun to map the 'human polyP-ome' [242]. The phenomenon of post-translational polyphosphorylation by inorganic polyphosphates primarily affects lysine residues of target proteins, which are suggested to form a nucleophilic attack on the polyP chain [243]. Modification of trimetaphosphate with biotin additions to each end of the polymer chain has allowed for the screening of 15000 human proteins, identifying 309 potential targets in the first instance, and opening the potential for many hundreds more [242].

The role of polyphosphate in both eukaryotic and prokaryotic cells creates interesting host/pathogen and pro-biotic interactions. There is evidence to suggest that the polyphosphate from probiotics in the intestine may play a key role in the maintenance of the epithelial barrier function [244]. When tissue damage occurs and a pathogen enters the host, short-chain polyphosphates in platelets play a role in the host's inflammatory response, encouraging clotting and neutrophil recruitment [228]. It is also suggested that host PolyP encourages proinflammatory (M1) phenotype differentiation in macrophages, which would encourage pathogen neutralisation and clearance [228, 235]. Prokaryotic cells carry polyphosphate which is on average much longer (1000+ units) than that of eukaryotic cells, and the pathogen may use these long-chain phosphates to counter the host response, encouraging M2 phenotype differentiation (anti-inflammatory) in macrophages and impairing MHC class II expression [228].

1.9 Sodium hexametaphosphate

Sodium hexametaphosphate (HMP), also known as Graham's salt, is a collection of high molecular weight inorganic polyphosphates, including linear, branched and cyclic structures [245]. Sodium HMP is formed when sodium phosphate (NaH_2PO_4) is heated at 800°C for a prolonged period, leading to the polymerisation of the phosphate units [245]. Rapid cooling is required to prevent the formation of the alternative sodium trimetaphosphate [246]. The resulting polyphosphate molecules are then hydrolysed by nucleophilic hydroxide (OH-) ions in water to form smaller linear polyphosphate molecules with a negative (anionic) charge and multiple binding sites [247, 248].

Sodium HMP can chelate metal ions and is commonly used to soften water or to decalcify and remove limescale in food manufacturing equipment and domestic

appliances [249]. Outside of mineralisation processes, HMP's chelating abilities can be used to interfere with processes dependent on calcium and magnesium ions, such as intercellular adhesion and cell membrane permeability [250, 251]. Polyphosphates including HMP are used in the ceramics industry as deflocculants [252, 253]. They are incorporated into colloidal suspensions of ceramic materials such as clay to alter their rheological properties and ensure they are optimal for different processing stages. With regard to the use of HMP in materials formation outside of ceramics, HMP has been used to crosslink chitosan through ionotropic gelation to form nanoparticles as a replacement for the more widely used tripolyphosphate (TPP) [254, 255]. The presence of monovalent and divalent metal ions is important for hydrogel formation, and chelating agents such as HMP can therefore be used to modulate the effects of these ions and the properties of the gel [256, 257].

Sodium HMP is also used in the food industry as an emulsifying agent and preservative [249, 258]. The role of HMP in food processing most typically utilises the ability of the ion to bind to protein, for example to separate whey protein [259] or metal ions, for example, to prevent accumulation of magnesium ions on the surface of fermented sausages [258]. The ability of HMP anions to bind to proteins can be used to stabilise emulsions, for example where the addition of HMP to egg white protein oil-in-water emulsions creates a 'creamier' – i.e. more stable - emulsion than those without HMP. This has been attributed to the ability of the HMP anions to crosslink the egg white protein, creating a viscoelastic network [260]. Additionally, in acidified milk drinks, HMP has been shown to interact with the protein pectin, again working to stabilise the milk emulsion [261]. Microencapsulation of stable oil particles in tuna and anchovy, through

the coacervation of HMP and gelatin, works to preserve the nutritionally valuable omega-3 fatty acids [262, 263].

In each of the varied functions that inorganic polyphosphates play, be that in ceramics, food or biological processes, the chain length of the phosphates involved is key to their activity. An investigation into polyphosphate-mediated blood clotting behaviour revealed that polyphosphate of shorter chain lengths (~100 units) accelerated factor V activation, whereas a length of 500 units or more was necessary for optimal activation of the contact pathway [264]. Variation of polyP chain length has been found throughout the anatomy of mammals, with that found in brain tissue consisting of a majority of chain lengths at 800 units or more, whereas that found in the plasma is around 60-100 units, and that in heart myofibrils is 25 units long [239, 240, 265, 266]. The composition of a solution of sodium hexametaphosphate at room temperature includes a majority of polyphosphates with 6 phosphate units or greater, with much smaller proportions of shorter chain (<5 phosphate units) polyphosphates [267]. Early studies into the composition of sodium hexametaphosphate (or Graham's salt), show that the temperature of formation is directly related to the lengths of the chains produced. Graham's salt can contain chains as long as 200 units or more [268] however there has previously been much variation in what is commercially available [269]. The polyphosphates present in sodium hexametaphosphate can be broken down when heated to form shorter-chain polyphosphates. When HMP was heated for 30 hours at 90°C, a viscous material consisting of orthophosphate and pyrophosphate was produced, signifying the end of the breakdown of the polyphosphate units [270]. The activation energy required for this breakdown was lowered when the solution into which the HMP was dissolved was made more basic [270]. This corresponds with

findings which investigate the role of heat treatment both in the presence and absence of $CaCl_2$ in the degradation of HMP. The proportion of polyphosphates with less than 6 phosphate units in a 0.5% HMP solution increased by 5% after treatment at 100ºC. When the HMP solution was heat-treated in the presence of $CaCl_2$, this compositional change was greater. When the same assessments were performed on pyrophosphate solutions, the presence of calcium appeared to instead inhibit the hydrolysis of pyrophosphate into orthophosphate, with 95% hydrolysis without $CaCl_2$ and 75% with [267]. There is little evidence outlining how HMP, or other polyphosphates, may break down over time without heat treatment when stored in ambient conditions in solution.

With regards to biomedical uses, research has shown that HMP can be used to de-calcify ectopically mineralised tissue [271] and dissolve kidney stones [272]. Due to its role in industry of modifying the surface of calcium ceramics, HMP is currently being investigated for various remineralisation and protective roles in dental care [273-279]. These studies have shown HMP to be safe for use in the oral cavity and to encourage human dental pulp cell and osteoblast proliferation [274, 275]. In the absence of serum, the population doubling time of human dental pulp cells was dramatically lowered by treatment with polyphosphate with a chain length of 60, at a concentration between 0.2 and 1mM [280]. HMP has also previously undergone toxicity testing due to its use in the food and cosmetic industries, with tests finding it safe for use in oral and dermal contexts [281].

Due to its unique properties, HMP presents as a viable potential agent in a topical treatment of BK which replaces the current EDTA/superficial keratectomy procedure.

2.

AIMS AND OBJECTIVES

The EDTA chelation procedure for the treatment of band keratopathy is well-regarded by clinicians, and it is considered effective [9]. There are, however, several limitations to this procedure, including:

(a) The threshold for treatment: it is common for patients to not receive treatment until their visual acuity is severely affected or they are experiencing unmanageable pain or discomfort.

(b) The risk of treatment: patients commonly develop corneal oedema after the procedure which in a small number of cases can lead to additional ocular complications.

(c) The removal of the epithelial layer: this leaves a higher risk of infection and is uncomfortable for the patient for days afterwards. The use of EDTA delays healing compared to eyes with similar corneal abrasions by up to 5 days, and there is also a risk of developing dry eye disease [10, 282].

(d) Exclusions from treatment: many patients develop CBK alongside additional ocular comorbidities which exclude them from receiving treatment for their CBK. An assessment of 89 cases in a UK hospital found that improvement in visual acuity after the procedure was not statistically significant, typically due to ocular co-morbidities [10].

(e) The availability of EDTA for chelation: clinicians are seeking alternatives to the usual Na-EDTA due to its scarcity in clinical settings.

(f) The aversion of patients to invasive procedures.

(g) The cost of invasive procedures: Where possible, surgical interventions should be considered a last resort in treatment.

(h) The risk of recurrence: A recent evaluation also showed that in 28% of cases the deposits recurred within 2 years, and some required a second procedure [10].

It is for these reasons that band keratopathy will sometimes be left untreated. The development of an effective topical treatment could circumvent some of these limitations, namely by reducing the threshold for and exclusions from treatment, reducing the risks compared with those associated with surgical intervention, improving the availability of the therapeutic agent, increasing the choices available to patients and clinicians, reducing the cost of treatment, and managing recurrences non-surgically.

The aim of this project was therefore to assess whether sodium hexametaphosphate could act as the therapeutic agent in an effective topical treatment for calcific band keratopathy, an ocular condition which is characterised by the ectopic formation of the calcium phosphate hydroxyapatite in the cornea. There are four key questions which form the basis of this investigation, each leading on from the last:

(a) Can sodium hexametaphosphate effectively demineralise and dissolve hydroxyapatite mineral within the time associated with the retention of an eye drop of the eye?

(b) Is sodium hexametaphosphate toxic to the ocular cells and tissue?

(c) Can the delivery of sodium hexametaphosphate to the eye be optimised by incorporating polymeric materials to modulate the viscoelastic properties of the formulation?

(d) Can a relevant *ex vivo* test be developed to assess the efficacy of sodium hexametaphosphate in treating band keratopathy?

Within these core questions and the investigations carried out to answer them, key parameters relevant to the wider context will be established, including the concentration of HMP in solution that is both effective and safe, how long this concentration of HMP would need to be resident on the ocular surface for, and whether the incorporation of said concentration of HMP into an organic polymeric material assists in the drug delivery. The development of an *ex vivo* model to test the HMP formulation within ties together the subsequent investigations.

3.

GENERAL METHODS

3.1 Table of Materials

Name	Supplier	Location of Supplier
10% Paraformaldehyde	Sigma Aldrich	The Old Brickyard, New Rd, Gillingham SP8 4XT, UK
10% Povidone Iodine solution (Videne)	WMS	Craiglas House, The Maerdy Industrial Estate, Rhymney NP22 5PY, UK
70% Ethanol	Sigma Aldrich	As above
Agar, powder	Sigma Aldrich	As above
Ammonium hydroxide	Sigma Aldrich	As above
Amphotericin B	ThermoFisher	Thermo Fisher Scientific UK, Bishop Meadow Road, Loughborough, LE11 5RG, UK
Calcium chloride	Sigma Aldrich	As above
Calcium nitrate	Sigma Aldrich	As above
Chitosan powder (medium chain length)	Sigma Aldrich	As above
Cytotox 96 non-radioactive LDH release assay kit	Promega	Science Park, 2 Benham Rd, Chilworth, Southampton SO16 7QJ, UK
Di-ammonium phosphate	Sigma Aldrich	As above
DMEM F-12 (Gibco)	ThermoFisher	As above
Esoin	Sigma Aldrich	As above
Ethylenediaminetetraacetic acid. crystalline	Sigma Aldrich	As above
Foetal Bovine Serum	Sigma Aldrich	As above
Glass cover slips	Sigma Aldrich	As above
Harris' Haemoxylin	Sigma Aldrich	As above
Histoclear	Sigma Aldrich	As above
Low acyl gellan powder (kelcogel)	CP Kelco	Cumberland Center II Atlanta, GA 30339, USA
Magnesium Chloride (anhydrous)	Sigma Aldrich	As above
Optimal cutting media	VWR	Hunter Blvd, Lutterworth LE17 4XN, UK
Penicillin/streptomycin	Sigma Aldrich	As above
pH controlled solutions (pH 4, 7, 10)	Fisher Scientific (ThermoFisher)	As above
Phosphate Buffered Saline solution (magnesium and calcium free)	Sigma Aldrich	As above
Potassium Chloride	Sigma Aldrich	As above
Propidium Iodide powder	ThermoFisher	As above
RPMI 1640	Sigma Aldrich	As above
Sodium Alginate powder	Sigma Aldrich	As above
Sodium Bicarbonate	Sigma Aldrich	As above
Sodium Chloride	Sigma Aldrich	As above

Sodium hexametaphosphate, crystalline	Sigma Aldrich	As above
Sodium Hydrogen Carbonate	Sigma Aldrich	As above
Sodium Hydrogen Phosphate	Sigma Aldrich	As above
Sodium hydroxide	Sigma Aldrich	As above
Synthetic mounting resin (vectamount)	2B Scientific	Office 4, Bldg A, Kirtlington Business Centre, Kirtlington, Kidlington OX5 3JA
Toluidine Blue O powder	Sigma Aldrich	As above
Von Kossa staining kit	Generon	11 Whittle Pkwy, Slough SL1 6DQ
Vybrant MTT assay kit	ThermoFisher	As above

3.2 Table of key apparatus

Type of equipment	Name	Supplier
Plate reader	Infiniti 2000	Tecan
pH meter	pH meter	Mettler Toledo
X-Ray Diffractor	D8 Autosampler	Bruker
X-Ray Fluorometer	X4 Tornado	Bruker
Fluorescence and brightfield microscope	EVOS 5000	ThermoFisher
Microscope camera	Moticam	Motic
Rheometer	Kinexus	Malvern Panalytical

3.3 Preparing aqueous solutions of chelating agents

Different concentrations of sodium hexametaphosphate solution were prepared by dissolving crystalline Na-HMP powder (Sigma Aldrich, UK) in Milli-Q distilled and filtered water under stirring until completely dissolved. EDTA solution was also prepared in by dissolving crystalline Na-EDTA powder (Sigma Aldrich, UK) in MiliQ water under stirring until completely dissolved. To create pH-neutral solutions of HMP, 1M NaOH was added dropwise to the relevant HMP solutions until pH 7 was reached and maintained, using a pH meter to measure the pH change. Changes in volume were accounted for by increasing the HMP concentration where necessary.

3.4 Preparing nanocrystalline hydroxyapatite sol

Powders of di-ammonium phosphate and calcium nitrate, and ammonium hydroxide solution (30%v/v) were acquired from Sigma-Aldrich, UK. An aqueous nanocrystalline hydroxyapatite sol was prepared using the precipitation method, adapted from that described by Raynaud et al. [283]. Aqueous solutions, both adjusted to pH 11 with the addition of dropwise ammonium hydroxide, were prepared of di-ammonium phosphate (12.5% w/v) and calcium nitrate (13% w/v). The phosphate solution was then added to the calcium solution in a dropwise manner, to form a final solution with a ratio of 7:5 v/v. The combined solutions were left under stirring for 100 hours. The white nanocrystalline hydroxyapatite precipitate was then centrifuged and washed three times before being re-suspended in fresh Milli-Q water to form a HA/water sol.

3.5 Absorbance readings

Absorbance readings were taken using a Tecan Infiniti 2000 plate reader. For each well of a 96-well plate, 9 readings were taken in a square profile. For the larger wells of a 6-well plate, 12 readings were taken per well in a 3x4 profile.

3.6 Hydroxyapatite demineralisation absorbance assay

To assess whether treatment of hydroxyapatite with Sodium hexametaphosphate dissolves the mineral and forms optically transparent by-products, absorbance readings were used to assess the demineralisation of HA by HMP. This method was adapted from previous investigations performed by Eisenstein et al. [271] and Robinson et al [272]. Hydroxyapatite sol was prepared to a concentration of 15% v/v. 50μL of sol was added to each well of a 96-well plate. Absorbance was read using a Tecan Infiniti 2000 plate reader at 375nm, with 9 reads per well to achieve a baseline (starting) absorbance reading. Baseline absorbance readings were included in the

range of 0.9-1.1, and the average baseline absorbance reading for each treatment group was within a 0.1 range. 50μL of treatment was added to each well. After each 60-minute interval, the absorbance was read at 375nm. As standard, the assay was performed at room temperature (20°C) with 5 repeats per group. The concentration and pH of the treatments and the temperature of the assay were all changed subsequent tests to investigate the effect of these parameters on the demineralisation reaction. The assay was also repeated using larger reactant volumes (4ml, 10ml) in a 6 well plate.

3.7 pH readings

The pH meter (Mettler-Toledo) was calibrated before use with pH-controlled solutions of pH 4, 7 and 10 (Fisher Scientific). pH readings were taken in triplicate, with the pH probe cleaned appropriately between readings.

3.8 X-Ray Diffraction (XRD)

A D8 Autosampler (Bruker, USA) with a copper tube was used for X-ray diffraction. X-ray diffraction allows analysis of the crystalline phases in a material, identifying the crystalline components of a powder. It also suggests when a material has an amorphous structure through the absence of defined peaks with a reduction in crystallinity being shown through broadening of the diffraction peaks. Dry, powdered samples are loaded into sample holder, around which the detector rotates. The x-ray tube directs rays towards the sample, and the detector detects the angle at which the x-rays leave the sample. The angle (θ) and intensity (count) are plotted as a diffraction pattern which is compared to the characteristic patterns of known materials. The XRD produced a diffraction pattern between $2\theta = 5°$ and 60° with a step size of 0.5s/°.

3.9 Preparation of Porcine eyes for culture

Whole porcine eyes were provided by Medical Meat Supplies, UK and received within 4 hours of death from a commercial abattoir. The eyes were waste from food production and animals were not killed for the purposes of research. Eyes were removed from the head after death but before scalding to maintain tissue viability. The eyes were transported in a vacuum sealed bag on ice. Once received, the eyes were disinfected for 5 minutes in 10% povidone iodine solution (Videne) and then rinsed in sterile PBS (Sigma Aldrich, UK). The eyes were then dissected, removing the anterior segment from the ocular globe, and then removing the lens, iris and scleral tissue, leaving the cornea. The corneas were then sterilised in 7.5% povidone iodine solution for 30 minutes and then rinsed three times in sterile PBS before further processing in a sterile laminar flow hood.

3.10 Preparation of assay plates for *in vitro* cellular toxicity assays

RPMI 1640, foetal bovine serum and penicillin/streptomycin were purchased from Sigma Aldrich, UK. Amphotericin B solution was purchased from ThermoFisher, UK. Clear, flat bottom, cell-culture treated 96- well plates (Corning CoStar) were seeded with cultured porcine stromal cells (passage 3) at a density of 5,000 cells per well with 100μl growth media (RPMI 1640 + 10% foetal bovine serum + 1% penicillin/streptomycin + 1% amphotericin B) and incubated for 48 hours at 37°C and 5% CO_2. Cells were counted using trypan blue exclusion. A cell curve was included from 0 – 20,000 cells/100μl for reference, and cell free wells (100μl media only) were also included for each treatment group. Once acclimatised (after 48 hours), the growth medium was removed and the wells gently washed with phenol-free and serum-free media, before being treated with 100μl treatment media (RPMI 1640, phenol-free and

serum-free). Treatment media was prepared by adding double-concentrate treatment solutions to phenol free media to reach final treatment concentrations of 0.125M, 0.25M, 0.5M, and 1M HMP, 2% EDTA. As both the EDTA and HMP are aqueous solutions, a water/media 50:50 group was included as a control. Treatments were performed in triplicate. All growth and treatment medias were sterile filtered before use. The cells and treatment were incubated at 37°C with 5% CO_2 for 4 or 6 hours.

For the propidium iodide assays, porcine corneal stromal cells (Passage 3) were seeded into a 24 well plate (Corning CoStar) at a density of 20,000 cells per well with 500µl growth media. 72 hours after seeding, the growth media was removed and treatment media were added including 0.125M, 0.25M, 0.5M, and 1M HMP, 2% EDTA, 50:50 media/water and untreated groups. Cells were incubated with treatments for 4 hours at 37°C and 5% CO_2.

3.11 Cryosectioning

Corneal samples obtained from porcine eyes and which had been used for testing were fixed in 4% Paraformaldehyde for 24 hours. For cyroportection of the samples, aqueous solutions of 15% w/v and 30% w/v sucrose (Sigma Aldrich, UK) were prepared, and samples were left in each for 12 hours successively. Samples were then embedded in optimal cutting media (VWR) in cuboidal cryomolds and snap frozen using dry ice. The embedded tissue was then cryosectioned at a thickness of 20µm onto glass slides (SuperFrost, ThermoFisher, UK). Slides were left in air to dry overnight (~16 hours) before staining, or freezing at -20°C for further processing.

3.12 Haemoxylin and Eosin staining

Slides were rehydrated in PBS for 5 minutes before staining. Slides were stained in Harris' haemoxylin for 5 minutes, differentiated in 5% acid alcohol and then 1% sodium bicarbonate before dehydration in 70% ethanol. Slides were then stained with eosin, before dehydration in 90%, 95% and 2x 100% ethanol. Slides were cleared with Histoclear II before mounting with synthetic resin (Vectamount®) and glass cover slips. Mounted slides were stored at room temperature (~20°C), protected from light, before imaging.

3.13 X-Ray Fluorescence (XRF)

X-ray fluorescence offers non-destructive elemental analysis of materials. When x-rays are fired at the atoms of a sample, characteristic secondary (fluorescent) x-rays are emitted depending on the electron configuration of the atom, allowing each element to have a characteristic signal. Corneal tissue sections were analysed with a X4 Tornado (Bruker) XRF to assess the phosphate levels present in the tissue. The stage height was adjusted to bring the sample into focus. The number of measurements per mm in the X direction was adjusted to ensure a spot size of 25μm maintained an unbroken line of readings across the sample. 75 cycles were performed per measurement with a measurement time of 150ms per pixel. Phosphate, calcium and sodium were all measured. Measurements were performed under vacuum to limit interference with light atom detection.

3.14 Von Kossa staining

Cryosections 20 μm in thickness were prepared of each cornea. Slides were rehydrated in distilled water for 5 minutes before staining. Sections were then

incubated in silver nitrate solution for 60 minutes under direct UV light. Slides were incubated in sodium thiosulfate solution, followed by nuclear fast red stain, then were dehydrated in 100% ethanol. Vectamount mounting resin was used to mount the slides with glass coverslips. Slides were imaged on an EVOS 5000 microscope, on the RGB Brightfield setting.

3.15 Statistics

Data processing and analysis was completed using Microsoft Excel and GraphPad Prism software respectively. Each experiment was repeated a minimum of three times. Normality and lognormality tests were performed on relevant numerical datasets (Anderson-Darling test, D'Agostino and Pearson test, Shapiro-Wilk test and Kolmogorov-Smirnov test). Statistical significance was assumed to be $p<0.0001$ (****).

4.

ASSESSING THE DEMINERALISATION EFFICACY OF SODIUM HEXAMETAPHOSPHATE

4.1 General introduction

Polyphosphates can form both soluble and insoluble complexes with metal ions. In bacteria, polyP has been found to regulate free iron in both stress and non-stress conditions, acting as either a reservoir or a sink [284]. Both the adsorption of HMP onto the surface of minerals and the ability of HMP to dissolve minerals relies on the chelation of calcium and other metal ions by HMP. Previous investigations have indicated that HMP has equal affinity for calcium and magnesium ions at a HMP concentration of 2mM [285]. HMP is also commonly used in meat preservation for its ability to regulate calcium and magnesium levels [258, 267, 286, 287]. However, it has also been shown that polyphosphate chain length influences the affinity of the polyp for calcium and magnesium, with longer chains having a higher affinity for calcium than magnesium, and the opposite being true for shorter chains [288]. Recent explorations have also found that polyphosphates can form coacervations when key ratios of divalent ions are reached [289].

Sodium hexametaphosphate has been investigated for use with both biological ceramics – for example, teeth and ectopically calcified soft tissue – and commercial ceramics – within clay processing for limescale removal. In clay processing, HMP is used as a deflocculant, adsorbing to the surface of the clay micelles and improving the rheological properties of the mixture [253, 290-292]. HMP acts as a deflocculant by altering the surface energy of clay micelles and introducing Na+ ions. Andreola *et al* describe how 'the chemi-adsorption produces a surface excess of negative charge and therefore the increase of the repulsion forces between the particles; as a consequence, the zeta potential value of the clay particles increases' [252]. It is suggested that HMP

adsorbs to aluminol present in clays. Furthermore the presence of HMP in kaolinite suspensions has been found to induce a cation exchange, where the increase in Na^+ ions causes an exchange of Ca^{2+} and Mg^{2+} ions on the kaolinite surface for the Na^+ ions [252]. An additional investigation into the role HMP plays in the dissolution of kaolinite, found that the adsorption of cationic surfactants on the surface of the clay was increased in the presence of HMP [291]. Tests involving montmorillonite show that this particular clay immobilises HMP, potentially through the formation of calcium-phosphate complexes [290, 293].

With regards to hydroxyapatite (HA) mineral specifically, sodium hexametaphosphate can be used to both degrade HA and as a source of phosphorous for its formation [271, 294]. It is widely thought that inorganic polyphosphates play a key role in bone generation, including osteoblast growth and differentiation [230-232]. It is suggested that enzymatic regulation of inorganic polyphosphate levels encourages or prevents apatite formation. The formation of polyphosphate can limit free orthophosphate, whilst the polyP created then limits the free calcium present. When mineralisation is desirable, the polyphosphates can then also be cleaved into orthophosphates by alkaline phosphates to encourage apatite formation [295]. When porous hydroxyapatite with or without polyP adsorption (average chain length of 60) was implanted in rabbit femurs, individuals with polyP adsorption elicited greater bone regeneration, affirming the suggestion that polyphosphates can act to encourage bone regeneration by providing phosphate for apatite formation [296]. Extensive studies have been carried out into the use of HMP for dental applications, where hydroxyapatite is the mineral of interest due to its presence in bone and enamel. When 1% or 8% HMP was applied to saliva coated hydroxyapatite disks, there was a

significant reduction in their dissolution rate when compared to control [297]. Where enamel is treated with 0.5% and 1% HMP, there is a greater adsorption post-treatment of calcium and phosphate ions to the enamel surface, which is suggested to be due to an increase in electron-door sites on the enamel surface once the HMP has been initially adsorbed [278, 298].

In vitro, HMP can be used to prevent re-agglomeration of physically deagglomerated nano-hydroxyapatite, again through changing the surface free energy of the nanoparticles [299, 300]. In addition to bone regrowth and protection, HMP has been used to demineralise hydroxyapatite, relying on the ability of the polyphosphate units to chelate calcium from the calcium phosphate salts. This is in line with the widespread use of Sodium HMP under the name ‘calgon’ as a water softener for limescale prevention and removal [301]. When investigated for the treatment and prevention of kidney stones, it was found that HMP was able to significantly dissolve and prevent the formation of various calcium phosphate salts, including calcium oxalate and hydroxyapatite [272, 302]. With regards to pathological ossification, HMP significantly demineralised samples of pathological bone [271]. Interestingly the demineralisation of bone, unlike its formation, did not appear to be mediated by the surface absorption kinetics, as the surface of the treated bone did not have an increased calcium or phosphate ratio when analysed through x-ray fluorescence [271].

The aim of this chapter is to determine whether sodium HMP could form the basis of a topical treatment that replaces the EDTA chelation procedure. The ability of HMP to demineralise hydroxyapatite mineral, and the influence of factors such as concentration, pH and time will be explored.

4.2 Materials and Methods

The hydroxyapatite demineralisation absorbance assay (Section 3.6, Page 75) was performed under a series of differing parameters to investigate the reaction between sodium hexametaphosphate and nano-hydroxyapatite mineral. The aim of this assay was to predict whether treating mineralised ocular tissue with HMP solution could result in the clearance of the obstructing mineral from the visual field.

4.2.1 Optimisation of the hydroxyapatite demineralisation absorbance assay

One measure of success for a novel treatment for band keratopathy would be the restoration of corneal transparency through the dissolution of the hydroxyapatite mineral. The passage of light through the tissue would be indicative of the mineral's dissolution. On this basis, the dissolution of hydroxyapatite could be assessed through the measurement of light passing through the material, using a typical plate reader.

Hydroxyapatite-in-water sols for testing were prepared within the range of 10%-95% v/v. A range of sols were then created by through the serial dilution of hydroxyapatite/water sol prepared at a concentration of 10% v/v, until a concentration of 3% v/v. 100μl of hydroxyapatite (HA) sol of each known, varying concentration was added to the wells of a clear 96-well plate. The plate was then scanned at a range of wavelengths between 230nm and 700nm, increasing in increments of 5nm for each reading (Tecan Infiniti 2000). To find the molar concentration of the 10% v/v HA sol, the sol was dried to a powder at 80°C for 48 hours. The powder was then weighed, and the molar concentration calculated. The range tested was therefore 0.724mM/ml at 10% v/v to 0.2175 mM/ml at 3% v/v.

To test the limits of this method, higher concentration HA sols were then tested at a single wavelength, ranging from 95% v/v to 16.5% v/v. 100μl of each concentration of HA sol was again plated in a clear 96-well plate. Absorbance was measured at 375nm with multiple reads per well.

4.2.2 Measuring the effect of time and HMP concentration on hydroxyapatite sol demineralisation

To investigate the relationship between HMP concentration and hydroxyapatite sol demineralisation, and to inform what concentration of HMP may be required to treat a cornea with hydroxyapatite deposits, 50μl of sodium hexametaphosphate solution of 2M, 1M, 0.5M and 0.25M concentration were added to pre-prepared and scanned wells containing 50μl of hydroxyapatite sol (15% v/v). Plates were prepared as previously described (Section 3.6, Page 75). The final concentration of the HMP treatment was calculated with consideration for the final volume of the HA sol and the added HMP treatment combined and was therefore half the concentration of HMP added, giving final treatment concentrations of 1M, 0.5M, 0.25M and 0.125M HMP. Absorbance measurements were taken at 375nm every hour for 9 hours.

4.2.3 Measuring pH changes that occur during hydroxyapatite sol demineralisation by HMP

To investigate the pH dependence of demineralisation behaviour of HA sol treated with 0.125M HMP, the nano-HA absorbance assay was repeated at 10ml total volume, with simultaneous pH readings and absorbance readings. To examine the changes in pH as the reaction progresses, 0.25M HMP was combined with 15% HA sol at 50:50 to a final volume of 10ml and a final HMP concentration of 0.125M. Absorbance was read

at 375nm every hour for 15 hours and then again at 24 hours and 72 hours. The pH was read with a pre-calibrated pH meter every hour for the 72-hour duration.

4.2.4 Measuring the effect of HA sol concentration on demineralisation

To establish the relationship between the demineralisation behaviour of HMP and the concentration of the hydroxyapatite sol, 50μl of differing sol concentrations within a range of 16.5% v/v and 95%v/v, and 50μl of 0.25M HMP, were combined in each well of a 96-well plate (giving a final concentration in the solution of 0.125M HMP). The absorbance of each well was measured at 375nm after 60 minutes of incubation.

4.2.5 X-Ray Diffraction analysis (XRD)

X-ray diffraction was performed as described previously (Section 3.8, page 76) on the precipitate formed in the reaction between 0.125M HMP and hydroxyapatite. The precipitate was washed with MiliQ water, centrifuged, and then air dried over several days before analysis. The XRD produced a diffraction pattern between $2\theta = 5°$ and 60° with a step size of 0.5s/°.

4.2.6 Measuring the effect of the pH of HMP on hydroxyapatite sol demineralisation

To assess the influence of pH on the reaction between HMP and HA, the assay was repeated with both pH neutralised (pH 7) and non-neutralised (pH ~5.2) 1M and 0.5M HMP treatments (final HMP concentrations of 0.5M and 0.25M). 96-well plates were prepared as previously described (Section 3.6, Page 75). The baseline absorbance reading was taken at 375nm as were subsequent readings taken after 60, 120, 180 and 240 minutes of treatment. A water control was included for reference.

4.2.7 Assessing the influence of temperature on the hydroxyapatite/Sodium hexametaphosphate reaction

96-well plates were prepared as previously described (Section 3.6, Page 75). HA sol and 0.5M HMP solution were brought to temperature at 5°C, 20°C, 37°C or 50°C in an incubator or fridge, sealed to reduce evaporation of the liquid phase. This temperature range was chosen to reflect the possibility of the solution being refrigerated, used at room temperature, at body temperature and above. 50 μl of temperature adjusted treatment was then added to each well and the plate was returned to a temperature-controlled environment for 60 minutes. After the 60-minute interval, the plate was scanned at 375nm to give a second absorbance reading.

4.2.8 Assessing of the affinity of HMP at various concentrations for forming precipitates with Magnesium and Calcium ions

To assess the affinity of HMP for divalent metal ions - beyond the chelation of calcium from hydroxyapatite – at different concentrations, 50μl HMP at a concentration of 0.25M, 0.5M, 1M or 2M was added to 6 wells each of a 96 well plate. Solutions of $MgCl_2$ and $CaCl_2$ were prepared by dissolving the appropriate mass of crystalline powder in Milli-Q water under stirring. 50μl of 1M $CaCl_2$, 1M $MgCl_2$, or a solution with a 1:1 ratio 2M $CaCl_2$:2M $MgCl_2$ was added to the HMP. The absorbance of each sample was read at 600nm every 60 minutes over 7 hours to detect the formation of precipitates.

4.2.9 Statistics

Statistical analysis was performed in Prism (Graph Pad). Comparison between the absorbance of HA treated with different concentrations of HMP, different pH levels and different temperatures was performed using a 2-way ANOVA (mixed-effects analysis in the case of HMP concentration) with multiple comparisons. A Pearson's correlation analysis was performed to analyse the relationship between measured pH and absorbance in the reaction between 0.125M HMP and HA.

4.3 Results

The aim of the assessments using nanocrystalline hydroxyapatite mineral is to establish whether HMP could adequately dissolve hydroxyapatite to restore corneal transparency and visual acuity. It is also necessary to establish the limitations of the efficacy of HMP, due to concentration, pH, time, or temperature.

4.3.1 Optimisation of the hydroxyapatite demineralisation absorbance assay

A plate reader was used to examine the passage of various wavelengths of light through samples of hydroxyapatite sol of a range of concentrations. This replicates the obstruction of light through the cornea in cases of band keratopathy.

This assessment showed that the measured absorbance increases linearly with HA concentration at all wavelengths tested (Figure 4.1). The absorbance of any single HA sample of a given concentration decreases with increasing wavelength. At wavelengths above 250 nm the gradient of the slope marking the relationship between HA sol concentration and absorbance becomes steeper. The relationship between absorbance and HA concentration remains the same above 280nm, where the gradients of the lines produced at each wavelength remain unchanged. Absorbance is therefore a relevant measure of the HA concentration of a sol within this range. Reductions in absorbance also, therefore, correspond to reductions in HA sol concentration.

Where the absorbance of higher concentrations of HA sol were tested (Figure 4.2), the relationship between concentration and absorbance remained linear only to a maximum 33%, where the gradient of the curve becomes increasingly shallow and

each incremental increase in HA sol concentration creates a smaller increase in absorbance. At these high concentrations of Hydroxyapatite in the sol (>33%), the difference in absorbance between different HA concentrations is minimal, and therefore the use of absorbance as a measure of concentration would be inaccurate and imprecise. HA sol concentrations of 15-25% create distinguishable results which can be accurately measured with this technique.

4.3.2 Measuring the effect of time and HMP concentration on hydroxyapatite sol demineralisation

Key to formulating a novel topical treatment is understanding the concentrations of the active agent necessary to achieve the desired effect. It is also essential to understand the contact time necessary between the drug and the targeted tissue for effective treatment. Previously, assessments of the demineralisation efficacy of HMP have used concentrations of HMP up to 0.2M and have measured the effect over many days. For the desired use under investigation in this work, it is necessary to find a concentration of HMP that is effective in a much shorter time – one that replicates the residence time of an eye drop at around 60 minutes.

Hydroxyapatite sol samples treated with 0.125M, 0.25M HMP, 0.5M HMP or 1M HMP (Figure 4.3) show a statistically significant ($p<0.0001$) decrease in absorbance from baseline after 60 minutes of treatment, and then at all subsequent time points, representing the demineralisation of hydroxyapatite by the HMP into soluble products. At the end of the assessment at 540 minutes, each treatment group had reached absorbance readings (±SEM) of 0.732 ±0.40, 0.735 ±0.046, 0.432 ±0.040 and 0.262 ±0.009 respectively, from a starting absorbance of 1.008 (±0.005). The water (control)

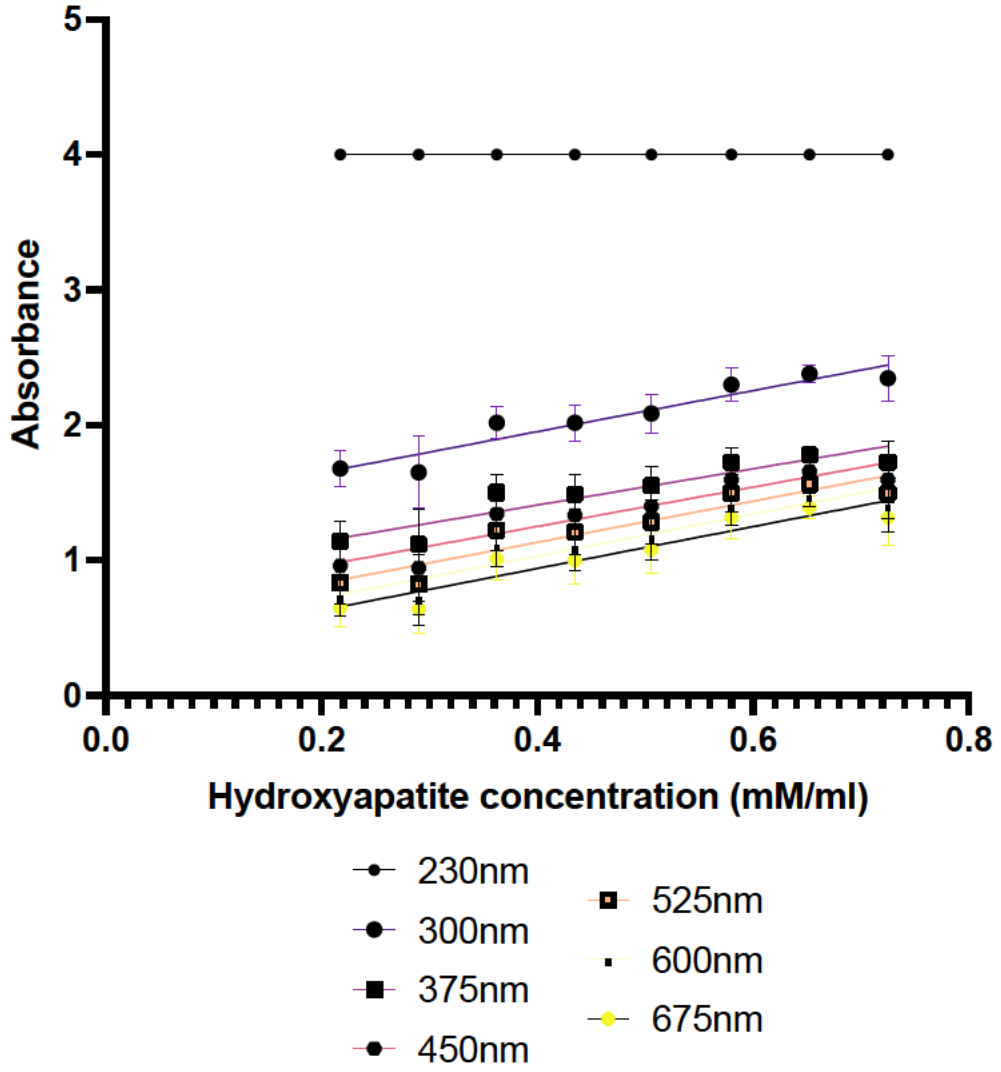

Figure 4.1: the absorbance measurements of 100µl of *varying concentrations of hydroxyapatite sol (0.2 – 0.75mM/ml) at a range of wavelengths from 230 – 675nm with interpolated lines of best fit. At each given concentration, the absorbance measured decreases with increasing wavelength. As concentration increases, so does absorbance. The change in absorbance is greater at wavelengths larger than 290nm. n=12. Error Bars = Standard Deviation (SD).*

group showed a small decrease from baseline, reading at 0.932 (±0.046). This is most likely due to evaporation of liquid over time.

The trend across 0.25M-1M HMP treated HA is that absorbance decreases with time, representing increases in demineralisation with increases in HMP concentration. From the same baseline, the 1M HMP treated group presented significantly lower absorbance readings than 0.25M and 0.5M at every time point up to 8 hours ($p<0.0001$). 1M HMP is therefore the most effective of the treatments assessed, reaching near maximum demineralisation at an absorbance of 0.295 (±0.012) within 2 hours and with no further significant changes in absorbance after 5 hours of treatment.

After the initial reading taken at 60 minutes post-baseline, 0.25M and 0.5M HMP treated sol both then show increases in absorbance, from 0.724 (±0.023) at 60 minutes to 0.779 (±0.047) at 360 minutes for 0.25M and from 0.518 (±0.021) at 60 minutes to 0.633 (±0.039) at 180 minutes. However, both groups then proceed in the same manner - steadily decreasing in absorbance over time, with each reading yielding a smaller value than the last over the time course of the reaction. From 7 hours of treatment onwards, 0.5M HMP shows significantly greater demineralisation (reduction in absorbance) than 0.25M HMP ($p<0.0001$).

0.125M HMP treated HA sol presents a different behaviour to the other treatment groups, with a preliminary decrease in absorbance to 0.395 (±0.012) within the first 60 minutes of treatment. The absorbance remains consistently low for the first four hours of treatment, with no significant difference between 1M HMP and 0.125M HMP

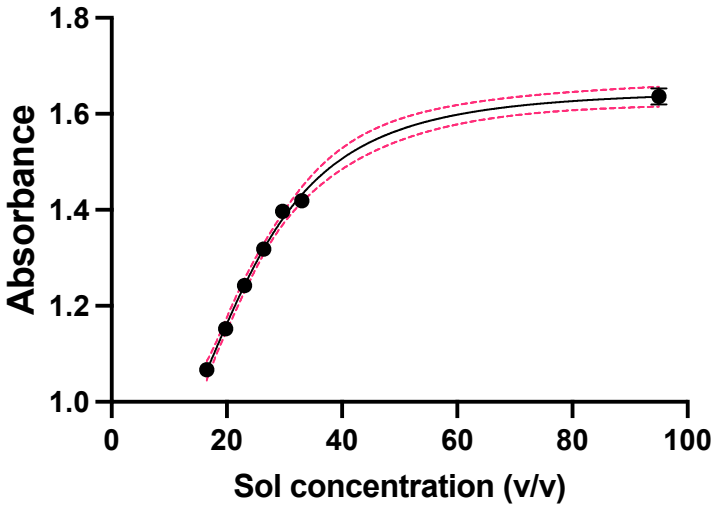

Figure 4.2: The measured absorbance of 100μl hydroxyapatite sol of various concentrations from 16.5% to 95% at 375nm. Line interpolated with 95% confidence interval bands (red). The measured absorbance increases proportionally with concentration until a limit of 33%, where increases in concentration produce increasing smaller increases in measured absorbance. Error Bars = Standard Error of Mean (SEM).

treated HA sol for the first 5 hours of treatment. This is then followed by subsequent increases in absorbance every hour onwards. At the 8-hour time point 0.125M treated HA sol shows no significant difference in absorbance to 0.25M treated sol.

4.3.3 Measuring the pH and absorbance changes that occur during hydroxyapatite sol demineralisation by HMP

There is a clear disparity in the results between hydroxyapatite treated with 0.125M HMP and that treated with 0.25, 0.5 or 1M HMP. It is therefore necessary to determine the factors responsible for this behaviour, for example whether it is due to the pH changes that occur during the reaction, so that this phenomena can be avoided in the desired application.

At the greater volume of 10 ml (Figure 4.4) the same trend in absorbance is replicated once more. A correlation analysis between pH and absorbance over the first 15 hours reveals a strong correlation ($r = -0.8318$ (Pearson's), $p = 8.681e\text{-}007$) between pH and absorbance. When compared to the corresponding pH readings, it is shown that as the demineralisation progresses and absorbance falls, the pH of the HMP/HA sol mixture increases. Where absorbance reaches a minimum of 1.026 (±0.122) at 420 minutes, the pH reaches a maximum of 6.55 at 480 minutes. However, this correlation is not maintained and as the absorbance then increases from 1.026 to 1.825 over the next 15 hours (hours 9 to 23), the pH only drops by 0.2. The absorbance is then maintained, and the pH slowly falls to 6.44 by the final reading at 72 hours.

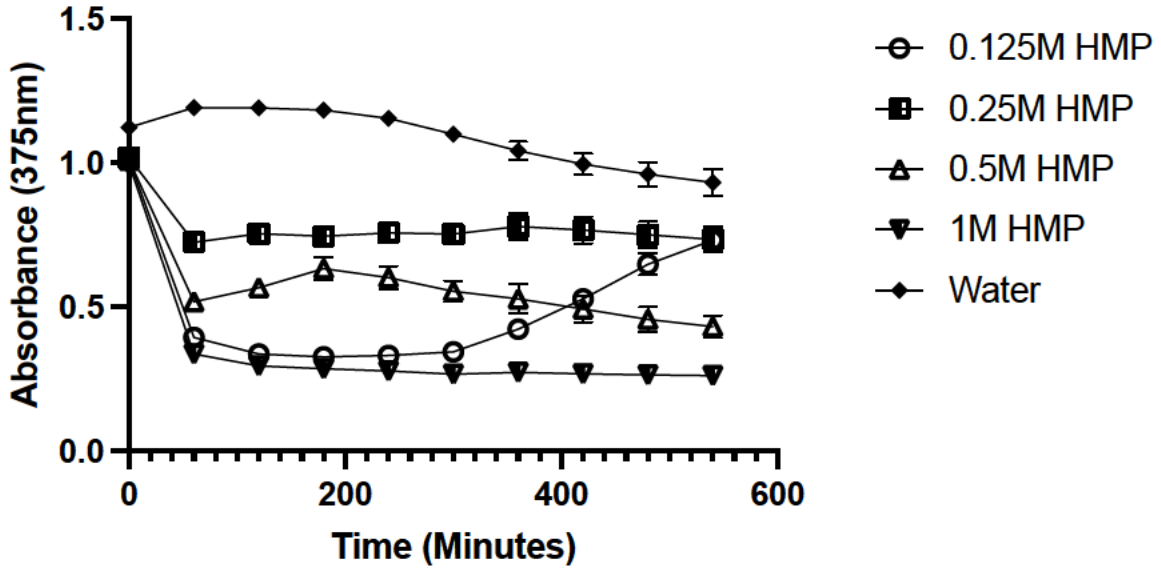

Figure 4.3: the measured absorbance at 375nm over time of 50µl hydroxyapatite sol treated with 50µl 0.25M, 0.5M, 1M and 2M sodium hexametaphosphate (giving a final concentration of 0.125M, 0.25M, 0.5M and 1M HMP in the combined solution). The 1M and 0.125M groups both show rapid decreases in absorbance. In 0.125M, this is followed by a subsequent increase. The 0.5M and 0.25M groups show a more steady but consistent decline in absorbance from baseline. Within and between group comparisons at each timepoint were performed using a 2way ANOVA with multiple comparisons. All HMP groups show significant demineralisation in the first 60 minutes ($p<0.0001$). The water (control) group shows a small decrease from baseline. N = 44. Error bars = SEM

4.3.4 Measuring the effect of HA sol concentration on demineralisation

To assess whether the 0.125M HMP/HA reaction is due to the ration of HMP to HA, the assessment was repeated using higher concentrations of HA. When the concentration of the hydroxyapatite sol is increased (Figure 4.5) the 0.125M HMP treatment still elicits the same response – rapid decreases followed by increases in absorbance. However, as the hydroxyapatite sol concentration increases, the time taken to reach the minimum absorbance (maximum demineralisation; the data points highlighted in red) - increases.

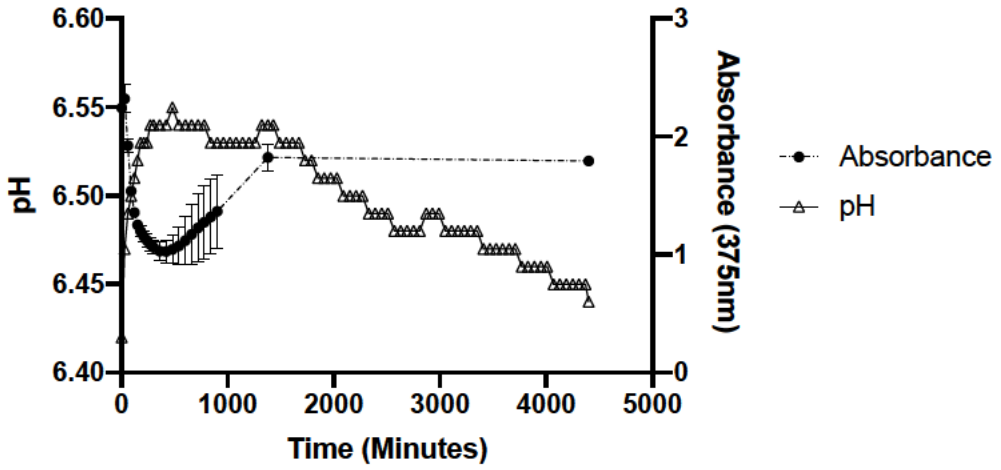

Figure 4.4: The measured pH and absorbance (375nm) over time (4400 minutes) of hydroxyapatite sol treated with 0.125M HMP (10ml). Pearson correlation analysis shows a strong correlation (r = -0.8318, p = 8.681e-007) between pH and absorbance which is reflected in the readings for the first 15 hours. n = 3. Error bars = Standard Deviation

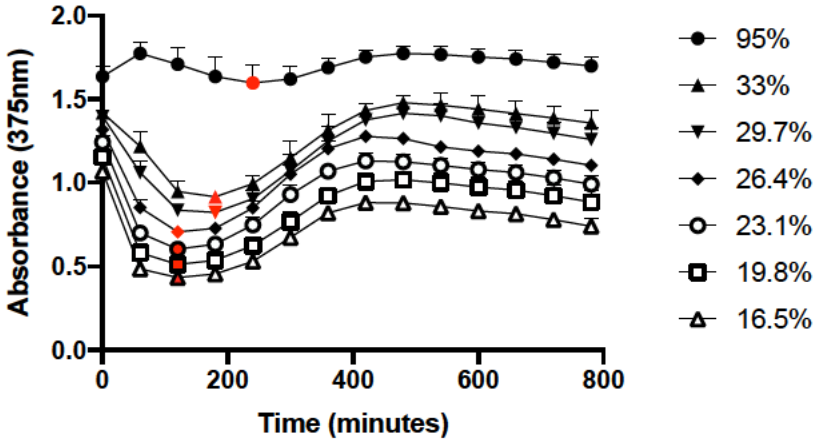

Figure 4.5: the measured absorbance over time of 100µl various concentrations of hydroxyapatite/water sol treated with 0.125M HMP (final concentration) n=12. The minimum absorbance value for each group is highlighted in red. Each HA concentration showed the same trend, an initial decrease in absorbance followed by an increase. As HA concentration increases, the time at which the minimum absorbance is reached increases. Error bars = Standard Deviation

4.3.5 X-Ray Diffraction analysis (XRD)

The reactions between 0.125M HMP and HA appear to show the precipitation of a solid after an initial dissolution. To understand the mechanisms at work, it is necessary to determine what is being reformed through XRD analysis – in particular whether it is a failed dissolution of HA. The XRD analysis revealed several peaks within the precipitate sample, the strongest at 17, and with others at 20, 26, 29, 29 and 34 (Figure 4.6). The diffraction pattern did not match that which would be expected from hydroxyapatite, which would present with a strong peak at 32, and it is unlikely that hydroxyapatite had reformed or reprecipitated in the reaction between 0.125M HMP and the nanocrystalline HA.

4.3.6 Measuring the effect of the pH of HMP on hydroxyapatite sol demineralisation

Eyedrops are commonly formulated to be pH neutral, mimicking the pH expected of the tear film and to avoid damage to the ocular tissues. In certain circumstances, the therapeutic benefits of an acidic or alkaline formulation may outweigh the risks, however where possible a neutral formulation should be the aim. It is therefore necessary to assess whether neutralised HMP solutions would provide the necessary therapeutic benefit.

Baseline absorbance was recorded at 1.435 (±0.012) (Figure 4.7). All treatment groups showed demineralisation in that in each there was a significant reduction ($p<0.0001$) in absorbance - from baseline to 0.471 (±0.017, 0.5M HMP), 1.082 (±0.011, 0.5M HMP - pH7), 0.965 (±0.010, 0.25M HMP) and 1.171 (±0.012, 0.25M HMP – pH 7) respectively after 240 minutes of treatment.

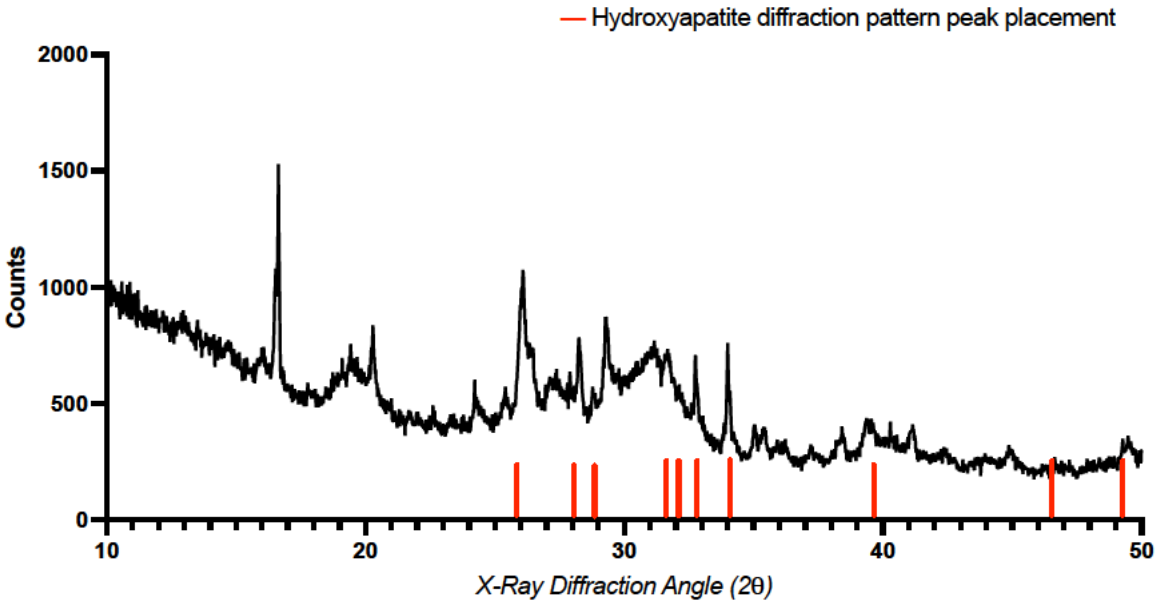

Figure 4.6: The measure X-Ray Diffraction Angle (2θ) versus the intensity of the precipitate formed in the later stages of the reaction between hydroxyapatite sol and 0.125M HMP. Red lines mark where defining peaks would be expected for an hydroxyapatite diffraction pattern.

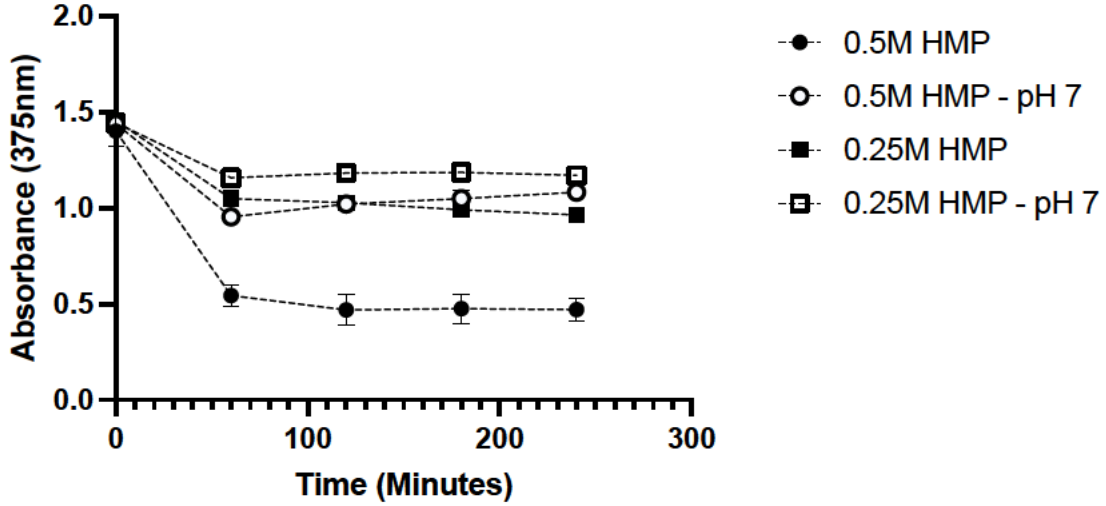

Figure 4.7: the measured absorbance (375nm) over time (0-240 minutes) of 50µl hydroxyapatite sol treated with 50µl 1M HMP, 1M HMP – pH 7, 0.5M HMP and 0.5M HMP – ph 7. Demineralisation over time and between treatment groups was compared using a 2way ANOVA with multiple comparisons. n=12. Error bars = Standard Deviation. Increases in pH lead to smaller reductions in absorbance at the same concentration of HMP.

As in the previous tests, the greatest single reduction in absorbance was in the first 60 minutes. Both non-neutralised HMP treatment groups showed significantly greater demineralisation than the same concentration of HMP at pH 7 at all time points ($p<0.0001$). There was no significant difference between 0.25M HMP and 0.5M HMP – pH7.

4.3.7 Measuring the effect of temperature on Hydroxyapatite sol demineralisation by HMP

The surface of the eye, although cooler than core body temperature at 32°C, will in most instances be warmer than room temperature (~20°C). It is therefore necessary to determine that the temperature of the eye will not inhibit the action of HMP, reducing the therapeutic benefits of the treatment.

From a baseline absorbance of 1.113 (±0.037), within 1 hour of treatment the hydroxyapatite sol in the group treated at 5 °C showed no significant demineralisation, with an absorbance of 1.094 (±0.009) (Figure 4.8). Treatment groups from 20°C and above all showed statistically significant reductions in absorbance from baseline within one hour of treatment ($p<0.0001$), with mean absorbance readings of 0.976 (±0.019, 20 °C), 0.536 (±0.004, 37.5 °C), 0.594 (±0.014, 50 °C). The increase in demineralisation between 20 °C and 37.5 °C was also significant ($p<0.0001$), but there was no significant difference between groups treated at 37.5 °C and 50 °C.

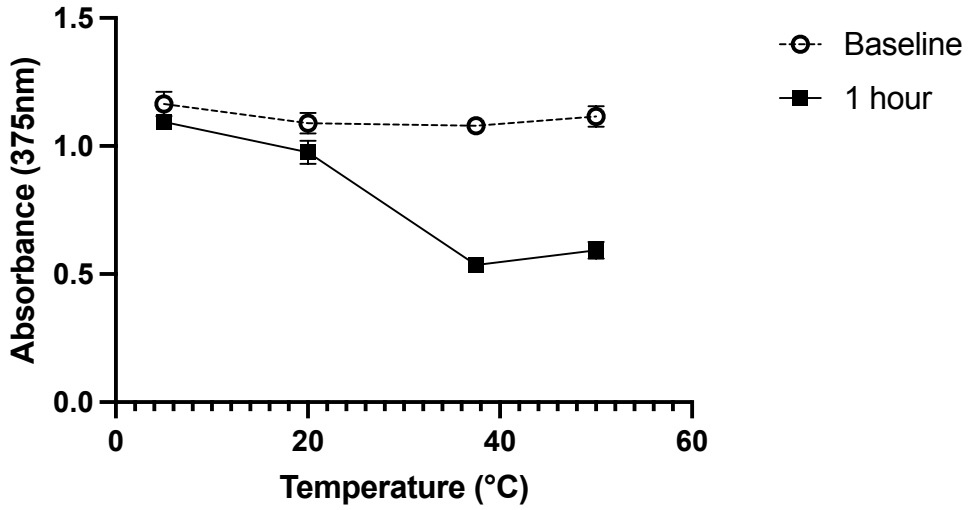

Figure 4.8: the measured absorbance (375nm) of 100µl hydroxyapatite sol treated with 0.5M HMP at 5°C, 20°C, 37.5°C and 50°C. Measurements taken at baseline (pre-treatment) and 1 hour. N = 6. Error bars = Standard Deviation. Between and within group comparisons were completed with a 2-way ANOVA. At lower temperatures a smaller reduction in absorbance occurs than that at higher temperatures.

4.3.8 Assessing of the affinity of HMP at various concentrations for forming precipitates with Magnesium and Calcium ions

The difference in behaviour of 0.125M HMP in comparison to 0.25M, 0.5M and 1M HMP brings into question whether at different concentrations, it is the affinity of the HMP solutions for calcium that is changing, and whether these differences are replicated with other metal ions such as magnesium. Magnesium forms insoluble precipitates with phosphate, which should be measurable through absorbance in the same way hydroxyapatite has been measured. Short-chain polyphosphates are also said to form insoluble precipitates with calcium ions, which again should be measurable in this way.

When the cumulative absorbance across the timepoints for each concentration of HMP is considered (Figure 4.9), 0.125M HMP and 0.25M HMP consistently show higher absorbance readings than 0.5M and 1M HMP on the addition of $CaCl_2$ and $MgCl_2$, and when both are present together. This suggests that 0.125M HMP and 0.25M HMP form a greater concentration of insoluble precipitates than 0.5M or 1M HMP. In the case of $CaCl_2$ it is 0.125M HMP that shows a marginally higher cumulative absorbance, and with $MgCl_2$ or with both metal-chlorides, it is 0.25M HMP that presents a higher cumulative absorbance. This suggests differing affinities for magnesium at different HMP concentrations.

When considering the absorbance over time, in each case within the first 10 minutes the absorbance of all concentrations of HMP tested increased with the addition of each metal-chloride solution. In the cases of $CaCl_2$ and $MgCl_2$ alone, the greatest increase at 10 minutes was exhibited by 1M HMP. However, after 1 hour and onwards, it

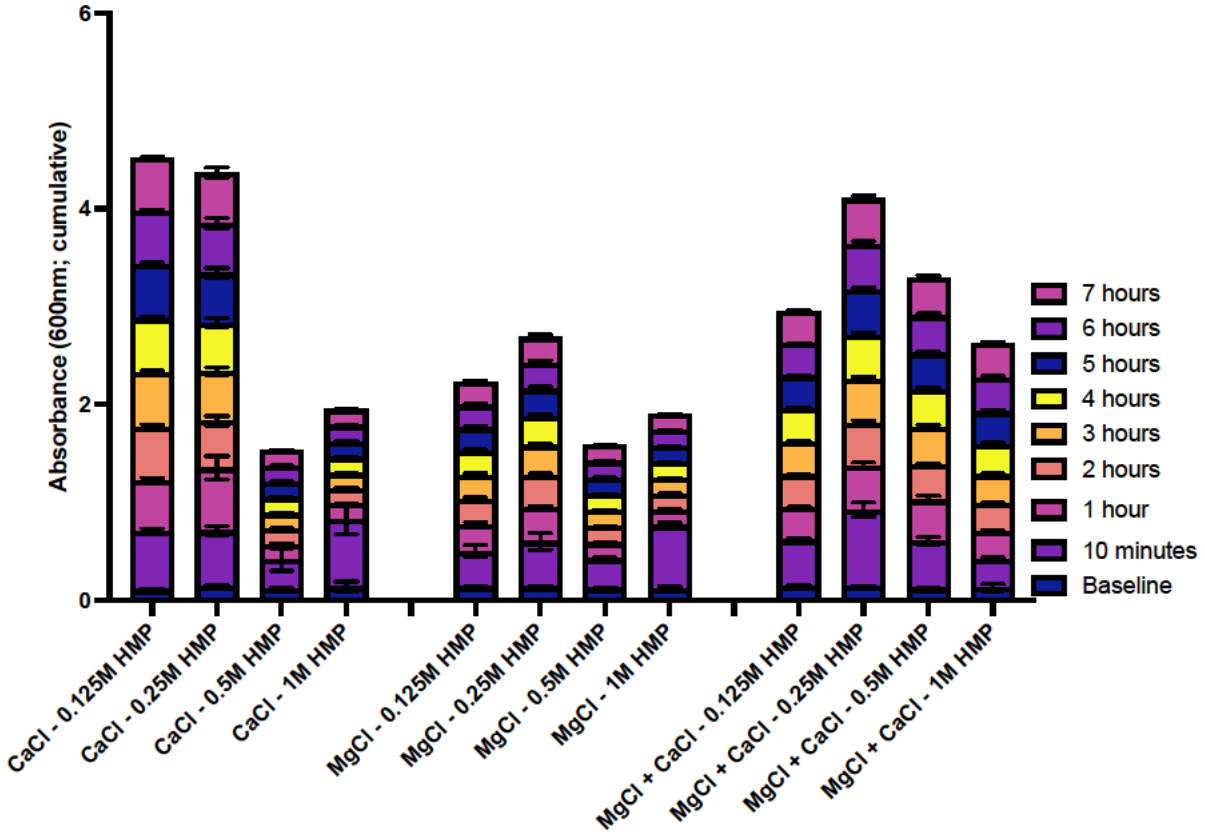

Figure 4.9: the measured absorbance (600nm) of HMP at concentrations of 0.125M, 0.25M, 0.5M and 1M with equal volume 1M $CaCl_2$, 1M $MgCl_2$ or 1M $MgCl_2$,$CaCl_2$, at time points up to 7 hours. Total reaction volume = 100µl n=6. Error bars = SEM. The cumulative absorbance readings over time reveal a higher absorbance for 0.125 and 0.25M concentrations of HMP with each metal-chloride additive.

is only 0.125M HMP and 0.25M HMP that continue to show increased absorbance readings when compared to baseline. Where both were both $CaCl_2$ and $MgCl_2$ are present, 0.25M HMP shows the highest mean absorbance consistently from 10 minutes onwards. Where the absorbance readings of the 0.5M and 1M groups returned to levels close to baseline after 10 minutes on the addition of $CaCl_2$ or $MgCl_2$ alone, when both $CaCl_2$ and $MgCl_2$ are present the absorbance remained elevated to levels comparable to those of 0.125M. 0.5M was consistently presenting the second highest mean absorbance readings after 0.25M, then 0.125M, then 1M.

4.4 Discussion

This assessment of the demineralisation of hydroxyapatite by sodium hexametaphosphate differs from previous investigations. Existing studies have largely focused on heat treated hydroxyapatite pellets, which are more relevant for potential applications concerning bone, dentistry or industrial ceramics processing but different to the precipitated mineral forming in the corneas of patients with band keratopathy [277, 297]. These previous assessments have also investigated the effects of HMP over munch longer time periods (days and weeks), compared to those of interest in this study, which is concerned with treatment times of up to 60 minutes [271, 273, 274, 277-279, 292]. The method presented here uses precipitated nanocrystalline hydroxyapatite which has not been heat treated, mimicking what we would expect to see in cases of calcific band keratopathy, where the mineral has most likely formed due to an Ca/P ionic imbalance. It is also worth noting that the range of concentrations of sodium HMP tested here are higher than those tested in other investigations, which tested a maximum of 0.2M HMP for biomedical applications [271, 272].

i) Absorbance as a measure of hydroxyapatite sol dissolution

The initial assessment of the relevance of absorbance as a measure of hydroxyapatite sol concentration (Figure 4.1) confirms the results of previous investigations using similar methods [271, 272]. This method is of particular relevance to the context considered in this work, as the aim for the hexametaphosphate treatment is to restore optical transparency to the cornea through the demineralisation of the hydroxyapatite mineral which has formed. This assessment found a limit to the proportional relationship between increases in absorbance and increases in hydroxyapatite sol concentration at 33%v/v HA sol, which corresponded to absorbance readings above

1.4 at 375nm. All further tests were therefore performed with HA sol of a concentration of 15%v/v with a starting absorbance of ~1.0.

ii) The influence of HMP concentration of HA sol dissolution

When assessing the concentration of HMP which most effectively demineralised nano-HA, all treatment concentrations of HMP tested yielded their greatest decrease in absorbance in the first 60 minutes of treatment compared to the subsequent 60-minute treatment intervals taken as individual changes. In fact, changes beyond the 1-hour mark appear to reflect evaporation of the liquid, as shown in the water control, rather than what is necessarily further demineralisation. This is of relevance to the desired application, which would see HMP being delivered topically to the ocular surface, as there is a brief treatment window in which topical treatments need to be effective. Eye drops can stay on the surface of the eye for between 10 minutes and a maximum of 6 hours depending on the properties of the drop. This can vary due to viscosity and mucoadhesion, but there is a normal assumed treatment window of around 1 hour [31, 59, 64, 66, 303]. It is therefore of considerable benefit that HMP can cause significant demineralisation within an hour. This will also be beneficial to a potential repeated dosing regimen, where each application yields the best possible action within its given limited window of bioavailability and activity. The amount and density of hydroxyapatite which has formed in the eye will differ between each patient, meaning the number of doses required to see an improvement in symptoms, or complete relief, may vary from patient to patient. The most effective treatment design would allow for this potential variability, allowing for as frequent dosage as is required whilst maintaining agreeable levels of cytotoxicity.

Each of the concentrations of HMP assessed for demineralisation of hydroxyapatite sol (0.125M – 1M) show a significant difference in comparison to each other concentration, however the lowest concentration – 0.125M – did not follow the trend of the higher concentration treatments (0.25M – 1M). In the case of 0.125M there appears to be a precipitation of a new mineral, after the first initial phase of demineralisation. This process is observed through an increase in absorbance over the latter hours of the test (Figures 4.3, 4.4 and 4.5). When this was assessed at a larger volume – 10 ml (Figure 4.4) – the changes in absorbance were mirrored in rises and falls in pH throughout the first demineralisation and reprecipitation phase – reprecipitation referring to the precipitation of what is likely a calcium phosphate but not necessarily hydroxyapatite. After this reprecipitation, the precipitated substance appears to remain stable, with no changes in absorbance whilst the pH then decreases. This pH decrease in itself is therefore not enough to trigger a second dissolution phase. It is also worth noting that despite reprecipitation occurring, the absorbance does not return to baseline levels.

iii) Examining the formation of a second precipitate with 0.125M HMP

When the reprecipitated substance was analysed using XRD, it did not present with the characteristic peaks of hydroxyapatite. Due to the ions available in the sol and the aqueous polyphosphate solution, the precipitate is almost certainly a calcium phosphate. However, the XRD shows that it is not hydroxyapatite which has been reformed, but a different water-insoluble calcium phosphate. There is the possibility of this representing a coacervation, however these have previously been formed through the addition of free calcium ions to polyphosphate solutions [289]. In this scenario, calcium has been added in the form of hydroxyapatite rather than as free ions. The

absorbance readings suggest that the hydroxyapatite is initially dissolved, which may release free calcium ions, as it would be expected that the polyphosphate chains form soluble complexes with the calcium they chelate [304]. An alternate possibility is the formation of insoluble calcium phosphates with a proportion of the polyphosphate chains available in HMP. It is known that shorter chain polyphosphates form insoluble complexes with calcium. This may not have been exhibited in the higher concentrations of HMP as there would be a higher availability of each of the longer chain lengths present, which have a higher affinity for calcium and form water-soluble precipitates. Therefore, it is possible that at a concentration of 0.125M, the longer polyP chains become saturated and this allows the shorter units to form complexes, whereas at the higher concentrations of HMP, saturation is not reached. It would therefore also stand to reason why increasing the HA concentration did not change this behaviour, as saturation would be reached in each instance (figure 4.5). This also suggests that the dictating factor is HMP concentration alone. At 95% HA sol concentration (Figure 4.5), the changes in absorbance are much less pronounced, however this is close to the maximum absorbance in which slight changes in demineralisation are translated through changes in absorbance and therefore detectable with this technique. However, this does not necessarily explain why 0.125M HMP appears to demineralise so rapidly in the first phase compared to 0.25M HMP and 0.5M HMP. If the proportion of chain lengths in each HMP solution stays the same for each concentration, and only the relative quantity increases with increasing concentration, it would be expected that the longer chain phosphates which have a high affinity for calcium should increase proportionally to the concentration of the HA sol, which remains the same for each test. This should mean that 0.25M and 0.5M HMP demineralise faster than 0.125M, and do not produce the precipitate as the same saturation is not reached.

When the simultaneous pH measurements are then assessed, it can be seen that the pH of the solution increases as the demineralisation progresses, most likely corresponding with the formation of Ca-P complexes which neutralise the HMP acidic end group. However, as the reprecipitation occurs – causing an increase in absorbance – the pH remains fairly stable. The subsequent decrease in pH is much more gradual than the primary increase, and no longer correlates with the absorbance readings. It is possible that the pH change represented allows the formation of this second precipitate, however it would be expected that as the pH then drops, the stability of the precipitate would be affected, and a further decrease in absorbance would be seen. It is also worth noting that although there are pH changes, they are not dramatic, remaining within a 0.15 range.

iv) The influence of pH on hydroxyapatite dissolution

With regards to the assessment of the influence of pH on the ability of HMP to demineralise HA sol (Figure 4.7), the results presented here are in line with those previously reported by Eisentstein et al. [271], showing that adjusting HMP to a pH of 7 reduces but does not prevent demineralisation of hydroxyapatite. It is generally advised that topical ocular treatments should aim for a neutral pH to best match the natural pH of the tear film. This helps to avoid side-affects such as dry eye disease or general ocular irritation [103, 305]. However, when considering whether neutralisation would be necessary in a topical treatment for band keratopathy, faster action of the treatment may be prioritised should the ocular toxicity of non-neutralised HMP be tolerable. If adjusting the pH allows for the HMP to be delivered in a way that enhances the treatment to a greater degree than that of maintaining the lower pH, for example in

combination with delivery in an agent that prolongs contact time on the ocular surface, it is beneficial to know that demineralisation is still achievable at a neutral pH. In each case, the benefits can be weighed. It is also of benefit that the optimum temperature for demineralisation amongst those assessed was found to be 37.5°C – representing normal body temperature and close to the temperature of the cornea, which is usually slightly cooler at between 32°C and 34°C [306].

v) Assessing whether each concentration of HMP reacts differently in the presence of metal-chlorides

When comparing the precipitates formed by HMP with $CaCl_2$ and $MgCl_2$ solutions, the 1M $CaCl_2$ assessment saw increases in absorbance at 0.125M and 0.25M HMP which were maintained across the entirety of the assessment. 0.5M and 1M HMP initially presented an increase in absorbance, but this was quickly lost, suggesting any precipitate redissolved and was unstable. The hydroxyapatite demineralisation assessments do not suggest that the ability of 0.5M or 1M HMP to chelate and complex calcium is impaired in comparison to that of 0.125M or 0.25M HMP – in fact suggesting the opposite. Therefore, 0.5M and 1M HMP may be forming water-soluble complexes with the calcium ions in the $CaCl_2$ solution, where 0.25M and 0.125M appear to be forming water-insoluble complexes. This adds weight to the suggestion that the increase in absorbance seen by 0.125M HMP-treated hydroxyapatite (after the initial decrease), could be due to the formation of such insoluble complexes.

Where $MgCl_2$ Is considered, again all concentrations of HMP appear to initially form insoluble magnesium complexes, represented as an increase in absorbance. However, the increase in absorbance is only maintained in 0.125M and 0.25M HMP,

and to a greater degree in the 0.25M HMP. Unlike calcium phosphates, magnesium phosphates are insoluble regardless of chain length. However, as stated previously, shorter chain polyphosphates appear to have a greater affinity for magnesium ions than longer chain polyphosphates. This assessment would therefore appear to further suggest that at lower HMP concentrations there may be a higher proportion of shorter phosphate chain lengths.

Where both Mg^{2+} and Ca^{2+} ions are available in equal 1M concentrations in solution, all concentrations of HMP show an increase in absorbance. In contrast to when each metal ion is singularly available, all HMP concentrations maintain this higher absorbance, suggesting each has formed stable precipitates. The increase in absorbance was again highest in 0.25M HMP, which was also higher than the other groups. The 1M, 0.5M and 0.125M groups showed minimal differences between them. This again suggests that at 0.25M there is a greater concentration of insoluble precipitates being formed, however there is no way to distinguish between whether Ca-polyP or Mg-polyP is being formed in any of the groups within this test. It is unclear why, when both ions are present in solution with the HMP, 0.5M and 1M form stable precipitates, but when only one ion is present they do not. It may be that the combination of ions allows for different complexes and arrangements to be formed, or that with double the total concentration of divalent ions present, a saturation is reached.

Sodium hexametaphosphate is proposed to dissolve in water to form a range of linear and cyclic polyphosphate anions with a range of lengths. Dirheimer et al [307] found that the largest fraction found in solutions of sodium hexametaphosphate (Graham's salt) were high molecular weight polyphosphates with a chain length >10, with smaller

fractions of smaller linear polyphosphates, tetrapolyphosphate, cyclotriphosphate, tripolyphosphate and pyrophosphate, respectively. A more recent study replicated these findings, showing that at 20°C a 0.5% solution of HMP was found to contain ~80% long chain (D>6) phosphates, ~15% trimetaphosphate and small fractions of orthophosphate, pyrophosphate and tetraphosphate [267]. It is claimed that shorter, linear polyphosphate ions are more effective in sequestering Mg^{2+} than Ca^{2+}, whereas the 'glassy phosphates', in which HMP is classed, are more effective at chelating Ca^{2+} than Mg^{2+} [286, 288]. This is supported by evidence from a recent study where it was found that polyphosphate solutions which contained a higher fraction of short chain length polyphosphates including Sodium hexametaphosphate, after heat treatment at 120°C, were less effective at chelating calcium ions than those with longer polyphosphate chains [267]. This has been investigated due to being of interest for meat preservation, as maintaining the levels of both calcium and magnesium is essential for maintaining the quality of the food and preventing mould growth [258, 267, 287]. When HMP underwent heat treatment and hydrolysis in the presence of calcium ions, a greater degree of trimetaphosphate was produced than with heat treatment alone [267].

It is possible, although this is a highly tentative suggestion, that at different concentrations of HMP the complexes the polyphosphates are encouraged to form in the presence of both calcium and magnesium ions differ. At a concentration of 0.25M HMP, where the affinity for calcium appears to be lower according to the demineralisation data, the affinity for magnesium may be higher. However, there is little evidence to suggest that the longer polyphosphates which make up the majority

of those present in HMP, and have a high affinity for calcium, are hydrolysed at low temperatures or without additional acidification.

vi) Summary

The aim of the work presented in this chapter is to establish whether sodium hexametaphosphate can effectively demineralise and dissolve hydroxyapatite mineral within the time-period associated with the ocular retention of an eye drop. Further to this, it has been necessary to establish the concentrations of HMP at which this effect can be achieved and whether the pH of the solution or the temperature at which the reaction takes place could hinder the potential therapeutic efficacy. Concentrations above 0.25M HMP were found to provide consistent demineralisation of hydroxyapatite sol within one hour of treatment. Although the same was true for 0.125M HMP, using this concentration created unexpected precipitation of mineral at later timepoints, which could limit therapeutic efficacy in practice or cause secondary mineralisation. It therefore stands to reason to use a concentration of HMP at 0.25M or above when formulating a potential treatment for band keratopathy. The efficacy of HMP at demineralising HA was limited by neutralising the pH of the solution. If the toxicity of the formulation allows, this should be avoided to see the maximum therapeutic benefit. The assumed ocular surface temperature of 32°C should enable successful demineralisation by HMP, other factors allowing.

5.

ASSESSING THE CORNEAL TOXICITY OF SODIUM HEXAMETAPHOSPHATE

5.1 General introduction

There are many possible mechanisms through which a treatment compound can be cytotoxic. The substance may damage the cellular membrane, interfere with mitochondrial metabolism, prevent protein synthesis or bind to cellular components, for example [308-310]. Cytotoxicity can be investigated using cellular monolayers in culture, a method which has become preferred due to the widely adopted aim to reduce the suffering and use of animals in biomedical research. *In vitro* cytotoxicity assays examine the effect of treatments on cell metabolism, adherence and structure. More specifically, they measure cell functions such as cell membrane permeability, enzyme activity and production, cellular adherence, ATP synthesis and cellular uptake of proteins [308]. Many assays work on the basis of colorimetry, fluorometry, luminosity or dye exclusion. Lactate dehydrogenase (LDH) and 3-(4,5-dimethylthiazol-2-yl)-2,5-diphenyl tetrazolium bromide) (MTT) reduction assays are common methods to provide preliminary evidence of the toxicity of a treatment, as is propidium iodide (dye exclusion) staining and imaging. Histopathology provides an idea of the effect of a treatment on a tissue as a whole, allowing the investigation of structural defects or the detection, through anti-body staining, of specific proteins.

The current procedure deployed to treat BK involves the removal of the epithelial layer of the cornea and the dissolution of the mineral build-up using EDTA of concentrations between 0.75% and 3.75% [10, 21, 311, 312]. EDTA has previously been shown to affect the health of the corneal epithelium, leading to additional discomfort and secondary ocular conditions, such as superficial punctate keratitis and lower sensory nerve density [217].

Sodium hexametaphosphate is commonly considered ‘safe’ for ingestion in low doses and is used in food production as a preservative [258, 286, 287, 313]. It is expected that HMP is hydrolysed into phosphoric acid in the intestines when ingested [281]. Early investigations of HMP examined its toxicity towards pathogens, and although it cannot be considered anti-bacterial or anti-microbial it is known for sensitising bacterial and fungal cells to anti-microbial agents such as silver nano-particles [314]. When examining the possibility of using these sensitising affects to target cancer cells, Oćwieja and Barbasz [315] found HMP to increase the ability of silver nano-particles to target and kill Histiocytic lymphoma (U-937) and human promyelocytic (HL-60) cells. They also found that HMP alone, at a concentration of 120mgL^{1} (0.196mM), decreases the cell viability of both cell lines, significantly more so the HL-60 line. This was investigated through LDH, MTT and lipid peroxidation (MDA) assays, with cytotoxicity increasing with HMP concentration up to the greatest test concentration, 120mgL^{1} [315]. The differences between the cell lines were postulated to be a result of differences in the structure of the cellular membranes. In contrast, when examining the influence of 0.05mM of HMP on the proliferation and migration of human dental pulp cells, Bae et al. found that HMP is favourable for the growth and differentiation of the cells [275]. This mirrors results from the assessment of the proliferation of human dermal fibroblasts treated with inorganic polyphosphates with a chain length of 65 phosphate units (representing a proportion of what has previously been found in Sodium hexametaphosphate/Graham’s salt) at 1.34mM [307, 316]. Inorganic Polyphosphates, the group of molecules which includes those present in sodium hexametaphosphate, have been shown in additional studies to have varying effects on different cell lines. In peripheral blood plasma cells and myeloma cells, the presence of polyP inhibited immunoglobulin secretion and triggered apoptosis. These effects

were not seen, however, in peripheral blood mononuclear cells, T cells, B cells, and non-lymphoid cell lines [265].

Understanding whether HMP is cytotoxic, or in other ways critically disruptive to the ocular environment, is a key milestone in preparing a formulation for therapeutic purposes. A degree of cytotoxicity is tolerable when considered against any therapeutic benefits, however a high level of toxicity would not be acceptable due to potential repercussions for the health of the cornea, and ultimately – the sight of the patient. It is therefore necessary to determine as best as possible the toxicity of demineralising concentrations of HMP towards ocular cell lines and tissues over a relevant time (treatment) period.

5.2 Materials and Methods

5.2.1 Growing primary cultures: Keratocytes

Corneal keratocytes are fast growing cells that reside in the corneal stroma, the layer of the cornea most commonly affected by hydroxyapatite build up in band keratopathy. Corneal keratocytes were cultured using an adaptation of the protocol published by Ramke et al [317]. This protocol has been verified as successfully culturing viable primary corneal cells from human corneal tissue in previous assessments, which examined the cells $CK3^{+/}$, $vimentin^{+/}$ and $5B5^{+/}$ stains [318]. Corneas from porcine eyes were prepared as previously described (Chapter 3, Section 3.9). The epithelial and endothelial corneal layers were removed from the washed corneas with scissors, and the stromal tissue was chopped into 1-2mm pieces. The tissue was placed in culture in sterile 60mm petri dishes with 15ml medium consisting of RPMI 1640 + 1% penicillin/streptomycin + 10% foetal bovine serum + 1% gentamycin + 1% amphotericin B (RPMI, PenStrep, FBS and gentamycin from Sigma Aldrich, UK; amphotericin B from Fisher Scientific, UK). The cultures were incubated at 37°C with 5% CO_2. After 48 hours 5ml of media was added. After 72 hours, the media was changed. The media was changed every 48 hours until cells were 50% confluent. After 5 days any non-adherent tissue was removed. Once 50% confluency was reached, cells were passaged and transferred into sterile, tissue culture coated T75 flasks at a density of 5000 cells/cm^2 to continue proliferating. The media was replaced every 2 days. When 70% confluent the cells were visually characterised to confirm the morphology was typical of healthy corneal keratocytes and the cells were seeded into assay plates for testing (Chapter 3, Section 3.10). Cells were imaged using a brightfield microscope and microscope camera (Moticam).

5.2.2 3-(4,5-dimethylthiazol-2-yl)-2,5-diphenyltetrazolium bromide (MTT) metabolism assay of porcine corneal keratocyte cell monolayers

3-(4,5-dimethylthiazol-2-yl)-2,5-diphenyltetrazolium bromide (MTT) metabolism assays provide an indication of cell health after treatment with a test substance. Viable cells convert the MTT dye into water-insoluble formazan, and the levels of formazan in each well can be measured to compare cell viability in each group. MTT assays were therefore performed to assess the viability of the corneal keratocyte cells after treatment with HMP. Cells and treatment media were prepared as previously described (Chapter 3, Section 3.10). For the MTT assays, the treatment media was removed from the wells as the end of the treatment period and replaced with 100μl fresh serum and phenol-free media. 1ml of MTT solution (Vybrant, ThermoFisher UK) was prepared with 1ml of sterile PBS and 5mg of desiccated MTT and vortexed to mix. 10μl 5mg/ml 3-(4,5-dimethylthiazol-2-yl)-2,5-diphenyltetrazolium bromide (MTT) solution was added to each 100μl of fresh media. The plates were returned to the incubator for a further 4 hours. After the incubation period, 85μl of the MTT containing media was removed and 50μl DMSO (Sigma Aldrich, UK) added to solubilize the formazan, ensuring thorough mixing. The plate was then incubated for a further 10 minutes before the absorbance was read at 540nm. The background absorbance from the media only wells was removed from the final readings. Treatment times of 4 hours and 6 hours were included such that the toxicity test reflect the extremes of the desired application, i.e. beyond the maximum residence time expected for an eye drop. The final absorbance readings for each treatment group were compared to the untreated control, to provide a % cell viability value.

5.2.3 Propidium Iodide assay

Cellular assay plates were prepared as previously described (Chapter 3, Section 3.10). The treatment media was removed from the treated porcine corneal keratocyte cells and replaced with media containing 0.02mg/ml propidium iodide (PI; ThermoFisher UK). Cells were incubated with propidium iodide for 10 minutes before being washed with sterile PBS. The media was then replaced with phenol and serum free media and cells were then imaged with an EVOS 5000 microscope. Cells were counted using the EVOS automatic cell count function, analysis the Texas Red filtered image.

5.2.4 *Ex-vivo* corneal biopsy assay

To assess the effect of treatments with various chelating agents on the structural integrity of the corneal tissue, an *ex vivo* corneal biopsy treatment assay was performed. Corneas from porcine eyes were prepared as previously described (Chapter 3, Section 3.9). Three 5 mm diameter biopsies were taken from each cornea with a disposable biopsy punch (Steifel) and randomised into each treatment group. The samples were placed with the epithelial layer facing upwards in specialised well inserts (Cellcrown) and placed in a 96-well plate, prepared with fresh 100µl media (HBSS + Penicillin/Streptomycin 1%). The epithelial surface of each corneal sample was then treated with 20µl of the chosen treatment. Treatments included 1M, 0.5M, 0.25M and 0.125M HMP, 2% EDTA and HBSS (control). The samples were incubated at 37°C for 4 hours. This assay was performed 5 times within each treatment group.

After 4 hours, the corneal biopsy samples were removed from the wells and fixed and embedded for cryosectioning. The corneal samples were then sectioned as previously described (Chapter 3, section 3.11) and placed onto positively charged glass slides

and slides from each group were stained with haematoxylin and eosin (H+E) as previously described (Chapter 3, section 3.12) and imaged.

5.2.5 3-(4,5-dimethylthiazol-2-yl)-2,5-diphenyltetrazolium bromide (MTT) assay of corneal tissue biopsies

To assess the viability of corneal tissue treated with HMP and EDTA, an *ex vivo* tissue MTT assay was performed. The tissue metabolism assay was adapted from that used by Erickson-DiRenzo et al [319]. Porcine corneas were prepared as previously described (Chapter 3, Section 3.9). DMEM/F12 media (Gibco) was prepared with HMP or EDTA to the appropriate concentrations and sterile filtered (0.2µm mesh, Corning). 5mm biopsies were taken from the corneas and one sample was placed in each well of a 24 well plate with 750µl of treatment media – 1M HMP, 0.5M HMP, 0.25M HMP, 0.125M HMP, 2% EDTA or DMEM/F12 only. Treatments were performed in triplicate. The plates were incubated at 37°C and 5% CO_2 for the duration of treatment. At the end of the treatment period (4 hours or 24 hours) the treatment media was removed and replaced with 750µl DMEM/F12 only. A recovery test was performed where after 4 hours of treatment, the biopsies remained in DMEM/F12 only for 18 hours before the MTT test was carried out. 75µl of 5mg/ml 3-(4,5-dimethylthiazol-2-yl)-2,5-diphenyltetrazolium bromide (MTT) solution was then added to each well and the plates were incubated at 37°C for a further 4 hours. The MTT solution and media was then removed and replaced with 750µl of Dimethyl Sulfoxide (DMSO) and the biopsies were finely minced. The plates were then wrapped in foil to protect from light and placed on a rotating plate (60rpm) for 1 hour. 100µl DMSO solution was then taken from each well in duplicate and placed in a 96-well plate. The absorbance of each well was read at 540nm.

5.2.6 X-Ray Fluorescence (XRF) analysis of corneal sections

To assess whether XRF could be used to analyse the penetration of HMP into the corneal tissue, 5mm biopsies of porcine corneal tissue were taken and embedded in optimal cutting media (OCT) for cryosectioning as previously described (Chapter 3, section 3.11). Unmounted 20µm sections were taken and assessed using X-Ray Fluorescence as previously described (Chapter 3, section 3.13).

5.2.7 *In vitro* and *ex vivo* cellular Lactate dehydrogenase release assay

Lactate dehydrogenase (LDH) release assays were performed to assess the cytotoxicity of the HMP treatments on the corneal keratocytes. CytoTox 96© non-radioactive assay kits were acquired from Promega, UK. Assay plates for both tissue biopsies and cellular monolayers were prepared as previously described (Chapter 3, General Methods, Section 3.10 and 3.11). For the cellular monolayer assays, a complete cell death group was included which was treated with 10µl 5% polyethylene glycol tert-octylphenyl ether solution for 45 minutes. The LDH measurements were performed by removing 50µl media from each well at the relevant time point and incubating them with the assay reagent (a solution of L-lactic acid (2-hydroxy propionic acid), β-NAD, DMSO, Tris-HCl and polyethylene glycol tert-octylphenyl ether) protected from light for 30 minutes. 50µl 5% acetic acid was then added to stop the reaction and the final absorbance was read at 490nm. The background absorbance from the media was subtracted from all values. Percentage cytotoxicity was calculated as follows:

$$\% \text{ Cytotoxicity} = \frac{Absorbance\ (Treated\ cells)}{Absorbance\ (Complete\ cell\ death)} \times 100$$

A positive control assessment was included to assess the functionality of the assay. Bovine Heart LDH was diluted to a ratio of 1:5000 in PBS + 1% bovine serum albumin. 50µl of the LDH control was added to a 96-well plate, and 50µl of medium containing 1M HMP was then added. HMP-free media was also included as a control. The solution was incubated for 30 minutes and then the absorbance was read at 490nm.

5.2.8 Statistics

Statistical analysis was performed in Prism (Graph Pad). Comparison between the treatment groups for the MTT assay was performed using a mixed-effect analysis with multiple comparisons.

Comparison between treatment groups for the propidium iodide assay was performed using an ordinary one-way ANOVA. Assessment of gaussian distribution showed the HMP treated groups to have normal distribution.

5.3 Results

Previous cytotoxicity assessments of HMP have created an inconclusive picture, with results showing both increased cell proliferation and reduced cell metabolism in different instances, depending on the cell line and concentration of HMP being used [274, 275, 315]. It is therefore necessary to determine the effect of HMP treatment on the health of ocular cells, to indicate whether a topical HMP treatment would be safe to use in cases of band keratopathy.

5.3.1 Keratocyte primary cell cultures

Healthy, rapidly proliferating monocultures of corneal keratocytes were successfully grown using this technique (Figure 5.1). Where tissue became adherent to the bottom of the petri dish, keratocytes would proliferate from this point and grow in dense clusters. The morphology of the PCK cells was consistent with the tightly packed, elongated cuboidal shape expected from keratocytes.

5.3.2 3-(4,5-dimethylthiazol-2-yl)-2,5-diphenyltetrazolium bromide (MTT) metabolism assay of cell monolayers

There are several mechanisms through which a test substance can be toxic to cells. MTT assays can demonstrate whether a test substance is interfering with normal cellular metabolism, either by killing the cells or by interfering with the metabolic pathway (which may ultimately lead to cell death).

In this assay, culture porcine corneal keratocytes were treated with various concentrations of HMP. Water, untreated control and EDTA treated groups were included for comparison.

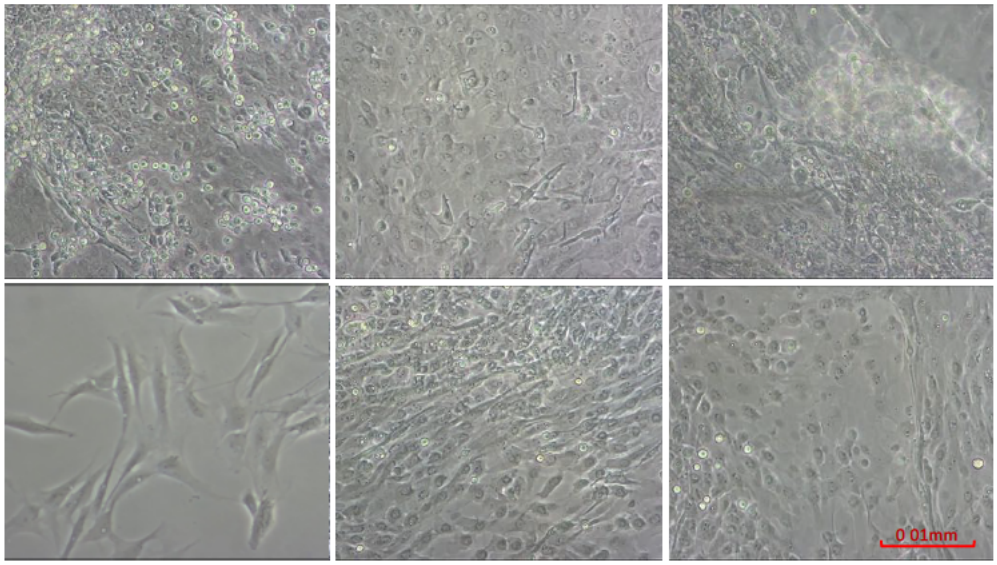

Figure 5.1: Brightfield microscope images of confluent cultured porcine corneal keratocytes in growth media (60mm petri dish, 15ml media). Visual comparison to images available in the literature confirm that the cell presented here share the morphology of corneal keratocytes. Images taken at X20 magnification. Scale bar = 0.01mm.

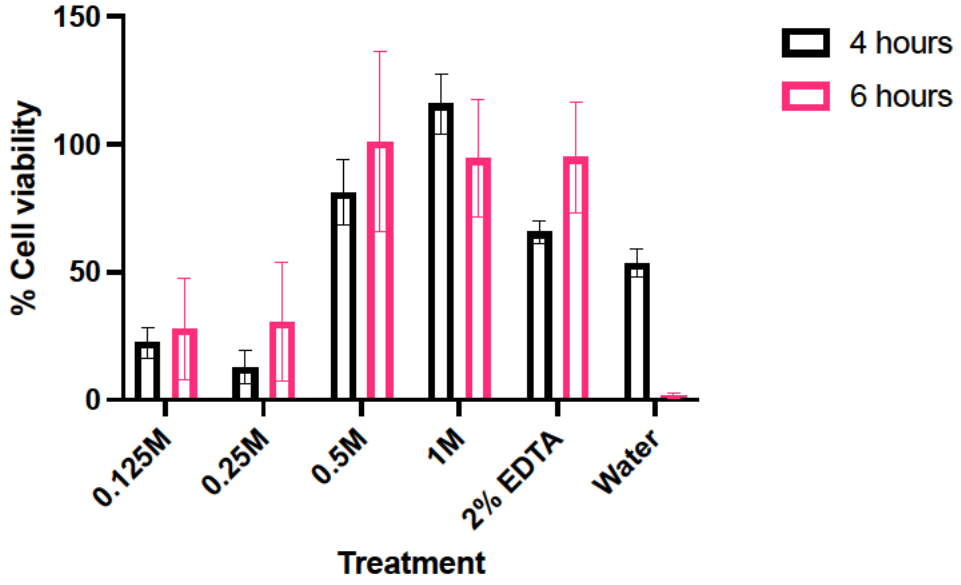

Figure 5.2: The MTT assay results presented as percentage cell viability. % cell viability was calculated against the untreated control group (normal growth media). Each test repeat included 5000 cells in 100μl treatment media. A 2way ANOVA (mixed effects analysis) with multiple comparisons was used to compare treatment groups. The 1M and 0.5M HMP groups show comparable results to the untreated control group. The 0.125M and 0.25M groups are significantly lower (125M HMP vs 1M HMP (p=0.0007) and 0.25M HMP vs 1M HMP (p=0.006)). Error bars = SEM. n=3

When calculated at % cell viability in comparison to the untreated PCK cells, the 1M and 0.5M HMP groups had the highest mean cell viability at 1M: 115%/106% (4 hours/6 hours), 0.5M: 100%/81%. 2% EDTA showed comparable results at 95%/66%. 0.125M HMP and 0.25M presented the lowest cell viability at 22%/27% and 13%/30% respectively (Figure 5.2). When the groups were compared (with the inclusion of both time points), there was a significant difference between 0.125M HMP vs 1M HMP ($p=0.0007$) and 0.25M HMP vs 1M HMP ($p=0.006$), with 1M HMP showing higher calculated % cell viability. 1M HMP was also significantly higher than the water control group, however this difference was associated with the 6-hour treatment and not the 4-hour treatment ($p=0.01$). There were no significant differences between the other treatment groups, however both the 0.5M HMP and 2% EDTA treatment groups showed higher calculated % cell viability than the 0.125 and 0.25M HMP groups.

5.3.3 Propidium Iodide assay

Propidium Iodide staining is commonly used to indicate cell death. Propidium Iodide is considered impermeable to live cells, therefore when cells are stained red by the dye this indicates that they are either dead or have otherwise been permeabilised to the dye. HMP and EDTA have both previously been shown to permeabilise cell membranes, which may allow for the penetration of the PI dye [60, 216].

Porcine corneal keratocytes were treated with various concentrations of HMP for 4 hours. Untreated, EDTA and water groups were included as controls for comparison. Untreated PCK cells presented with minimal propidium iodide staining and were still confluent in the base of the well (Figure 5.3). The same was true of the water treated (vehicle control) PCK cells. The 2% EDTA treated PCK cells were no longer confluent,

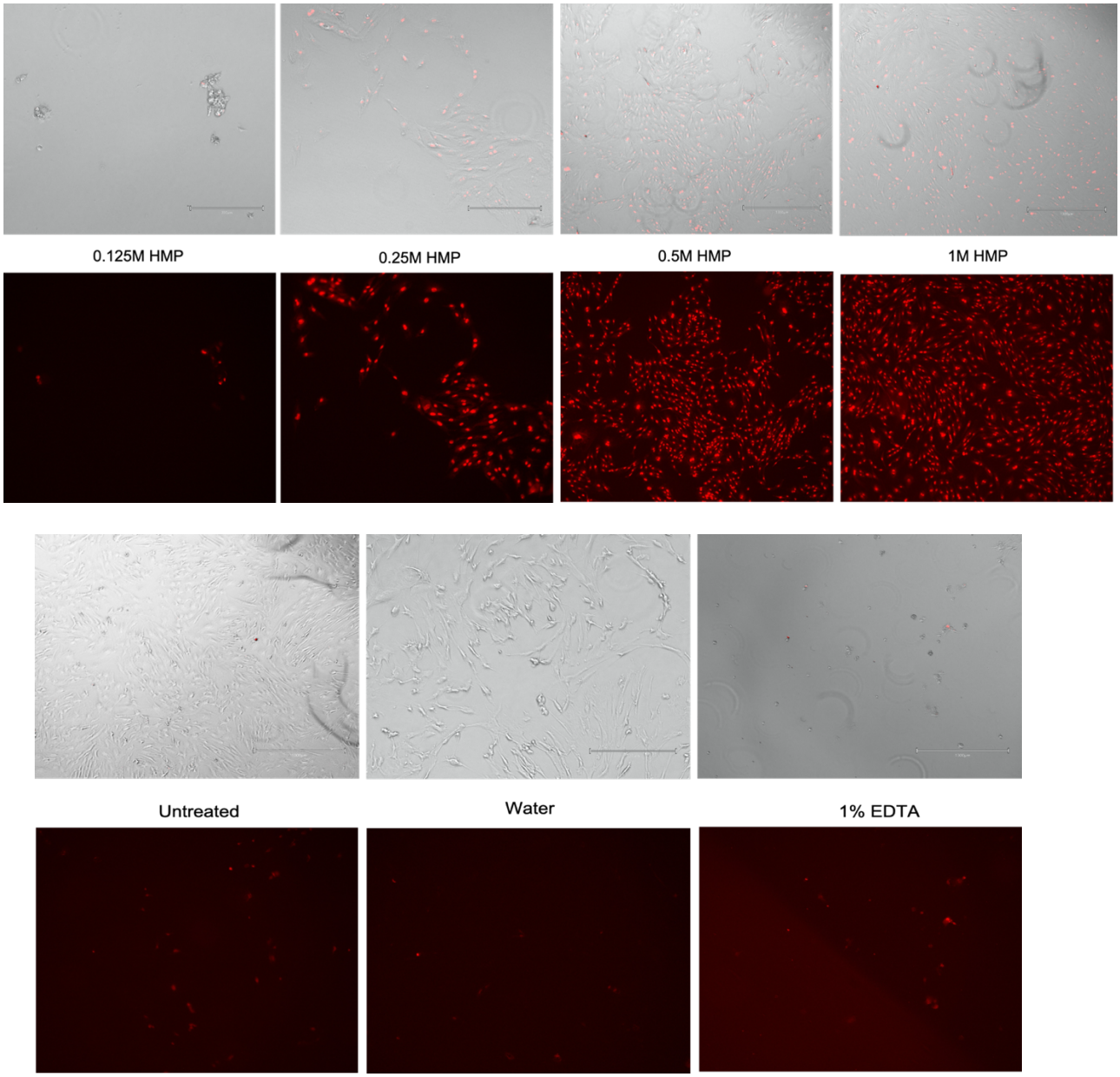

Figure 5.3: Top row: Brightfield images Bottom row: Texas Red images, of propidium iodide stained porcine corneal keratocyte cells after 4 hours treatment with HMP (0.125-1M), 1% EDTA, or sterile water. Magnification: X20. Scale bar: 1200μm. 24-well plate, 500μl media per well. All HMP treated cells stained positive for Propidium Iodide. Cell adherence appears to increase with HMP treatment concentration. 1% EDTA treated cells lose adherence. Water treated (vehicle control) and Untreated (normal growth media control) cells included for reference.

with the majority of PCK cells losing adherence (Figure 5.4). The cells which remained stained positive for propidium iodide, suggesting a breach in the membrane. The same was true of PCK cells treated with 0.125M and 0.25M HMP. Both groups lost a large proportion of cells through reduction in adhesion, and the remaining cells stained positive for propidium iodide. In fact, all PCK cells treated with HMP stained positive with propidium iodide suggesting a breached membrane in each case. However, where 0.25M and 0.125M treated cells lost adherence, 0.5M and 1M treated cells did not.

Through image analysis the PCK cells were quantified (Figure 5.4). The 1M HMP treated group had a significantly greater cell count than the 0.125M ($p<0.0001$), 0.25M, ($p<0.0001$) and 0.5M ($p=0.0003$) groups. The trend across the HMP treated groups was that cell count increased with HMP concentration.

5.3.4 **Re-analysis of the MTT assay results to include measures of cellular adherence**

The % cell viability calculations performed to analyse the MTT assay data do not distinguish between loss of cell metabolism/cell death and loss of cell density. When then the propidium iodide cell count data and MTT assay data (Figure 5.5) are compared, the propidium iodide cell count data appears to partially explain the MTT assay results. When the MTT results for each treatment group are divided by the average quantified propidium iodide cell count for that group (Figure 5.5), a different trend emerges. 0.125M HMP and 2% EDTA treated PCK cells appear on average to show a greater rate of metabolism per cell than those treated with higher concentrations of HMP. 0.25M HMP shows the lowest relative cell metabolism, followed by the 0.5M and 1M groups which show comparable results.

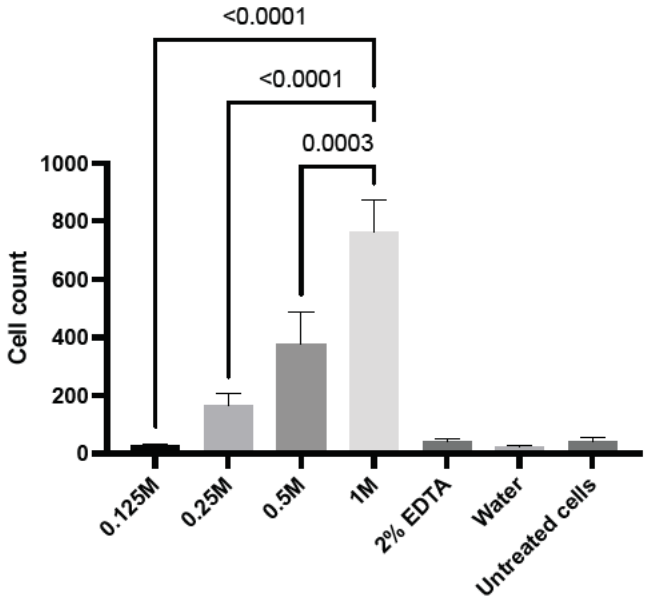

Figure 5.4: Cell count (mean values) of propidium iodide stained porcine corneal keratocyte cells for each treatment group (0.125-1M HMP, 2% EDTA, water and untreated control). Groups were compared with a one-way ANOVA. There were significant differences between the 1M treated group and all other HMP treatment groups. n = 5. Error bars = SEM.

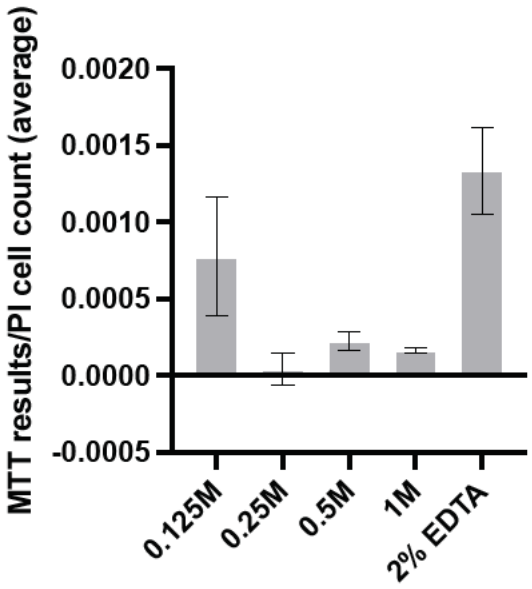

Figure 5.5: The relative average values for each treatment group when the MTT assay results are divided by the average values from the propidium iodide cell count. Water and untreated group are excluded due to the absence of propidium iodide staining in those groups. Error Bars = Standard Deviation (SEM).

5.3.5 *Ex vivo* corneal biopsy assay

The H&E-stained images of the sectioned treated corneas (Figure 5.6) reveal structural differences between the groups. The corneas treated with 2% EDTA, 0.125M HMP and 0.25M HMP show epithelial cell detachment when compared to the HBSS control, and also in comparison to the 0.5M and 1M HMP treated corneas. The 0.5M and 1M treated corneas show dense epithelial layers in comparison to the HBSS (control) group, suggesting some desiccation may have occurred. None of the treatment groups present with structural abnormalities deeper than the epithelial layer.

5.3.6 3-(4,5-dimethylthiazol-2-yl)-2,5-diphenyltetrazolium bromide (MTT) metabolism assay of tissue biopsies

Although cellular monolayer assays are useful for providing an indication of cytotoxicity, cells can behave differently *in vitro* than *ex vivo* or *in vivo*. *Ex vivo* tissue biopsy assays were performed on porcine corneas to investigate the effect of HMP treatment on the corneal structure. EDTA and HBSS treatment groups were included as controls for comparison.

When the corneal biopsies were treated in media containing each of the chelating agents, there were no significant differences in the measured formazan metabolism and calculated tissue viability between the groups other than at 24 hours (Figure 5.7), where the 1M treated group presented with significantly higher % tissue viability than the other groups (23%). At the same time point, the 0.125M HMP and 2% EDTA groups showed similar viability at 15.5% and 16% respectively. 0.25M and 0.5M HMP presented the lowest mean values of tissue viability at 7% and 8% respectively. The trend is similar at 4 hours treatment, with the exception of 1M HMP

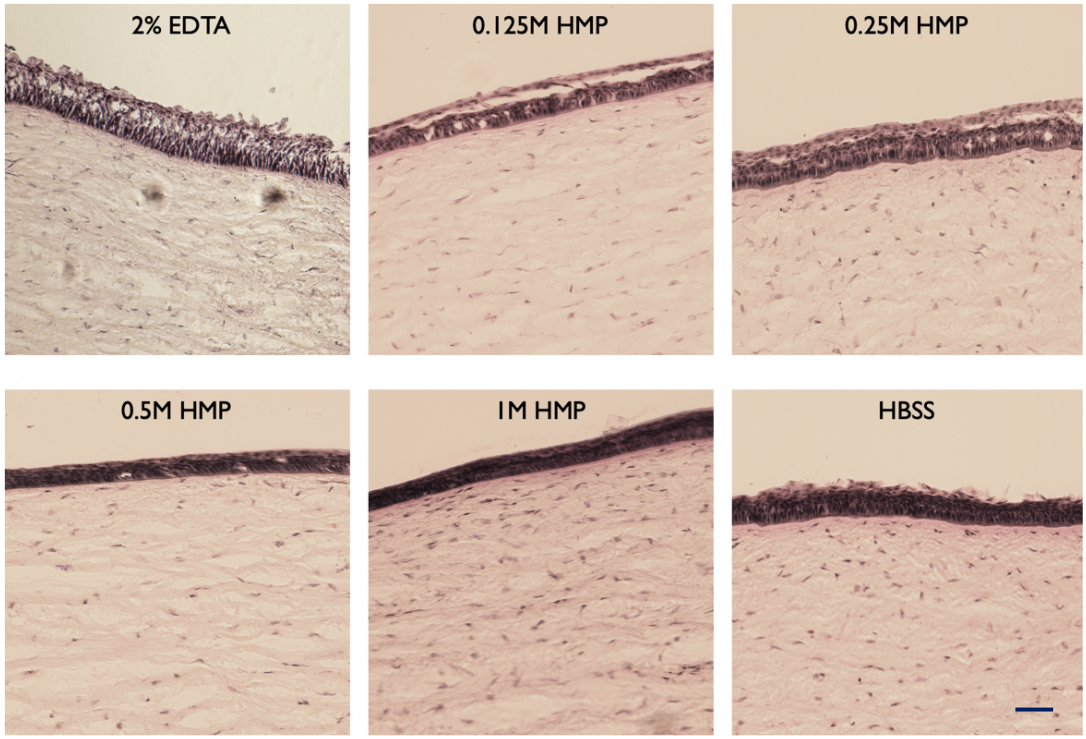

Figure 5.6: Brightfield microscope images at X20 magnification, of Haemoxylin and eosin (H&E) stained porcine corneal sections after 4 hours treatment with 2% EDTA, HBSS or 0.125M-1M HMP. 2% EDTA, 0.125M and 0.25M HMP groups show epithelial detachment. The 0.5M and 1M HMP show a dense epithelial layer in comparison to the HBSS control, potentially due to a degree of desiccation. Scale bar = 250μm

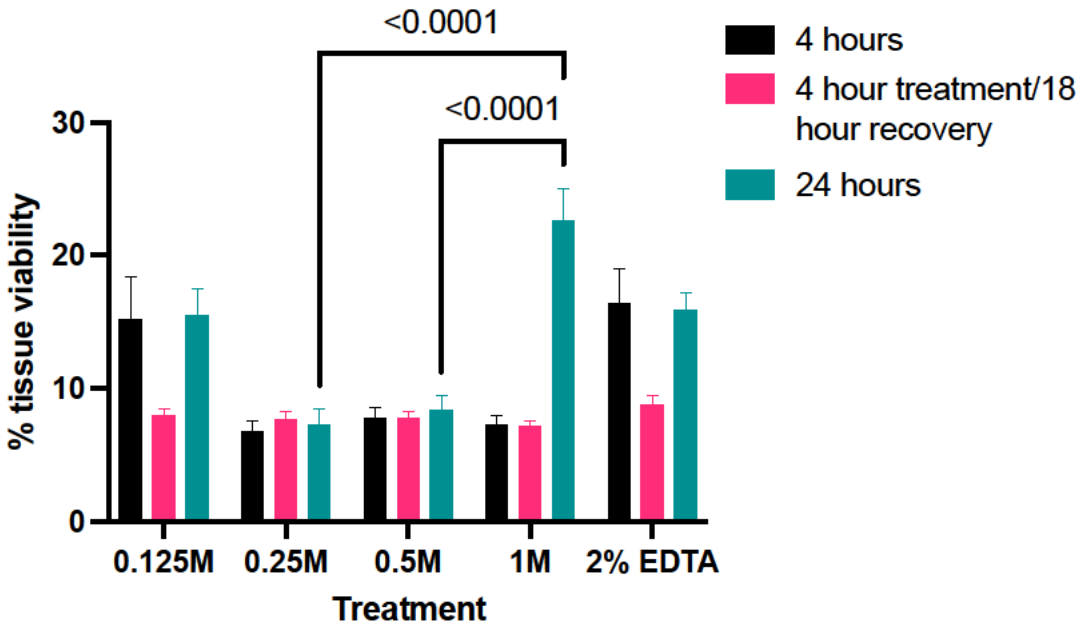

Figure 5.7: The calculated percentage (%) tissue viability based on MTT assay measurements for the 5mm diameter, circular biopsy of corneal tissue after exposure to each treatment after 4 hours (Black), 4 hours treatment and 18 hours recovery in normal media (Pink) or 24 hours treatment (Green). Values within and between each time point were compared using a mixed effects analysis. % tissue viability was calculated in comparison to untreated controls. Tissue viability was low across all groups. A noticeable change occurred in the trend between the treatment groups at 24 hours treatment, where the 1M group exhibited significantly greater tissue viability than the 0.25 and 0.5M groups ($p<0.0001$). N=6. Error Bars = Standard Error of Mean (SEM).

which presents a lower cell viability (7%) in line with 0.25M and 0.5M HMP. The inclusion of an 18-hour recovery period post-treatment altered the trend, bringing all groups in line with similar viability measurements (7-9%).

5.3.7 XRF analysis of corneal sections

The XRF images revealed a consistent distribution of calcium and sodium throughout the corneal tissue (Figure 5.8a). The detection of phosphate, however, revealed a higher concentration of phosphate throughout the epithelial layer, showing as a bright, thin band along the length of the tissue. This was further confirmed by cross-sectional line analysis (Figure 5.8b), which detected a higher phosphate count in the epithelial layer. This was not replicated in the measurement of sodium.

5.3.8 *In vitro* and *ex vivo* Lactate Dehydrogenase release assay

The results of the LDH release assays in both *in vitro* cellular monolayer assays and tissue biopsy assays (Figure 5.9) showed a consistent trend of a reduction in the measured absorbance with increasing HMP concentration. In the case of the tissue biopsy assay, the readings for all HMP treated groups were significantly lower than those of the untreated tissue. A test using an LDH positive control (bovine heart LDH), revealed that the group including 0.5M HMP in the media produced lower absorbance readings on the completion of the assay. This suggests that HMP interferes with the LDH assay so that measured absorbance is no longer an indicator of LDH release, and that this assay is not an appropriate method for assessing the cytotoxicity of HMP. The positive control assessment included using bovine serum albumin, which appeared to form an insoluble precipitate with low concentrations of HMP (0.0625M and 0.125M), leading to an increase in measured absorbance.

a)

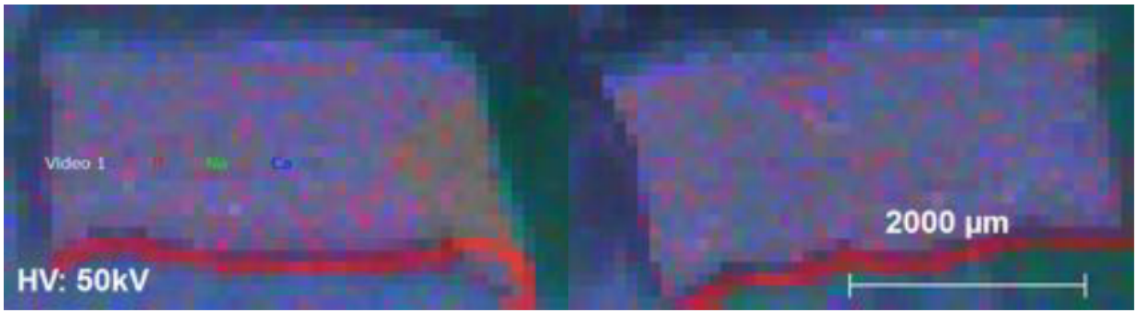

b)

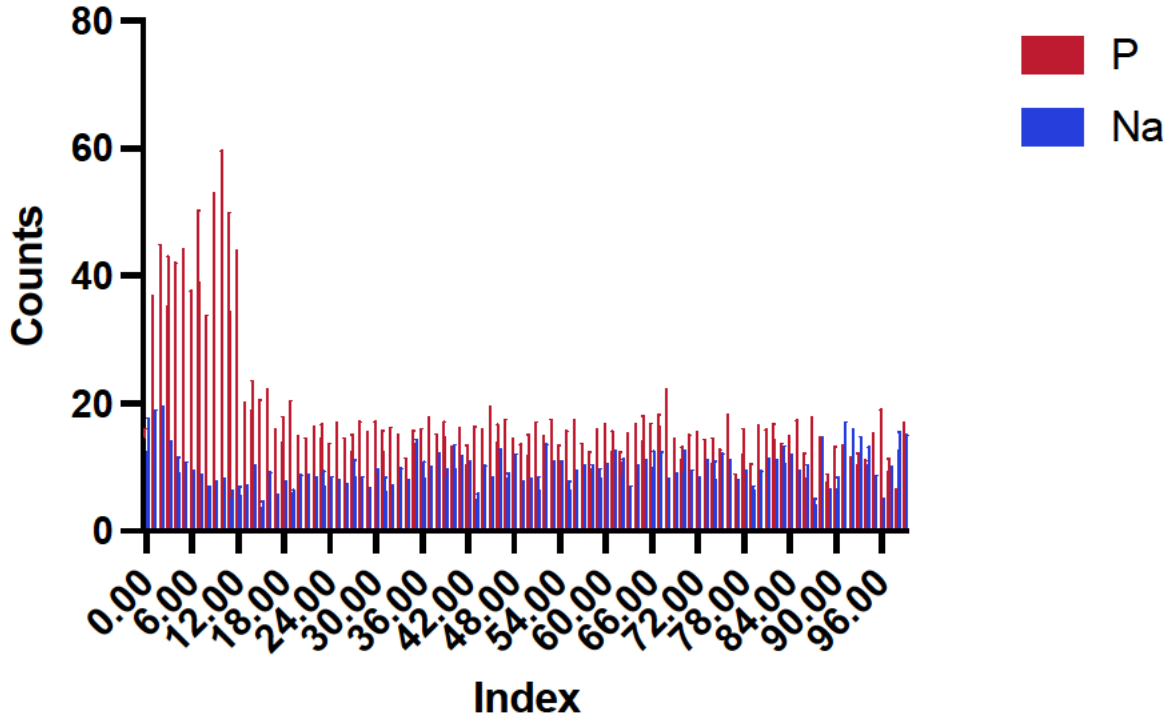

Figure 5.8: a) Contrast images of the detection of Phosphate (Red), Sodium (Green) and Calcium (Blue) within porcine corneal sections using X-Ray Fluorescence (XRF). A consistent distribution of calcium and sodium is revealed throughout the corneal tissue. The detection of Phosphate revealed a concentration throughout the epithelial layer, showing as a bright, thin red band along the length of the tissue.

b) measurement of the levels of calcium and phosphate (counts) along a bisecting line through the tissue, from the epithelial layer through to the endothelial layer. The higher levels of phosphate in the epithelial layer are demonstrated by the higher phosphate count. N=4. Error Bars = Standard Deviation).

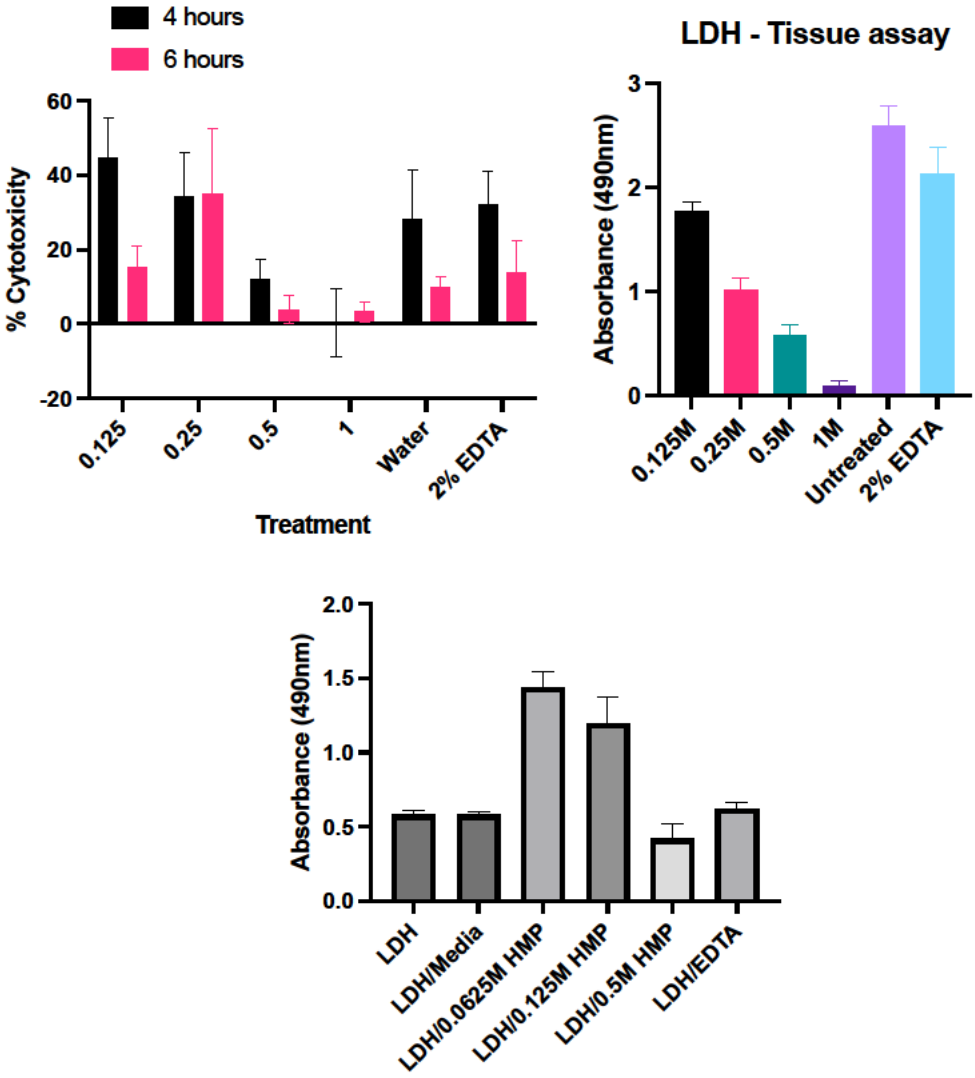

Figure 5.9: Error bars = SEM.
a) In vitro cellular monolyaer assay - values of percentage cytotoxicity calculated using absorbance values indicating lactate dehydrogenase release against the untreated control group. The 0.5M and 1M HMP groups present lower values of percentage cytotoxicity compared to 0.125M and 0.25M HMP and 2% EDTA. N=9. b) Tissue biopsy assay - absorbance values indicating lactate dehydrogenase release for each treatment group. The HMP groups are significabtly lower than the untreated control group, bringing into question the accuracy of the assay. N=8. c) A comparison of the absorbance values of samples containing the same concentration of LDH, with and without the presence of HMP. The sample containing 0.5M HMP reads lower despite containing the same concentration of LDH. The samples containing 0.0625M and 0.125M HMP read higher, having formed an insoluble precipitate. N=5

5.4 Discussion

In most cases it is assumed that as the concentration of a cytotoxic agent increases – the cytotoxicity induced also increases. However, the HMP assay results presented in this chapter have not consistently followed this trend.

Previous investigations into the cytotoxicity of sodium hexametaphosphate have also shown conflicting results. When examining the possibility of using these sensitising affects to target cancer cells, Oćwieja and Barbasz [315] found that HMP alone, at a concentration of 120mgL^{1} (0.196mM), decreases the cell viability of Histiocytic lymphoma (U-937) and human promyelocytic (HL-60) cell lines, and significantly more so the HL-60 line. The differences between the cell lines were postulated to be a result of differences in the structure of the cellular membranes. In contrast, when examining the influence of 0.05mM of HMP on the proliferation and migration of human dental pulp cells, Bae et al. found that HMP is favourable for the growth and differentiation of the cells [275]. This mirrors results from the assessment of the proliferation of human dermal fibroblasts treated with inorganic polyphosphates with a chain length of 65 phosphate units at 1.34mM [316]. These assessments included concentrations of HMP much lower than those tested here and over much longer time periods - over 24 hours in the case of the cancer cells and up to 14 days in the case of the human dental pulp cells.

i) Concentration-dependent affects

With such an increase in the HMP concentrations we tested compared to previous assessments, it was expected that our assessments would see an increase in cell death or malfunction, even over a shorter time period. However, this was not reflected

in the results of the MTT metabolism assay performed on the cellular monolayer (Figure 5.2), which appeared to show the porcine keratocyte cells in higher concentration HMP treatment groups metabolising a rate more comparable to untreated controls (shown through % viability calculations). When comparing these results to those of the Propidium Iodide penetration assay (Figure 5.5), it is clear that this may be due to the loss of cellular adhesion at 0.125M and 0.25M HMP, meaning the metabolism values are in reality reported for a smaller number of PCK cells in comparison to the higher concentrations. When the propidium iodide cell count values and MTT assay values are combined (Figure 5.5), the trend for the *in vitro* cellular monolayer assays becomes comparable to that found at the 4 hour treatment time in the tissue biopsy assays, where 0.125M HMP and 2% EDTA show the highest % viability (metabolism compared to controls) compared to the other treatment groups (Figure 5.7). However, at the 24-hour time point, the 1M HMP group records significantly higher tissue metabolism than the 0.25M and 0.5M groups.

It is possible for mammalian cells to metabolise inorganic polyphosphates [229]. Over the last 30 years the suggestion that inorganic polyP is involved in mitochondrial metabolism pathways has gained traction, and there is evidence to suggest that inorganic polyP depletion interferes with inner membrane potential and causes increased NADH levels [320]. These results highlight the potential limitations of using a metabolism assay to assess the cytotoxicity of a molecule which may interfere with normal cellular metabolism.

ii) The role of metal cations in cellular adhesion and permeabilization

However, the trend in cellular adhesion is also yet to be explained. This same trend was evident in the *ex vivo* tissue assays, where the epithelial layer can be seen to be detaching from the corneas treated with 0.125M and 0.25M HMP and 2% EDTA. It also appears as though HMP treatment causes the permeabilization of cell membranes, but in 0.5M and 1M HMP treated PCK cells this does not appear fatal. These phenomena are likely related to the impact of HMP on metal cations both in the cell culture media, and the adhesion mechanisms of the cells. HMP's many uses in the food and ceramics industries rely on its ability to form stable complexes with calcium and other divalent metal ions [252, 253, 292, 321]. Calcium plays a vital role in cell-to-cell and cell-to-substrate adhesion in that cadherin membrane glycoproteins have been highlighted as key players in cell-to-cell adhesion in most tissues. Cadherins depend on Calcium ions for their function [213]. Additionally, calcium and magnesium play a key role in cell permeabilization, and HMP has already been shown to permeabilize the cell membranes of various cell types [212, 216, 322]. In bacterial culture HMP has been shown to cause cell lysis, which is then alleviated by the addition of NaCl or $MgSO_4 \cdot 7H_2O$ into the culture medium, suggesting the interference is with metal cation metabolism [323]. The *in vitro* cytotoxicity of HMP will likely be mediated by how HMP interacts with metal ions in the culture media as well as within the structure of the PCK cells, impacting adherence, permeability and metabolism of the cells.

The earlier assessment (Chapter 4, Figure 4.8) of the interaction between HMP and $MgCl_2$ and $CaCl_2$ offers additional evidence to the theory that there could be a variation in the behaviour of HMP solutions of different concentrations towards metal cations. Our previous assessment of the formation of insoluble precipitates by HMP and $CaCl_2$

and $MgCl_2$ suggested that there was a higher affinity for magnesium in the 0.125M and 0.25M treatment groups than the 0.5M and 1M groups. When compared to the results of the propidium iodide and *ex vivo* biopsy assays, it is also seen that 0.125M and 0.25M HMP reduce cellular adhesion in comparison to the 0.5M and 1M groups. It is possible that the trend in cytotoxicity exhibited is related to the affinity of each concentration of HMP for magnesium ions, which may in turn be related to the length of the polyphosphate chains at each HMP concentration, or the formation of certain complexes with specific orientations at these concentrations.

iii) Potential interference of HMP with LDH assay reaction

The positive control performed to test the viability of the LDH assay showed that HMP interferes with the assay, possibly producing false results in the *in vitro* cellular monolayer tests. The fact that higher concentrations of HMP produced lower absorbance results suggests that the HMP may be binding with one of the reactants needed to create the colour change necessary for the colorimetric assay to work. The assay reagent includes L-Lactic acid (2-hydroxy propionic acid), β-NAD (nicotinamide adenine dinucleotide), DMSO, Tris-HCl and polyethylene glycol tert-octylphenyl ether, and the presence of LDH is necessary to create the colour change necessary. It is known that HMP does not mix with DMSO, however as it is not the HMP but the LDH which is being read this should not interfere with the colour change of the assay. The interaction between polyphosphates and LDH has been subject to previous investigations, which showed that where LDH upon heating unfolds irreversibly, LDH which was heated in the presence of polyphosphate ($polyP_{300}$) did not unfold completely but formed a thermally stable intermediate structure [324]. However, this previous study found no evidence that polyP binds to LDH in the absence of high

temperatures, as in the work performed here. The LDH assay relies on a coupled enzymatic reaction that converts iodonitrotetrazolium (INT) into formazan by diaphorase. The released LDH converts lactate to pyruvate (as in anaerobic metabolism) reducing NAD to NADH/H^+. Diaphorase then uses the NADH/H^+ to reduce the INT to red formazan [308]. Further investigation would be necessary to determine exactly where HMP is interfering with this assay mechanism.

The positive control assessment also revealed that at lower concentrations, HMP appears to complex with bovine serum albumin. HMP is known for its ability to complex proteins [249, 313, 325] and the aggregation of BSA by HMP has been previously studied [326] - therefore this finding is unsurprising. However, it is notable that this only occurred in the lower concentrations (0.00625 and 0.125M) and not at 0.5M HMP, again suggesting a change in the ability of HMP to form certain complexes at higher concentrations.

iv) Mechanisms of cell injury and death

LDH assays, in combination with other methods such as cell membrane permeation dye exclusion assays, are used to provide an indication of cell death by necrosis [327]. Necrosis is unprogrammed cell death, caused by chemical or physical insult, which leads to the membrane of the cell being breached and the internal contents leaking out [327]. Evidence of cell membrane permeabilization by HMP has been revealed in the work presented here, and in previous studies performed with HMP and similar calcium chelating agents [250, 251, 328]. What is unclear, is whether this cell permeabilization is reversible, or as a result of necrosis. Neither MTT assays nor LDH assays are reliable measures of other forms of cell death, in particular apoptosis. Apoptosis is

programmed cell death, strictly mediated by caspases and genetically programmed to occur as a natural part of a cell's life-cycle [329]. Apoptosis can be triggered by both internal and external insults, including membrane injury or mitochondrial injury [330]. To examine fully the potential mechanism of cytotoxicity by HMP both apoptosis and necrosis will need to be measured.

v) XRF analysis of corneal phosphate content

The XRF analysis revealed that even in untreated corneas there is a high natural phosphate content of the epithelial tissue, relative to the other tissues in the cornea. This could provide some explanation to the formation of hydroxyapatite occurring at the interface between the epithelial tissue and stromal tissue. However, phosphate is naturally present in multiple forms in all cells and therefore this reading may just be indicative of the higher density of cells in the epithelial layer, which is tightly packed and organised in comparison to the relatively open network of cells and collagen in the corneal stroma and the much thinner endothelial layer.

vi) Summary

The aim of the work in this chapter is to provide an assessment of the potential danger to the ocular environment of using a topical HMP treatment. *In vitro* and *ex vivo* cell metabolism, cell death and histochemical assays were performed to gain an understanding on the cytotoxic effects of HMP on corneal cells (porcine corneal keratocytes) and tissue (porcine corneal biopsies). HMP treatment did not create the expected trend, where an increase in concentration of a test substance causes an increase in measured cell viability (cell metabolism compared to healthy controls). It has therefore not been possible to determine which concentration of HMP might be

safest to use, as 0.5 and 1M HMP appear to allow greater cellular retention and maintenance of tissue integrity, whereas 0.125M HMP appears to facilitate greater cell metabolism than at higher concentrations.

6.

FORMULATION OF A SODIUM HEXAMETAPHOSPHATE DELIVERY MATERIAL

6.1 General Introduction

When aiming to deliver therapeutic agents to the ocular tissues, a range of eye drop formulations or alternative ocular devices can be employed. Both drops and inserts most commonly aim for properties which do not inhibit clarity of vision, and therefore offer minimal disruption to the patient.

This is one of the major advantages of gellan fluid gel-based drops, which share the same refractive index as water and therefore offer optimal optical properties. Gellan is a thermally gelling polymer with an anionic charge, which crosslinks in the presence of sodium (and other metal) ions. Gellan fluid gels have been developed by shearing crosslinked low-acyl gellan hydrogels, creating a macrostructure of individual 'cells' of crosslinked gellan which flow around one another whilst otherwise maintaining the gel structure [95, 131, 133]. Gellan fluid gels are shear thinning, a property which can be advantageous in an eye drop for the purposes of comfort and wettability [331]. As an eye drop, low-acyl gellan fluid gel shows optimal retention and when formulated with hrDecorin, successfully sustained release of the drug to reverse corneal opacity in a murine model [332]. It has also been shown that the sodium present in tears is sufficient to crosslink gellan, meaning in situ gelation is a possibility [333].

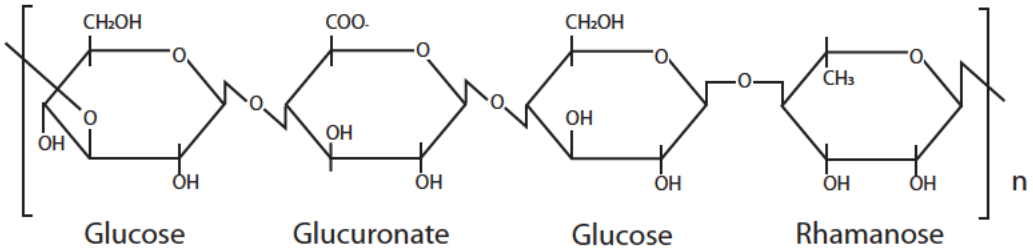

Figure 6.1: The polymeric structure of gellan

Alginate is a naturally occurring polymer, routinely harvested from various species of seaweed. The monomeric composition and arrangement of the alginate can vary depending on the species from which it was harvested, namely through variation in the mannuronic (M) and guluronic (G) acid monomer blocks [334]. Two adjacent G blocks are required in the monomeric composition to create a binding site for polyvalent cations and to allow gelling behaviour [334, 335]. Due to the interest in both natural polymers and polymeric hydrogels for drug delivery alginate has been assessed for a variety of applications [70, 79, 91, 256, 336-340]. With regards to ocular uses, drug-eluting calcium alginate inserts have been assessed as a potential novel option for ocular therapies [107]. In concurrence with the conventional eye drop polymers listed previously, alginate has been examined as a thickening agent to improve eye drop retention and improve delivery of carteolol for increased treatment efficacy for ocular hypotension [341] and as a protective agent for the ocular surface in the treatment of dry eye disease [342]. Calcium alginate has also been formulated to gel in-situ and used to encapsulate therapeutic nanoparticles [343, 344]. Alginate is a readily available polymer, and is widely considered non-toxic and capable of offering improved ocular retention in comparison to aqueous drops. Alginate with a high proportion of guluronic acid (G blocks) in the polymer backbone show a reversible liquid to gel transition, and this has been examined for the delivery of pilocarpine [345]. Compared to other polymers like hyaluronic acid or cationic chitosan, alginate gels show poorer mucoadhesion on the ocular surface [219], however the wettability of the drop is improved compared to more viscous formulations – a trade-off which needs to be balanced to reach the optimum retention and drug delivery for an eye drop. To form a crosslinked hydrogel with alginate, calcium is the usual choice of agent, however other divalent and trivalent ions can be considered [346, 347]. Photo-crosslinkable alginate

formulations have also been developed [348]. Alginate has been widely investigated for tissue engineering purposes, with studies showing that phosphates and other ions may contribute to the degradation of the gel, particularly in combination with cell encapsulation [337, 349]. It is also commonly used in combination with other, positively charged polymers such as chitosan, forming ionotropic gel materials [336, 350-353]. Co-polymer formulations offer tuneable properties, and alginate in combination with Arjun bark resin offers an in-situ gelling eye drop which offers extended release [354]. A colloidal alginate formulation has previously been employed to deliver sodium hexametaphosphate through injection for the treatment of pathological bone growth [302].

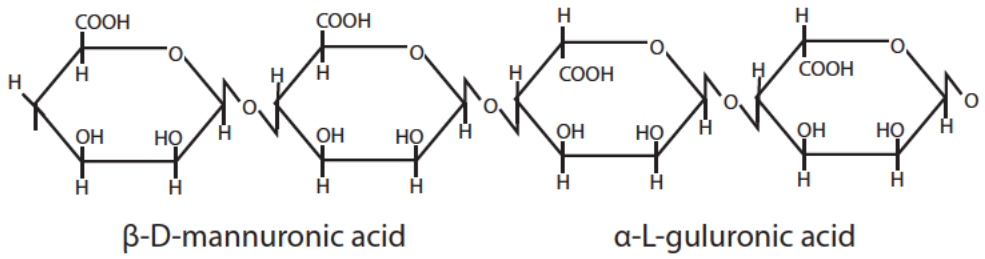

Figure 6.2: The polymeric structure of Alginate

Chitosan is a derivative of chitin, found in shells of crustaceans. Unlike many other polymers, chitosan has the distinct property of being positively charged (cationic), allowing it to crosslink and interact with molecules that other polymers do not, including other anionic polymers such as carbopol or alginate [355]. This makes chitosan gels incredibly tuneable and has allowed for the development of sensitive chitosan gels, including pH sensitive, ion sensitive and thermosensitive formulations which can gel in-situ [355]. Chitosan is a naturally occurring polymer, which has previously been shown to crosslink with inorganic polyphosphates including HMP [350, 356-358]. As a

cationic polymer, chitosan shows optimal mucoadhesion properties, but can also be at risk of degradation by tear film proteins [346, 359]. It has been suggested that chitosan may be able to open the corneal epithelial tight junctions to allow for greater penetration into the ocular tissue [360]. Chitosan can form comparatively rigid hydrogels, which have been examined for orthopaedic applications (in combination with additional anionic polymers) [340]. There have also been multiple investigations into chitosan dressings for wound and burn repair [361-366]. Chitosan readily forms nanoparticles, which have been widely investigated for their ability to cross the ocular (and other) barriers and improve drug delivery [60, 254, 255, 352, 356, 367-370]. Chitosan can also act as an emulsion stabiliser, allowing for the formation of a wide range of chitosan-based materials with a range of macro and microstructures [152, 366, 371]. Most importantly for the context considered within this work, chitosan crosslinks ionotropically with inorganic polyphosphates [350, 356, 369]. In the formation of nanoparticles, HMP was compared to phytic acid and tripolyphosphate, and it was found that tripolyphosphate provided the fastest drug release, and greater stability in storage than those formed with HMP [356, 369]. Chitosan-HMP beads have been shown to be affective at removing dyes, particularly anionic dyes, from water and are being investigated further for water purification purposes [372].

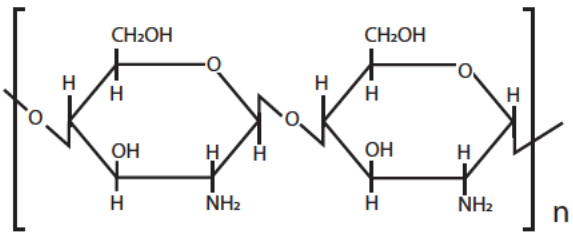

Figure 6.3: the polymeric structure of Chitosan

The aim of incorporating HMP into a polymeric delivery material would be to improve the retention of HMP on the surface of the eye, extending the window in which the HMP is bioavailable and providing therapeutic effects – in this case dissolving the hydroxyapatite mineral. A higher viscosity has been shown to improve drop retention, however in this case the therapeutic efficacy is dependant also on the ability of the delivery material to release HMP at effective doses. It is common for the release properties of drug delivery materials to be assessed *in vitro* by sampling and testing solution within which the material has eluted its carried drug.

Assessing the concentration of polyphosphate in a solution can be done through methods which break the polyphosphate chains into orthophosphates or single Pi units which can then be quantified with molybdenum blue or similar colorimetric assays [373]. This process involves hazards such as boiling the sample in acid. Various alternative methods for quantifying polyphosphates have been developed, namely to quantify the small amount of inorganic polyphosphates that can be found in cells, and to examine the activity of enzymes such as PFK on the chain length of those inorganic polyphosphates [373]. Such novel methods include enzymatic assays, and additional colorimetric assays such as those involving toluidine blue O dye. Toluidine blue O is most commonly used for immunohistochemistry, allowing the differential staining of various tissue types. The dye ranges in colour from blue to pink, depending on the properties of the tissue being stained. It is suggested that this metachromatic shift is induced through polymerisation of the dye when in contact with anionic chromophores, such as DNA or RNA [374].

Sodium hexametaphosphate (HMP) exists in aqueous solution as a negatively charged inorganic polymer of multiple phosphate units [375]. HMP is a chelating agent, readily chelating metal ions such as calcium and magnesium. In addition, the positive sodium ions delivered alongside the HMP molecules can in certain formulations crosslink anionic organic polymers to form hydrogels [248, 331, 376]. Each of these three factors allows HMP to, in theory, exhibit multiple different effects on an organic polymer formulation. The charge of the polymeric phosphate units will determine interactions with other charged polymers, whilst the ability to chelate metal ions may interfere with the structure of other polymeric materials, by sequestering the metal ions necessary for crosslinks to form. It is therefore necessary to incorporate HMP into various polymers in order to establish the optimum properties for ocular drug delivery.

It remains to be seen how demineralising concentrations of HMP interact with various organic polymeric materials. The optimum formulation for an HMP-eluting eye drop would maintain enough viscosity to remain on the surface of the eye for the desired, without compromising vision and whilst delivering a therapeutic dose of HMP to the cornea.

6.2 Materials and Methods

6.2.1 Preparing Alginate gels with Sodium hexametaphosphate

Sodium alginate has previously been used to deliver an injectable dose of HMP for the purpose of dissolving ectopic mineral [302]. Alginate has also been used in other ocular formulations [341, 342, 344, 345]. Sodium alginate was prepared as a 2% w/v gel through the dissolution of powdered sodium alginate (Sigma Aldrich, UK) in MiliQ deionised filtered water under stirring (800rpm, 5 minutes) at room temperature. Once a homogenous gel had formed, HMP was then added to form gels of 0-0.1M HMP.

6.2.2 Preparing Gellan gels and fluid gels with Sodium hexametaphosphate

Due to its optical properties, i.e. that it shares the refractive index of the tear film, gellan makes an attractive choice for ocular formulations. Gellan was prepared as a 1.0% w/v gel by combining powdered low-acyl gellan (kelcogel) in Milli-Q water at a starting temperature of 80°C. To form a crosslinked gellan fluid gel, the gellan was subsequently cooled under stirring to 40°C and 10% 0.2M NaCl was added. Na-HMP of various concentrations was then added to the cooled gellan (both crosslinked and non-crosslinked) under stirring to form gels of 0-0.1M HMP. To compare the effect of NaCl to that of HMP, 2M NaCl was added to non-crosslinked gellan to form gels of 0-0.1M NaCl.

6.2.3 Creating chitosan solutions and crosslinked chitosan gels

Chitosan has previously shown to crosslink on the addition of HMP [356, 369, 370]. This may allow for the development of a formulation with tuneable properties. 2% chitosan gel was prepared by dissolving medium chain length chitosan powder (Sigma

Aldrich, UK) in 1% v/v aqueous acetic acid under stirring. 5ml samples of 2% chitosan gel were taken and mixed with increasing proportions of 0.1M HMP to form crosslinked gels of 0-0.01M HMP.

6.2.4 Creating chitosan films

Topical ocular drug delivery most commonly takes the form of eye drops, however ocular inserts offer an attractive alternative due to their increased retention [32, 103, 104, 377]. Crosslinked chitosan has previously been used to create ocular inserts [359, 367]. 2% and 3% chitosan gels were prepared in 1% acetic acid. Clean glass slides were then dipped into each gel until coated. The coated slides were then placed in 0.001M, 0.01M, 0.125M, 1M or 2M HMP for 24 hours. The gels were imaged, and then a razorblade was used to detach the films from the glass slide for further testing.

6.2.5 Viscometry - Shear Stress Ramp

To investigate the relationship between HMP and the polymeric hydrogel carriers, the alginate and gellan gels containing a range from 0-0.1M HMP and chitosan gels containing 0-0.01M HMP were then assessed using a shear stress ramp from 0.1Pa to 250Pa over 5 minutes (Malvern Rheometer). HMP solutions of 1M and 2M were also tested for comparison. 10 samples were taken per decade. The maximum shear stress was chosen to mimic the maximum stresses expected under blinking conditions on the surface of the eye. Flat parallel plate geometry was used, and the test was performed at a temperature of 32°C to mimic the ocular surface.

6.2.6 Submersion of gellan in HMP and NaCl

To further investigate the interaction between gellan and HMP, gellan was prepared as described both with and without 10mM NaCl crosslinking agent. Equal samples of each were submerged in 1ml HMP (1M, 0.5M, 0.25M or 0.125M) or NaCl (1M) for 48 hours. After 48 hours the gellan pieces were retrieved and imaged for comparison.

6.2.7 Oscillatory stress sweep test - limit of the Viscoelastic Region determination

To characterise the films developed by crosslinking chitosan with HMP, an oscillatory sweep test was performed. Using a Malvern Rheometer with flat plate geometry, the chitosan films were exposed to stresses in the range of 0.03 to 400 Pa at a constant frequency of 0.1 Hz. Complex shear stress and complex shear strain were recorded and used to determine the limit of the viscoelastic region (LVER). This sets the maximum stress/strain which can be applied to the films in further testing before failure or permanent changes to the structure of the material. The test was performed at 25°C

6.2.8 Fixed strain Frequency Sweep analysis

At a fixed strain of 1% (previously determined as within the LVER), the chitosan films were exposed to frequencies increasing from 0.01 to 50Hz and the Shear modulus (elastic component) and shear modulus (viscous component) were recorded.

6.2.9 Toludine Blue Assay development

To develop a safe and simple method of measuring HMP release, a 0.1% w/v dye of toluidine blue O was prepared using toluidine blue O powder (Sigma, UK) and Milli-Q water. 50µl of dye was added to the wells of a clear flat bottomed 96-well plate

(Corning). 50µL of reactant – either milli-Q water or HMP of concentrations from 0.01M-2M – was then added and the absorbance of the plate was read by a plate reader (Tecan Infiniti 2000) at a range of wavelengths from 290nm-1000nm, at 10nm increments.

6.2.10 HMP Release assay – Toluidine Blue

In order to assess the release of HMP from alginate gel and chitosan films, 50µl of alginate containing 0.5M HMP or a 5mm diameter circular biopsy sample of chitosan film prepared in 1M HMP was added to the base of the well of a 96 well plate. 100µl of Milli-Q water was then added. 5 wells were prepared for each time point – 10 minutes, 30 minutes, 60 minutes, 120 minutes, 240 and 360 minutes. At the relevant time, 50ul of water was removed from the top of the well and placed into 50ul toluidine blue O dye and incubated for 1 hour. The absorbance of the toluidine blue O mixture was then read at 450-700nm at 10nm increments. To prepare the controls, 50ul of each control substance was added to 50ul toluidine blue dye and incubated for 1 hour. The absorbance was again read at 450-700nm at 10nm increments. The calculation determined through the experiments performed above (viii) was then applied to the absorbance results, allowing for comparison to a standard curve which predicts HMP concentration in the sample.

6.2.11 HMP release assay – Hydroxyapatite sol

As above (6.2.10), 50µl of alginate containing 0.5M HMP or a 5mm diameter circular biopsy sample of chitosan film prepared in 1M HMP was added to the base of the well of a 96 well plate. 100µl of Milli-Q water was added on top. 5 wells were prepared for each time point – 10 minutes, 30 minutes, 60 minutes, 120 minutes, 240 and 360

minutes. 50 µl of hydroxyapatite was added to each well of a separate, corresponding plate and the absorbance was measured at 380nm. At the relevant time, 50µl of water was removed from the top of the wells containing the hydrogel formulations and placed into the wells with 50µl hydroxyapatite sol and incubated for 1 hour. The absorbance of the HA sol was then read at 380nm.

6.2.12 Contact angle

The contact angle of formulations relative to the ocular surface is an important predictor of the drop behaviour and retention under blinking. Unscalded whole porcine eyes were received from a commercial abattoir within 4 hours of death. Eyes were rinsed with HBSS and placed in the top of 50ml falcon tubes with the cornea facing upwards. A camera and tripod were positioned to be level with and focused on the corneal surface. 300µl of each formulation (0.5M HMP/alginate, 1M HMP or HBSS) was added to the surface of each eye and the travel of the drop was filmed. Each formulation was assessed on the surface of three different eyes, three times. Frames were subsequently taken from the footage and the contact angle of each formulation was measured in ImageJ.

6.2.13 **Statistics**

The results of the HMP release assay using hydroxyapatite sol were analysed using a paired t-test to compare baseline and post-treatment absorbance measurements at each time point. Prior to this the data was assessed for normal distribution using a Shapiro-Wilk test.

The contact angle measurements for each formulation were compared using a one-way ANOVA. A Shapiro-Wilk test confirmed normal distribution prior to comparison.

6.3 Results

6.3.1 Visual observations of gellan, alginate and chitosan gels with HMP

In order to create a HMP delivery material, HMP was mixed with alginate, chitosan and gellan aqueous gels.

When 2% alginate gel was combined with increasing proportions of 2M HMP, it was observed that at a concentration of 1M, separation occurred in the formulation (Figure 6.4a). A homogenous formulation is necessary to ensure both consistency and comfort, therefore for further testing a maximum of 0.5M HMP was used in combination with alginate.

On the addition of HMP into the Gellan fluid gel, the formulation appeared to develop opacity at 0.04M HMP (Figure 6.4b). This increased with increasing HMP addition, with the formulation becoming both less resistant to inversion – i.e. weaker - and cloudier.

Where HMP was added to 2% chitosan at proportions from 0.001 to 0.01M, a clear colour gradient appeared, with increasing HMP correlating to an increase in the opacity of the gel and a change in colour from light brown to white (Figure 6.4c). This visual gradient was assumed to correspond to increased crosslinking in the material.

6.3.2 Creating chitosan films

In the case of the formulations prepared with 1M and 2M HMP, the films formed by 3% chitosan were optically opaque compared to those formed with 2% chitosan (Figure 6.5). The films formed with 0.1M HMP and 0.001M HMP were optically

a)

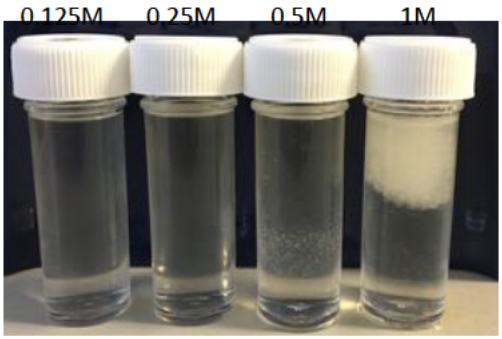

b)

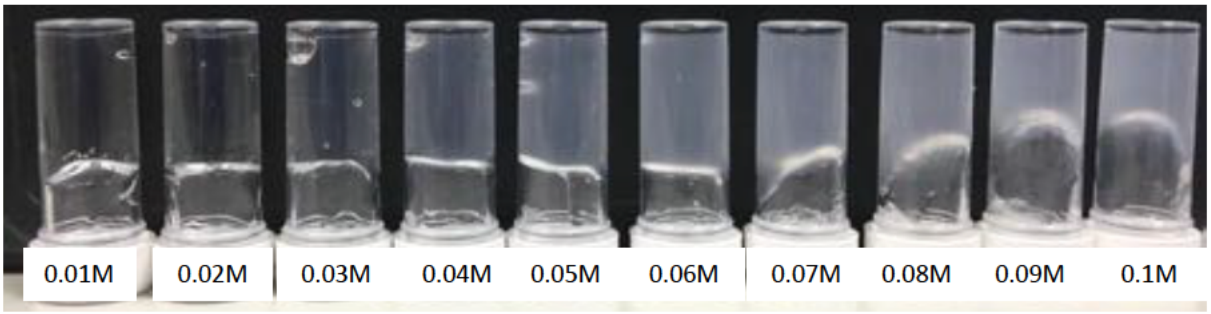

c)

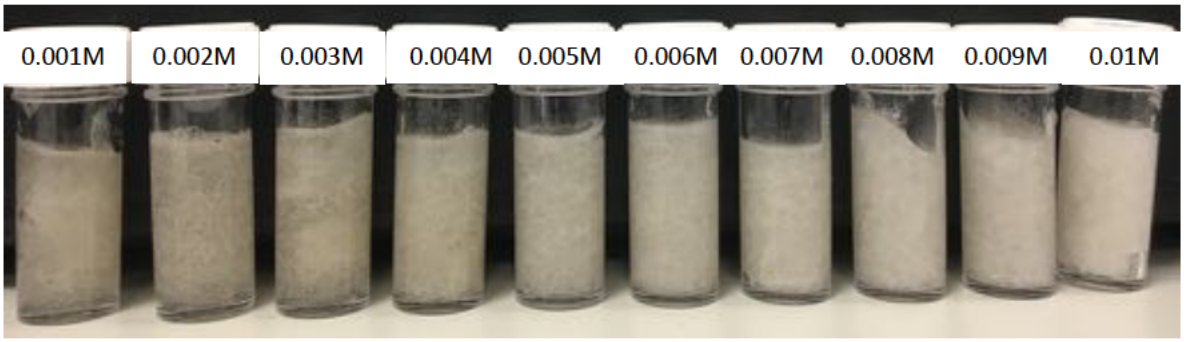

Figure 6.4: a) *2% alginate gel with increasing (from left to right) concentrations of HMP. At 1M, the formulation appears to segregate into two phases, no longer forming a visibly homogenous mixture.* ***b)*** *1% gellan fluid gel with increasing (from left to right) concentrations of HMP. As the concentration of HMP within the formulation increases, the optical properties of the gel change and the gel loses transparency.The gel also become less resistant to inversion, shown by the gel beginning to travel upon inversion at concentrions of HMP above 0.06M* ***c)*** *From left to right: 2% chitosan gel in 1% aqueous aectic acid with increasing concentrations of 0.1M HMP solution (from 1% to 10%) corresponding to a HMP concentration of 0.001M to 0.01M HMP. As the proportion of 0.1M HMP in the gel increases, the colour of the gel progressively changes from light brown to white and the opacity of the gel increases.*

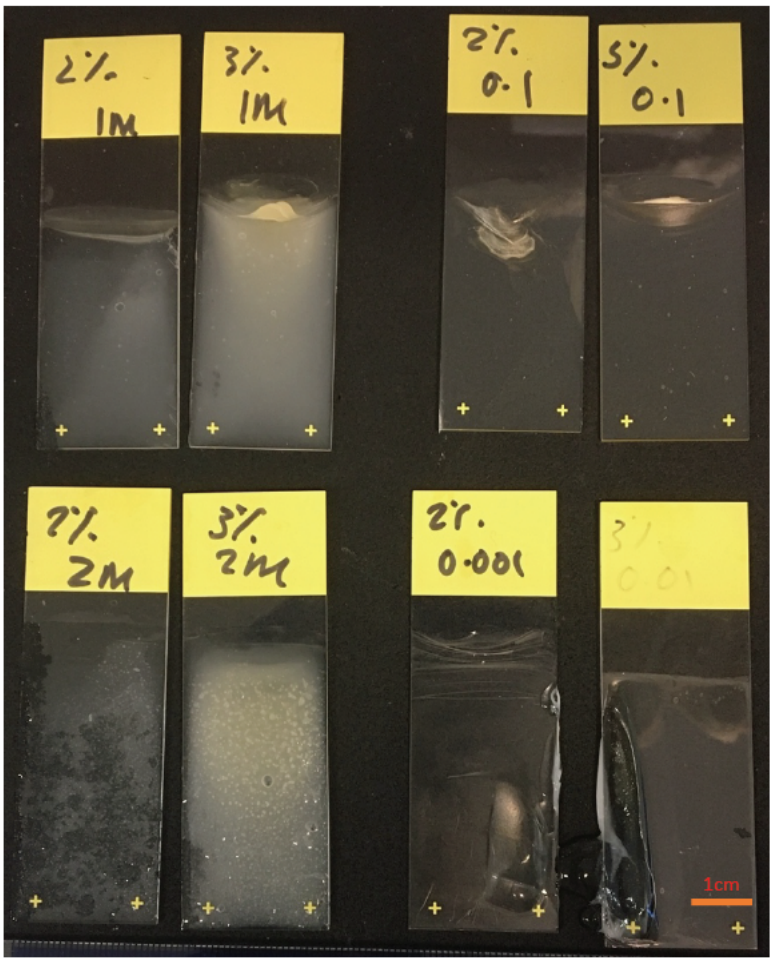

Figure 6.5: *From top left to bottom right – 2% and 3% chitosan gels crosslinked for 24 hours with 1M, 0.1M, 2M or 0.001M HMP. The opacity of the gels increased both with chitosan content and HMP concentration.*

transparent and brittle in comparison with the films prepared with the higher concentrations of HMP, at both 2% and 3% chitosan. The films prepared with 0.1M and 0.001M HMP broke once removed from the glass slides and could not be subject to further testing.

6.3.3 Viscometry - Shear Stress Ramp

Viscometry is used to determine the viscoelastic properties of a formulation, revealing possible structural changes in a formulation, and providing an indication of the behaviour of a gel under shear conditions such as blinking. When Gellan with added HMP or NaCl underwent a shear stress ramp (Figure 6.6), each showed a shear thinning profile, maintaining a peak shear viscosity at lower shear stresses (up to the range of 10^1 Pa), before shear viscosity then rapidly decreases with incremental increases in shear stress. This creates a characteristic shear stress profile, with a 'cliff' shape – a flat top followed by a steep drop, representing the yield stress of the material. gellan with no additives also has a shear thinning profile, but the gradient of the thinning (the decrease in shear viscosity at each increase in shear stress) is greatly reduced when compared to that of gellan with crosslinking additives.

The addition of HMP and NaCl to the gellan gels appeared to induce increases in shear viscosity up to and including 0.04M in both. In both groups the peak shear viscosity at low shear rates was ~1000 Pa S at 0.02M and ~10000 Pa S at 0.04M. Gellan + NaCl consistently maintained or increased this peak shear viscosity at shear stresses $<10^1$ Pa as NaCl concentration continued to increase. Gellan + HMP, however, did not maintain this peak shear viscosity as HMP concentration rose. From 0.06M HMP and

onwards there is a steady decline in the shear viscosity of gellan + HMP across all shear stresses, but most noticeably in the 'cliff top' peak achieved at pre-yield stresses. This peak dropped to the range of 10^3 Pa S at 0.1M and was only maintained up to the range of 10^1 Pa at 0.08M.

At 0.06M there is a noticeable difference between gellan + HMP and gellan + NaCl, with the yield stress of gellan + HMP decreasing, represented by poorer maintenance of the peak viscosity value at low shear stresses in comparison to gellan + NaCl. Gellan + NaCl however, mostly maintains the maximum peak viscosity even as NaCl concentration continues to increase.

At 0.06M in the HMP group and 0.08M in the NaCl group, each formulation had developed a middle 'step' in the shear profile, representing an intermediate yield stress or two yield points. In the gellan + HMP formulations, this middle 'step' becomes more pronounced as the peak shear viscosity drops and the initial yield point recedes.

Alternatively, Alginate shows a shear thinning profile (Figure 6.7), with shear viscosity decreasing gradually with increasing shear stress – from just below 10^1 Pa S to just below 10^1 Pa S. Increases in HMP concentration decreased the shear viscosity of the alginate gradually, with each increase in HMP concentration decreasing the average shear viscosity until the highest concentration of 0.1M HMP, which shows the lowest shear viscosity values (consistently in the range below 10^1) at the respective shear stresses.

Chitosan gel with 0% HMP addition shows a shear thinning profile, with shear viscosity steadily decreasing with increasing shear stress – from 10^1Pa S to 10^2 Pa S (Figure

6.8). At 0.01M HMP there is a dramatic increase in shear viscosity, with the peak shear viscosity at low shear stress reaching close to 10^4Pa S. With subsequent increases in HMP addition, the peak shear viscosity of the chitosan continues to increase, and the threshold for the drop in shear viscosity, representing shear thinning, occurs at higher shear stresses.

When average shear viscosity values across the entire shear stress ramp test are compared at each concentration of HMP in each material, the differences in the response to HMP addition can be shown. Chitosan shows increasing shear viscosity with HMP addition. Gellan shows an initial increase in average shear viscosity with HMP addition, followed by a steady decrease. Alginate shows a consistent and steady decrease in average shear viscosity as HMP is added (Figure 6.9).

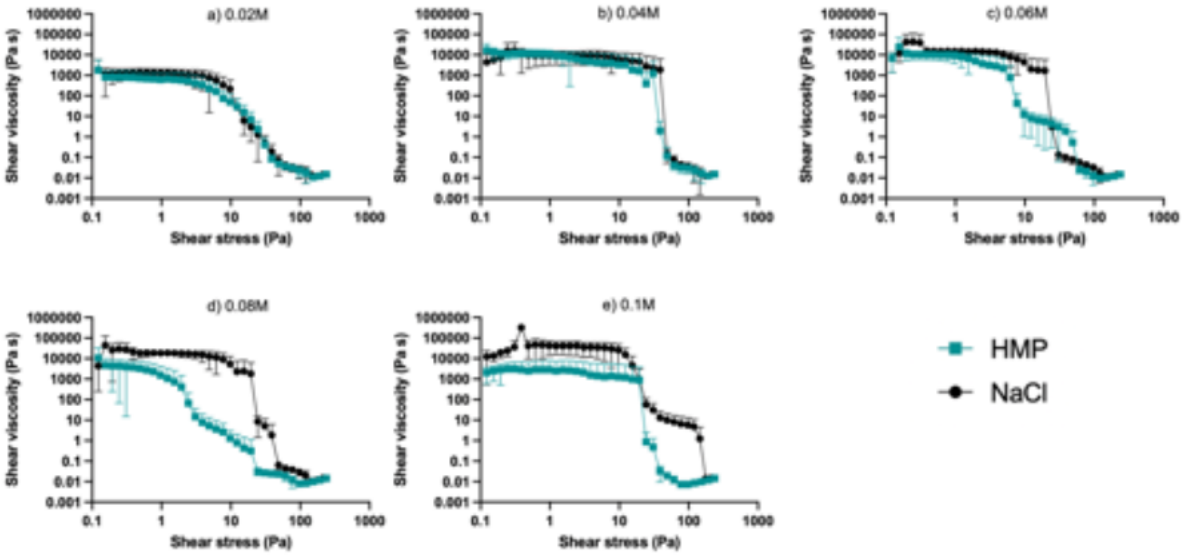

***Figure 6.6**: The shear stress ramp viscometry assessment, presented as Shear Viscosity (Pa S) over Shear Stress (Pa) for 1% Low-Acyl Gellan and HMP (green/square) or NaCl (black/circle) at a concentration of a) 0.02M, b) 0.04M, c) 0.06M, d) 0.08M and e) 0.1M. Test performed at a temperature of 32ºC. The profiles of each material (HMP vs NaCl) show similar trends until 0.06M, where the shear viscosity of Gellan + HMP falls compared to Gellan + NaCl. Error Bars = Standard Deviation (SD).*

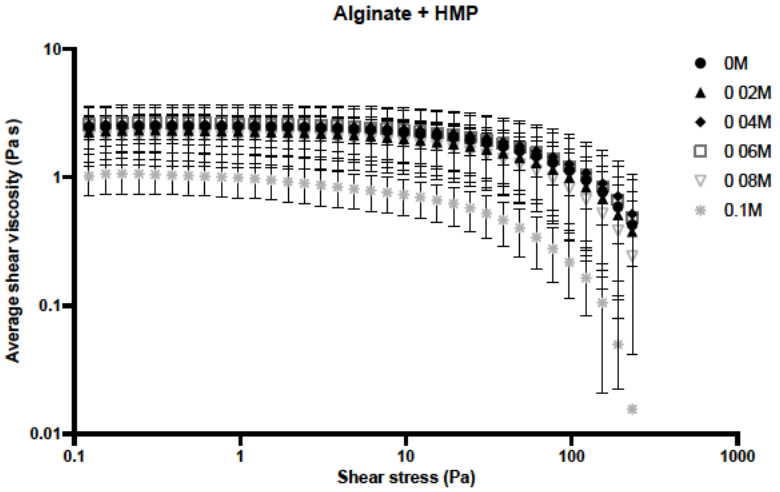

***Figure 6.7:** The shear stress ramp viscometry assessment, presented as Shear Viscosity (Pa S) over Shear Stress (Pa) for 2% Na-Alginate and HMP. Test performed at a temperature of 32ºC. As the concentration of HMP in the formulation increases, the average shear viscosity decreases across all shear rates. Each formulation shows a shear thinning profile independent of HMP concentration. N=4. Error Bars = Standard Deviation (SD).*

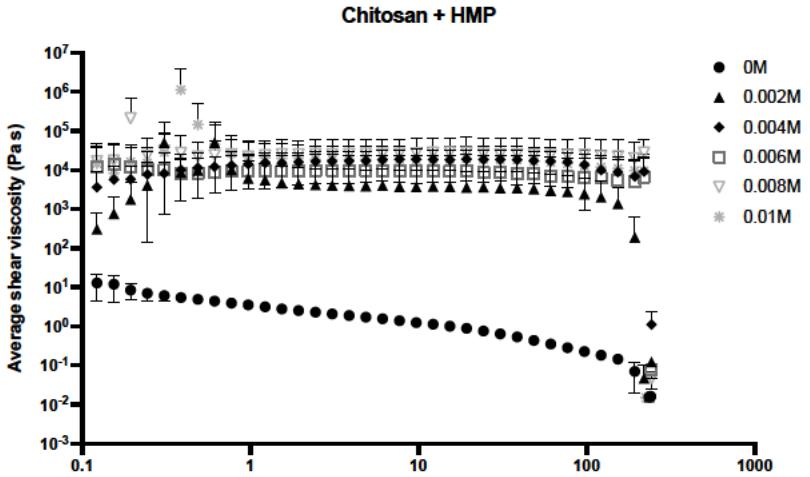

Figure 6.8: *The shear stress ramp viscometry assessment, presented as Shear Viscosity (Pa S) over Shear Stress (Pa) for 2% medium chain length chitosan in 1% aqueous acetic acid with increasing concentrations of HMP. Test performed at a temperature of 32ºC. As the concentration of HMP in the formulation increases, the average shear viscosity increases across all shear rates. Each formulation below 0.06M HMP shows a shear thinning profile, however at concentrations above this shear thinning is not apparent at these shear rates. N=6. Error Bars = Standard Deviation (SD).*

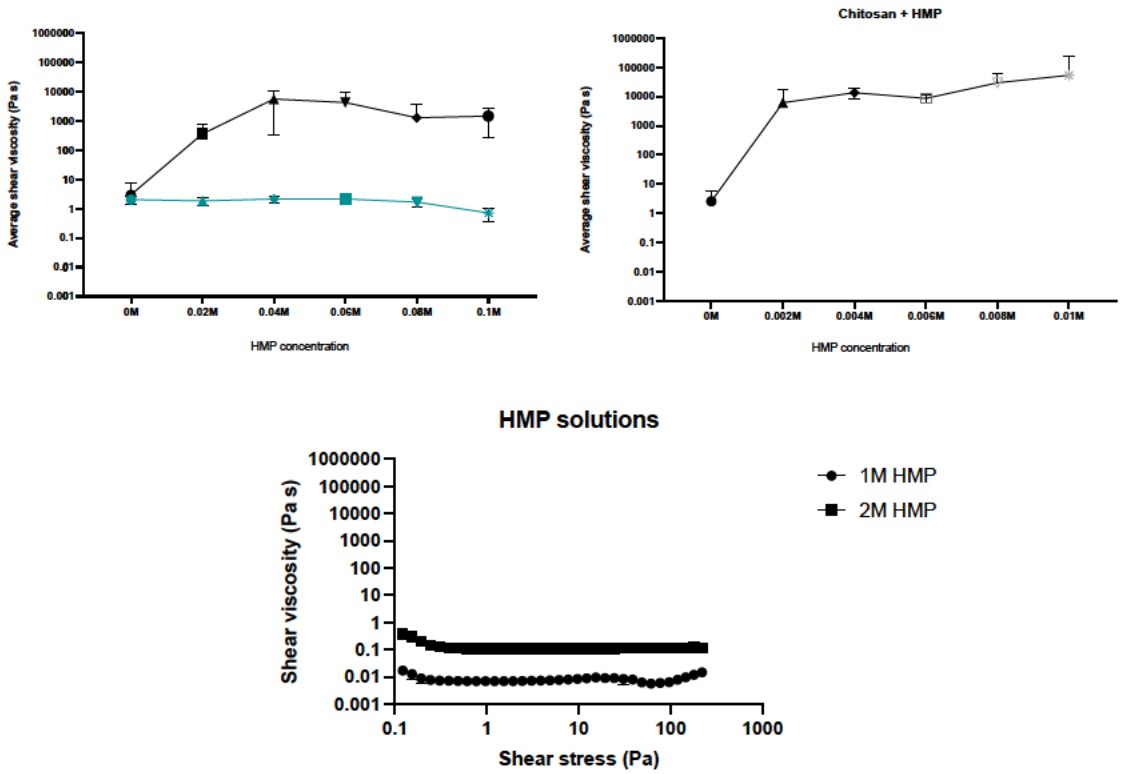

Figure 6.9: *When the average shear viscosity for each material (32ºC) is compared across HMP concentration, the differences between in material are displayed. Alginate (Top Left; Green) presents the lowest average shear viscosity of the three materials tested, with shear viscosity decreasing with HMP concentration. Chitosan (Top Right) shows the highest, increasing with HMP addition. Gellan shows a biphasic response, with shear viscosity increasing up to a point then beginning to decrease with HMP addition. The shear viscosity of HMP alone (Bottom) is included for reference.*

6.3.4 Submersion of Gellan in HMP and NaCl

The shear stress ramp revealed that addition of HMP to gellan appears to reduce the shear viscosity of the formulation. There are multiple ways in which the addition of HMP could disrupt the structure of the gellan fluid gel. To investigate whether the HMP degrades the gellan itself, samples of gellan 'cells' with and without NaCl pre-crosslinking were placed in 1ml of HMP (0.125M-1M) or NaCl (1M) for 48 hours, each sample formed a robust crosslinked gellan pellet (Figure 6.10). There was an observed difference in the size of the pellets, both across the two starting materials (crosslinked or non-crosslinked) and across the solutions into which they were placed.

The pre-crosslinked gellan fluid gel had formed the characteristic gellan particles pre-submersion (Figure 6.10). These were relatively irregular in their size and therefore there was a greater variation within each group, however with this accounted for, in both the Gellan and pre-crosslinked Gellan + 20mM NaCl groups, there was a noticeable decrease in the final size of the pellets as HMP concentration increased. In the pre-crosslinked group, the 1M NaCl submerged pellets were the largest, however this was not the case in the non-crosslinked group.

The key finding of this assessment was that exposure to HMP alone was not sufficient to decrease the shear viscosity of the gellan, instead creating a crosslinked, rubbery pellet.

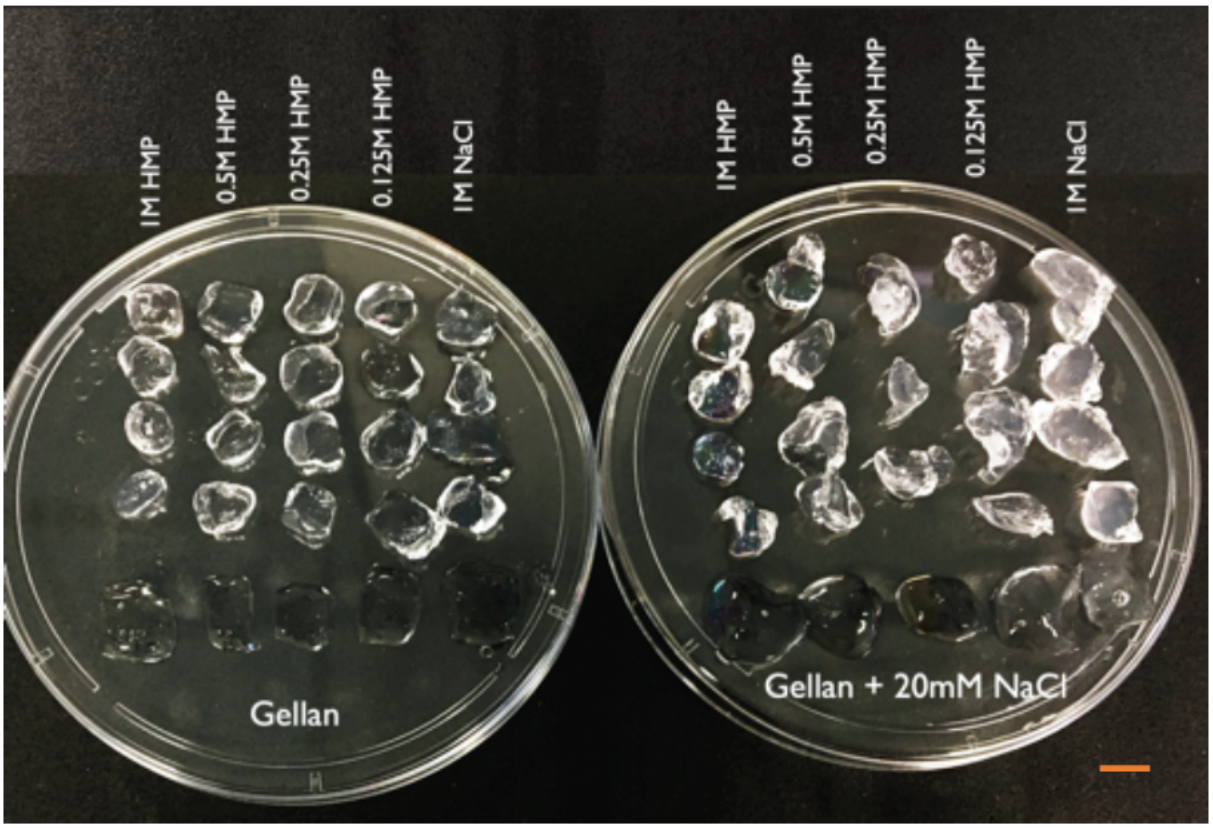

Figure 6.10: Samples of gellan and gellan prepared with 20mM NaCl after 48 hours submersion in (from left to right each side) 1M HMP, 0.5M HMP, 0.25M HMP, 0.125M HMP and 1M NaCl. in both the Gellan and Gellan + 20mM NaCl groups there is a noticeable decrease in the final size of the pellets as HMP concentration increased. Scale bar = 1cm.

6.3.5 Oscillatory stress sweep test with LVER determination

Prior to further characterisation of polymer films, it is key to determine the limit of the viscoelastic region – the maximum strain that a material can experience before it no longer behaves in a viscoelastic manner and the structure of the material changes or is damaged irreversibly, meaning stress is not absorbed but is causing transformations in the material.

The oscillatory stress sweep test revealed the LVER in each chitosan material (Figure 6.11). For both groups it was determined that a shear strain of 1% was within the LVER, therefore this was the parameter used for the following tests. The films formed with 2M HMP presented with a greater average shear stress at LVER compared with those prepared with 1M HMP – 28.5 Pa vs 11.5 Pa respectively.

6.3.6 Fixed strain Frequency Sweep analysis

The frequency sweep test revealed differences between the two formulations (Figure 6.12). At each frequency, both the elastic and viscous shear modulus was higher in the 2M HMP/chitosan compared to the 1M HMP/chitosan. There was also a greater difference between the two complex modulus components in the 1M group than the 2M group, which appeared to be due to a further drop in the viscous component of the 1M group.

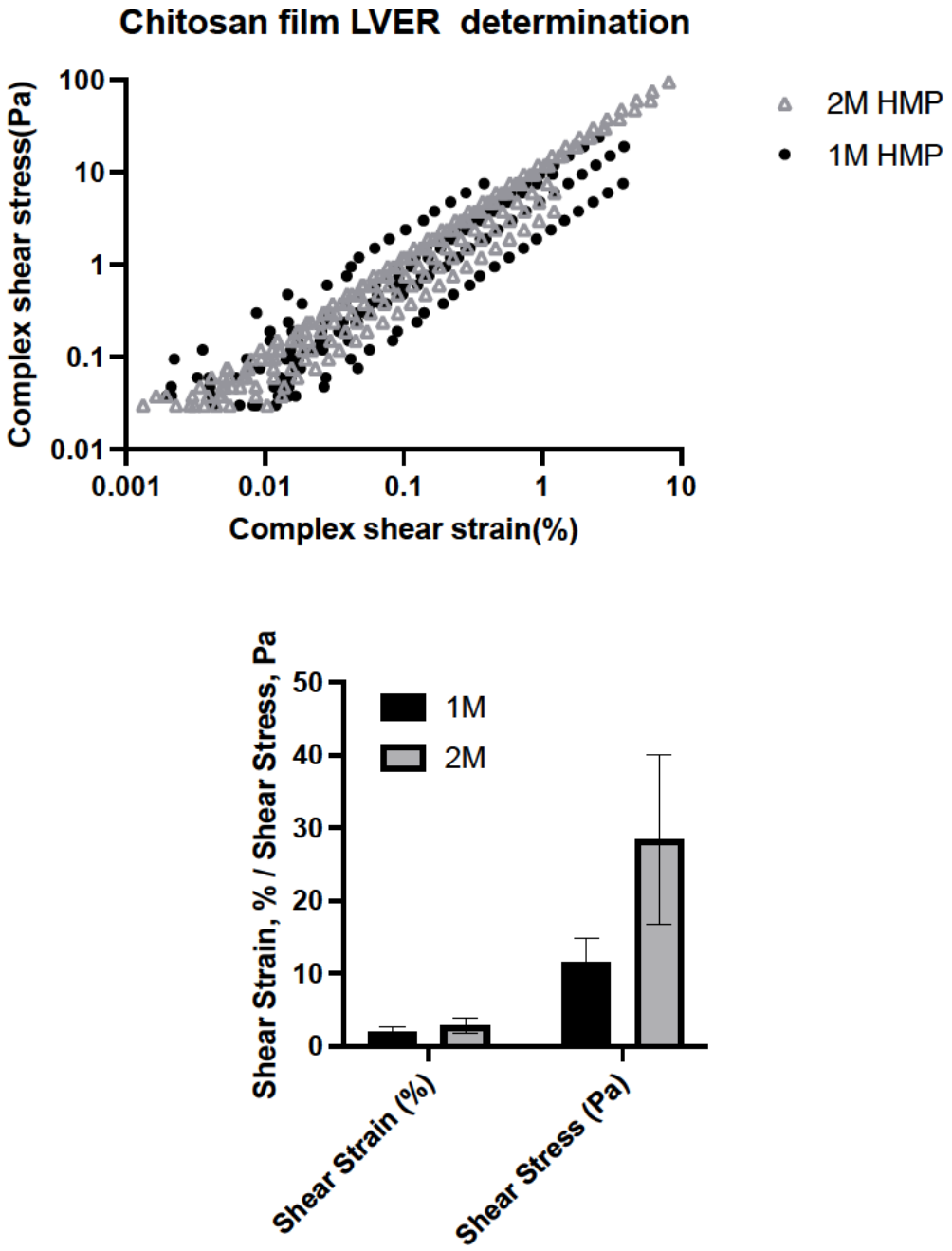

Figure 6.11: The results of the Oscillatory Sweep Test of chitosan films formed with 1M and 2M HMP, a) presented as complex shear stress (Pa) vs complex shear strain (%) and b) the calculated LVER for each group. Tests performed at a temperature of 25ºC.The 2M HMP group showed a higher stress limit of the LVER at 28.420Pa (±33.16) compared to the 1M group at 11.535Pa (±8.19). N=6. Error Bars = Standard Error of Mean (SEM).

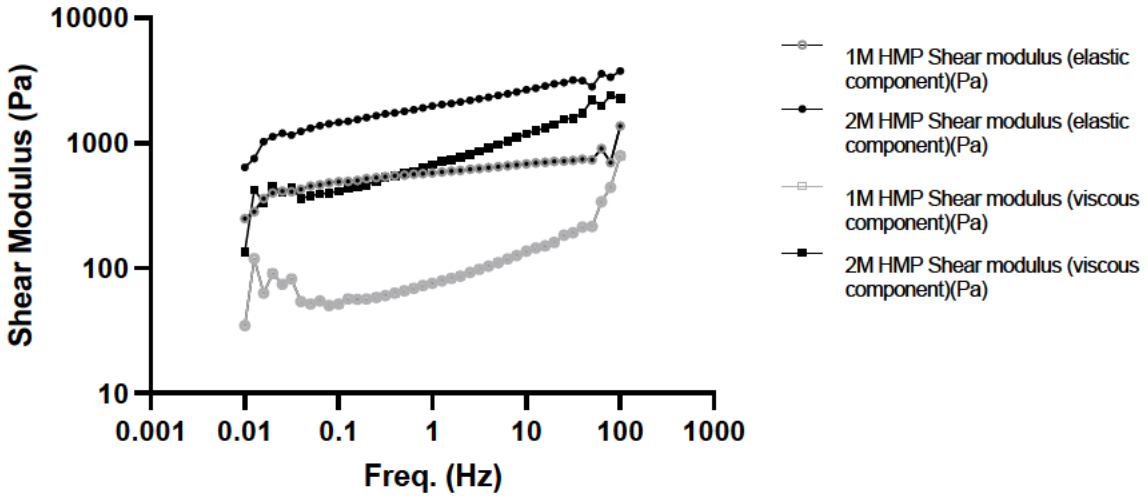

Figure 6.12: The results of the fixed strain frequency sweep test presented as shear modulus (Pa) over Frequency (Hz) for chitosan films formed with 1M and 2M HMP. Test performed at a temperature of 25ºC. At each frequency, both the elastic and viscous shear modulus was higher in the 2M HMP/chitosan compared to the 1M HMP/chitosan. N=6. Error Bars = Standard Error of Mean (SEM).

6.3.7 Developing a toluidine Blue O HMP release assay

Key to determining the optimum delivery material for a topical dose of HMP to the ocular surface, is determining which materials can deliver the appropriate concentration of HMP in the given time. In order to simply and safely measure HMP release, a colorimetric assay can be developed using toluidine blue O dye.

On visual inspection the reaction between toluidine blue and HMP creates a blue to purple shift. When the absorbance of the toluidine blue without added HMP was read, it was shown to have a characteristic curve, with a major peak at 580nm and a minor overlapping peak at between 630nm and 640nm (Figure 6.13). This suggests that the dye strongly absorbs light within the yellow (590-565nm) and red (625-700nm) wavelengths. This therefore explains the blue appearance of the dye under white light. HMP addition creates a shift in the absorbance spectrum, with the peak occurring between 590nm (lower concentrations of HMP) and 550nm (higher concentrations of HMP), indicating a shift to absorb more green light with increasing concentrations of HMP. There is also a reduction in the absorbance of red light, as the minor peak at 630-640nm is lost. This change in the absorbance spectrum corresponds to the change in the colour under white light, which appears to shift from blue to purple.

There is additional variance between the spectra of toluidine blue + HMP of different concentrations. At lower concentrations of HMP the absorbance at the peak wavelength appears to generally be much lower than that of higher concentrations This corresponds to visual assessments of it being ‘lighter’ in colour. The absorbance at the peak wavelength appears to increase with increasing HMP concentration.

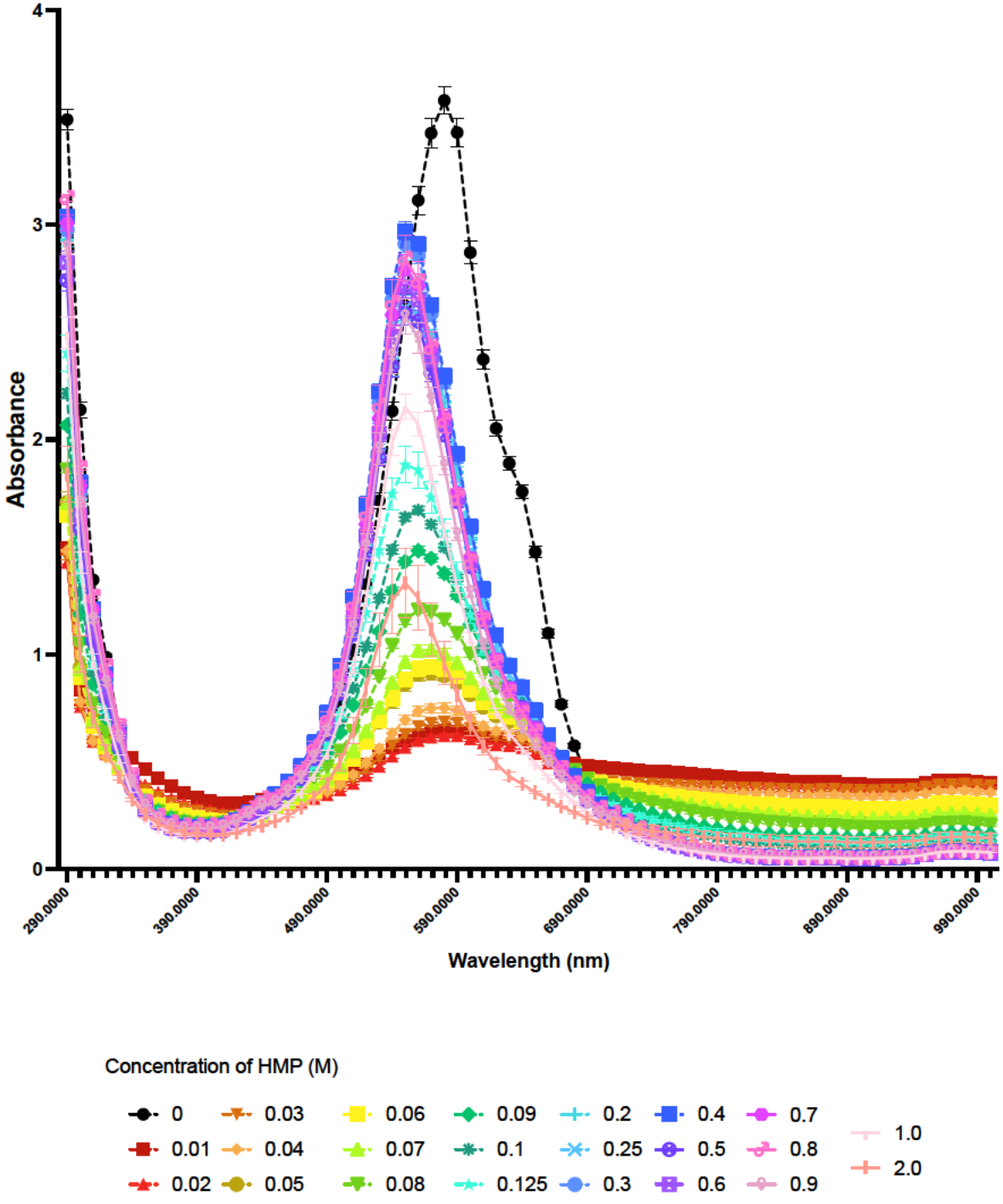

Figure 6.13: The spectra of toluidine blue O dye with various concentrations of HMP (0-2% w/v), measured at wavelengths between 290nm and 1000nm. Toludine blue O alone (Black) has a characteristic curve, with a major peak at 580nm and a minor overlapping peak at between 630nm and 640nm. HMP addition creates a shift in the absorbance spectrum, with the peak occurring between 590nm (lower concentrations of HMP) and 550nm (higher concentrations of HMP). N= 11. Error Bars = Standard Deviation (SD).

A correlation analysis was performed between absorbance values and HMP concentration at each wavelength. Despite the shift of the peaks occurring between the wavelengths of 590-550nm, the correlation analysis reveals that readings at 690nm have the highest correlation to HMP concentration (R^2= 0.5595, p = <0.0001), relating to the absorbance of red light.

This spectral shift presents several opportunities for assessing the HMP concentration in samples. At any HMP concentration there appears to be a peak shift, and the size of this shift is an indication of HMP concentration, with a greater shift indicating greater HMP concentration. Secondly, lower absorbance values at the peak correspond with lower concentrations of HMP, and higher absorbance values with higher concentrations of HMP.

Additionally, readings at the wavelength 690nm have a high correlation to HMP concentration (Figure 6.14a and 6.14b). Therefore, it is logical to assume a formula could be developed including the terms peak wavelength, absorbance reading at peak wavelength, absorbance at 690nm. When (peak wavelength * absorbance reading at peak)/absorbance at 690nm was plotted against HMP concentration, a curve was produced (Figure 6.14c and 6.14d) with which the absorbance spectra of toluidine blue samples could be used to predict HMP concentration at concentrations between 0.01 and 0.2M HMP. At concentrations above 0.2M HMP, the curve flattens and the difference between concentrations becomes indistinguishable.

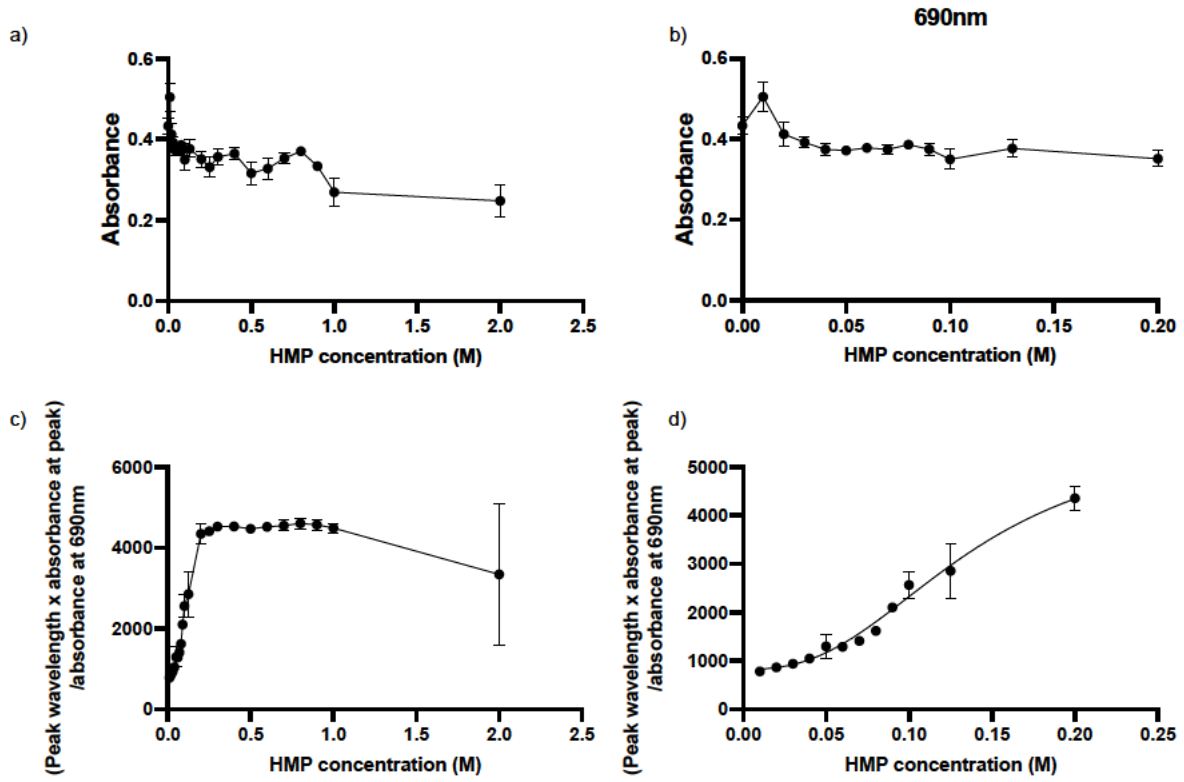

*Figure 6.14: a) The measured absorbance at 690nm of Toludine blue O dye with various concentrations of HMP from 0 to 2M. b) The measured absorbance of Toludine blue O dye with various concentrations of HMP from 0 to 0.2M. c) (peak wavelength * absorbance reading at peak)/absorbance at 690nm against HMP concentrations from 0 to 2M. d) (peak wavelength * absorbance reading at peak)/absorbance at 690nm against HMP concentrations from 0 to 0.2M. Error Bars = Standard Deviation (SD)*

6.3.8 Measuring HMP release – toluidine blue assay

The developed toluidine blue O assay was then used to analyse samples of water into which the alginate and chitosan delivery materials would have released their carried HMP. The absorbance readings of the combined toluidine blue/chitosan release media showed the spectral shift that is indicative of HMP release. This steadily increased with release time until a peak at 360 minutes (Figure 6.15). The absorbance readings at 360 minutes corresponded to concentration of 0.2M HMP on the generated curve. The corresponding concentrations of HMP to the absorbance readings at each time point are recorded in table 4.1.

The absorbance readings of the combined toluidine blue/alginate release media also showed the spectral shift that is indicative of HMP release. This again increased over time, with a final peak which corresponded to a HMP concentration of 0.145M HMP at 360 minutes (Figure 6.16). The corresponding concentrations of HMP to the absorbance readings at each time point are recorded in table 4.2.

6.3.9 Measuring HMP release – hydroxyapatite demineralisation assay

In addition to the colorimetric detection of HMP release, the released HMP also need to be effective at demineralising hydroxyapatite. When the release assays were repeated using hydroxyapatite sol instead of toludine blue O (Figure 6.17), contrasting results were recorded. The alginate group showed a significant decrease in the absorbance of the HA sol at each time point, indicating significant demineralisation ($p=0.0008$). In the chitosan group, no decrease in absorbance was measured at any time point, suggesting no demineralisation occurred.

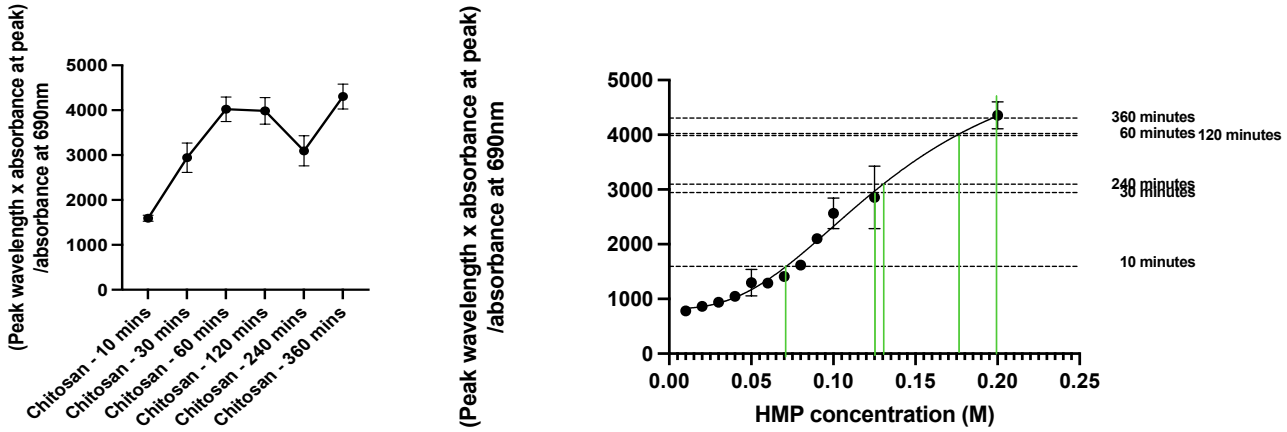

*Figure 6.15: The absorbance readings of the combined toluidine blue/chitosan release media, a) plotted as (peak wavelength * absorbance reading at peak)/absorbance at 690nm, N=10 and b) the average for each time point compared to the standard curve. Error Bars = Standard Error of Mean (SEM).*

	Release concentration (M/l)
10 mins	0.07
30 mins	0.125
60 mins	0.175
120 mins	0.175
240 mins	0.13
360 mins	0.2

Table 4.1: The interpolated HMP release concentrations (M/l) of the chitosan films at each time point

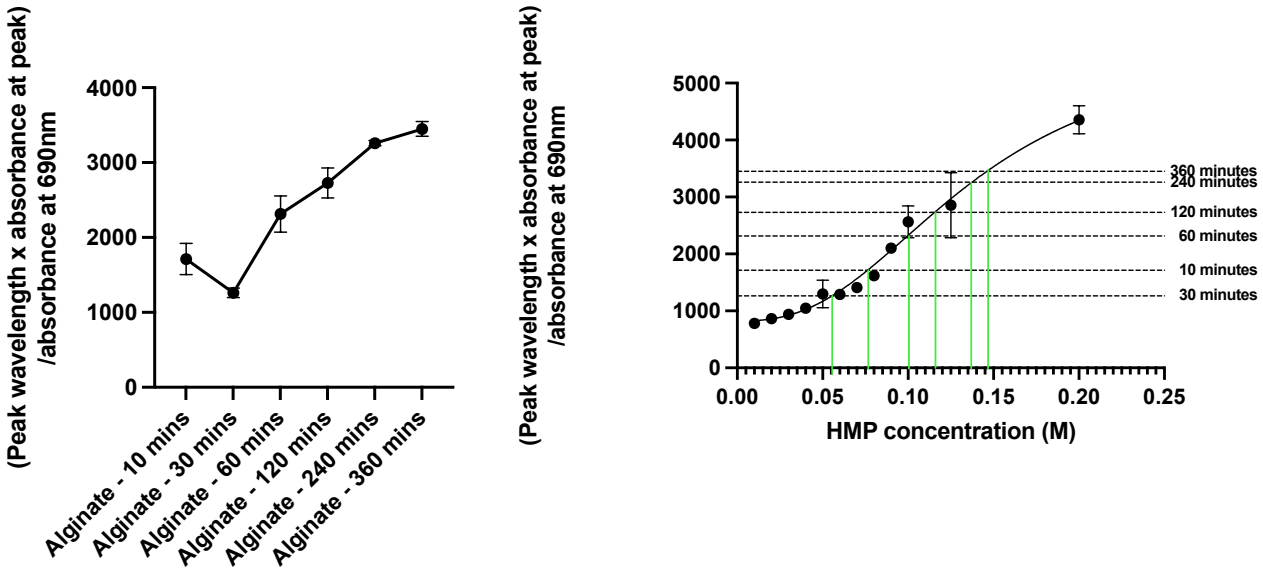

*Figure 6.16: The absorbance readings of the combined toluidine blue/alginate release media, a) plotted as (peak wavelength * absorbance reading at peak)/absorbance at 690nm, N=10 and b) the average for each time point compared to the standard curve. Error Bars = Standard Error of Mean (SEM).*

	HMP release (M)	% of maximum
10 mins	0.055	33.000132
30 mins	0.075	45.00018
60 mins	0.1	60.00024
120 mins	0.115	69.000276
240 mins	0.135	81.000324
360 mins	0.145	87.000348

Table 4.2: The interpolated HMP release concentrations (M/l) of the alginate at each time point

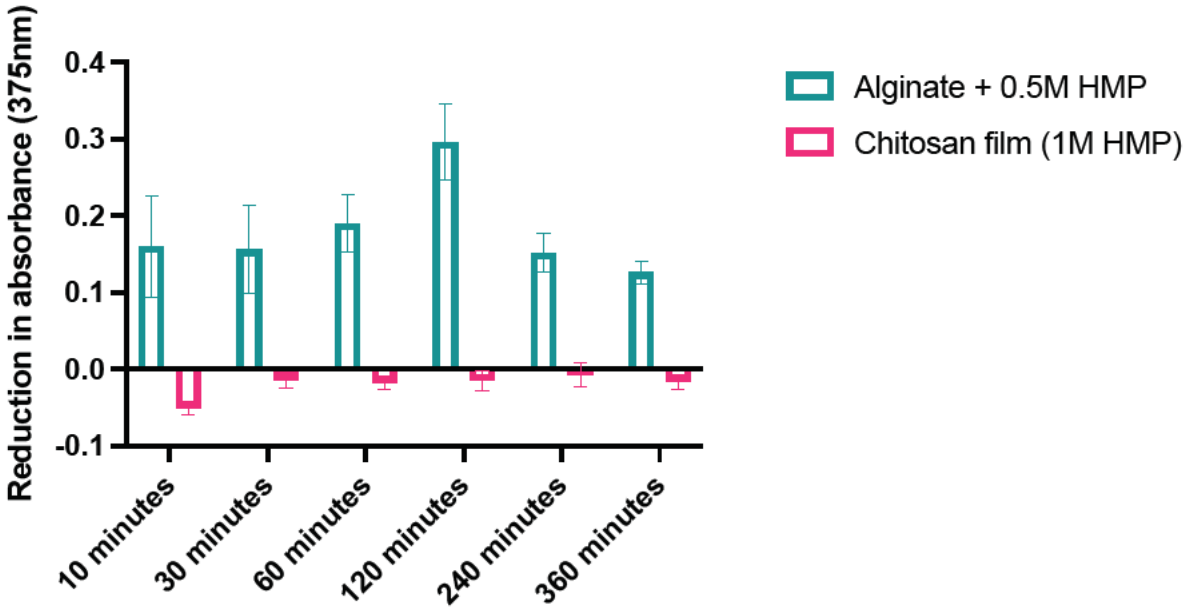

Figure 6.17: the reduction in absorbance, representing demineralisation, of hydroxyapatite sol after 1 hour incubation with release media from alginate+0.5M HMP or chitosan film made with 1M HMP at time points (release) from 10 minutes to 6 hours. The alginate+0.5M HMP showed significant reduction in absorbance (p=0.0008), however no reduction in absorbance was achieved in the chitosan group. Error Bars = Standard Error of Mean (SEM).

6.3.10 Formulation contact angle

Changes in viscosity, surface tension and surface chemistry effect the 'wetting' of applied eye drops relative to the surface of the eye – i.e. how easily blinking and natural flow spread an eye drop across the eye's surface [192-194]. The surface tension of an eye drop formulation, which is directly linked to the contact angle, has also been highlighted to have an important relationship with the drop size, and its consistency over multiple applications [195, 196]. It is therefore a useful comparison to measure the contact angle of the HMP-polymer formulations and HMP-alone solutions.

Of the three formulations tested, 1M HMP had the largest contact angle, significantly greater than Alginate/0.5M HMP ($p=0.0004$) and HBSS ($p<0.0001$) with a mean of 34.75° (Figure 6.18). The alginate/0.5M HMP formulation had a slightly larger average contact angle than the HBSS control at 21.7° vs 18.19° respectively, however this was not statistically significant.

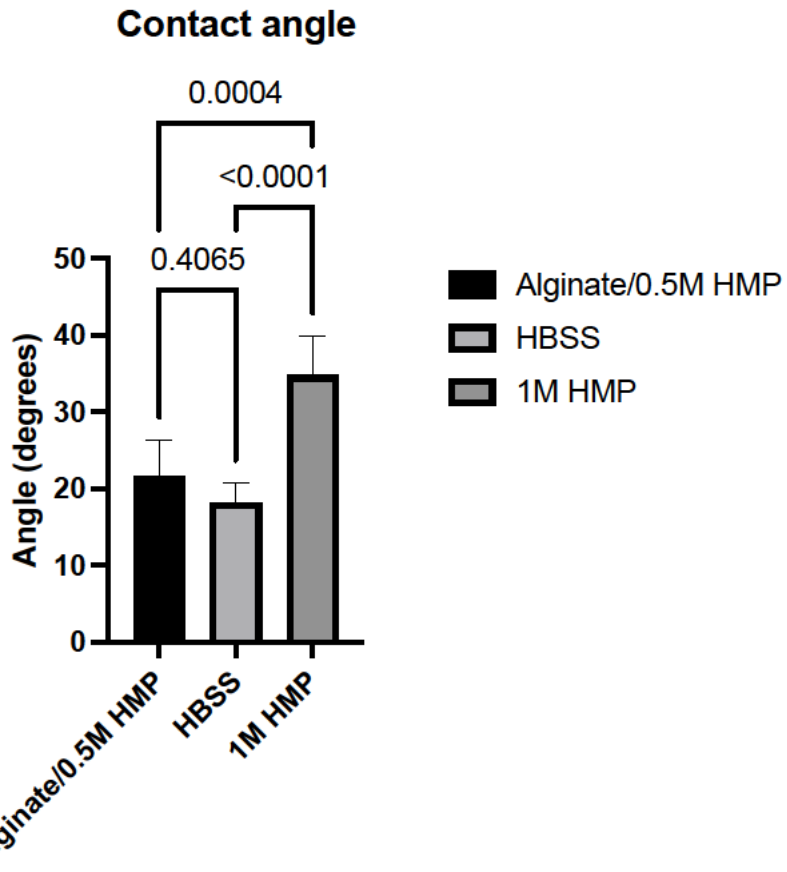

Figure 6.18: The average contact angle of each formulation when applied to the anterior ocular surface of a fresh porcine eye. Groups were compared using a one-way ANOVA. The average contact angle of the 1M HMP group was significantly higher than that of the HBSS control ($p<0.0001$). N=3. Error Bars = Standard Error of Mean (SEM).

6.4 Discussion

Each of the polymeric materials examined – gellan, alginate and chitosan - presented a different reaction to HMP addition, with gellan and chitosan appearing to crosslink with the addition of HMP, increasing in viscosity, and alginate appearing to decrease in viscosity as HMP is added.

i) Gellan

The rheological assessment appeared to reveal equal degrees of crosslinking in each Gellan formulation upon initial addition of NaCl or HMP. Crosslinking can be assumed to be represented by an increase in the shear viscosity (peak) at shear stresses up to around 10^1 Pa. Both NaCl and HMP appeared to crosslink the gellan, most likely because both solutions would provide sodium (Na^+) ions with which the gellan can crosslink. However, the relative increases in viscosity do not directly correspond with the predicted amount of sodium available in each solution – 0.04M HMP should deliver six times the equivalent amount of sodium in a 0.04M NaCl solution. There has been much disagreement over the last 7 decades as to the appropriate representation of the structure of sodium hexametaphosphate/grahams salt. The 6-phosphate ring structure remains prolific, despite widespread rejection of that hypothesis. The more likely composition of so called hexametaphosphate is many different linear short and long chain polyphosphates [246, 270]. This therefore changes the idea of molar concentrations of the salt solution, as there are many molecular weights present. It may be better to consider HMP solutions in their percentage weight/volume. In this case, 0.125M HMP would be 7.65%, 0.25M would be 15.29%, 0.5M would be 30.59% and 1M would be 61.18% in water. Without a clear idea of the molecular make-up of

the HMP solution, it is difficult to assume what concentration of free sodium should be available in any given solution, and therefore hard to compare with NaCl.

Up to and including the addition of 0.04M of each crosslinking agent, there appears to be no difference in the shear viscosity at pre-yield shear rates between the different formulations. The increase in concentration of NaCl or HMP from this point does not correspond with any significant further increase in the peak shear viscosity of the formulations. The NaCl formulations maintain this maximum shear viscosity at pre-yield shear rates, whereas the HMP formulations show a decrease as HMP concentration increases. This suggests that unlike NaCl, HMP is in some way disrupting the structure of the crosslinked gellan and reducing its viscosity at pre-yield shear stresses.

The peak shear viscosity of the HMP + gellan formulations never decreases as far as to be comparable to that of non-crosslinked gellan, suggesting there is not full disintegration of the crosslinked structure. Additionally, when both crosslinked (10mM NaCl) and non-crosslinked gellan were added to NaCl or various concentrations of HMP for 48 hours, each sample of gellan did not disintegrate, but crosslinked, becoming robust pellets. This is further evidence that it is not the crosslinks themselves that HMP disturbs as the peak pre-yield shear viscosity decreases.

The fluid gel created by crosslinking gellan with sodium under stirring is suggested to consist of many units or ‘cells’ of crosslinked gellan rather than one homogenous crosslinked system, which allows the fluid gel to retain fluid like properties such as flow. It is possible that HMP addition disrupts the interactions between these crosslinked

units. It is well documented that HMP is used as a deflocculant in ceramics processing, adsorbing to the surface of micelles present in kaolin dispersions and altering the rheological properties of said dispersions by disrupting the interactions between the micelles [290]. It is possible that HMP is playing a similar role as a deflocculant in the gellan fluid gel, disrupting the interactions between the gellan particles either through adsorption onto their surface, such as with kaolin, or through a different mechanism. It is therefore again important to note the differences in the response of gellan to increasing HMP addition, compared to that of increasing NaCl addition. It is possible that increased crosslinking density or increases in sodium availability alone are responsible for this behaviour, through saturation of crosslinking within the individual particles changing their surface chemistry and limiting inter-particle interactions. However, since the effect is much more pronounced in the HMP formulations, we would in turn expect a steeper increase in shear viscosity from 0M to 0.04M addition in the HMP formulations compared to the NaCl formulations, as they would reach the threshold crosslinking density faster.

Further to the rheological analysis, there is a noticeable change in the optical properties of gellan as the HMP and NaCl content increases. Crosslinked gellan fluid gel as prepared prior to HMP addition is optically transparent, with the same refractive index as water, allowing it to ‘disappear’ when immersed. However, as HMP is added the gellan loses its transparency and becomes cloudy. This becomes noticeable at around 0.04M addition, which correlates to the appearance of the middle ‘step’ (second yield point) in the rheological profile of the gellan. In addition to the suggestion that HMP anion could be in some way disrupting the relationship between the sodium-crosslinked gellan units, this change in the rheological profile and the change in optical

properties could also indicate an introduction of an interstitial phase by the HMP between the gellan units. This phase may in part consist of the polyphosphate chains themselves and may cause the repulsion of the gellan particles.

For the context considered within this thesis, the optical properties of the drop are of lesser importance, as the vision of those with BK is already greatly compromised, so use of a non-transparent agent could be considered. However, due to the structural changes occurring within the gellan, and the resulting 'grainy' texture, the formulation would be uncomfortable on the surface of the eye and is therefore unsuitable.

ii) Alginate

The sodium alginate gels did not crosslink with HMP addition, instead decreasing in shear viscosity as HMP addition increased. There was not a dramatic change in the shear viscosity profile of alginate as HMP was added, and the alginate largely retained the same flow properties. This could allow alginate to act as a suitable carrier for HMP as an eyedrop. However, previous investigations into the use of alginate gels with chelating agents, with the aim of improving drop retention and corneal permeability, found that there was no benefit to drug delivery of using alginate alone, or alginate with the agent. There was also evidence to suggest the alginate gel inhibited the action of the chelating agent [219]. Further investigation is therefore necessary to determine whether alginate improves the retention and performance of HMP on the ocular surface. This investigation also found an upper tolerance of HMP within alginate gels, as the alginate + 1M HMP appeared to separate. This is a limit to the transportation capacity of alginate gels, and may therefore be a limit to the demineralisation possible with an alginate formulation.

iii) Chitosan

Similarly to Gellan, chitosan crosslinks with HMP addition. As chitosan carries the opposite charge to gellan, the crosslinking mechanism is different, with chitosan interacting with the negative HMP molecule rather than the positive sodium ion. It is thought that chitosan and HMP undergo ionotropic gelation. This creates a much stiffer gel, hence why $1/10^{th}$ the concentration of HMP is required to create a crosslinked chitosan gel with the same shear viscosity of gellan + HMP. The crosslinked chitosan gel does not have appropriate properties for an eye drop, however the formulated gels offered a potential alternative delivery mechanism in the form of topical films.

Ocular inserts in the form of hydrogel films present an attractive alternative to eye drops, due to the ability to simplify treatment regimens and increase drug retention. An obvious area for innovation is drug-eluting contact lenses [61, 104-106, 108, 359], however other biological films can also be used. Amniotic membrane transplants are already used in some cases to expediate the wound healing post-superficial keratectomy for band keratopathy [21, 378, 379].

The results of the mechanical testing of the chitosan films followed an expected trend, with the Shear modulus of the films increasing with the HMP concentration with which they were crosslinked. The films formed at the lowest concentrations of HMP were fragile, and could not be removed from the glass slides for testing. The gels formed with 1M and 2M HMP were more robust when handled and subjected to further analysis. This quantified the observed changes, with an increase in shear modulus as the formulation concentration of HMP increased from 1M to 2M. This is likely to

represent an increase in the crosslinking density of the gels as HMP concentration increases. However, as 2M HMP is a highly saturated solution, there may also be a degree of dehydration which is impacting the properties of the gel. This could be further examined by hydrating the gels in solutions of different osmolarity and repeating the assessments.

iv) HMP release testing

The release assessments of the chitosan films revealed that an effective dose of HMP was not released from the films formulated with either 1M or 2M HMP. This was confirmed by the hydroxyapatite demineralisation assay. The toluidine blue O assay indicated the release of a reagent from the films into the solution, which when compared to the control values suggested HMP at a concentration of 0.2M. However, this was rejected by the mineralisation data.

The development of the toluidine blue assay was attempted in an effort to simplify the methods available for analysing the presence and concentration of HMP in a sample. The assay works most effectively in a sequence of two steps – identifying a spectral shift that corresponds with the presence of HMP, then appropriately quantifying the size and shape of that shift to estimate the HMP concentration. When considering HMP alone in a controlled way, the assay was effective, however when in combination with other materials and ions it became much harder to distinguish between the detection of HMP and the detection of other species. Although it cannot be used as a direct method of quantification, the demineralisation release assay is a much more relevant release assay protocol for the context under consideration. When the results of the two

assays were compared, it became clear that in the case of the chitosan films, an effective does of HMP was not released within the given time. It is likely that due to the reaction between chitosan and HMP to form crosslinks within the gel, that insufficient free HMP remained for the purposes of demineralisation. The alginate, however, was effective in releasing a dose of HMP that caused demineralisation in the HA sol within one hour.

v) Contact angle measurements

When the contact angle of the formulations (alginate + 0.5M HMP, 1M HMP and HBSS) were compared, 1M HMP had the highest average contact angle which likely responds to the highest surface tension and lowest 'wettability' of the drop. This is likely due to the low osmolarity of the solution, which is 61% Na-HMP w/v. The alginate formulation did have a larger average contact angle than that of the HBSS control, which suggests some viscosity is maintained compared to simple aqueous solutions. The shear stress ramp revealed that alginate formulations decreased in viscosity with HMP addition, likely due to the disruption of the tangled polymer network by repulsive anionic HMP molecules.

vi) Summary

The aim of the assessments carried out in this chapter is to establish whether the incorporation of HMP into an organic polymer gel would maximise the bioavailability of the delivered HMP and improve therapeutic efficacy. As a charged polymeric molecule, HMP elicited changes in the properties of the organic polymer gels, through the introduction of crosslinks or the disruption of the similarly-charged entangled polymer networks. Overall, these assessments revealed only one organic polymer/HMP

formulation which might present as a viable HMP delivery vehicle – sodium alginate gel. The alginate delivery material did not crosslink, creating a weaker gel than the other formulations, however this was more desirable than the crosslinked gels which developed heterogenous phases and became too stiff for the desired application.

7.

CREATING A MODEL OF BAND KERATOPATHY

7.1 General Introduction

Ocular toxicity testing has been established as an important step in ensuring consumer products are safe for use in the case of accidental ocular contact when used by the general public. This testing has largely taken the form of *in vivo* animal testing, such as the Draize test on rabbits [310], which involves administering 100µl of a test substance into the lower conjunctival sac of each rabbit and observing changes such as corneal clarity and ocular discharges for up to 1 week [380]. For multiple decades this testing has been endorsed by both industry and governments as necessary for ensuring public safety. However, concerns over the use of animals in research have pushed forward attempts to create more humane tests for such purposes. Additionally, the accuracy and cost of such testing has been called into question. As the scientific community moves away from animal testing unless absolutely necessary, the importance of developing relevant and accurate *ex vivo* and *in vitro* tests has been heightened. This shared effort and purpose has therefore greatly increased the number of ocular toxicity models available.

As a further step to reduce the unnecessary use of animals in research, various *ex vivo* tests make use of 'waste' tissue from commercial abattoirs – namely porcine and bovine eyes. Porcine eyes are a good surrogate for the human eye and various models have been established where the tissue can remain healthy for a prolonged period [381, 382]. This has also been achieved in rabbit and rat eyes, although these are not comparable in size and some structures differ to those of human eyes [383, 384].

In order to thoroughly assess both the ocular toxicity and therapeutic efficacy of HMP as a treatment for band keratopathy, a viable *ex vivo* band keratopathy model needs to be established. A review of *ex vivo* corneal models found in the literature revealed that most models maintain the corneal tissues in culture from 60 minutes up to 30 days (Table 5). The majority of studies sourced tissue from commercial food supply chains, most likely due to the ease and cost effectiveness. All models cited (Table 4) used fresh tissue that was processed within 24 hours of slaughter. The majority cultured the tissue in under 4 hours post-slaughter to maintain optimum tissue viability. All models excluded eyes with visual defects, and some assessed with fluorescein before dissecting also. Sodium fluorescein is the clinical standard test for assessing the ocular surface for damage. Most models (Table 5) included transporting the ocular globe in a balanced salt solution or PBS to prevent desiccation of the ocular surface before use, and some maintained lids or conjunctiva as an extra degree of protection. The ocular surface desiccates easily, and prolonged desiccation will lead to loss of epithelial cell viability and as a result, ocular barrier function, which is critical for ocular penetration or wound healing tests. A number of models alternatively froze the tissue to preserve it before use. This is not appropriate for all models, as freezing can compromise the fine tissue structure and there is a risk of freeze-burn if not done correctly.

For models which lasted less than 24 hours, no antimicrobial agents were listed in the preparation of the tissue, either as a washing step or as part of the culture medium (if used). This is likely due to the fact that infection would not have a significant impact on the results within that time frame, unless it was a pre-existing pathology which would have most likely presented as an ocular defect, leading to exclusion regardless. Many of these sub-24-hour tests were perfusion studies, looking at the permeation of a drug

or other substance through the corneal barrier. These assessments would require the corneal barrier to remain intact, which would factor into the shorter time periods for testing, as the tissue would lose viability and swelling might occur post 24 hours. Cultures which were established for longer periods introduced washing steps to the tissue preparation, most commonly with povidone iodine which replicates the common surgical procedure. In some cases, antibiotic/antimycotic washing steps were also included. Tissue from commercial sources poses a risk of infection, and in a laboratory environment these steps would be necessary to prevent infection of the culture and possible cross-contamination. For cultures lasting over 24 hours, the tissue was supplemented with medium, most commonly MEM or DMEM, supplemented with antibiotics, antimycotics and foetal bovine serum. Some models included dextran in the medium to reduce swelling of the corneas (corneal oedema). Cultures were incubated at temperatures between 32 and 37°C, representing the lower and upper limits of eye surface temperature and core body temperature. Cultures were also incubated with 5% CO_2 as is common tissue and cell culture practice. Media was either changed regularly or continuously supplied through perfusion. Maintaining a regularly supply of fresh nutrients is key to maintaining tissue viability, and renewal of antimycotic and antibiotic solutions is necessary for infection control. Where cultures were not submerged, artificial tears or media were regularly applied to the epithelial surface to prevent desiccation, and cultures were also maintained at high humidity (~95%) for the same purpose. Models used multiple methods to maintain the corneal tissue shape, either a modified artificial anterior chamber, a scaffold or by filling the anterior chamber with agar. For corneal wound healing studies, wound healing was most commonly evaluated visually with sodium-fluorescein. Some models included

regular swabs of the corneal surface and medium to check for infection, or analysis of the outflow medium to ensure the tissue was metabolising at a healthy rate.

Band keratopathy (BK) is characterised by the formation of opaque, grey/white mineral deposits in the cornea, most commonly just below the epithelial layer [11, 385]. BK is mostly commonly treated through a superficial keratectomy including EDTA chelation, however topical treatments are under investigation. At the time of writing, a clinical trial is underway investigating the use of twice-daily EDTA eye drops for BK treatment over a period of 6 months (ClinicalTrials.gov Identifier: NCT03985371). An *ex vivo* model of BK was previously inadvertently created by Schrage et al [383]. Using the established *ex vivo* eye irritation test, healthy *ex vivo* rabbit corneas were mineralised using phosphate buffered eye drops, further confirming the link between this formulation and cases of BK [383, 386, 387]. Some animals are known to develop band keratopathy, including horses, alpacas and dogs [11, 388-390], however trying to use naturally occurring cases to harvest tissue for testing would be unsustainable. The aim of the work presented in this chapter is to establish whether a combination of the tissue culture techniques previously deployed in successful corneal models could be used to develop an intentional model of band keratopathy, through which formulations could be tested for the potential to treat the disease.

Table 5: Published literature on the development of *ex vivo* corneal models for various tests, with their preparation, cleaning and maintenance steps outlined. Organised on length of test/culture time from shortest to longest

Title	Animal	Length of test	Transport Cleaning, preparation and maintenance
Depth- and direction-dependent changes in solute transport following cross-linking with riboflavin and UVA light in *ex vivo* porcine cornea [391]	Porcine	60 minutes	• Stored on ice or in moist chambers at 4 C. • Warmed to room temperature for 45 min pre-treatment. • Used within 12 hours post-mortem. • No disinfection or washing listed. • Only eyes with clear corneas that showed no signs of abrasion or opacity were used.
***Ex vivo* rabbit cornea diffusion studies with a soluble insert of moxifloxacin [377]**	Rabbit	3 hours	• Corneas stored in PBS for up to 1 hour pre-study • Eyeballs were rinsed with a saline solution.
***Ex vivo* permeation of erythropoietin through porcine conjunctiva, cornea, and sclera [392]**	Porcine	6 hours	• Collected from a slaughterhouse, kept refrigerated immersed in PBS, and 1 h later conjunctivas, corneas and scleras were surgically dissected
An *Ex Vivo* Evaluation of Moxifloxacin Nanostructured Lipid Carrier Enriched In Situ Gel for Transcorneal Permeation on Goat Cornea [393]	Goat	12 hours	• Eyes procured from catering supply chain. • Immediately stored in Krebs ringer solution. • Once dissected, tissue pieces were stored in Krebs ringer solution under −80 C.
A simple corneal perfusion chamber for drug penetration and toxicity studies [394]	Porcine	< 1 day	• Eyes were obtained from a local abattoir, transported to the laboratory at 4 C, and used within 2–3 hours of enucleation. • Corneas were perfused with BSS-Plus at a flow rate of 1 ml/min. • The perfusion chamber was heated to 35 C. • The corneal epithelial surface was kept moist by applying BSS-Plus eye drops every 20 minutes. • Excess fluid was removed through the drainage channel.
Bovine Cornea Opacity and Permeability Test: An in Vitro Assay of Ocular Irritancy [395, 396]	Bovine	8 hours+	• Eyes procured from local abattoir, transported Hanks Balanced Salt Solution. • The corneas were mounted into holders. Both chambers were then filled with MEM supplemented with 1% fetal bovine serum (FBS), and corneas were incubated for 1 hr in a water bath at 32 C.
1,25-dihydroxyvitami	Mouse	48h +	• Eyes were enucleated and stored in sterile PBS.

n D_3 inhibits corneal wound healing in an ex-vivo mouse model [397]			• Eyes were fixed with subdermal injection needles in a 24-well cell culture plate prepared with 500 µL paraffin, and kept submerged with PBS. • Post burn, eyes were incubated in DMEM/F12 (with stable glutamine) supplied with antibiotics (Gentamicin (10 µg/ml), Amphotericin B (0.25 µg/ml); without serum.
Corneal wound healing is modulated by topical application of amniotic fluid in an *ex vivo* organ culture model [379] and [398]	Rabbit	36 hours	• Eyes were enucleated immediately following euthanization and placed in 50 ml tubes containing Dulbecco Modified Eagle Medium, on ice. • A circular central epithelial defect was created on each cornea 2 hours post- enucleation. The sclero-corneal ring was excised leaving 3–5 mm of sclera. • The ends of laboratory test tubes were glued tightly concave-side down into each well using acrylic glue. Dulbecco Modified Eagle Medium with antibiotic/antimycotic solution (1/200) was then added to each well to just cover each dome (12 ml per well). • The sclero-corneal rings were placed in the culture plates to be incubated at 37C with 5% CO_2. Culture medium was changed once during the experiment.
An *ex vivo* cornea infection model [109, 399]	Rabbit	2 days+	• Frozen • 10% Povidone Iodine for 30 minutes in a sterile field, 5x wash with sterile PBS • The sterilized cornea is placed into a supporting mould, and is filled with soft agar.
***Ex vivo* injury model [400, 401]**	Rabbit	48 hours	• Stored overnight in DMEM and antibiotics during transit • Dissected corneas were placed anterior side down in a glass spot plate containing DMEM, and their endothelial side filled with melted 0.75% agar (50 C). • After the agar solidified, corneas were turned over and cultured at 37 C in a humidified 5% CO_2 incubator in a 12 well plate using DMEM (high glucose) containing 1× MEM NEAA, 1× RPMI 1640 vitamins, 0.1 mg/ml ascorbic acid and 0.01 mg/ml ciprofloaxin
***Ex vivo eye irritation test [402] [403]* [383]**	Rabbit	3 days	• Rabbit corneas obtained from slaughterhouse. • Corneas excised and placed in an artificial anterior ocular chamber. • Corneas are prepared and cultivated within 8 hours postmortem. • Chamber supplied with a culture medium containing Earle salts and HEPES buffer (Eagle minimal essential medium [MEM], HEPES buffer 5.8 g/L). • Medium was constantly replenished by a micropump with an entrance pH value of 7.4 ± 0.2 and a flow rate of 6.44 µL/min. • The corneas were incubated at a temperature of 32 C and a humidity of more than 95% throughout all the experiments. • There was no additional moisturizing with culture medium MEM.
Microvesicle delivery of a lysosomal transport protein	Rabbit	96h	• Removed immediately post-mortem. • Washed three times in sterile PBS • globes were incubated at 37Cin a 5%CO_2 incubator in 150 ml flasks with gas-permeable stoppers containing 50 ml Ham's F12 medium

to *ex vivo* rabbit cornea [404]			
***Ex Vivo* Corneal Organ Culture Model for Wound Healing Studies [405]**	Porcine	5 days +	• Immediately put into PBS • Eyes dipped 3x in 10% iodine then 2x in PBS. • Wound the centre of the cornea. Remove cornea with limbus from globe. • Fill endothelial side with Agar + DMEM + Collagen. • Add 4 ml of SSFM to the 60mm plate, maintaining corneas at an air-liquid interface at the limbal border in 5% CO_2 at 37 C. • Refresh media after 24 h and thereafter every other day. Wet the corneal surface once daily by adding 1 drop of SSFM from the conditioned media in the dish to maintain moisture.
Establishing a porcine *ex vivo* cornea model for studying drug treatments against bacterial keratitis [406]	Rabbit and Porcine	5 days +	• Transferred in sterile PBS solution • process them immediately upon arrival. • Once all eyes are cleared of surrounding tissue, place in 3% (v/v) povidone iodine in PBS and leave for 1 min. Rinse with sterile PBS. • Excise the cornea leaving about 3 mm of sclera surrounding the cornea. • Briefly rinse it in 1.5% (v/v) povidone iodine solution in PBS. • Place Each CSR in a 34mm petri dish with 3ml media (DMEM with insulin, EGF, FCS, Penicillin-Streptomycin, Amphotericin B and Dextran). • Change media after 24 hours. • After 48 hours rinse with PBS.
Evaluation of 2 *ex vivo* Bovine Cornea Storage Protocols for Drug Delivery Applications [407]	Bovine	1, 4 and 7 days	• Storage in optimized organ culture (OC) medium at 37 C or phosphate-buffered saline (PBS) at 2-8 C • Histology revealed that storage in OC consistently caused detachment of the epithelial layer by day 4 of storage, whereas both storage conditions caused a significant increase in stromal thickness and tissue vacuolation.
Development of a novel *ex vivo* equine corneal model [408]	Equine	7 days	• Immediately post-euthanasia, the ocular surface was washed with a 1% dilute betadine solution. • The cornea along and 2–3 mm of perilimbal sclera was harvested. • CSRs were immediately placed into a sterile 50-ml test tube filled with 20 ml of MEM placed on ice for transport • The CSR was again washed with a 1% betadine solution followed by copious rinsing with sterile PBS. • CSR was sterilely placed into a 50-ml tissue culture plate epithelial side up. 15ml of MEM media supplemented with 10% fetal bovine serum, essential amino acids, penicillin, streptomycin, fungizone, sodium pyruvate, and MEM vitamins added. • Each CSR was visibly inspected to ensure it was completely submerged. • The total culture media were changed once daily.
***Ex Vivo* Organotypic Corneal Model of Acute Epithelial Herpes**	Rabbit	7 days	• Explanted corneas are cultured in Minimum Essential Medium (MEM) supplemented with Non-Essential Amino Acids (1X), L-Glutamine (2 mM), Penicillin (200 U/ml), and Streptomycin (200 µg/ml).

Simplex Virus Type I Infection [409]			• Thoroughly rinse the cornea in sterile PBS containing Penicillin (200 U/ml) and Streptomycin (200 µg/ml). • Add the 1% agarose-containing medium to the endothelial concavity of the cornea. • Place the cornea with the supporting gel scaffold epithelial side up into a 35 mm tissue culture dish and add culture medium to cover the epithelial surface. The cornea may be cultured in this way for over a week, with medium changes every 48 hr.
Establishment of a porcine corneal endothelial organ culture model for research purposes [410]	Porcine	15 days	• Whole porcine eyes were purchased from a local abattoir. • The eyes were enucleated without thermal treatment of the pigs and were processed within 12 h after death. • The eyes were kept at 21 C. Eyes were disinfected for 5 min in a 1:20-solution of iodine and Dulbeccos's PBS. • Corneoscleral buttons, central corneal buttons and split corneal buttons were harvested. Each was transferred into a 12-well plate with the endothelial-side upwards. • Wells were filled with 3 ml Culture Medium supplemented with 2.5% fetal bovine serum. Afterwards the samples were cultured at 37 C and a CO_2 content of 5% for 15 days in an incubator. • Culture medium was renewed after the third and eighth day of cultivation.
Ex vivo Caprine Model to Study Virulence Factors in Keratitis [411]	Goat	15 days	• Eyes washed five times with PBS. • Incubated in 2.5% povidone iodine solution for 5 minutes, washed three times with PBS, and then incubated in 0.1% gentamicin for 15 minutes, then washed 3 more times in PBS. • The dissected cornea was placed on an agarose-gelatin solid support in a culture plate containing 1 ml DMEM with 10% FBS and antibiotics (penicillin, 100 I. U./ml and streptomycin, 75 µg/ml) and gentamycin (35 µg/ml) and placed in a CO_2 incubator at 37 C. • The medium was changed after every 24 hours.
Development and assessment of a novel *ex vivo* corneal culture technique [412]	Dog and Rabbit	21 days	• 8 dog corneas and 10 rabbit corneas were wounded with an excimer laser. • Corneas were cultured for 21 days on agarose based dome scaffolds or on flat-topped scaffolds.
Assessment of Topical Therapies for Improving the Optical Clarity Following Stromal Wounding in a Novel *Ex Vivo* Canine Cornea Model [413]	Dog	21 days	• Each globe received a stromal excimer laser phototherapeutic keratectomy (PTK). • Each identical black scaffold was then centred of a 6-well plate well and affixed using methyl cyanoacrylate adhesive. The scaffold- microplate assembly cured for 24 hours before being sterilized with ethylene oxide. • Each wounded corneoscleral rim was placed epithelium side-up onto a black scaffold • Culture wells were then filled with medium up to the limbus. • Each plate was covered, placed on a nutating plate at 24 rpm and incubated at 37.8C in a humid atmosphere containing 5% CO_2. • For the first 24 hours, Dulbecco's modified Eagle's medium and Ham's F-12 nutrient mixture with L-glutamine at a ratio of 1:1 supplemented with 10% fetal bovine serum, HEPES, dextran 40. chondroitin sulfate

			and 10% antimicrobial solution (streptomycin, penicillin, and amphotericin) was used. Thereafter, only 1% antimicrobial solution (streptomycin, penicillin, and amphotericin) was used.
An experimental study to test the efficacy of MSCs in reducing corneal scarring in an ex-vivo organ culture model [414]	Human	28 days	• Modified artificial anterior chamber
Development and Assessment of a Novel Canine Ex Vivo Corneal Model [415]	Canine	28 days	• At the time of euthanasia, a neomycin–polymixin B–bacitracin ophthalmic ointment (Vetropolycin®) was applied. • The eyelids were then secured closed with 1 in. surgical adhesive dressing for transport. • Periocular skin and conjunctival sacs were decontaminated with 0.2% povidone-iodine. CSR were excised and rinsed with sterile PBS three times for 10s each. • A scaffold was constructed by modifying a standard six-well plate with syringe covers secured concave side down in 4 of 6 wells with adhesive. The scaffold was decontaminated by gas autoclave sterilization. • Each CSR was placed epithelial side up on the scaffold. Media was added dropwise to each CSR culture well until reaching the limbus (7 ml). The scaffold was placed on a nutating plate that rotates clockwise in three-dimensional axes at 24 cycles/min in incubator conditions: 37 C, 5% CO_2, and 95% humidity. • A random cornea was sampled, using sterile swab technique of the cornea and media, for microbial culture at each time point days 0, 3, 7, 14, and 28 for routine aerobic culture analysis. • All corneas were also stained with fluorescein sodium 0.5% with 160 µL of eye wash to rinse at each media change. Corneas were assessed with cobalt blue filter for stain retention that would highlight epithelial defects. At days 0, 7, 14, and 28, two CSR were removed from culture for histology.
Development of ex vivo organ culture models to mimic human corneal scarring [416]	Human	30 days	• Corneas were cultured for 30 days at 37 C in 5% CO_2 using 10 ml of medium per six-well plate. • DMEM/Glutamax and Ham's F-12 mixed in a 1:1 ratio with 10% fetal bovine serum, 50 µg/ml vitamin C, 100 UI/ml penicillin, 20 µg/ml streptomycin, and 1 µg/ml Fungizone was used. • The medium was changed three times a week. The posterior face of the cornea was in contact with sterile blotting paper, soaked with culture medium, and placed on a conformer to maintain the curved shape of the cornea, while the anterior face was in contact with air. • A drop of medium was added twice a day either to the top of the cornea or directly into the wound.

7.2 Materials and Methods

7.2.1 Preparation of 10x Simulated Bodily Fluid (SBF)

Simulated Bodily Fluid is commonly used to create mineral coatings on the surface of various materials, for example titanium [417-419]. SBF was prepared as described by Chen et al [420]. NaCl (5.84% w/v), KCl (0.037% w/v), $CaCl_2$ (0.277% w/v), $MgCl_2 \cdot 6H_20$ (0.102% w/v), NaH_2PO_4 (0.120% w/v) and $NaHCO_3$ (0.084% w/v) were added to Milli-Q water sequentially, under stirring. The next reagent was added after the previous was fully, visibly dissolved. The solution was then sterile filtered (0.2µm) before use.

7.2.2 *Ex vivo* corneal biopsy SBF mineralisation

In order to test the formation of mineral deposits in tissue treated with SBF, un-scalded, whole porcine eyes were prepared as previously described (chapter 3: general methods, section 3.7). 5mm biopsies were taken from the porcine corneas using a disposable biopsy punch. The samples were placed with the epithelial layer facing upwards in specialised well inserts (Cellcrown) and placed in a 96-well plate, prepared with fresh 100µl media (HBSS + Penicillin/Streptomycin 1%). The epithelial surface of each corneal sample was then treated with 20µl of 10x simulated bodily fluid (SBF) and incubated at 37°C for 24 hours. After 24 hours, the 10x SBF solution was removed from the well of the ocular insert. The corneal biopsies were removed from the inserts, and fixed in 4% PFA overnight. The samples were the appropriately prepared for cryosectioning as previously described (Chapter 3, section 3.11). Slides were stained with Von Kossa stain (as described, Chapter 3, Section 3.14) or haemoxylin and eosin

(H&E) (as described, Chapter 3, section 3.12) and imaged under bright field microscopy (EVOS 5000).

7.2.3 Whole cornea model – optimisation

An accurate assessment of the efficacy of HMP as a treatment for band keratopathy relies upon the creation of an ex vivo model in which mineral deposits are induced in viable whole corneas. In developing the *ex vivo* organ culture model, it was decided that a combination of 10x SBF and high concentration (0.5M) sodium phosphate solutions would both be used to treat the ocular surface to increase the chances of rapid mineralisation. Previous investigations have shown that high concentrations of phosphate preservatives in eye drops can induce band keratopathy [14, 383, 386, 387]. Povidone iodine washes were introduced after repeated infections on initiation of the organ culture. DMEM-F12 has been highlighted by multiple previous organ culture studies as an appropriate medium for maintaining ocular tissue health and viability (Table 4). Agar was used to maintain the shape of the corneal-scleral rim and to provide an additional nutrient source for the tissue.

Whole unscalded porcine corneas were received within 4 hours of death from a commercial abattoir. The superficial conjunctival tissue was removed before the globe was sterilised for 5 minutes in 10% povidone iodine solution. The cornea of each eye was wounded using a handheld miniature drill, creating abrasions around 4mm in diameter at 3 positions around the cornea. The globe was then dissected to remove the posterior tissues, leaving the cornea with a rim of sclera 5mm wide. The corneal-scleral rim (CSR) was then placed in 7.5% povidone iodine solution for 30 minutes before moving into a sterile tissue culture hood. The CSR was rinsed three times in

sterile PBS and placed inverted (endothelial side upwards) in the well of a 12 well plate. 2% agar/DMEM was prepared prior to dissection and sterilised via autoclave. Prior to dissection the autoclaved agar was placed in a water bath at 80°C to prevent solidification. Immediately before use, the water bath with the agar was reduced in temperature to 37°C. The anterior chamber was then filled with liquid 2% agar. The agar was allowed to solidify before the CSR was reinverted and placed in a well of a 6 well plate and supplemented with DMEM:F12 media, with added 10% foetal bovine serum, 10% penicillin/streptomycin, 1% amphotericin B and 0.2% gentamycin. The medium was added to the volume at which is reached the limbus of the CSR. The CSRs were then acclimatised overnight in a humid incubator at 36.5ºC and 5% CO_2.

To mineralise the corneas, 0.5M $NaPO_4$ solution and 10x SBF solution were added to the epithelial surface alternately, three times daily. Media was changed twice daily - before mineralisation treatments and 2 hours after the final treatment. When the media was changed, fresh media was used to bathe the corneal surface to prevent desiccation. Mineralisation was assessed by visualising corneal opacity. This was performed by directing an LED light through the posterior of the CSR, revealing mineralisation in the form of opacities on the corneal surface.

Wound healing was assessed through fluorescein staining. Once the fluorescein stain showed no obvious wound, and the wounded eyes started to show opacities which were representative of mineral formation, the eyes were fixed in 4% paraformaldehyde and cryosectioned as previously described (Chapter 3, section 3.11).

For comparison, corneas were prepared and wounded and maintained in culture without the mineralisation treatments. These corneas were included as non-mineralised controls and were removed from culture at the same time points as the mineralised corneas.

7.2.4 BK model and tests of formulation

Topical demineralisation treatments were then assessed using the mineralised cornea model. Once corneas were mineralised, 0.3ml of sterile-filtered treatment solution– 1M HMP, 0.5M HMP, 2% EDTA or 0.5M HMP/alginate - was applied to the surface of each cornea 5 times over 48 hours, with a minimum of 4 hours between treatments. Treatment was applied in a sterile laminar flow hood. Corneas remained in DMEM throughout treatment and continued to be incubated at 36.5ºC and 5% CO_2 in between treatments. Media was changed in between treatments. After 5 treatments/48 hours, mineralisation was then reassessed as described (section 7.2.3), and the corneas were fixed and embedded for cryosectioning as previously described (Chapter 3, section 3.11).

7.2.5 Stain Quantification

Silver staining was quantified using the ImageJ software and calculated as area stained. To do this, images of each cornea taken at 20x magnification were converted to the RGB stack type, and the threshold was set at Red 240. The measurement was then taken of the above threshold area.

7.3 Results

7.3.1 *Ex vivo* Corneal biopsy SBF mineralisation

The aim of treating the corneal biopsies with 10x SBF was to induce mineralisation in the tissue. After 24 hours of treatment with 10x simulated bodily fluid, the sectioned and stained corneal biopsies showed some evidence of mineralisation (Figure 7.1, visualised as black staining). When assessing the tissue integrity, the epithelial layer of the corneas showed disintegration or complete detachment, as evidenced by the absence of the characteristic bright pink (nuclear fast red) stained band at the edge of the stromal tissue. Although the 10x SBF treatment was applied to the corneal surface, evidence of mineralisation was not localised only to the epithelial/stromal interface. Clusters of stained particles were dispersed throughout the stromal tissue also. The level of mineralisation indicated was not substantive enough to be considered a replica of that shown in cases of Band Keratopathy.

7.3.2 Assessing the whole cornea model as a replication of BK

Whole corneas were cultured and treated with mineralising agents in an attempt to replicate band keratopathy. Sections from the visibly mineralised corneas were positive for calcium in the Von Kossa stain (Figure 7.2), appearing as black/brown staining. Image analysis quantified an average of 67490μm^2 stained per 305,731 μm^2 imaged, an average of 21.7% of the total area. Both the non-wounded and wounded corneas mineralised, however there was a higher level of mineralisation in the wounded corneas - 101021 μm^2 in the wounded corneas and 25767.8 μm^2 in the non-wounded corneas ($p<0.0001$) (Figure 7.3). The depth of the mineralisation was also visibly greater in the wounded corneas, penetrating further into the stromal tissue. In

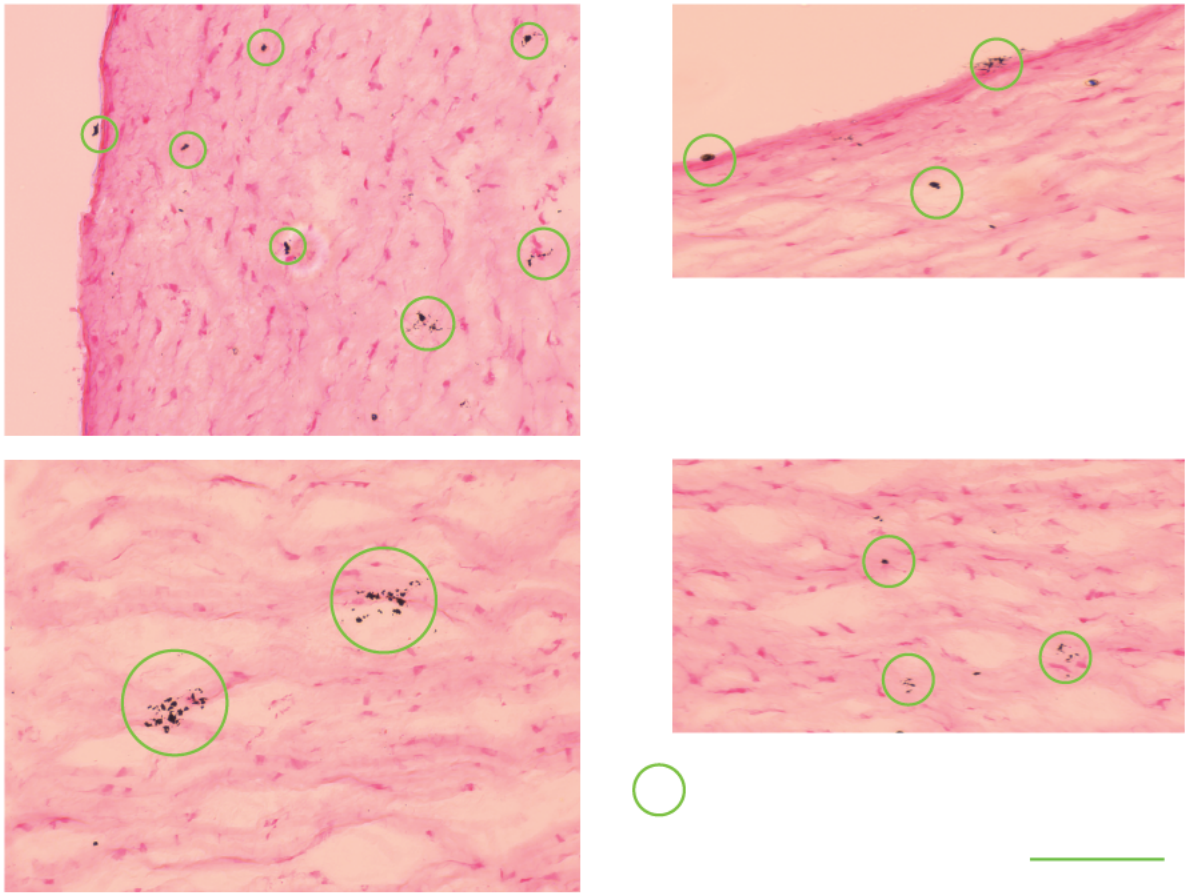

Figure 7.1: Von Kossa stained sections of porcine corneal biopsies post-incubation in 10x Simulated Bodily Fluid. Evidence of mineralisation in the form of clusters of stained particles (green circles) were dispersed throughout the stromal tissue, not localised to the epithelial/stromal boundary as would be anticipated in Band Keratopathy. Scale bar = 150μm.

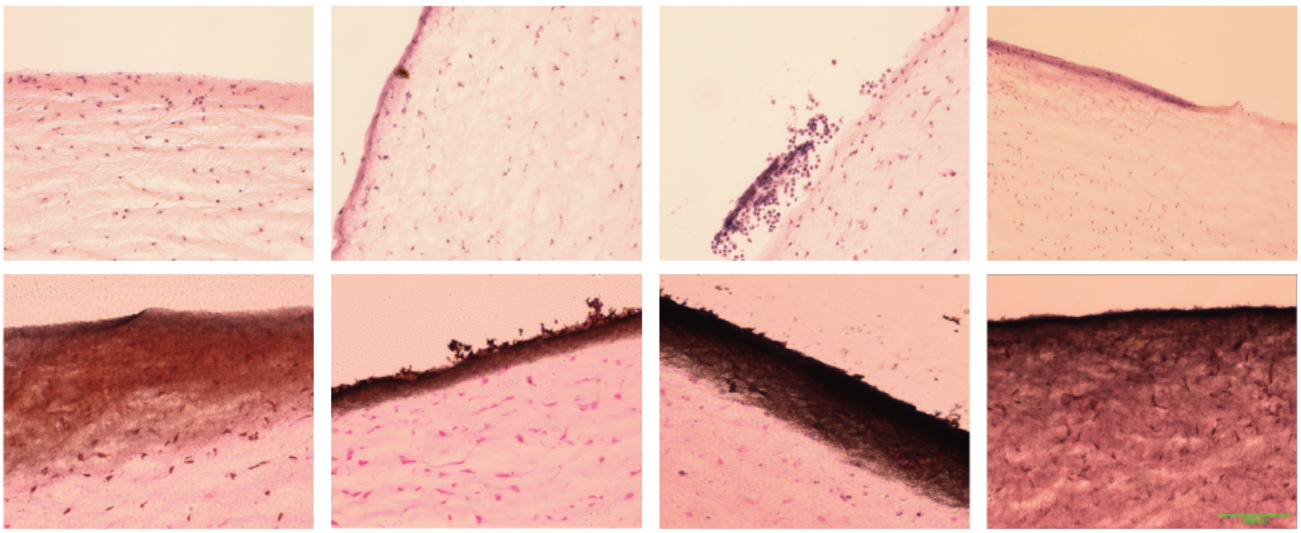

Figure 7.2: a) H&E stained sections of mineralised porcine corneas b) Von Kossa stained sections of mineralised porcine corneas. Both the Haemoxylin and Eosin staining and the Nuclear Fast Red/Von Kossa staining show minimal epithelial retention in the mineralised corneas. Epithelial surface oriented to top of page in each image. The strong black/brown staining is indicative of calcium mineral formation.

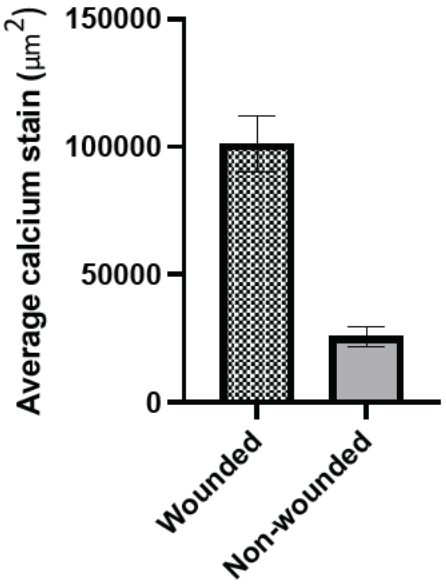

Figure 7.3: The average quantified positive calcium staining (μm^2; Von Kossa) in the wounded and non-wounded mineralised corneas. N=4. There was a higher level of mineralisation in the wounded corneas - 101021 μm^2 in the wounded corneas and 25767.8 μm^2 in the non-wounded corneas, suggesting the injured tissue provides a greater nucleation surface than the non-wounded tissue.

comparison, the average quantified area stained in the non-mineralised group was 380 μm^2, significantly lower than the mineralised corneas ($p<0.0001$).

Both the H&E staining and the nuclear fast red/Von Kossa staining showed minimal epithelial retention in the mineralised corneas. In the non-mineralised corneas (Figure 7.4), epithelial retention was visibly greater, but there was still major epithelial layer degradation compared to what would be expected of a healthy corneal surface.

There were also noticeable differences in the stromal tissue, with minimised nuclear staining in some areas leading to the tissue to appear smoother. In heavily calcified areas, as evidenced by the level of staining, the nuclei of the cells also often appeared stained black, whereas this is not the case in the other areas of the stroma.

7.3.3 Assessing the efficacy of various HMP formulations to treat band keratopathy

The mineralisaed corneas were then treated with topical demineralising formulations. Visualisation of the corneas prior to treatment confirmed corneal opacities consistent with the wounding patterns of each cornea (Figure 7.5). Post-treatment visualisation also confirmed the removal (absence) of the opacities in each cornea in each treatment group after 48 hours of treatment (five doses). All treatment groups showed a significant reduction in calcium staining (Figure 7.6) compared to the non-treated, mineralised controls ($p<0.0001$). Between the treatment groups, 1M HMP had the smallest quantified area stained, showing no evidence of remaining mineralisations.

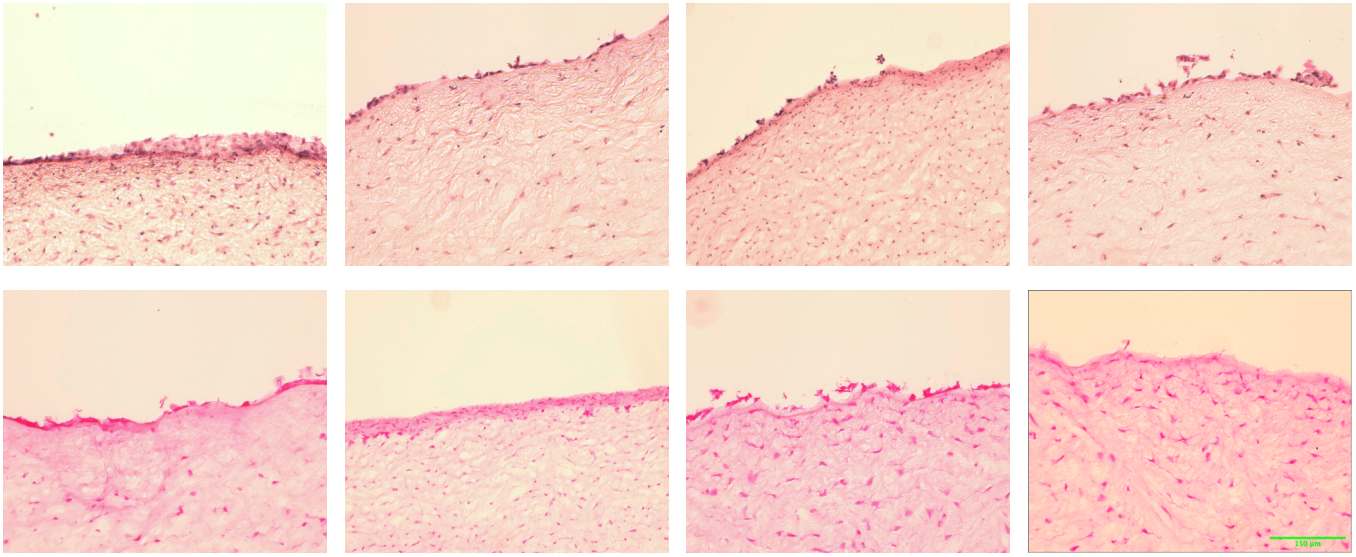

Figure 7.4: Top: H&E stained sections of non-mineralised porcine corneas. Bottom: Von Kossa stained sections of non-mineralised porcine corneas. Anterior corneal surface oriented to top of page. Both the Haemoxylin and Eosin staining and the Nuclear Fast Red/Von Kossa staining show marginally improved, but still minimal, epithelial retention in comparison to the mineralised corneas. The lack of black/brown staining is indicative of the absence of calcium mineral formation. Scale bar = 150μm

The 0.5M HMP/Alginate group also showed no evidence of substantial remaining mineralisation. In the 2% EDTA group, substantial mineralisation was found in once instance, but this was not consistent. The 0.5M HMP (alone) treatment group consistently showed evidence of residual mineralisation, showing as clusters of black marks. There was, however, still a reduction in comparison to the untreated corneas in both the quantity (area stained) and depth of the mineral remaining. There were no significant differences in the average quantified stained area between each treatment group, nor was there a significant difference between the non-mineralised corneas and the treated corneas.

All but one cornea in the 1M treated group showed complete absence of any remaining epithelial layer, and in each group there was evidence of loss of nuclear staining in areas which were wounded.

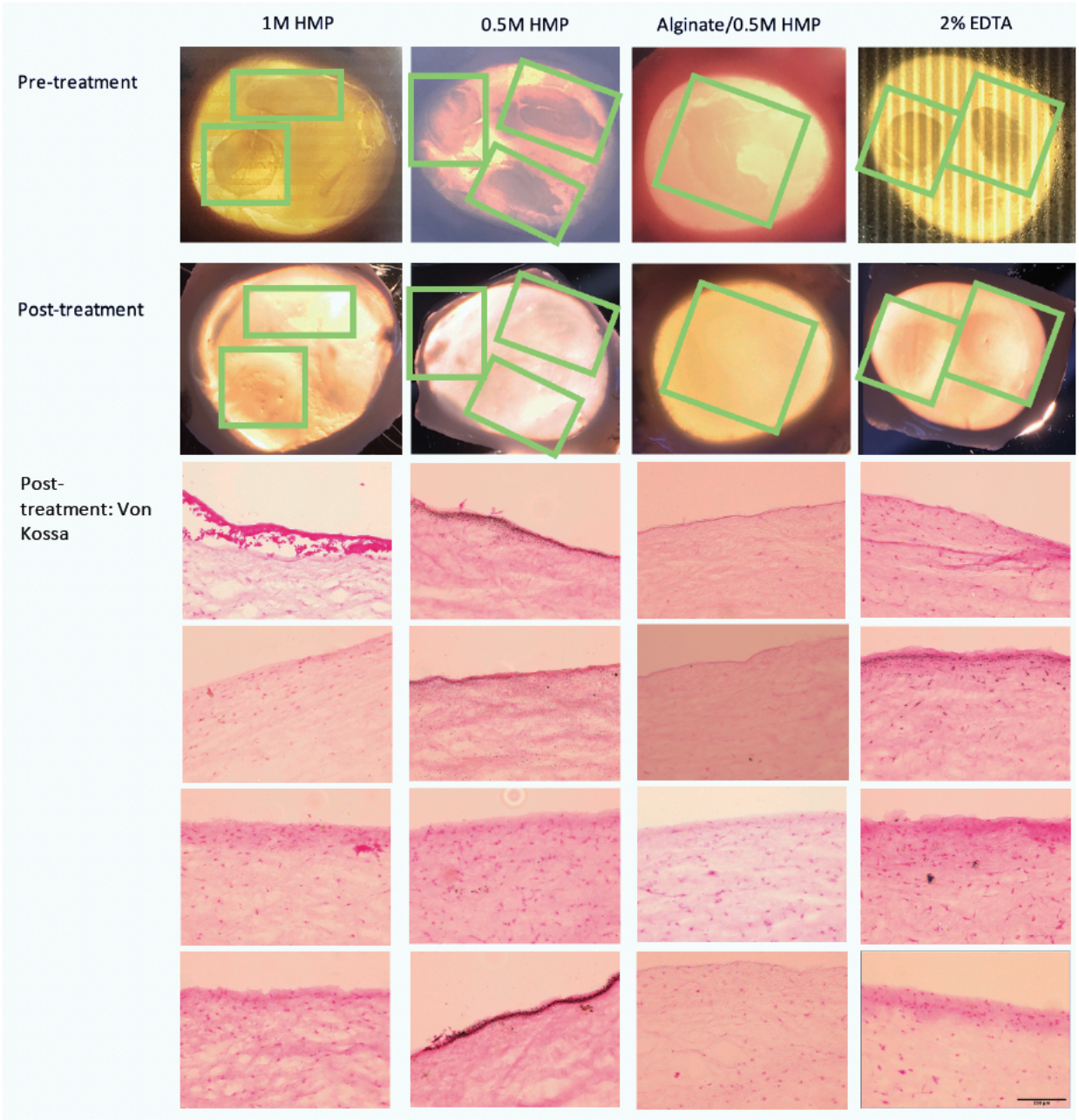

Figure 7.5: Images of the whole porcine cornea pre-treatment and post-treatment for each treatment group, followed by Von Kossa stained sections of the corneas from each treatment group. Scale bar = 150μm

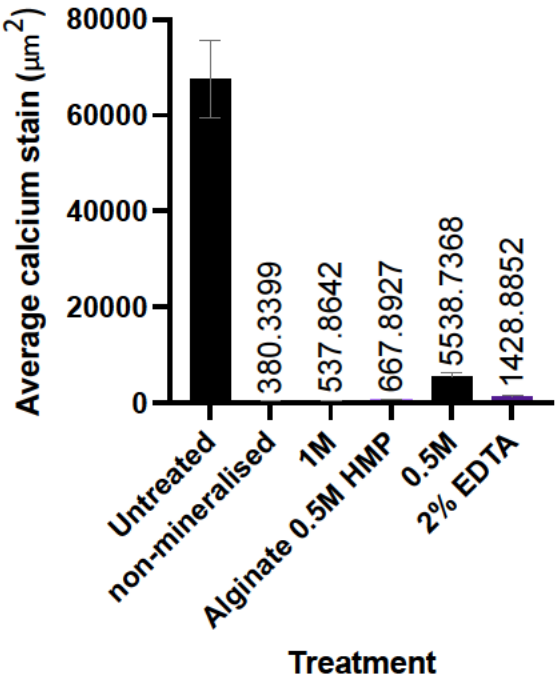

Figure 7.6: Quantified area stained (µm²; Von Kossa) post-treatment in each treatment group, with untreated included for reference. All treatment groups showed a reduction in calcium staining compared to the non-treated, mineralised controls. Between the treatment groups, 1M HMP had the smallest quantified area stained, showing no evidence of remaining mineralisation. The 0.5M HMP/Alginate group also showed no evidence of widespread remaining mineralisation. In the 2% EDTA group, remaining mineralisation was found in once instance, but this was not consistent. The 0.5M HMP (alone) treatment group consistently showed evidence of residual mineralisation, showing as clusters of black marks. There was, however, still a reduction in comparison to the untreated corneas in both the quantity (area stained) and depth of the mineral remaining. N=4. Error Bars = Standard Error of Mean (SEM).

7.4 Discussion:

i) Mineralisation of tissue using 10x SBF

In an attempt to create a rapid and simple model of BK, mineralisation of corneal tissue biopsies was attempted with 10x SBF, which is used to create mineral coatings on material surfaces [417-419]. The corneal biopsies treated with 10x SBF for 24 hours showed some evidence of mineralisation, however this was not substantive enough or localised enough to be considered a replica of band keratopathy. Epithelial detachment was obvious both on visualisation of the samples during processing – epithelial layers were clearly visible detached from the tissue body in solution – and on analysis of the stained sections. These observations indicated that to successfully replicate BK, an organ culture model would be necessary, to allow for maintained tissue viability whilst mineralisation occurred.

ii) Assessment of the *ex vivo* band keratopathy model

The corneas which were successfully cultured and mineralised revealed several important findings with regards to the viability of the *ex vivo* model created. Firstly, the wounding was not necessary for mineral formation. However, where the corneas were wounded, the mineral reached deeper into the stromal layer and the staining reveal was more diffuse, suggesting the mineralisation was less granular in nature. Although the wounding may not be necessary for mineralisation of the tissue, it provides multiple advantages for the model, namely some control of level of mineralisation and the size of the mineral ‘patches’. By creating wounds in which the mineral can form, the mineralisation process was more easily visualised and monitored with the use of the LED light and without the need for additional techniques. Band Keratopathy can form

with or without ocular injury, but is likely more severe in ocular injury cases, as was replicated in this model development.

It can be observed from the model deployed that all corneas maintained their clarity post-treatment, indicating tissue viability and lack of induced inflammation and associated scarring.

The model created in this work is designed to represent band keratopathy in the human eye. Band keratopathy can form through systemic imbalances of calcium and phosphate or local challenges to the ocular environment. This model replicated local challenges, similar to the reports of band keratopathy occurring in patients who use phosphate buffered eye drops [383]. In order to accelerate mineralisation and shorten the model timeframe in an attempt to maintain optimal tissue viability, high concentrations of sodium phosphate and SBF were used. This method induced mineralisation quickly, however it appears the formation of the mineral disrupted the epithelial layer. Only one of the treatment groups showed any evidence of epithelial retention, which was a single instance in the 1M group, and this was not consistent. It is possible that the corneal wounding was too extensive, and the mineralising agents too concentrated, for corneal epithelial healing to occur. It also known that extracellular calcium ions play a crucial role in encouraging cell proliferation for wound healing, and depriving the ocular surface of calcium with the application of calcium chelating agents may well have also prevented successful re-epithelialisation [421].

Even where the corneas were not wounded, the mineralisation appears to destabilise the epithelial layer. In the Von Kossa stain images, clusters of cells and mineral could be seen detaching from the ocular surface. This is not dissimilar to the progression of

severe Band Keratopathy, which can cause corneal erosion and the development of severe dry eye syndrome. This is, however, a potential limitation to the testing of the demineralising formulations, as the epithelial barrier may have been compromised, aiding in the demineralisation process. It is also possible that the tissue was losing viability, however this was not reflected in a loss of corneal clarity (aside from the mineralisation) as would be expected. The use of povidone iodine to sterilise the eyes prior to culture may also limit wound healing and challenge the ocular surface [422], however optimisation of the process previously showed that this step was necessary to prevent infection of the culture. Previous attempts to create a corneal organ culture model have faced similar issues where medium has been used to cover the ocular surface [407] (Table 4).

Although calcification can appear in both H&E and Von Kossa staining, in the former as dark purple/black and in the latter as brown/black – our assessments showed that Von Kossa, is much more sensitive for detecting calcification, with the Von Kossa-stained samples indicating much higher levels of mineralisation across all samples than the H+E-stained samples (Figure 7.2). The H+E-stained samples were, however, much clearer for assessing epithelial retention, particularly as in the Von Kossa stained samples the presence of calcium often masked whether the epithelial layer was still present.

The Von Kossa images also showed evidence of the cell nuclei in the stromal layer potentially acting as nucleation sites for the mineralisation process. In areas of mineralisation, in the surrounding stromal tissue the nuclei of the stromal cells appeared as black, indicating silver/calcium staining, instead of the expected pink of

the nuclear fast red stain. As cell nuclei store an abundance of phosphates, it is possible that as the extracellular phosphate and calcium levels rise due to the mineralising treatments, the nuclei of the cells provide a rich environment for mineral nucleation to occur. This would be different to the process through which mineralisation occurs for processes such as bone formation, which rely on the matrix production and vesicle release of osteoblasts [423].

iii) Utilising the *ex vivo* BK model to assess the efficacy of topical demineralisation treatments

When formulating a treatment to replace the superficial keratectomy procedure, it is of primary importance that the chemical agents deployed do not trigger an ocular challenge so great that opacity-inducing inflammation or corneal scarring is induced.

When considering the ability of each of the treatments tested to remove the formed mineral, the 1M HMP and 0.5M HMP/alginate groups were the most effective demineralising agents when comparing the average quantified area stained. With regards to the 1M HMP group, this would be expected, as it is in agreement with the hydroxyapatite demineralisation assessment performed previously (Chapter 4, Figure 4.3). The improvement of 0.5M HMP/alginate in comparison to 0.5M HMP alone could indicate greater ocular retention of the alginate formulation, creating a longer window of bioavailability of the demineralising agent. The previous formulation assessment (Chapter 6, Figure 6.18) showed that the alginate/HMP and 1M HMP solutions had a higher viscosity than that which would be expected for a simple aqueous salt solution, and both also showed a higher contact angle than HBSS (control).

It is however, worth considering that all groups tested were effective at demineralising compared to the untreated controls.

iv) Summary

The aim of the work presented in this chapter is to create, assess and then utilise an ex vivo porcine corneal organ culture model as a replica of band keratopathy. 10x SBF and 0.5M phosphate solutions were effective and inducing corneal mineralisation, as confirmed by Von Kossa staining. The model was then used to test potential topical treatments for BK. All formulations tested – 1M HMP, alginate/0.5M HMP and 2% EDTA – were successful at demineralising the corneas. The choice of which agent would be most effective as a topical treatment for band keratopathy will therefore rely on further evidence of the toxicity and long-term effects of their use on the ocular surface. Further development of this model as a corneal wound healing model could offer an additional avenue for the exploration of the toxicity of HMP based treatments.

8.

GENERAL DISCUSSION, LIMITATIONS, AND SUGGESTED FUTURE WORKS

The aim of this project was to assess whether sodium hexametaphosphate could form the basis of an effective topical treatment for calcific band keratopathy, an ocular condition which is characterised by the ectopic formation of the calcium-phosphate hydroxyapatite in the cornea. This larger topic was approached through four key questions:

(a) Can Sodium hexametaphosphate effectively demineralise hydroxyapatite within the time period associated with the retention of an eye drop of the eye

With the view of using Sodium hexametaphosphate as a topical agent for the treatment of corneal calcification, this investigation has firstly highlighted the potential for HMP to demineralise precipitated hydroxyapatite quickly. 1M HMP was the most effective of the concentrations of HMP assessed, inducing significant demineralisation within 1 hour of treatment. The HMP treatment concentrations did not produce a linear trend as would have been anticipated for a test of this nature. 0.125M HMP, the lowest concentration tested, appeared to rapidly demineralise the hydroxyapatite before producing a second precipitate, most likely an insoluble calcium-phosphate. These data highlight the narrow line dividing sodium hexametaphosphate as a mineralisation aid, as in the human body and in its role in dental protection, and a demineralising agent, as in its commercial use as Calgon and in the studies conducted with ectopic calcification [273, 274, 297, 298, 302]. For the context considered within this work, reliable demineralisation is key to the efficacy of a HMP formulation to treat calcific band keratopathy, therefore where possible it appears a higher concentration is desirable.

The majority of the investigation into the efficacy of HMP as a demineralising agent used absorbance readings of synthesised nanohydroxyapatite. Although the relevant number of repeats were performed to ensure the appropriate power in the calculations, there is naturally a high variability in this technique, both through differences in batches of synthesised HA and pipetting errors, as the HA sol is not a homogenous solution. Additional checks could be performed on the synthesised HA to ensure homogeneity between batches, such as XRD analysis. In the case of the Calcium and Magnesium Chloride metal ion affinity assays, the main limitation of those results is the lack of further analysis of the precipitations produced. Again, further analysis through XRD or elemental analysis through XRF would provide an explanation as to which precipitates had formed in each case. Where possible, it would also be beneficial to investigate further the properties of the hydroxyapatite formed in cases of band keratopathy, to ensure that the *in vitro* testing of possible treatments accurately reflects the characteristics of the naturally occurring mineral.

(b) Is Sodium hexametaphosphate toxic to the ocular tissue

Neither the demineralisation nor the cell metabolism assay results show a strictly linear relationship with HMP concentration. It is therefore relevant to compare the demineralisation efficacy and cell metabolism assay results of the different treatment concentrations of HMP, to see if in combination they speak to the relationship between HMP concentration and its ability to chelate calcium ions. When cell viability and demineralisation (reduction in absorbance) are compared (Figure 8.1), there is a loose trend of higher relative demineralisation pairing with higher relative cell viability at

0.125M and 0.25M HMP. It is reasonable to assume that the demineralisation of hydroxyapatite by HMP is dependent on the ability of the polyphosphate anions to chelate calcium, forming soluble, stable Ca-HMP complexes. The cytotoxic effects of HMP will, however, be a combination between its effect on Calcium ions as well as other metal ions critical for maintaining cell homeostasis and adhesion such as sodium (Na^+), potassium (K^+) and magnesium (Mg^{2+}).

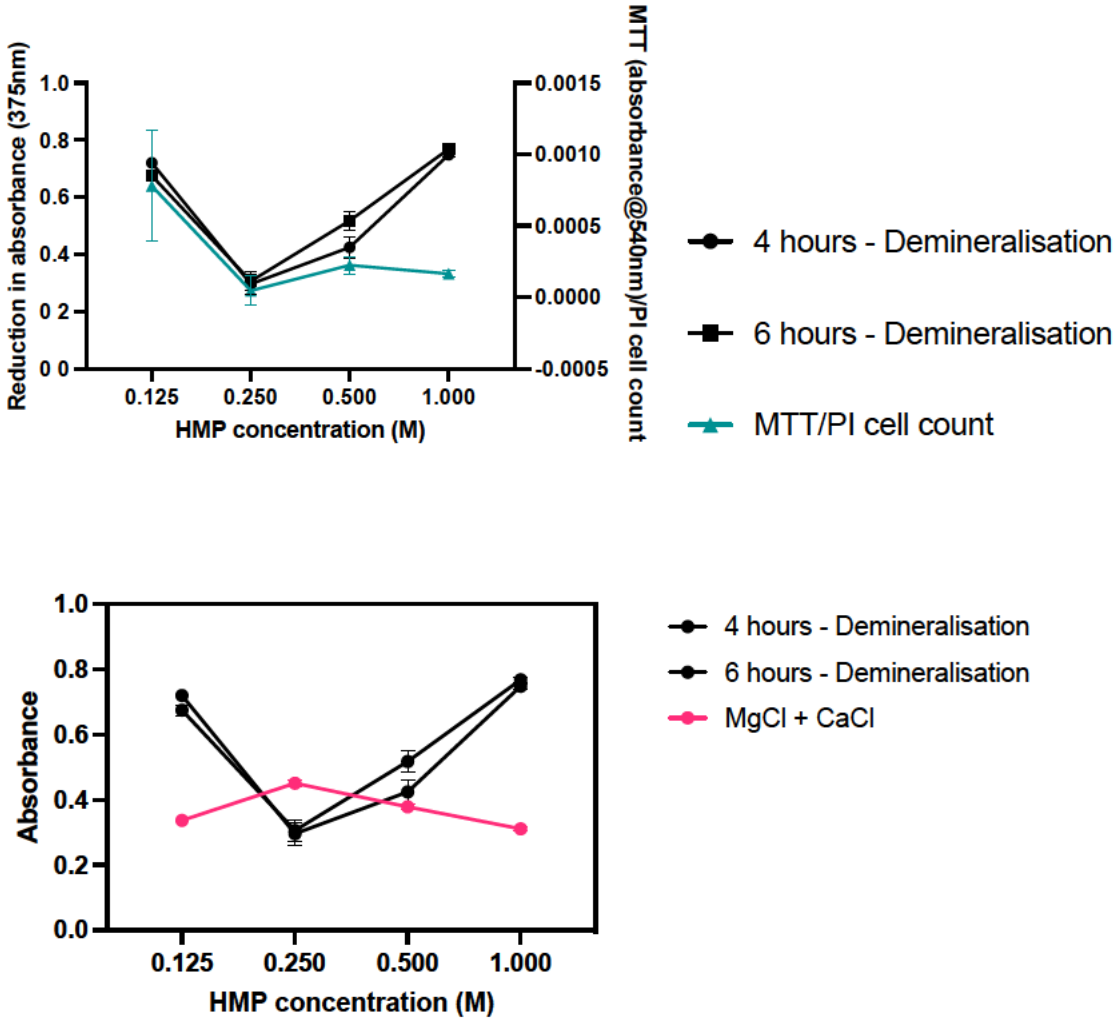

Figure 8.1: Reduction in absorbance (demineralisation, average across all time points) and Cell viability (MTT assay results/PI cell count) plotted against HMP concentration. There is a loose correlation between the two assessments, which is stronger in 0.125M and 0.25M HMP. Demineralisation can be assumed to be driven by the ability of HMP to chelate calcium, where as cytotoxicity is much more complex. b) absorbance of HMP and $MgCl_2$+$CaCl_2$ solution, plotted against HMP concentration.

Previous studies have shown that polyphosphates have a higher affinity for sodium than potassium. As there is abundant sodium in the sodium hexametaphosphate solutions, it is unlikely that HMP is depriving cells of K^+ ions [288], however sodium overload may be a contributing factor.

When the demineralisation results are compared to the results of the $MgCl_2$ and $CaCl_2$ absorbance assay (Figure 16b), we see a mirroring – where demineralisation is lowest, precipitation formation is highest, as would be expected. A comparison of these results may suggest that greater sequestration of ions from the cell culture medium at 0.25M HMP may be inducing greater toxicity and loss of cellular adhesion.

Further investigation is necessary to explain the trends seen in demineralisation efficacy and cytotoxicity across the concentrations of HMP presented, potentially focussing on the affinity at different concentrations to different metal ions. A recurring theme within the results presented here, is the non-linearity of the relationship between the concentration of HMP and its affects. This can be seen in the demineralisation of hydroxyapatite, the MTT assay results, the interaction between HMP and BSA, and the interaction between HMP and Gellan. The trends exhibited could in theory link to the findings in previous studies which link polyphosphate behaviour to chain length, however, there has not been any suggestion previously that changing the concentration of a solution of sodium hexametaphosphate might change the proportion of different chain lengths within the solution. As a best estimate, the highly saturated solutions formed at 1M HMP may incur incomplete hydrolysis of the polyphosphate salt, however this would need to be investigated with chain length determination, such

as size fractionation through gel electrophoresis or column fractionation, end group titration and light scattering [239, 267, 307, 373, 424].

As polyphosphates may play a key role in cellular metabolism, metabolic assays cannot be relied upon to provide a full picture of the cytotoxicity of sodium hexametaphosphate. Additionally, these investigations have found that HMP also interferes with the commonly used LDH colorimetric assay, and our propidium iodide staining assay produced unexpected results. Therefore, the toxicity data is inconclusive. It has, on the other hand, raised some interesting avenues for further investigation.

When considering the apparent permeabilization of the cellular membrane by HMP, it could be examined whether it is possible to deliver therapeutic or genetic agents such as mRNA to the cells as a result of this permeabilization. Additionally, it would need to be seen whether this permeabilization is recoverable and reversible, potentially with the replenishment of metal ions in the media. A traditional wound healing/scratch assay on relevant corneal cells (epithelial cells or keratocytes) may offer evidence as to whether the cells can recover from HMP treatment [361, 384]. This would be relevant to the higher concentrations of HMP, as we have shown the lower concentrations of HMP cause the cells to lose adherence. Again, it remains to be seen whether the cells that lose attachment may recover if placed in HMP-free media, as they do with trypsin-EDTA for example.

During this investigation, unsuccessful attempts were made to culture both human (HCE-2) and porcine corneal epithelial cells. The use of multiple cell lines for future

investigations would be advantageous, as it has previously been noted that HMP can illicit different effects on different cell lines [315]. An additional area of exploration could be the impact of HMP on the epithelial barrier function, for example with transepithelial resistance measurement [360]. As a calcium chelating agent, it would be anticipated that HMP would interfere with the epithelial tight junctions (cadherins). However, through this same line of reasoning it would be expected that the higher concentrations of HMP which demineralise HMP rapidly would also cause the cells to lose adherence, and it would therefore make a relevant comparison. It is worth noting that the propidium iodide assay performed in this investigation would normally be performed as a live/dead assay with a green fluorescein or other counterstain to counter the red stain. Both fluorescein and calcein counterstains were unsuccessfully attempted, with neither green stain successfully appearing under fluorescent microscopy. The brightfield images of the cells provide appropriate evidence for the exclusion of the red propidium iodide dye in the cases of the untreated control and give and idea of cell confluency, however a counterstain analysis which allowed contrast between permeated and non-permeated cells would have been preferrable. This would have allowed for better comparison between the treated and untreated cells, allowing the contextualisation of cell metabolism assay results based on the number of recorded live or dead cells.

An angle not fully investigated in this project is the binding of HMP to proteins, either on ocular cells or within the tear film. As this is a known property of inorganic polyphosphates, and this work has highlighted the ability of HMP to form complexes with BSA. It would be reasonable to investigate the potential impact of this in the desired context, with investigations into the binding of HMP to various proteins found in the ocular environment [242]. Additionally, inorganic polyphosphates play a role in

the host immune response, and any immunogenic properties of HMP would need to be considered. In particular, the recruitment and any induced phenotype changes of macrophages and neutrophils could be analysed [164, 425].

In relation to the toxicity assays, the osmolarity of the HMP solutions needs to be considered in the context of the results presented. In all cases other than the 1M HMP, the tissues visibly swelled in the treatment media. In the case of 1M HMP, the tissue shrank and desiccated, recovering once the treatment media was replaced. Potential desiccation can also be seen in the treated corneal biopsies (Figure 5.6). The effect of this desiccation is not clear based on the results achieved, but in moving towards a potential *in vivo* model, the effects of this would need to be considered. An additional limitation of these investigations is the ration of volumes within the assay. A relatively small piece of tissue 5mm in diameter and around 3 mm thickness, creating a volume of ~24mm^3 is placed in a 750ml (750mm^3) volume of treatment media, creating a ratio of 125:4. In the context for which HMP is being assessed, the ratio would be reversed, with a much larger tissue body compared to the eye drop (between 20µl and 100µl).

Many ocular formulations are designed within strict pH limits, usually within 6.8-7.4, in order to preserve the pH of the tear film and to protect the ocular surface. In this context, we have shown that increasing the pH of HMP to 7 from 5.2 limits but does not prevent demineralisation (Figure 4.7). The benefits of a neutral pH therefore need to be weighed against the cost of a loss in demineralisation efficacy. This decision should be informed by relevant toxicity data, however the toxicity data acquired within our investigations do not give a clear idea of the impact of concentration or pH on the cytotoxicity of the HMP concentrations tested. Further work with relevant cytotoxicity

tests could be done to determine which would be more beneficial – rapid demineralisation at the potential cost of toxicity, or a gentler treatment which may require longer treatment periods.

(c) Can the delivery of Sodium hexametaphosphate to the eye be optimised by incorporating polymeric hydrogel materials

With regards to the formulation of the optimal delivery vehicle for HMP to the ocular surface, it is clear that HMP has a dramatic impact on the properties of the polymers tested. Due to the high concentration necessary to induce rapid demineralisation, a useful further comparison would be between the ocular surface retention of HMP and HMP/polymer formulations. This can be performed *in vivo* using fluorescein loaded drops and allows for the potential to analyse further the influence of the formulation on the tissue structure and function through anterior chamber OCT and immune cell imaging [62, 63]. Performing such analysis *in vivo* would give valuable additional information as to the behaviour of the formulations under blinking conditions. It would also provide an opportunity to perform whole mount immunofluorescence immunohistochemical analysis of immune markers such as CD45 (differentiated hematopoietic cells), CD68 (monocytes), MHC class II (antigen presenting cells), IBA-1 (macrophage specific protein), F4/80 (antigen presenting cells) and ZO-1 (tight junction protein) which would provide a well-rounded idea of the ocular immune response to the different formulations. The materials chosen for this investigation have all previously been developed for ocular formulations and are considered safe for this purpose when the right preparation techniques are used to maintain sterility. However, due to reactions that occur between HMP and the carrier materials, further toxicity

assessments of the HMP/hydrogel formulations would need to be performed in addition to HMP alone, to ensure the HMP/hydrogel combinations do not incur other adverse responses.

Within the formulation work performed here within, data from rheological tests such as the shear stress ramp (Figures 6.3, 6.4, 6.5) are used to predict how each gel might behave in the desired context – as a drop administered topically to the ocular surface. The assumption is that a higher viscosity leads to a greater eye drop retention. However, although a relationship between viscosity and residence time has previously been extrapolated for eye drop formulations, these tests can only provide a suggestion as to how a drop might behave *in vivo*. Several factors are not taken into account in these tests, including the storage time of the formulation, the curvature of the eye, mucoadhesion, lacrimal clearance, true blinking mechanics and the potential acceleration of clearance through ocular irritation. In particular, the dilution of HMP delivered to the ocular surface needs to be further considered. The demineralisation assessment results could suggest that a higher concentration of HMP would produce faster and more consistent results, however if that higher concentration, say 1M HMP, is diluted by tears to 0.125M HMP, the results presented here suggest that re-mineralisation may be a risk.

The toluidine blue assay developed in this work was not successful in distinguishing between HMP and other molecules in the solutions including the polymeric carriers being assessed, however toluidine blue could be redeployed to investigate the penetration of HMP into the corneal tissue. Sections of treated corneas could be stained with toluidine blue, and a colour shift within the tissue would indicate the

presence of HMP [374]. The penetration of HMP into the tissue would be a relevant measure of therapeutic potential, indicating an advantageous release profile form the carrier material or optimum retention of the drop on the ocular surface.

The chitosan films developed using 1M and 2M HMP did not release therapeutically effective doses of HMP, however, such films may be useful in a host of other application, including as moisture-retaining, anti-microbial wound dressings [363-366, 426]. Dermal models could be employed to assess the efficacy of the developed material in this context [361, 366].

A future avenue to be explored, is the potential for HMP to form stable lipid emulsions, either in combination with polymers such as chitosan, or alone. As elucidated in the introductory literature review, lipid based formulations for ocular drug delivery offer an attractive alternative where hydrogel or polymer formulations may fall short. Particularly in a disease where the development of dry eye is common, as is true for patients with BK, the delivery of lipids in tandem with the demineralising agent may offer additional symptomatic relief [51, 52, 143]. The interactions between the lipid and HMP would need to be examined, alongside the toxicity of the combined agents and the release profile, however.

In addition to the physical properties assessed herein, any potential treatment would need to be further optimised with sterilisation in mind. HMP solutions can be sterile filtered, however this is not true of gels which may need to be sterilised by heat treatment of radiation. These processes can further change the structure of the material, and this would have to be taken into account.

(d) Can a relevant *ex vivo* test be developed to assess the efficacy of sodium hexametaphosphate in treating band Keratopathy

The *ex vivo* porcine model of band keratopathy developed to test the HMP formulations can be best compared to the very late stages of severe disease, where the epithelial layer has been ruptured and mineral is deeply embedded in the stromal tissue. The model provides evidence of the potential efficacy of HMP in the context of treating band keratopathy topically, however there are limitations to the model. The wounding performed on each eye was not necessarily consistently sized in either diameter or depth due to the method of wounding – a handheld miniature drill. Previous methods of wounding were attempted including abrasion using an algebrush or scalpel, and the drill provided the most consistent results, however this could be further optimised. The assay was designed to provide rapid mineralisation in order to maintain tissue viability. Viability was monitored with visual assessments of corneal clarity and media colour, however testing of the culture media would allow for constant monitoring of lactate levels and other markers of tissue viability which would allow for the exclusion of non-viable tissue earlier in the model. Additionally, alternative models have developed media pumping systems through which the tissue media is constantly replenished and monitored, which would aid in this [383, 384, 402, 403].

Within this model, 300µl of each formulation was applied to each eye at each treatment. This is large than the average eye drop, which usually have a volume between 10 and 100µl. This was due to the fact that with no conjunctiva or eye lids, the majority of the formulation ran immediately off the surface of the eye and into the

media. Of course, *in vivo* the same can happen as the blinking reflex occurs and some is lost to the tears, but to test the formulations it was necessary to ensure a portion of the treatment remained on the eye. This highlights a limitation that occurs across demineralisation, toxicity and *ex vivo* model work – without an accurate idea of the contact time of each formulation, the data created was working on estimates of the minimum and maximum residence times for an eye drop. For the demineralisation assessment, we assumed a minimum contact time of 1 hour as previous studies have provided evidence that aqueous drops are still resident at this time. For the *in vitro* toxicity assays, a maximum residence time of between 4 and 6 hours was assumed, as this represents a time point beyond the upper limit of data on more viscous eye drop formulations. Both the *ex vivo* model and the toxicity assessments could be repeated with a more accurate treatment regime relative to residence time data. For the toxicity assessment, it would be vital to examine the effect of a repeated dosing regimen with recovery in between, something that was only touched on in the work begun here.

Analysis of previous *ex vivo* models (Table 4) revealed multiple considerations for the development of an *ex vivo* band keratopathy organ culture model. Porcine tissue was chosen for our model development for both the similarities in size and structure to a human eye, and the availability of fresh tissue. Smaller rabbit eyes had been previously used in an organ culture model – the ex-vivo eye irritation model – which successfully replicated topical phosphate induced band keratopathy [383]. Smaller eyes are potentially easier to maintain in culture, however this model relied on specialised perfusion chamber apparatus.

An additional consideration relates to how important the presence of the Bowman's membrane is to the aetiology of BK in the human eye. It is presumed that in many cases mineralisation begins here, before spreading into the stroma or rupturing the epithelial layer in more severe cases. This is separate to the development of BK in cases of injury or ulceration. In animals, cases of BK are commonly reported in horses and dogs [11, 388]. Neither horses not dogs have a Bowman's layer, suggesting that it may not be essential in the development of the disease, but still may affect the likelihood and progression [388, 427, 428]. There has been disagreement over whether porcine corneas have a Bowman's layer, with multiple conflicting reports. However, recent scanning electron microscope (SEM) and tunnelling electron microscope (TEM) images strongly suggest that the Bowman's layer is present in the porcine cornea [429]. This should allow a model developed with porcine cornea to more accurately replicate the development of BK in humans.

A consistent limitation of the model developed in this work is the degradation of the epithelial layer. Multiple steps could be taken to improve this limitation of the model, including the incorporation of agents which encourage epithelial cell growth such as Insulin, EGF and hydrocortisone into the culture media. Additionally, if alternative sterilisation steps could be explored to remove the need for povidone iodine treatment, the epithelial layer may be better protected before the tissue enters culture. A further optimisation step would include the homogenisation of the wounding performed on each eye to ensure each eye is wounded as similarly as possible, to increase consistency between samples.

Although an *ex vivo* model was chosen to replicate band keratopathy in this work, future studies could include the development of more complex *in vitro* 3-D cellular assays, which allow for the investigation of the response of various immune cells to HMP treatment. 3D models are suitable for the investigation of injury and regeneration models, which would be complimentary to the research questions proposed here [430]. 3D models would also allow for investigation into the responses of human corneal cells (as opposed to porcine) without the issues of sourcing high volumes of *ex vivo* human donor tissue, and would also enable the assessment of intra-cellular mechanisms between epithelial and stromal cells (as opposed to a single cell type), without the risks and challenges associated with *ex vivo* organ culture models such as infection and loss of tissue viability [430].

Relevant to the toxicity investigation for this potential treatment is the passage of the drop from the ocular surface to surrounding tissues, including through the nasal passage to the stomach or bloodstream. An ocular residence time analysis using fluorescein could be adapted to also include endpoints which investigate the final destinations of the drop. Due to the previous evidence, as well as that presented through our own investigations, suggesting the possibility of multiple reactions to HMP by different tissues and cell lines, it may be necessary to investigate the toxicity of HMP on conjunctival, vascular and other tissues.

Despite the development of increasingly accurate *ex vivo* and *in vitro* assays, it is still necessary for any treatment hoping to reach clinical trial or use to create *in vivo* animal data. Testing HMP formulations *in vivo* on an animal with induced band keratopathy would be a robust test of the potential for further development. Wound healing and

related models are common in animal work, and a similar mineralisation protocol could potentially be followed to induce band keratopathy in a murine eye using high phosphate eye drops and/or 10x SBF. However, this may be unnecessary, as multiple investigations have induced band keratopathy as an unintended side-effect without the need for wounding. One of these found that the use of ketamine/xylazine anaesthetic agents appeared to induce corneal cloudiness, which was later diagnosed as band keratopathy with a slit lamp [431]. Additionally, excess systemic or topical vitamin D can induce band keratopathy without the need for corneal abrasion [20]. The same is true of silicon oil. Each of these avenues could be explored to develop a less invasive *in vivo* model to continue this investigation.

e) Emergent questions for future analysis

In addition to the questions raised by the investigation into each of the four primary areas covered here (demineralisation, toxicity, formulation and *ex vivo* modelling), the success of any future formulation developed using HMP will rely on factors outside of the scope of this investigation. This includes the practicality of manufacturing the solution on a larger scale for clinical use, and the behaviours of the patients it is prescribed to. A comparative study (likely a clinical trial) would need to be performed between outcomes of patients who have the current standard superficial keratectomy treatment, and the new formulation. The efficacy of the new formulation, beyond it's biochemical characteristics, will depend on adherence from the patient to the desired treatment regime – something which is a barrier to all eye drop-based treatments [110-112, 114].

9.

CONCLUSIONS

Four questions were highlighted as key to this investigation –

(a) Can sodium hexametaphosphate effectively demineralise hydroxyapatite within the time period associated with the retention of an eye drop of the eye

(b) Is sodium hexametaphosphate toxic to the ocular tissue

(c) Can the delivery of sodium hexametaphosphate to the eye be optimised by incorporating polymeric hydrogel materials

(d) Can a relevant *ex vivo* test be developed to assess the efficacy of sodium hexametaphosphate in treating band keratopathy

The experiments performed have gone some of the way to answering each of these. It was found that Sodium hexametaphosphate at concentrations at and greater than 0.125M can induce significant reductions in the measured absorbance of hydroxyapatite sol within 1 hour of treatment, with 1M HMP appearing the most effective of the concentrations tested.

The toxicity of HMP remains to be further explored, with the work presented here suggesting that HMP negatively effects cell adhesion and metabolism and induces permeabilization of the cellular membrane, in a concentration dependant manner, but with a non-linear relationship between concentration and these behaviours.

HMP was found to induce dense crosslinking in gellan and chitosan, creating materials unsuitable for an eye drop. Chitosan films were developed, but these failed to release therapeutically effective levels of HMP. Alginate, however, appeared to present as a viable option for carrying concentrations of HMP below 0.5M.

Finally, an *ex vivo* model of band keratopathy was developed in porcine eyes, but with limited epithelial retention. This model was used to successfully show mineralisation and demineralisation of the tissue by HMP and the current clinical standard, EDTA. When compared, 1M HMP appeared to be more successful in demineralising the tissue when following the same treatment course as 2% EDTA.

Further work needs to be performed to investigate the toxicity of concentrations of HMP which could effectively demineralise calcified ocular tissue *in vitro*, avoiding metabolism assays which may provide misleading results due to the role of polyphosphate in cellular metabolism. In addition, the *ex vivo* model of band keratopathy should be further optimised to maintain epithelial barrier function if possible, and create a more accurate assessment of treatment efficacy. An analysis of the chain lengths of polyphosphates present in sodium hexametaphosphate could shed light on some of the behaviours described throughout this work.

References

1. Mantelli, F., J. Mauris, and P. Argueso, *The ocular surface epithelial barrier and other mechanisms of mucosal protection: from allergy to infectious diseases.* Curr Opin Allergy Clin Immunol, 2013. **13**(5): p. 563-8.
2. Kirsch, T., *Determinants of pathological mineralization.* Current Opinion in Rheumatology, 2006. **18**(2).
3. Li, Q., Q. Jiang, and J. Uitto, *Ectopic mineralization disorders of the extracellular matrix of connective tissue: molecular genetics and pathomechanisms of aberrant calcification.* Matrix Biol, 2014. **33**: p. 23-8.
4. Giachelli, C.M., *Ectopic Mineralization: New Concepts in Etiology and Regulation*, in *Handbook of Biomineralization*. 2007. p. 349-360.
5. Giachelli, C.M., *Ectopic Calcification.* The American Journal of Pathology, 1999. **154**(3): p. 671-675.
6. Blair, H.C., et al., *Osteoblast Differentiation and Bone Matrix Formation In Vivo and In Vitro.* Tissue Eng Part B Rev, 2017. **23**(3): p. 268-280.
7. Golub, E.E., *Biomineralization and matrix vesicles in biology and pathology.* Semin Immunopathol, 2011. **33**(5): p. 409-17.
8. Bergen, A.A., et al., *On the origin of proteins in human drusen: The meet, greet and stick hypothesis.* Prog Retin Eye Res, 2019. **70**: p. 55-84.
9. Jhanji, V., C.J. Rapuano, and R.B. Vajpayee, *Corneal calcific band keratopathy.* Curr Opin Ophthalmol, 2011. **22**(4): p. 283-9.
10. Al-Hity, A., K. Ramaesh, and D. Lockington, *EDTA chelation for symptomatic band keratopathy: results and recurrence.* Eye (Lond), 2018. **32**(1): p. 26-31.
11. Berryhill, E.H., et al., *Comparison of corneal degeneration and calcific band keratopathy from 2000 to 2013 in 69 horses.* Vet Ophthalmol, 2017. **20**(1): p. 16-26.
12. Nascimento, H., et al., *Uveitic band keratopathy: child and adult.* J Ophthalmic Inflamm Infect, 2015. **5**(1): p. 35.
13. Nevyas, A.S., et al., *Acute band keratopathy following intracameral Viscoat.* Arch Ophthalmol, 1987. **105**(7): p. 958-64.
14. Prasad Rao, G., et al., *Rapid Onset Bilateral Calcific Band Keratopathy Associated with Phosphate-containing Steroid Eye Drops.* European journal of Implant and Refractive Surgery, 1995. **7**(4): p. 251-252.
15. Weng, S.F., et al., *Risk of Band Keratopathy in Patients with End-Stage Renal Disease.* Sci Rep, 2016. **6**: p. 28675.
16. Das, A.V., L.N. Pillutla, and S. Chaurasia, *Clinical profile and demographic distribution of band shaped keratopathy in India: A study of 8801 patients.* Indian J Ophthalmol, 2022. **70**(5): p. 1582-1585.
17. Goel, S., et al., *Ocular manifestations of Wilson's disease.* BMJ Case Rep, 2019. **12**(3).
18. Suvarna, J.C., *Kayser-Fleischer ring.* J Postgrad Med, 2008. **54**(3): p. 238-40.
19. O'Connor, G.R., *Calcific band keratopathy.* Transactions of the American Ophthalmological Society, 1972. **70**: p. 58-81.
20. Doughman, D.J., et al., *Experimental Band Keratopathy.* Archives of Ophthalmology, 1969. **81**(2): p. 264-271.
21. Kwon, Y.S., Y.S. Song, and J.C. Kim, *New treatment for band keratopathy: superficial lamellar keratectomy, EDTA chelation and amniotic membrane transplantation.* Journal of Korean medical science, 2004. **19**(4): p. 611-615.

22. Transplant, N.B.a., *Organ and Tissue Donation and Transplantation Activity Report 2020/21*. 2021.
23. Bourne, R.R.A., et al., *Magnitude, temporal trends, and projections of the global prevalence of blindness and distance and near vision impairment: a systematic review and meta-analysis.* The Lancet Global Health, 2017. **5**(9): p. e888-e897.
24. Pezzullo, L., et al., *The economic impact of sight loss and blindness in the UK adult population.* BMC Health Serv Res, 2018. **18**(1): p. 63.
25. Forrester, J.V., et al., *Embryology and early development of the eye and adnexa*, in *The Eye*. 2016. p. 103-129.e8.
26. Terakita, A., *The opsins.* Genome Biology, 2005. **6**(3): p. 213.
27. Forrester, J.V., et al., *Anatomy of the eye and orbit*, in *The Eye*. 2016. p. 1-102.e2.
28. Giora, E. and W. Büttemeyer, *Roberto Ardigò as a forerunner of George M. Stratton's experiments on inverted vision.* Hist Psychol, 2020. **23**(1): p. 26-39.
29. Baranowski, P., et al., *Ophthalmic drug dosage forms: characterisation and research methods.* ScientificWorldJournal, 2014. **2014**: p. 861904.
30. Baba, K., et al., *A method for enhancing the ocular penetration of eye drops using nanoparticles of hydrolyzable dye.* J Control Release, 2011. **153**(3): p. 278-87.
31. Di Colo, G., et al., *Selected polysaccharides at comparison for their mucoadhesiveness and effect on precorneal residence of different drugs in the rabbit model.* Drug Dev Ind Pharm, 2009. **35**(8): p. 941-9.
32. Singh, V., et al., *Polymeric ocular hydrogels and ophthalmic inserts for controlled release of timolol maleate.* J Pharm Bioallied Sci, 2011. **3**(2): p. 280-5.
33. Bravo-Osuna, I., et al., *Microspheres as intraocular therapeutic tools in chronic diseases of the optic nerve and retina.* Adv Drug Deliv Rev, 2018. **126**: p. 127-144.
34. Skopiński, P., P. Krawczyk, and A.M. Ambroziak, *Immunology of the ocular surface and contact lens wear: theoretical fundamentals.* Central European Journal of Immunology, 2013. **2**: p. 254-259.
35. McDermott, A.M., *Antimicrobial compounds in tears.* Exp Eye Res, 2013. **117**: p. 53-61.
36. Gipson, I.K. and P. Argüeso, *Role of Mucins in the Function of the Corneal and Conjunctival Epithelia*, in *International Review of Cytology*. 2003, Academic Press. p. 1-49.
37. Hodges, R.R. and D.A. Dartt, *Tear film mucins: front line defenders of the ocular surface; comparison with airway and gastrointestinal tract mucins.* Exp Eye Res, 2013. **117**: p. 62-78.
38. Ruponen, M. and A. Urtti, *Undefined role of mucus as a barrier in ocular drug delivery.* Eur J Pharm Biopharm, 2015. **96**: p. 442-6.
39. Forrester, J.V., et al., *Immunology*, in *The Eye*. 2016. p. 370-461.e2.
40. Nho, Y.-C., J.-S. Park, and Y.-M. Lim, *Preparation of Poly(acrylic acid) Hydrogel by Radiation Crosslinking and Its Application for Mucoadhesives.* Polymers, 2014. **6**(3): p. 890-898.
41. Park, C.G., et al., *Mucoadhesive microparticles with a nanostructured surface for enhanced bioavailability of glaucoma drug.* J Control Release, 2015. **220**(Pt A): p. 180-188.
42. Takeuchi, H., et al., *Novel mucoadhesion tests for polymers and polymer-coated particles to design optimal mucoadhesive drug delivery systems.* Adv Drug Deliv Rev, 2005. **57**(11): p. 1583-94.

43. Woertz, C., et al., *Assessment of test methods evaluating mucoadhesive polymers and dosage forms: an overview.* Eur J Pharm Biopharm, 2013. **85**(3 Pt B): p. 843-53.
44. Yan, J., et al., *Comparison of different in vitro mucoadhesion testing methods for hydrogels.* Journal of Drug Delivery Science and Technology, 2017. **40**: p. 157-163.
45. Yu, T., G.P. Andrews, and D.S. Jones, *Mucoadhesion and Characterization of Mucoadhesive Properties*, in *Mucosal Delivery of Biopharmaceuticals*. 2014. p. 35-58.
46. Schechter, M.C., S.W. Satola, and D.S. Stephens, *27 - Host Defenses to Extracellular Bacteria*, in *Clinical Immunology (Fifth Edition)*, R.R. Rich, et al., Editors. 2019, Content Repository Only!: London. p. 391-402.e1.
47. Garreis, F., et al., *Expression and Regulation of Antimicrobial Peptide Psoriasin (S100A7) at the Ocular Surface and in the Lacrimal Apparatus.* Investigative Ophthalmology & Visual Science, 2011. **52**(7): p. 4914-4922.
48. Zierhut, M., et al., *Immunology of the lacrimal gland and ocular tear film.* Trends Immunol, 2002. **23**(7): p. 333-5.
49. Lan, J.X., et al., *Effect of tear secretory IgA on chemotaxis of polymorphonuclear leucocytes.* Australian and New Zealand Journal of Ophthalmology, 1998. **26**(S1): p. S36-S39.
50. Mudgil, P., *Antimicrobial role of human meibomian lipids at the ocular surface.* Invest Ophthalmol Vis Sci, 2014. **55**(11): p. 7272-7.
51. Essa, L., D. Laughton, and J.S. Wolffsohn, *Can the optimum artificial tear treatment for dry eye disease be predicted from presenting signs and symptoms?* Cont Lens Anterior Eye, 2018. **41**(1): p. 60-68.
52. Martin, E., et al., *Effect of tear supplements on signs, symptoms and inflammatory markers in dry eye.* Cytokine, 2018. **105**: p. 37-44.
53. Tomlinson, A., M. Hair, and A. McFadyen, *Statistical approaches to assessing single and multiple outcome measures in dry eye therapy and diagnosis.* Ocul Surf, 2013. **11**(4): p. 267-84.
54. Cunha-Vaz, J., R. Bernardes, and C. Lobo, *Blood-Retinal Barrier.* European Journal of Ophthalmology, 2011. **21**(6_suppl): p. 3-9.
55. Janagam, D.R., L. Wu, and T.L. Lowe, *Nanoparticles for drug delivery to the anterior segment of the eye.* Adv Drug Deliv Rev, 2017. **122**: p. 31-64.
56. Calles, J.A., et al., *Polymers in Ophthalmology*, in *Advanced Polymers in Medicine*. 2015. p. 147-176.
57. Eghrari, A.O., S.A. Riazuddin, and J.D. Gottsch, *Overview of the Cornea: Structure, Function, and Development.* Prog Mol Biol Transl Sci, 2015. **134**: p. 7-23.
58. Pepic, I., et al., *Toward the practical implementation of eye-related bioavailability prediction models.* Drug Discov Today, 2014. **19**(1): p. 31-44.
59. Imperiale, J.C., G.B. Acosta, and A. Sosnik, *Polymer-based carriers for ophthalmic drug delivery.* J Control Release, 2018. **285**: p. 106-141.
60. Kaur, I.P. and R. Smitha, *Penetration enhancers and ocular bioadhesives: two new avenues for ophthalmic drug delivery.* Drug Dev Ind Pharm, 2002. **28**(4): p. 353-69.
61. Gause, S., et al., *Mechanistic modeling of ophthalmic drug delivery to the anterior chamber by eye drops and contact lenses.* Adv Colloid Interface Sci, 2016. **233**: p. 139-154.
62. Gagliano, C., et al., *Measurement of the Retention Time of Different Ophthalmic Formulations with Ultrahigh-Resolution Optical Coherence Tomography.* Curr Eye Res, 2018. **43**(4): p. 499-502.

63. Jiao, H., et al., *Anterior segment optical coherence tomography: its application in clinical practice and experimental models of disease.* Clin Exp Optom, 2019. **102**(3): p. 208-217.
64. IPINAZAR UNDURRAGA, M., et al., *Ocular surface retention time and extensions of TFBUT of a lubricating eye drop.* Acta Ophthalmologica Scandinavica, 2007. **85**(s240): p. 0-0.
65. Mochizuki, H., et al., *Fluorophotometric measurement of the precorneal residence time of topically applied hyaluronic acid.* Br J Ophthalmol, 2008. **92**(1): p. 108-11.
66. Paugh, J.R., et al., *Precorneal residence time of artificial tears measured in dry eye subjects.* Optom Vis Sci, 2008. **85**(8): p. 725-31.
67. Subrizi, A., et al., *Design principles of ocular drug delivery systems: importance of drug payload, release rate, and material properties.* Drug Discov Today, 2019.
68. Craig, J.P., et al., *TFOS DEWS II Definition and Classification Report.* Ocul Surf, 2017. **15**(3): p. 276-283.
69. Bulletin, D.T., *The management of dry eye.* BMJ, 2016. **353**: p. i2333.
70. Kumar, K., et al., *Bioadhesive polymers: novel tool for drug delivery.* Artif Cells Nanomed Biotechnol, 2014. **42**(4): p. 274-83.
71. Sannino, A., C. Demitri, and M. Madaghiele, *Biodegradable Cellulose-based Hydrogels: Design and Applications.* Materials, 2009. **2**(2): p. 353-373.
72. Aravamudhan, A., et al., *Natural Polymers*, in *Natural and Synthetic Biomedical Polymers*. 2014. p. 67-89.
73. Zheng, X., T. Goto, and Y. Ohashi, *Comparison of in vivo efficacy of different ocular lubricants in dry eye animal models.* Invest Ophthalmol Vis Sci, 2014. **55**(6): p. 3454-60.
74. Madruga, L.Y.C., et al., *Effect of ionic strength on solution and drilling fluid properties of ionic polysaccharides: A comparative study between Na-carboxymethylcellulose and Na-kappa-carrageenan responses.* Journal of Molecular Liquids, 2018. **266**: p. 870-879.
75. Fekete, T., et al., *Synthesis of carboxymethylcellulose/acrylic acid hydrogels with superabsorbent properties by radiation-initiated crosslinking.* Radiation Physics and Chemistry, 2016. **124**: p. 135-139.
76. Kyyronen, K. and A. Urtti, *Improved Ocular - Systemic Absorption Ratio of Timolol by Viscous Vehicle and Phenylephrine.* Investigative Ophthalmology & Visual Science, 1990. **31**(9): p. 1827-1833.
77. Sharma, M., S. Kohli, and A. Dinda, *In-vitro and in-vivo evaluation of repaglinide loaded floating microspheres prepared from different viscosity grades of HPMC polymer.* Saudi Pharm J, 2015. **23**(6): p. 675-82.
78. Reverchon, E., G. Lamberti, and A. Antonacci, *Supercritical fluid assisted production of HPMC composite microparticles.* The Journal of Supercritical Fluids, 2008. **46**(2): p. 185-196.
79. Arthanari, S., P. Renukadevi, and V. Saravanakumar, *Evaluation of lactose stabilized tetanus toxoid encapsulated into alginate, HPMC composite microspheres.* Journal of Industrial and Engineering Chemistry, 2014. **20**(4): p. 2018-2022.
80. West, D.C. and S. Kumar, *Hyaluronan and angiogenesis.* Ciba Found Symp, 1989. **143**: p. 187-201; discussion 201-7, 281-5.
81. Krause, W.E., E.G. Bellomo, and R.H. Colby, *Rheology of sodium hyaluronate under physiological conditions.* Biomacromolecules, 2001. **2**(1): p. 65-9.

82. Salzillo, R., et al., *Optimization of hyaluronan-based eye drop formulations.* Carbohydr Polym, 2016. **153**: p. 275-283.
83. Brignole, F., et al., *Efficacy and safety of 0.18% sodium hyaluronate in patients with moderate dry eye syndrome and superficial keratitis.* Graefes Arch Clin Exp Ophthalmol, 2005. **243**(6): p. 531-8.
84. Mencucci, R.C.B., Roberto Caputo, Eleonora Favuzza, *Effect of a hyaluronic acid and carboxymethylcellulose ophthalmic solution on ocular comfort and tear-film instability after cataract surgery.* Journal of Cataract & Refractive Surgery, 2015. **41**(8): p. 1699-1704.
85. Aragona, P.P., V.; Micali, A.; Santocono, M.; and G. Milazzo, *Long term treatment with sodium hyaluronate-containing artificial tears reduces ocular surface damage in patients with dry eye.* British Journal of Ophthalmology, 2002.
86. McDermott, M.L. and H.F. Edelhauser, *Drug binding of ophthalmic viscoelastic agents.* Archives of Ophthalmology, 1989. **107**(2): p. 261-263.
87. Lin, C.C. and K.S. Anseth, *PEG hydrogels for the controlled release of biomolecules in regenerative medicine.* Pharm Res, 2009. **26**(3): p. 631-43.
88. G, T., *The effects of lubricant eye drops on visual function as measured by the inter-blink interval Visual Acuity Decay test.* Clin Ophthalmol, 2009. **3**: p. 501 - 506.
89. Aguilar, A., et al., *Efficacy of polyethylene glycol-propylene glycol-based lubricant eye drops in reducing squamous metaplasia in patients with dry eye disease.* Clin Ophthalmol, 2018. **12**: p. 1237-1243.
90. Asbell, P., et al., *Clinical Outcomes of Fixed Versus As-Needed Use of Artificial Tears in Dry Eye Disease: A 6-Week, Observer-Masked Phase 4 Clinical Trial.* Investigative Ophthalmology & Visual Science, 2018. **59**(6): p. 2275-2280.
91. Shtenberg, Y., et al., *Alginate modified with maleimide-terminated PEG as drug carriers with enhanced mucoadhesion.* Carbohydr Polym, 2017. **175**: p. 337-346.
92. Veronese, F.M. and A. Mero, *The impact of PEGylation on biological therapies.* BioDrugs, 2008. **22**(5): p. 315-29.
93. Buske, J., et al., *Influence of PEG in PEG-PLGA microspheres on particle properties and protein release.* Eur J Pharm Biopharm, 2012. **81**(1): p. 57-63.
94. Jang, H.J., C.Y. Shin, and K.B. Kim, *Safety Evaluation of Polyethylene Glycol (PEG) Compounds for Cosmetic Use.* Toxicol Res, 2015. **31**(2): p. 105-36.
95. Cooke, M.E., et al., *Structuring of Hydrogels across Multiple Length Scales for Biomedical Applications.* Adv Mater, 2018. **30**(14): p. e1705013.
96. Mammadova, S.M., et al., *Synthesis, Structure and Swelling Properties of Hydrogels Based on Polyacrylic Acid*. Vol. 29. 2017. 576-580.
97. Islam, M.T., et al., *Rheological characterization of topical carbomer gels neutralized to different pH.* Pharm Res, 2004. **21**(7): p. 1192-9.
98. Lyapunov, A.N., et al., *Studies of Carbomer Gels Using Rotational Viscometry and Spin Probes.* Pharmaceutical Chemistry Journal, 2015. **49**(9): p. 639-644.
99. Ochoa-Andrade, A., et al., *Study of the Influence of Formulation Variables in Bioadhesive Emulgels Using Response Surface Methodology.* AAPS PharmSciTech, 2017. **18**(6): p. 2269-2278.
100. Suchaoin, W., et al., *Mucoadhesive polymers: Synthesis and in vitro characterization of thiolated poly(vinyl alcohol).* Int J Pharm, 2016. **503**(1-2): p. 141-9.
101. Leone, G., et al., *Modified low molecular weight poly-vinyl alcohol as viscosity enhancer.* Materials Today Communications, 2019. **21**.

102. Peppas, N.A., et al., *Hydrogels in Biology and Medicine: From Molecular Principles to Bionanotechnology.* Advanced Materials, 2006. **18**(11): p. 1345-1360.
103. Baranowski, P., et al., *Ophthalmic Drug Dosage Forms: Characterisation and Research Methods.* The Scientific World Journal, 2014. **2014**: p. 861904.
104. Bertens, C.J.F., et al., *Topical drug delivery devices: A review.* Exp Eye Res, 2018. **168**: p. 149-160.
105. Chauhan, A., *Ocular Drug Delivery Role of Contact Lenses.* Delhi Journal of Ophthalmology, 2015. **26**(2).
106. Cooper, R.C. and H. Yang, *Hydrogel-based ocular drug delivery systems: Emerging fabrication strategies, applications, and bench-to-bedside manufacturing considerations.* J Control Release, 2019. **306**: p. 29-39.
107. Fuchs, B., et al., *A New Calcium-alginate Insert for Drug Delivery to the Eye: A Tolerance Study.* Investigative Ophthalmology & Visual Science, 2002. **43**(13): p. 4196-4196.
108. Ross, A.E., et al., *Topical sustained drug delivery to the retina with a drug-eluting contact lens.* Biomaterials, 2019. **217**: p. 119285.
109. Ubani-Ukoma, U., et al., *Evaluating the potential of drug eluting contact lenses for treatment of bacterial keratitis using an ex vivo corneal model.* Int J Pharm, 2019. **565**: p. 499-508.
110. Carpenter, D.M., et al., *Exploring the influence of patient-provider communication on intraocular pressure in glaucoma patients.* Patient Educ Couns, 2015.
111. Davies, I., A.M. Williams, and K.W. Muir, *Aids for eye drop administration.* Surv Ophthalmol, 2017. **62**(3): p. 332-345.
112. Friedman, D.S., et al., *Risk factors for poor adherence to eyedrops in electronically monitored patients with glaucoma.* Ophthalmology, 2009. **116**(6): p. 1097-105.
113. Newman-Casey, P.A., et al., *The Most Common Barriers to Glaucoma Medication Adherence: A Cross-Sectional Survey.* Ophthalmology, 2015. **122**(7): p. 1308-16.
114. Okeke, C.O., et al., *Interventions improve poor adherence with once daily glaucoma medications in electronically monitored patients.* Ophthalmology, 2009. **116**(12): p. 2286-93.
115. Sleath, B., et al., *The relationship between glaucoma medication adherence, eye drop technique, and visual field defect severity.* Ophthalmology, 2011. **118**(12): p. 2398-402.
116. Waterman, H., et al., *Interventions for improving adherence to ocular hypotensive therapy.* Cochrane Database Syst Rev, 2013(4): p. CD006132.
117. Ahmed, E.M., *Hydrogel: Preparation, characterization, and applications: A review.* J Adv Res, 2015. **6**(2): p. 105-21.
118. Al-Kinani, A.A., et al., *Ophthalmic gels: Past, present and future.* Adv Drug Deliv Rev, 2018. **126**: p. 113-126.
119. Kirchhof, S., A.M. Goepferich, and F.P. Brandl, *Hydrogels in ophthalmic applications.* Eur J Pharm Biopharm, 2015. **95**(Pt B): p. 227-38.
120. Ma, S., et al., *Structural hydrogels.* Polymer, 2016. **98**: p. 516-535.
121. van der Meer, P.F., J. Seghatchian, and D.C. Marks, *Quality standards, safety and efficacy of blood-derived serum eye drops: A review.* Transfus Apher Sci, 2016. **54**(1): p. 164-7.
122. Shelley, H., et al., *In Situ Gel Formulation for Enhanced Ocular Delivery of Nepafenac.* J Pharm Sci, 2018. **107**(12): p. 3089-3097.

123. Wu, Y., et al., *Research progress of in-situ gelling ophthalmic drug delivery system.* Asian Journal of Pharmaceutical Sciences, 2019. **14**(1): p. 1-15.
124. Madni, A., et al., *Non-invasive strategies for targeting the posterior segment of eye.* Int J Pharm, 2017. **530**(1-2): p. 326-345.
125. Francisco J. Otero-Espinar, A.F.-F., Miguel González-Barcia, José Blanco-Méndez, Asteria Luzardo, *Chapter 6 - Stimuli sensitive ocular drug delivery systems.* 2018: p. 211 - 270.
126. Barreiro-Iglesias, R., C. Alvarez-Lorenzo, and A. Concheiro, *Incorporation of small quantities of surfactants as a way to improve the rheological and diffusional behavior of carbopol gels.* Journal of Controlled Release, 2001. **77**(1-2): p. 59-75.
127. Islam, M.T., et al., *Fourier transform infrared spectroscopy for the analysis of neutralizer-carbomer and surfactant-carbomer interactions in aqueous, hydroalcoholic, and anhydrous gel formulations.* Aaps Journal, 2004. **6**(4).
128. Mills, T., A. Koay, and I.T. Norton, *Fluid gel lubrication as a function of solvent quality.* Food Hydrocolloids, 2013. **32**(1): p. 172-177.
129. Mahdi, M.H., B.R. Conway, and A.M. Smith, *Evaluation of gellan gum fluid gels as modified release oral liquids.* Int J Pharm, 2014. **475**(1-2): p. 335-43.
130. Fernández Farrés, I. and I.T. Norton, *Formation kinetics and rheology of alginate fluid gels produced by in-situ calcium release.* Food Hydrocolloids, 2014. **40**: p. 76-84.
131. Chouhan, G., et al., *A self-healing hydrogel eye drop for the sustained delivery of decorin to prevent corneal scarring.* Biomaterials, 2019. **210**: p. 41-50.
132. Moya-Ortega, M.D., et al., *Dexamethasone eye drops containing gamma-cyclodextrin-based nanogels.* Int J Pharm, 2013. **441**(1-2): p. 507-15.
133. Ter Horst, B., et al., *A gellan-based fluid gel carrier to enhance topical spray delivery.* Acta Biomater, 2019. **89**: p. 166-179.
134. Bradbeer, J.F., et al., *Low acyl gellan gum fluid gel formation and their subsequent response with acid to impact on satiety.* Food Hydrocolloids, 2015. **43**: p. 501-509.
135. Fernández Farrés, I., R.J.A. Moakes, and I.T. Norton, *Designing biopolymer fluid gels: A microstructural approach.* Food Hydrocolloids, 2014. **42**: p. 362-372.
136. Mahdi, M.H., et al., *Gellan gum fluid gels for topical administration of diclofenac.* Int J Pharm, 2016. **515**(1-2): p. 535-542.
137. Mahdi, M.H., B.R. Conway, and A.M. Smith, *Development of mucoadhesive sprayable gellan gum fluid gels.* Int J Pharm, 2015. **488**(1-2): p. 12-9.
138. Simmons, P.A., C. Carlisle-Wilcox, and J.G. Vehige, *Comparison of novel lipid-based eye drops with aqueous eye drops for dry eye: a multicenter, randomized controlled trial.* Clin Ophthalmol, 2015. **9**: p. 657-64.
139. Simmons, P.A., et al., *Efficacy, safety, and acceptability of a lipid-based artificial tear formulation: a randomized, controlled, multicenter clinical trial.* Clin Ther, 2015. **37**(4): p. 858-68.
140. Suda, K., et al., *High-density lipoprotein mutant eye drops for the treatment of posterior eye diseases.* J Control Release, 2017. **266**: p. 301-309.
141. Alvarez-Trabado, J., Y. Diebold, and A. Sanchez, *Designing lipid nanoparticles for topical ocular drug delivery.* Int J Pharm, 2017. **532**(1): p. 204-217.
142. Peng, C.C., et al., *Emulsions and microemulsions for ocular drug delivery.* Journal of Drug Delivery Science and Technology, 2011. **21**(1): p. 111-121.

143. Di Pascuale, M.A., E. Goto, and S.C. Tseng, *Sequential changes of lipid tear film after the instillation of a single drop of a new emulsion eye drop in dry eye patients.* Ophthalmology, 2004. **111**(4): p. 783-91.
144. Qiao, J. and X. Yan, *Emerging treatment options for meibomian gland dysfunction.* Clin Ophthalmol, 2013. **7**: p. 1797-803.
145. Jaiswal, P., B. Gidwani, and A. Vyas, *Nanostructured lipid carriers and their current application in targeted drug delivery.* Artif Cells Nanomed Biotechnol, 2016. **44**(1): p. 27-40.
146. Ahsan, F., et al., *Targeting to macrophages: role of physicochemical properties of particulate carriers—liposomes and microspheres—on the phagocytosis by macrophages.* Journal of Controlled Release, 2002. **79**(1): p. 29-40.
147. Akbarzadeh, A., et al., *Liposome: classification, preparation, and applications.* Nanoscale Res Lett, 2013. **8**(1): p. 102.
148. Szebeni, J. and S.M. Moghimi, *Liposome triggering of innate immune responses: a perspective on benefits and adverse reactions.* J Liposome Res, 2009. **19**(2): p. 85-90.
149. Samimi, S., et al., *Lipid-Based Nanoparticles for Drug Delivery Systems*, in *Characterization and Biology of Nanomaterials for Drug Delivery*. 2019. p. 47-76.
150. Lim, A., M.R. Wenk, and L. Tong, *Lipid-Based Therapy for Ocular Surface Inflammation and Disease.* Trends Mol Med, 2015. **21**(12): p. 736-748.
151. Dave, V., et al., *Lipid-polymer hybrid nanoparticles: Synthesis strategies and biomedical applications.* J Microbiol Methods, 2019. **160**: p. 130-142.
152. Ying, L., K. Tahara, and H. Takeuchi, *Drug delivery to the ocular posterior segment using lipid emulsion via eye drop administration: effect of emulsion formulations and surface modification.* Int J Pharm, 2013. **453**(2): p. 329-35.
153. Sindt, C.W., et al., *Dendritic immune cell densities in the central cornea associated with soft contact lens types and lens care solution types: a pilot study.* Clin Ophthalmol, 2012. **6**: p. 511-9.
154. Yureeda Qazi, A.C., Neda Baniasadi, Lixin Zheng, Deborah Witkin, Douglas B. Critser, Amy Watts, Jill Beyer, Christine W. Sindt, Pedram Hamrah, *Early Effects of Contact Lens Wear on Immune Cell Density of the Ocular Surface: Preliminary Results of a Laser In Vivo Confocal Microscopy Study.* Invest. Ophthalmol. Vis. Sci., 2011.
155. Chao, C., et al., *Non-invasive objective and contemporary methods for measuring ocular surface inflammation in soft contact lens wearers - A review.* Cont Lens Anterior Eye, 2017. **40**(5): p. 273-282.
156. Gad, A., et al., *Tear film inflammatory cytokine upregulation in contact lens discomfort.* Ocul Surf, 2019. **17**(1): p. 89-97.
157. Pili, K., et al., *Dry eye in contact lens wearers as a growing public health problem.* Psychiatr Danub, 2014. **26 Suppl 3**: p. 528-32.
158. Greiner, K.L. and J.J. Walline, *Dry eye in pediatric contact lens wearers.* Eye & contact lens, 2010. **36**(6): p. 352-355.
159. Sweeney, D., et al., *Clinical Characterization of Corneal Infiltrative Events Observed with Soft Contact Lens Wear*. Vol. 22. 2003. 435-42.
160. Espana, E.M. and S.C.G. Tseng, *Analysis of contact lens intolerance by exploring neuroanatomic integration of ocular surface defense.* Contact Lens and Anterior Eye, 2003. **26**(3): p. 131-137.
161. Meng, T., et al., *Therapeutic implications of nanomedicine for ocular drug delivery.* Drug Discov Today, 2019. **24**(8): p. 1524-1538.

162. Chinnery, H.R., P.G. McMenamin, and S.J. Dando, *Macrophage physiology in the eye.* Pflugers Arch, 2017. **469**(3-4): p. 501-515.
163. Hamrah, P., et al., *Novel characterization of MHC class II-negative population of resident corneal Langerhans cell-type dendritic cells.* Invest Ophthalmol Vis Sci, 2002. **43**(3): p. 639-46.
164. McWhorter, F.Y., et al., *Modulation of macrophage phenotype by cell shape.* Proc Natl Acad Sci U S A, 2013. **110**(43): p. 17253-8.
165. Sadtler, K., et al., *Divergent immune responses to synthetic and biological scaffolds.* Biomaterials, 2019. **192**: p. 405-415.
166. Wynn, T.A. and K.M. Vannella, *Macrophages in Tissue Repair, Regeneration, and Fibrosis.* Immunity, 2016. **44**(3): p. 450-462.
167. Dana, M.R., *Corneal antigen-presenting cells: diversity, plasticity, and disguise: the Cogan lecture.* Invest Ophthalmol Vis Sci, 2004. **45**(3): p. 722-7; 721.
168. Chinnery, H.R., et al., *Turnover of bone marrow-derived cells in the irradiated mouse cornea.* Immunology, 2008. **125**(4): p. 541-548.
169. Thill, M., et al., *A Novel Population of Repair Cells Identified in the Stroma of the Human Cornea.* Stem Cells and Development, 2007. **16**(5): p. 733-746.
170. Ferenbach, D. and J. Hughes, *Macrophages and dendritic cells: what is the difference?* Kidney Int, 2008. **74**(1): p. 5-7.
171. Chung, L., et al., *Key players in the immune response to biomaterial scaffolds for regenerative medicine.* Adv Drug Deliv Rev, 2017. **114**: p. 184-192.
172. Tan, C., et al., *Unlike Th1/Th17 cells, Th2/Th9 cells selectively migrate to the limbus/conjunctiva and initiate an eosinophilic infiltration process.* Experimental Eye Research, 2018. **166**: p. 116-119.
173. KNOP, N. and E. KNOP, *Conjunctiva-associated lymphoid tissue (CALT) – the physiological protective MALT of the conjunctiva.* Acta Ophthalmologica, 2008. **86**(s243): p. 0-0.
174. Knop, N. and E. Knop, *Ultrastructural anatomy of CALT follicles in the rabbit reveals characteristics of M-cells, germinal centres and high endothelial venules.* J Anat, 2005. **207**(4): p. 409-26.
175. Chung, B.J., D. Platt, and A. Vaidya, *The mechanics of clearance in a non-Newtonian lubrication layer.* International Journal of Non-Linear Mechanics, 2016. **86**: p. 133-145.
176. Tomlinson, A. and S. Khanal, *Assessment of Tear Film Dynamics: Quantification Approach.* The Ocular Surface, 2005. **3**(2): p. 81-95.
177. Washington, N., C. Washington, and C. Wilson, *Physiological Pharmaceutics—Barriers to Drug Absorption*. Vol. 93. 2001.
178. Uchino, Y., *The Ocular Surface Glycocalyx and its Alteration in Dry Eye Disease: A Review.* Invest Ophthalmol Vis Sci, 2018. **59**(14): p. DES157-DES162.
179. Khutoryanskiy, V.V., *Mucoadhesive Materials and Drug Delivery Systems*. 2014, New York, UNITED KINGDOM: John Wiley & Sons, Incorporated.
180. Mansuri, S., et al., *Mucoadhesion: A promising approach in drug delivery system.* Reactive and Functional Polymers, 2016. **100**: p. 151-172.
181. Al-shohani, A., *Hydrogel Formulations for Opthalmic Delivery*, in *School of Pharmacy*. 2016, University College London.
182. Xu, X., et al., *Sustained release of Avastin(R) from polysaccharides cross-linked hydrogels for ocular drug delivery.* Int J Biol Macromol, 2013. **60**: p. 272-6.

183. Deepthi, S. and J. Jose, *Novel hydrogel-based ocular drug delivery system for the treatment of conjunctivitis.* Int Ophthalmol, 2018.
184. Grover, L.M. and A.M. Smith, *Hydrocolloids and Medicinal Chemistry Applications*, in *Handbook of Biopolymers and Biodegradable Plastics*. 2013. p. 365-384.
185. De Souza Ferreira, S.B., et al., *Linear correlation between rheological, mechanical and mucoadhesive properties of polycarbophil polymer blends for biomedical applications.* J Mech Behav Biomed Mater, 2017. **68**: p. 265-275.
186. Rahman, M.Q., et al., *The effect of pH, dilution, and temperature on the viscosity of ocular lubricants--shift in rheological parameters and potential clinical significance.* Eye (Lond), 2012. **26**(12): p. 1579-84.
187. Mansour, M., et al., *Ocular poloxamer-based ciprofloxacin hydrochloride in situ forming gels.* Drug Dev Ind Pharm, 2008. **34**(7): p. 744-52.
188. Tamburic, S. and D.Q.M. Craig, *A comparison of different in vitro methods for measuring mucoadhesive performance.* European Journal of Pharmaceutics and Biopharmaceutics, 1997. **44**(2): p. 159-167.
189. Laffleur, F., et al., *Evaluation of modified hyaluronic acid in terms of rheology, enzymatic degradation and mucoadhesion.* Int J Biol Macromol, 2019. **123**: p. 1204-1210.
190. Rossi, S., et al., *Rheological analysis and mucoadhesion: A 30 year-old and still active combination.* J Pharm Biomed Anal, 2018. **156**: p. 232-238.
191. Jones, D.S., et al., *Statistical modelling of the rheological and mucoadhesive properties of aqueous poly(methylvinylether-co-maleic acid) networks: Redefining biomedical applications and the relationship between viscoelasticity and mucoadhesion.* Colloids Surf B Biointerfaces, 2016. **144**: p. 125-134.
192. Abdulrazik, M. and S. Benita, *Interfacial Interactions Of Cationic And Anionic Artificial Tears With Ionic Hydrogel Contact Lens Surface.* Investigative Ophthalmology & Visual Science, 2012. **53**(14): p. 6111-6111.
193. Shanker, R.M., et al., *An in vitro technique for measuring contact angles on the corneal surface and its application to evaluate corneal wetting properties of water soluble polymers.* International Journal of Pharmaceutics, 1995. **119**(2): p. 149-163.
194. Purslow, C., R. Wilcox, and F. Drijfhout, *A novel method to measure the contact angle of dry eye drop solutions.* Contact Lens and Anterior Eye, 2018. **41**: p. S72.
195. German, E.H., MA; Wood, D, *Reliability of drop size from multi-dose eye drop bottles: is it cause for concern?* Eye, 1999. **13**: p. 93-100.
196. Van Santvliet, L. and A. Ludwig, *Determinants of eye drop size.* Surv Ophthalmol, 2004. **49**(2): p. 197-213.
197. Malkin, A.Y. and A.I. Isayev, *2 - VISCOELASTICITY*, in *Rheology Concepts, Methods, and Applications (Second Edition)*, A.Y. Malkin and A.I. Isayev, Editors. 2012, Elsevier: Oxford. p. 43-126.
198. Malkin, A.Y. and A.I. Isayev, *3 - LIQUIDS*, in *Rheology Concepts, Methods, and Applications (Second Edition)*, A.Y. Malkin and A.I. Isayev, Editors. 2012, Elsevier: Oxford. p. 127-221.
199. Cheng, X., et al., *Imaging the microscopic structure of shear thinning and thickening colloidal suspensions.* Science, 2011. **333**(6047): p. 1276-9.
200. Mutharasan, R. and S. Srinivas, *Topographic Distribution Of Blink Induced Shear Stress (BLISS) On The Corneal Surface.* Investigative Ophthalmology & Visual Science, 2002. **43**(13): p. 974-974.

201. Wilson, D.I., *What is rheology?* Eye (Lond), 2018. **32**(2): p. 179-183.
202. Edsman, K., J. Carlfors, and K. Harju, *Rheological evaluation and ocular contact time of some carbomer gels for ophthalmic use.* International Journal of Pharmaceutics, 1996. **137**(2): p. 233-241.
203. Aragona, P., et al., *Physicochemical Properties of Hyaluronic Acid-Based Lubricant Eye Drops.* Transl Vis Sci Technol, 2019. **8**(6): p. 2.
204. Ceulemans, J. and A. Ludwig, *Optimisation of carbomer viscous eye drops: an in vitro experimental design approach using rheological techniques.* European Journal of Pharmaceutics and Biopharmaceutics, 2002. **54**(1): p. 41-50.
205. Kate Gurnon, A. and N.J. Wagner, *Large amplitude oscillatory shear (LAOS) measurements to obtain constitutive equation model parameters: Giesekus model of banding and nonbanding wormlike micelles.* Journal of Rheology, 2012. **56**(2): p. 333-351.
206. Bhattarai, N., J. Gunn, and M. Zhang, *Chitosan-based hydrogels for controlled, localized drug delivery.* Adv Drug Deliv Rev, 2010. **62**(1): p. 83-99.
207. Wang, K. and Z. Han, *Injectable hydrogels for ophthalmic applications.* J Control Release, 2017. **268**: p. 212-224.
208. Kaklamani, G., et al., *Mechanical properties of alginate hydrogels manufactured using external gelation.* J Mech Behav Biomed Mater, 2014. **36**: p. 135-42.
209. George, A., P.A. Shah, and P.S. Shrivastav, *Natural biodegradable polymers based nano-formulations for drug delivery: A review.* Int J Pharm, 2019. **561**: p. 244-264.
210. Subrizi, A., et al., *Design principles of ocular drug delivery systems: importance of drug payload, release rate, and material properties.* Drug Discov Today, 2019. **24**(8): p. 1446-1457.
211. Ramsay, E., et al., *Corneal and conjunctival drug permeability: Systematic comparison and pharmacokinetic impact in the eye.* Eur J Pharm Sci, 2018. **119**: p. 83-89.
212. M. Fabrizio Saettonea, P.C., Riccardo Cerbaia, Gabriela Mazzantib, Laura Braghirolib, *Evaluation of ocular permeation enhancers: in vitro effects on corneal transport of four fl-blockers, and in vitro/in vivo toxic activity.* International Journal of Pharmaceutics, 1996. **142**: p. 103-113.
213. Hirano, S., et al., *Calcium-dependent cell-cell adhesion molecules (cadherins): subclass specificities and possible involvement of actin bundles.* J Cell Biol, 1987. **105**(6 Pt 1): p. 2501-10.
214. Xu, L., P.A. Overbeek, and L.W. Reneker, *Systematic analysis of E-, N- and P-cadherin expression in mouse eye development.* Exp Eye Res, 2002. **74**(6): p. 753-60.
215. Chifflet, S., et al., *Effect of membrane potential depolarization on the organization of the actin cytoskeleton of eye epithelia. The role of adherens junctions.* Exp Eye Res, 2004. **79**(6): p. 769-77.
216. Morrison, P.W. and V.V. Khutoryanskiy, *Enhancement in corneal permeability of riboflavin using calcium sequestering compounds.* Int J Pharm, 2014. **472**(1-2): p. 56-64.
217. Villani, E., et al., *The Ocular Surface in Medically Controlled Glaucoma: An In Vivo Confocal Study.* Invest Ophthalmol Vis Sci, 2016. **57**(3): p. 1003-10.
218. Johannsdottir, S., et al., *Topical drug delivery to the posterior segment of the eye: The effect of benzalkonium chloride on topical dexamethasone penetration into the eye in vivo.* Journal of Drug Delivery Science and Technology, 2018. **48**: p. 125-127.

219. Rodriguez, I., et al., *Enhancement and inhibition effects on the corneal permeability of timolol maleate: Polymers, cyclodextrins and chelating agents.* Int J Pharm, 2017. **529**(1-2): p. 168-177.
220. Ahn, K. and A. Kornberg, *Polyphosphate kinase from Escherichia coli. Purification and demonstration of a phosphoenzyme intermediate.* J Biol Chem, 1990. **265**(20): p. 11734-9.
221. Ishige, K., H. Zhang, and A. Kornberg, *Polyphosphate kinase (PPK2), a potent, polyphosphate-driven generator of GTP.* Proc Natl Acad Sci U S A, 2002. **99**(26): p. 16684-8.
222. Nocek, B., et al., *Polyphosphate-dependent synthesis of ATP and ADP by the family-2 polyphosphate kinases in bacteria.* Proc Natl Acad Sci U S A, 2008. **105**(46): p. 17730-5.
223. Zhang, H., K. Ishige, and A. Kornberg, *A polyphosphate kinase (PPK2) widely conserved in bacteria.* Proc Natl Acad Sci U S A, 2002. **99**(26): p. 16678-83.
224. Gautam, L.K., P. Sharma, and N. Capalash, *Attenuation of Acinetobacter baumannii virulence by inhibition of polyphosphate kinase 1 with repurposed drugs.* Microbiol Res, 2021. **242**: p. 126627.
225. Cui, C., et al., *Characterization of polyphosphate kinases for the synthesis of GSH with ATP regeneration from AMP.* Enzyme and Microbial Technology, 2021. **149**.
226. Zhang, A., et al., *The structure of exopolyphosphatase (PPX) from Porphyromonas gingivalis in complex with substrate analogs and magnesium ions reveals the basis for polyphosphate processivity.* J Struct Biol, 2021. **213**(3): p. 107767.
227. Xie, L. and U. Jakob, *Inorganic polyphosphate, a multifunctional polyanionic protein scaffold.* J Biol Chem, 2019. **294**(6): p. 2180-2190.
228. Bowlin, M.Q. and M.J. Gray, *Inorganic Polyphosphate in Host and Microbe Biology.* Trends Microbiol, 2021.
229. Ali, A., et al., *A novel mammalian glucokinase exhibiting exclusive inorganic polyphosphate dependence in the cell nucleus.* Biochem Biophys Rep, 2017. **12**: p. 151-157.
230. Hacchou, Y., et al., *Inorganic polyphosphate: a possible stimulant of bone formation.* Journal of Dental Research, 2007. **86**(9): p. 893-897.
231. Yuan, Q., et al., *Effect of combined application of bFGF and inorganic polyphosphate on bioactivities of osteoblasts and initial bone regeneration.* Acta Biomater, 2009. **5**(5): p. 1716-24.
232. Tsutsumi, K., et al., *Morphogenetic study on the maturation of osteoblastic cell as induced by inorganic polyphosphate.* PLoS One, 2014. **9**(2): p. e86834.
233. Raposo, G., M.S. Marks, and D.F. Cutler, *Lysosome-related organelles: driving post-Golgi compartments into specialisation.* Curr Opin Cell Biol, 2007. **19**(4): p. 394-401.
234. Docampo, R. and S.N. Moreno, *Acidocalcisomes.* Cell Calcium, 2011. **50**(2): p. 113-9.
235. Morrissey, J.H., S.H. Choi, and S.A. Smith, *Polyphosphate: an ancient molecule that links platelets, coagulation, and inflammation.* Blood, 2012. **119**(25): p. 5972-9.
236. Muller, F., et al., *Platelet polyphosphates are proinflammatory and procoagulant mediators in vivo.* Cell, 2009. **139**(6): p. 1143-56.
237. Ruiz, F.A., et al., *Human platelet dense granules contain polyphosphate and are similar to acidocalcisomes of bacteria and unicellular eukaryotes.* J Biol Chem, 2004. **279**(43): p. 44250-7.

238. Solesio, M.E., et al., *Inorganic polyphosphate is required for sustained free mitochondrial calcium elevation, following calcium uptake.* Cell Calcium, 2020. **86**: p. 102127.
239. Dedkova, E.N., *Inorganic polyphosphate in cardiac myocytes: from bioenergetics to the permeability transition pore and cell survival.* Biochem Soc Trans, 2016. **44**(1): p. 25-34.
240. Seidlmayer, L.K., et al., *Inorganic polyphosphate is a potent activator of the mitochondrial permeability transition pore in cardiac myocytes.* J Gen Physiol, 2012. **139**(5): p. 321-31.
241. Wang, L., et al., *Inorganic polyphosphate stimulates mammalian TOR, a kinase involved in the proliferation of mammary cancer cells.* Proc Natl Acad Sci U S A, 2003. **100**(20): p. 11249-54.
242. Azevedo, C., et al., *Screening a Protein Array with Synthetic Biotinylated Inorganic Polyphosphate To Define the Human PolyP-ome.* ACS Chem Biol, 2018. **13**(8): p. 1958-1963.
243. Azevedo, C., T. Livermore, and A. Saiardi, *Protein polyphosphorylation of lysine residues by inorganic polyphosphate.* Mol Cell, 2015. **58**(1): p. 71-82.
244. Segawa, S., et al., *Probiotic-derived polyphosphate enhances the epithelial barrier function and maintains intestinal homeostasis through integrin-p38 MAPK pathway.* PLoS One, 2011. **6**(8): p. e23278.
245. *The Chemical Structures and Properties of Condensed Inorganic Phosphates*, in *The Biochemistry of Inorganic Polyphosphates*. 2004. p. 3-13.
246. Cooper, D.R. and J.A. Semlyen, *Equilibrium ring concentrations and the statistical conformations of polymer chains: Part 9. Sodium metaphosphates in Graham's salt.* Polymer, 1972. **13**(9): p. 414-418.
247. Crowther, J. and A.E.R. Westman, *THE HYDROLYSIS OF THE CONDENSED PHOSPHATES: III. SODIUM TETRAMETAPHOSPHATE AND SODIUM TETRAPHOSPHATE.* Canadian Journal of Chemistry, 1956. **34**(7): p. 969-981.
248. Thilo, E., *The Structural Chemistry of Condensed Inorganic Phosphates.* Angewandte Chemie International Edition in English, 1965. **4**(12): p. 1061-1071.
249. Chee, K.L. and M.K. Ayob, *Optimization of hexametaphosphate-assisted extraction and functional characterization of palm kernel cake protein.* Food Sci Technol Int, 2013. **19**(2): p. 109-22.
250. Helander, I.M. and T. Mattila-Sandholm, *Fluorometric assessment of gram-negative bacterial permeabilization.* J Appl Microbiol, 2000. **88**(2): p. 213-9.
251. Letham, D.S., *Separation of plant cells with hexametaphosphate and the nature of intercellular bonding.* Experimental Cell Research, 1962. **27**(2): p. 352-355.
252. Andreola, F., et al., *Effect of sodium hexametaphosphate and ageing on the rheological behaviour of kaolin dispersions.* Applied Clay Science, 2006. **31**(1-2): p. 56-64.
253. Andreola, F., et al., *The role of sodium hexametaphosphate in the dissolution process of kaolinite and kaolin.* Journal of the European Ceramic Society, 2004. **24**(7): p. 2113-2124.
254. Rassu, G., et al., *Intranasal Delivery of Genistein-Loaded Nanoparticles as a Potential Preventive System against Neurodegenerative Disorders.* Pharmaceutics, 2018. **11**(1).
255. Thandapani, G., et al., *Size optimization and in vitro biocompatibility studies of chitosan nanoparticles.* Int J Biol Macromol, 2017. **104**(Pt B): p. 1794-1806.

256. Chueh, B.H., et al., *Patterning alginate hydrogels using light-directed release of caged calcium in a microfluidic device.* Biomed Microdevices, 2010. **12**(1): p. 145-51.
257. Melero, A., et al., *Chelating Effect of Cellulose Acetate Hydrogel Crosslinked with EDTA Dianhydride Used as a Platform for Cell Growth.* Advances in Materials Science and Engineering, 2019. **2019**: p. 1-11.
258. Walz, F.H., et al., *Optimum hexametaphosphate concentration to inhibit efflorescence formation in dry fermented sausages.* Meat Sci, 2018. **139**: p. 35-43.
259. Hidalgo, J., J. Kruseman, and H.U. Bohren, *Recovery of Whey Proteins with Sodium hexametaphosphate.* Journal of Dairy Science, 1973. **56**(8): p. 988-993.
260. Alavi, F., L. Chen, and Z. Emam-Djomeh, *Structuring of acidic oil-in-water emulsions by controlled aggregation of nanofibrillated egg white protein in the aqueous phase using sodium hexametaphosphate.* Food Hydrocolloids, 2021. **112**.
261. Mocanu, M., et al., *The effect of sodium hexametaphosphate on the efficiency of pectin in stabilizing acidified milk drinks.* Food Hydrocolloids, 2021. **118**.
262. Wang, B., B. Adhikari, and C.J. Barrow, *Optimisation of the microencapsulation of tuna oil in gelatin-sodium hexametaphosphate using complex coacervation.* Food Chem, 2014. **158**: p. 358-65.
263. Wang, B., et al., *Anchovy oil microcapsule powders prepared using two-step complex coacervation between gelatin and sodium hexametaphosphate followed by spray drying.* Powder Technology, 2019. **358**: p. 68-78.
264. Smith, S.A., et al., *Polyphosphate exerts differential effects on blood clotting, depending on polymer size.* Blood, 2010. **116**(20): p. 4353-9.
265. Hernandez-Ruiz, L., et al., *Inorganic polyphosphate and specific induction of apoptosis in human plasma cells.* Haematologica, 2006. **91**(9): p. 1180-6.
266. Kumble, K.D. and A. Kornberg, *Inorganic polyphosphate in mammalian cells and tissues.* J Biol Chem, 1995. **270**(11): p. 5818-22.
267. Rulliere, C., et al., *Heat treatment effect on polyphosphate chain length in aqueous and calcium solutions.* Food Chem, 2012. **134**(2): p. 712-6.
268. Callis, C.F., J.R. Van Wazer, and P.G. Arvan, *The Inorganic Phosphates as Polyelectrolytes.* Chemical Reviews, 1954. **54**(5): p. 777-796.
269. Gustavson, K.H., A. Larsson, and E. Olsen, *The Interaction of Polymetaphosphates with Hide Protein.* Acta Chemica Scandinavica, 1951. **5**: p. 1221-1243.
270. Casas, J.M., et al., *31P NMR spectroscopic studies of the influence of the environment in the degradation process of the Graham's salt.* Ceramics International, 2010. **36**(1): p. 39-46.
271. Eisenstein, N., et al., *Enzymatically regulated demineralisation of pathological bone using sodium hexametaphosphate.* Journal of Materials Chemistry B, 2016. **4**(21): p. 3815-3822.
272. Robinson, T.E., et al., *Hexametaphosphate as a potential therapy for the dissolution and prevention of kidney stones.* Journal of Materials Chemistry B, 2020.
273. da Camara, D.M., et al., *Effect of low-fluoride toothpastes combined with hexametaphosphate on in vitro enamel demineralization.* J Dent, 2014. **42**(3): p. 256-62.
274. Bae, W.J., et al., *Effects of sodium tri- and hexameta-phosphate in vitro osteoblastic differentiation in Periodontal Ligament and Osteoblasts, and in vivo bone regeneration.* Differentiation, 2016. **92**(5): p. 257-269.

275. Bae, W.J., et al., *Effects of sodium tri- and hexametaphosphate on proliferation, differentiation, and angiogenic potential of human dental pulp cells.* J Endod, 2015. **41**(6): p. 896-902.
276. Conceicao, J.M., et al., *Fluoride gel supplemented with sodium hexametaphosphate reduces enamel erosive wear in situ.* J Dent, 2015. **43**(10): p. 1255-60.
277. Bartizek, R.D., P. Walters, and A.R. Biesbrock, *The prevention of induced stain using two levels of sodium hexametaphosphate in chewing gum.* J Clin Dent, 2003. **14**(4): p. 77-81.
278. Neves, J.G., et al., *Surface free energy of enamel treated with sodium hexametaphosphate, calcium and phosphate.* Arch Oral Biol, 2018. **90**: p. 108-112.
279. da Camara, D.M., et al., *Synergistic effect of fluoride and sodium hexametaphosphate in toothpaste on enamel demineralization in situ.* J Dent, 2015. **43**(10): p. 1249-54.
280. Kawazoe, Y., et al., *Activation of the FGF signaling pathway and subsequent induction of mesenchymal stem cell differentiation by inorganic polyphosphate.* Int J Biol Sci, 2008. **4**(1): p. 37-47.
281. *Final Report on the Safety Assessment of Sodium Metaphosphate, Sodium Trimetaphosphate, and Sodium hexametaphosphate.* International Journal of Toxicology, 2001. **20**(3_suppl): p. 75-89.
282. Farid, M., et al., *Corneal Edema and Opacification Preferred Practice Pattern(R).* Ophthalmology, 2019. **126**(1): p. P216-P285.
283. Raynaud, S., et al., *Calcium phosphate apatites with variable Ca/P atomic ratio I. Synthesis, characterisation and thermal stability of powders.* Biomaterials, 2002. **23**(4): p. 1065-72.
284. Beaufay, F., et al., *Polyphosphate Functions In Vivo as an Iron Chelator and Fenton Reaction Inhibitor.* mBio, 2020. **11**(4): p. e01017-20.
285. Vujicic, I., S.C. Batra, and J.M. DeMan, *Interaction of alkaline earth metal ions with polyphosphates and citrate in the presence and absence of casein.* Journal of Agricultural and Food Chemistry, 1967. **15**(3): p. 403-407.
286. Sofos, J.N., *Use of phosphates in low-sodium meat products; Utilisation des phosphates dans les produits carnés à faible teneur en sodium.* Food technology (Chicago), 1986. **40**(9): p. 52-69.
287. Walz, F.H., et al., *Inhibitory effect of phosphates on magnesium lactate efflorescence formation in dry-fermented sausages.* Food Res Int, 2017. **100**(Pt 1): p. 352-360.
288. Van Wazer, J.R. and C.F. Callis, *Metal Complexing By Phosphates.* Chemical Reviews, 1958. **58**(6): p. 1011-1046.
289. Momeni, A. and M.J. Filiaggi, *Comprehensive study of the chelation and coacervation of alkaline earth metals in the presence of sodium polyphosphate solution.* Langmuir, 2014. **30**(18): p. 5256-66.
290. Castellini, E., et al., *Thermodynamic aspects of the adsorption of hexametaphosphate on kaolinite.* J Colloid Interface Sci, 2005. **292**(2): p. 322-9.
291. Choi, I.K., W.W. Wen, and R.W. Smith, *The effect of a long chain phosphate on the adsorption of collectors on kaolinite.* Minerals Engineering, 1993. **6**(11): p. 1191-1197.
292. Han, Y., et al., *Interactions between kaolinite Al OH surface and sodium hexametaphosphate.* Applied Surface Science, 2016. **387**: p. 759-765.
293. Castellini, E., et al., *Sodium hexametaphosphate interaction with 2:1 clay minerals illite and montmorillonite.* Applied Clay Science, 2013. **83-84**: p. 162-170.

294. Zhou, H., et al., *Mesoporous hydroxyapatite nanoparticles hydrothermally synthesized in aqueous solution with hexametaphosphate and tea polyphenols.* Mater Sci Eng C Mater Biol Appl, 2017. **71**: p. 439-445.
295. Omelon, S., et al., *Control of vertebrate skeletal mineralization by polyphosphates.* PLoS One, 2009. **4**(5): p. e5634.
296. Morita, K., et al., *Enhanced initial bone regeneration with inorganic polyphosphate-adsorbed hydroxyapatite.* Acta Biomater, 2010. **6**(7): p. 2808-15.
297. do Amaral, J.G., et al., *Effects of polyphosphates and fluoride on hydroxyapatite dissolution: A pH-stat investigation.* Arch Oral Biol, 2016. **63**: p. 40-46.
298. Goncalves, F.M.C., et al., *Remineralizing effect of a fluoridated gel containing sodium hexametaphosphate: An in vitro study.* Arch Oral Biol, 2018. **90**: p. 40-44.
299. Luo, W., et al., *The effect of disaggregated nano-hydroxyapatite on oral biofilm in vitro.* Dent Mater, 2020. **36**(7): p. e207-e216.
300. Nguyen, V.S., et al., *Effect of ultrasonication and dispersion stability on the cluster size of alumina nanoscale particles in aqueous solutions.* Ultrason Sonochem, 2011. **18**(1): p. 382-8.
301. Abd-El-Khalek, D.E. and B.A. Abd-El-Nabey, *Evaluation of sodium hexametaphosphate as scale and corrosion inhibitor in cooling water using electrochemical techniques.* Desalination, 2013. **311**: p. 227-233.
302. Robinson, T.E., et al., *Local injection of a hexametaphosphate formulation reduces heterotopic ossification in vivo.* Mater Today Bio, 2020. **7**: p. 100059.
303. Xiao, Q., et al., *A comparative assessment of the efficacy of carbomer gel and carboxymethyl cellulose containing artificial tears in dry eyes.* J Huazhong Univ Sci Technolog Med Sci, 2008. **28**(5): p. 592-5.
304. Chow, L.C., *Solubility of calcium phosphates.* Monogr Oral Sci, 2001. **18**: p. 94-111.
305. Lim, L.T., E.Y. Ah-Kee, and C.E. Collins, *Common eye drops and their implications for pH measurements in the management of chemical eye injuries.* Int J Ophthalmol, 2014. **7**(6): p. 1067-8.
306. Kessel, L., et al., *The relationship between body and ambient temperature and corneal temperature.* Invest Ophthalmol Vis Sci, 2010. **51**(12): p. 6593-7.
307. Felter, S., G. Dirhiemer, and J.P. Ebel, *Fractionnemnt des polyphostphates inorganique de longue chaine sur sephadex G100.* Journal of Chromatography A, 1968. **35**: p. 207-210.
308. Aslantürk, Ö.S., *In Vitro Cytotoxicity and Cell Viability Assays: Principles, Advantages, and Disadvantages*, in *Genotoxicity - A Predictable Risk to Our Actual World*. 2018.
309. Barile, F.A., *Validating and troubleshooting ocular in vitro toxicology tests.* J Pharmacol Toxicol Methods, 2010. **61**(2): p. 136-45.
310. Wilson, S.L., M. Ahearne, and A. Hopkinson, *An overview of current techniques for ocular toxicity testing.* Toxicology, 2015. **327**: p. 32-46.
311. Arjamaa, O., *EDTA chelation for calcific band keratopathy.* Am J Ophthalmol, 2005. **139**(1): p. 216; author reply 216.
312. Najjar, D.M., et al., *EDTA chelation for calcific band keratopathy: results and long-term follow-up.* Am J Ophthalmol, 2004. **137**(6): p. 1056-64.
313. Hu, Y., et al., *Effects of sodium hexametaphosphate, sodium tripolyphosphate and sodium pyrophosphate on the ultrastructure of beef myofibrillar proteins investigated with atomic force microscopy.* Food Chem, 2021. **338**: p. 128146.

314. Mendes-Gouvea, C.C., et al., *Sodium trimetaphosphate and hexametaphosphate impregnated with silver nanoparticles: characteristics and antimicrobial efficacy.* Biofouling, 2018. **34**(3): p. 299-308.
315. Oćwieja, M. and A. Barbasz, *Sodium hexametaphosphate–induced enhancement of silver nanoparticle toxicity towards leukemia cells.* Journal of Nanoparticle Research, 2020. **22**(6).
316. Shiba, T., et al., *Modulation of mitogenic activity of fibroblast growth factors by inorganic polyphosphate.* J Biol Chem, 2003. **278**(29): p. 26788-92.
317. Ramke, M., et al., *Porcine corneal cell culture models for studying epidemic keratoconjunctivitis.* Mol Vis, 2013. **19**: p. 614-22.
318. Pathak, M., et al., *The effect of culture medium and carrier on explant culture of human limbal epithelium: A comparison of ultrastructure, keratin profile and gene expression.* Experimental eye research, 2016. **153**: p. 122-132.
319. Erickson-DiRenzo, E., M.P. Sivasankar, and S.L. Thibeault, *Utility of cell viability assays for use with ex vivo vocal fold epithelial tissue.* Laryngoscope, 2015. **125**(5): p. E180-5.
320. Abramov, A.Y., et al., *Targeted polyphosphatase expression alters mitochondrial metabolism and inhibits calcium-dependent cell death.* Proc Natl Acad Sci U S A, 2007. **104**(46): p. 18091-6.
321. Damodaran, S. and K.L. Parkin, *12.6 Antioxidants*, in *Fennema's Food Chemistry (5th Edition)*. CRC Press.
322. Vaara, M., *Agents That Increase the Permeability of the Outer Membrane.* Microbiological Reviews, 1992. **56**(3): p. 395 - 411.
323. Post, F.J., G.B. Krishnamurty, and M.D. Flanagan, *INFLUENCE OF SODIUM HEXAMETAPHOSPHATE ON SELECTED BACTERIA.* Applied microbiology, 1963. **11**(5): p. 430-435.
324. Yoo, N.G., et al., *Polyphosphate Stabilizes Protein Unfolding Intermediates as Soluble Amyloid-like Oligomers.* J Mol Biol, 2018. **430**(21): p. 4195-4208.
325. Power, O.M., et al., *Dephosphorylation of caseins in milk protein concentrate alters their interactions with sodium hexametaphosphate.* Food Chem, 2019. **271**: p. 136-141.
326. Vandegrift, V. and R.R. Evans, *Polyphosphate binding interactions with bovine serum albumin in protein-polyphosphate precipitates.* J Agric Food Chem, 1981. **29**(3): p. 536-9.
327. Chan, F.K., K. Moriwaki, and M.J. De Rosa, *Detection of necrosis by release of lactate dehydrogenase activity.* Methods Mol Biol, 2013. **979**: p. 65-70.
328. Vogel, K.G., *Effects of hyaluronidase, trypsin, and EDTA on surface composition and topography during detachment of cells in culture.* Experimental Cell Research, 1978. **113**(2): p. 345-357.
329. Renehan, A.G., C. Booth, and C.S. Potten, *What is apoptosis, and why is it important?* Bmj, 2001. **322**(7301): p. 1536-8.
330. Cruickshanks, N., et al., *Apoptosis*, in *Brenner's Encyclopedia of Genetics (Second Edition)*, S. Maloy and K. Hughes, Editors. 2013, Academic Press: San Diego. p. 166-169.
331. García, M.C., M.C. Alfaro, and J. Muñoz, *Creep-recovery-creep tests to determine the yield stress of fluid gels containing gellan gum and Na+.* Biochemical Engineering Journal, 2016. **114**: p. 257-261.

332. Hill, L.J., et al., *Sustained release of decorin to the surface of the eye enables scarless corneal regeneration.* NPJ Regen Med, 2018. **3**: p. 23.
333. Rupenthal, I.D., C.R. Green, and R.G. Alany, *Comparison of ion-activated in situ gelling systems for ocular drug delivery. Part 1: physicochemical characterisation and in vitro release.* Int J Pharm, 2011. **411**(1-2): p. 69-77.
334. Bor, S., et al., *Alginates: From the ocean to gastroesophageal reflux disease treatment.* The Turkish journal of gastroenterology : the official journal of Turkish Society of Gastroenterology, 2019. **30**(Suppl2): p. 109-136.
335. Dettmar, P.W., et al., *A comparative study on the raft chemical properties of various alginate antacid raft-forming products.* Drug Dev Ind Pharm, 2018. **44**(1): p. 30-39.
336. George, M. and T.E. Abraham, *Polyionic hydrocolloids for the intestinal delivery of protein drugs: alginate and chitosan--a review.* J Control Release, 2006. **114**(1): p. 1-14.
337. Hunt, N.C., R.M. Shelton, and L.M. Grover, *Reversible mitotic and metabolic inhibition following the encapsulation of fibroblasts in alginate hydrogels.* Biomaterials, 2009. **30**(32): p. 6435-43.
338. Jahromi, S.H., et al., *Degradation of polysaccharide hydrogels seeded with bone marrow stromal cells.* J Mech Behav Biomed Mater, 2011. **4**(7): p. 1157-66.
339. Lee, K.Y. and D.J. Mooney, *Alginate: properties and biomedical applications.* Prog Polym Sci, 2012. **37**(1): p. 106-126.
340. Venkatesan, J., et al., *Alginate composites for bone tissue engineering: a review.* Int J Biol Macromol, 2015. **72**: p. 269-81.
341. Demailly, P., et al., *Ocular hypotensive efficacy and safety of once daily carteolol alginate.* Br J Ophthalmol, 2001. **85**(8): p. 921-4.
342. Tokuda, N., et al., *Effects of a long-acting ophthalmic formulation of carteolol containing alginic acid on the corneal epithelial barrier function and water retentive effect.* Journal of ocular pharmacology and therapeutics : the official journal of the Association for Ocular Pharmacology and Therapeutics, 2012. **28**(2): p. 123-128.
343. Xin, G., et al., *Ophthalmic Drops with Nanoparticles Derived from a Natural Product for Treating Age-Related Macular Degeneration.* ACS Appl Mater Interfaces, 2020. **12**(52): p. 57710-57720.
344. Liu, Y., et al., *In situ gelling gelrite/alginate formulations as vehicles for ophthalmic drug delivery.* AAPS PharmSciTech, 2010. **11**(2): p. 610-620.
345. Cohen, S., et al., *A novel in situ-forming ophthalmic drug delivery system from alginates undergoing gelation in the eye.* Journal of Controlled Release, 1997. **44**(2): p. 201-208.
346. Dubashynskaya, N., et al., *Polysaccharides in Ocular Drug Delivery.* Pharmaceutics, 2019. **12**(1).
347. Liu, S., et al., *Scaling law and microstructure of alginate hydrogel.* Carbohydr Polym, 2016. **135**: p. 101-9.
348. Jeon, O., et al., *The effect of oxidation on the degradation of photocrosslinkable alginate hydrogels.* Biomaterials, 2012. **33**(13): p. 3503-14.
349. Hunt, N.C., et al., *Encapsulation of fibroblasts causes accelerated alginate hydrogel degradation.* Acta Biomater, 2010. **6**(9): p. 3649-56.
350. Alfatama, M., L.Y. Lim, and T.W. Wong, *Chitosan oleate-tripolyphosphate complex-coated calcium alginate bead: physicochemical aspects of concurrent core-coat formation.* Carbohydrate Polymers, 2021.

351. Guo, J., et al., *Effective immobilization of Bacillus subtilis in chitosan-sodium alginate composite carrier for ammonia removal from anaerobically digested swine wastewater.* Chemosphere, 2021. **284**: p. 131266.
352. Hosseini, S. and M. Varidi, *Optimization of Microbial Rennet Encapsulation in Alginate - Chitosan Nanoparticles.* Food Chem, 2021. **352**: p. 129325.
353. Rocha, C.E.V., et al., *Alginate-chitosan microcapsules improve vaccine potential of gamma-irradiated Listeria monocytogenes against listeriosis in murine model.* Int J Biol Macromol, 2021. **176**: p. 567-577.
354. Noreen, S., et al., *Terminalia arjuna gum/alginate in situ gel system with prolonged retention time for ophthalmic drug delivery.* Int J Biol Macromol, 2020. **152**: p. 1056-1067.
355. Irimia, T., et al., *Chitosan-Based In Situ Gels for Ocular Delivery of Therapeutics: A State-of-the-Art Review.* Marine drugs, 2018. **16**(10): p. 373.
356. Abdelgawad, A.M. and S.M. Hudson, *Chitosan nanoparticles: Polyphosphates cross-linking and protein delivery properties.* Int J Biol Macromol, 2019. **136**: p. 133-142.
357. Berger, J., et al., *Structure and interactions in covalently and ionically crosslinked chitosan hydrogels for biomedical applications.* European Journal of Pharmaceutics and Biopharmaceutics, 2004. **57**(1): p. 19-34.
358. Sánchez-Díaz, J.C., et al., *Effect of sodium hexametaphosphate concentration on the swelling and controlled drug release properties of chitosan hydrogels.* Journal of Applied Polymer Science, 2010: p. n/a-n/a.
359. Silva, D., et al., *Chitosan/alginate based multilayers to control drug release from ophthalmic lens.* Colloids Surf B Biointerfaces, 2016. **147**: p. 81-89.
360. Smith, J., E. Wood, and M. Dornish, *Effect of chitosan on epithelial cell tight junctions.* Pharm Res, 2004. **21**(1): p. 43-9.
361. Bazmandeh, A.Z., et al., *Dual spinneret electrospun nanofibrous/gel structure of chitosan-gelatin/chitosan-hyaluronic acid as a wound dressing: In-vitro and in-vivo studies.* Int J Biol Macromol, 2020. **162**: p. 359-373.
362. Boucard, N., et al., *The use of physical hydrogels of chitosan for skin regeneration following third-degree burns.* Biomaterials, 2007. **28**(24): p. 3478-88.
363. Colobatiu, L., et al., *Development of bioactive compounds-loaded chitosan films by using a QbD approach – A novel and potential wound dressing material.* Reactive and Functional Polymers, 2019. **138**: p. 46-54.
364. Escarcega-Galaz, A.A., et al., *Mechanical, structural and physical aspects of chitosan-based films as antimicrobial dressings.* Int J Biol Macromol, 2018. **116**: p. 472-481.
365. Kaczmarek, B., et al., *The characterization of thin films based on chitosan and tannic acid mixture for potential applications as wound dressings.* Polymer Testing, 2019. **78**.
366. Zhang, M., et al., *High-mechanical strength carboxymethyl chitosan-based hydrogel film for antibacterial wound dressing.* Carbohydr Polym, 2021. **256**: p. 117590.
367. Alonso, M.J. and A. Sanchez, *The potential of chitosan in ocular drug delivery.* J Pharm Pharmacol, 2003. **55**(11): p. 1451-63.
368. Pella, M.C.G., et al., *Chitosan-based hydrogels: From preparation to biomedical applications.* Carbohydr Polym, 2018. **196**: p. 233-245.
369. Sang, Z., et al., *Comparison of three water-soluble polyphosphate tripolyphosphate, phytic acid, and sodium hexametaphosphate as crosslinking agents in chitosan nanoparticle formulation.* Carbohydr Polym, 2020. **230**: p. 115577.

370. Sarkar, S., et al., *Chitosan: A promising therapeutic agent and effective drug delivery system in managing diabetes mellitus.* Carbohydr Polym, 2020. **247**: p. 116594.
371. Zhang, Y., et al., *Fabrication of chitosan gel droplets via crosslinking of inverse Pickering emulsifications.* Carbohydr Polym, 2018. **186**: p. 1-8.
372. Raval, N.P., et al., *Hexametaphosphate cross-linked chitosan beads for the eco-efficient removal of organic dyes: Tackling water quality.* J Environ Manage, 2021. **280**: p. 111680.
373. Christ, J.J., S. Willbold, and L.M. Blank, *Methods for the Analysis of Polyphosphate in the Life Sciences.* Anal Chem, 2020. **92**(6): p. 4167-4176.
374. Sridharan, G. and A.A. Shankar, *Toluidine blue: A review of its chemistry and clinical utility.* Journal of oral and maxillofacial pathology : JOMFP, 2012. **16**(2): p. 251-255.
375. Kulaev, I.S., *Biochemistry of inorganic polyphosphates.* Rev Physiol Biochem Pharmacol, 2004. **73**: p. 131-58.
376. Mosby, B.M., S. Shah, and P.V. Braun, *Salt Water-Triggered Ionic Cross-Linking of Polymer Composites by Controlled Release of Functional Ions.* ACS omega, 2018. **3**(11): p. 16127-16133.
377. Sebastian-Morello, M., et al., *Ex vivo rabbit cornea diffusion studies with a soluble insert of moxifloxacin.* Drug Deliv Transl Res, 2018. **8**(1): p. 132-139.
378. Anderson, S.B.F.d.S., R.; Hofmann-Rummelt, C.; Seitz, B., *Corneal calcification after amniotic membrane transplantation.* 2003.
379. Castro-Combs, J., et al., *Corneal wound healing is modulated by topical application of amniotic fluid in an ex vivo organ culture model.* Exp Eye Res, 2008. **87**(1): p. 56-63.
380. Teixeira, L. and R.R. Dubielzig, *Eye*, in *Haschek and Rousseaux's Handbook of Toxicologic Pathology*. 2013. p. 2095-2185.
381. Piehl, M., et al., *Novel cultured porcine corneal irritancy assay with reversibility endpoint.* Toxicol In Vitro, 2010. **24**(1): p. 231-9.
382. Seyed-Safi, A.G. and J.T. Daniels, *A validated porcine corneal organ culture model to study the limbal response to corneal epithelial injury.* Exp Eye Res, 2020. **197**: p. 108063.
383. Schrage, N.F., M. Frentz, and M. Reim, *Changing the composition of buffered eye-drops prevents undesired side effects.* Br J Ophthalmol, 2010. **94**(11): p. 1519-22.
384. Dutescu, R.M., C. Panfil, and N. Schrage, *Comparison of the effects of various lubricant eye drops on the in vitro rabbit corneal healing and toxicity.* Exp Toxicol Pathol, 2017. **69**(3): p. 123-129.
385. Donaghy, C.L.V., J. M.; Greiner, M. A.; Goins, K. M.; Wagoner, M. D.;, *Calcific Band Keratopathy*. 2015.
386. Schrage, N.F., ; Schlobmacher, B.; Aschenbernner, W.; Langefeld, S., *Phosphate buffer in alkali eye burns as an inducer of experimental corneal calcification.* Burns, 2000. **27**.
387. Schrage, N.F., et al., *Relationship of eye burns with calcifications of the cornea?* Graefes Arch Clin Exp Ophthalmol, 2005. **243**(8): p. 780-4.
388. Brooks, D.E., *Equine Stromal and Endothelial Keratopathies: Medical Management of Stromal Abscesses, Eosinophilic Keratitis, Calcific Band Keratopathy, Striate Band Opacities, and Endotheliitis in the Horse.* Clinical Techniques in Equine Practice, 2005. **4**(1): p. 21-28.
389. Pucket, J.D., M.J. Boileau, and M.J.M. Sula, *Calcific band keratopathy in an alpaca.* Veterinary Ophthalmology, 2014. **17**(4): p. 286-289.

390. Nevile, J.C., et al., *Diamond burr debridement of 34 canine corneas with presumed corneal calcareous degeneration.* Veterinary Ophthalmology, 2016. **19**(4): p. 305-312.
391. Hepfer, R.G., et al., *Depth- and direction-dependent changes in solute transport following cross-linking with riboflavin and UVA light in ex vivo porcine cornea.* Exp Eye Res, 2021. **205**: p. 108498.
392. Resende, A.P., et al., *Ex vivo permeation of erythropoietin through porcine conjunctiva, cornea, and sclera.* Drug Deliv Transl Res, 2017. **7**(5): p. 625-631.
393. Gade, S., et al., *An Ex Vivo Evaluation of Moxifloxacin Nanostructured Lipid Carrier Enriched In Situ Gel for Transcorneal Permeation on Goat Cornea.* J Pharm Sci, 2019. **108**(9): p. 2905-2916.
394. Thiel, M.A., et al., *A simple corneal perfusion chamber for drug penetration and toxicity studies.* Br J Ophthalmol, 2001. **85**(4): p. 450-3.
395. Gautheron, P., et al., *Bovine corneal opacity and permeability test: An in vitro assay of ocular irritancy.* Fundamental and Applied Toxicology, 1992. **18**(3): p. 442-449.
396. Kolle, S.N., et al., *In-house validation of the EpiOcular(TM) eye irritation test and its combination with the bovine corneal opacity and permeability test for the assessment of ocular irritation.* Altern Lab Anim, 2011. **39**(4): p. 365-87.
397. Sel, S., et al., *1,25-dihydroxyvitamin D3 inhibits corneal wound healing in an ex-vivo mouse model.* Graefes Arch Clin Exp Ophthalmol, 2016. **254**(4): p. 717-24.
398. Sriram, S., et al., *Assessment of anti-scarring therapies in ex vivo organ cultured rabbit corneas.* Exp Eye Res, 2014. **125**: p. 173-82.
399. Ubani-Ukoma, U., et al., *An ex vivo cornea infection model.* MethodsX, 2020. **7**: p. 100876.
400. Goswami, D.G., et al., *Efficacy of anti-inflammatory, antibiotic and pleiotropic agents in reversing nitrogen mustard-induced injury in ex vivo cultured rabbit cornea.* Toxicol Lett, 2018. **293**: p. 127-132.
401. Tewari-Singh, N., et al., *Silibinin, dexamethasone, and doxycycline as potential therapeutic agents for treating vesicant-inflicted ocular injuries.* Toxicol Appl Pharmacol, 2012. **264**(1): p. 23-31.
402. Pinheiro, R., et al., *Comparison of the lubricant eyedrops Optive(R), Vismed Multi(R), and Cationorm(R) on the corneal healing process in an ex vivo model.* Eur J Ophthalmol, 2015. **25**(5): p. 379-84.
403. Spöler, F., et al., *The Ex Vivo Eye Irritation Test as an alternative test method for serious eye damage/eye irritation.* Altern Lab Anim, 2015. **43**(3): p. 163-79.
404. Thoene, J.G., M.A. DelMonte, and J. Mullet, *Microvesicle delivery of a lysosomal transport protein to ex vivo rabbit cornea.* Mol Genet Metab Rep, 2020. **23**: p. 100587.
405. Castro, N., S.R. Gillespie, and A.M. Bernstein, *Ex Vivo Corneal Organ Culture Model for Wound Healing Studies.* J Vis Exp, 2019(144).
406. Okurowska, K., et al., *Establishing a Porcine Ex Vivo Cornea Model for Studying Drug Treatments against Bacterial Keratitis.* J Vis Exp, 2020(159).
407. Thakur, S.S., D. Shrestha, and I.D. Rupenthal, *Evaluation of 2 ex vivo Bovine Cornea Storage Protocols for Drug Delivery Applications.* Ophthalmic Res, 2019. **61**(4): p. 204-209.
408. Marlo, T.L., et al., *Development of a novel ex vivo equine corneal model.* Veterinary Ophthalmology, 2017. **20**(4): p. 288-293.

409. Alekseev, O., A.H. Tran, and J. Azizkhan-Clifford, *Ex vivo organotypic corneal model of acute epithelial herpes simplex virus type I infection.* J Vis Exp, 2012(69): p. e3631.
410. Kunzmann, B.C., et al., *Establishment of a porcine corneal endothelial organ culture model for research purposes.* Cell Tissue Bank, 2018. **19**(3): p. 269-276.
411. Madhu, S.N., et al., *Ex vivo Caprine Model to Study Virulence Factors in Keratitis.* J Ophthalmic Vis Res, 2018. **13**(4): p. 383-391.
412. Berkowski, W.M., Jr., et al., *Development and assessment of a novel ex vivo corneal culture technique involving an agarose-based dome scaffold for use as a model of in vivo corneal wound healing in dogs and rabbits.* Am J Vet Res, 2020. **81**(1): p. 47-57.
413. Berkowski, W.M., et al., *Assessment of Topical Therapies for Improving the Optical Clarity Following Stromal Wounding in a Novel Ex Vivo Canine Cornea Model.* Invest Ophthalmol Vis Sci, 2018. **59**(13): p. 5509-5521.
414. Rose, J.S., et al., *An experimental study to test the efficacy of Mesenchymal Stem Cells in reducing corneal scarring in an ex-vivo organ culture model.* Exp Eye Res, 2020. **190**: p. 107891.
415. Proietto, L.R., et al., *Development and Assessment of a Novel Canine Ex Vivo Corneal Model.* Curr Eye Res, 2017. **42**(6): p. 813-821.
416. Janin-Manificat, H., et al., *Development of ex vivo organ culture models to mimic human corneal scarring.* Mol Vis, 2012. **18**: p. 2896-908.
417. Baino, F. and S. Yamaguchi, *The Use of Simulated Body Fluid (SBF) for Assessing Materials Bioactivity in the Context of Tissue Engineering: Review and Challenges.* Biomimetics (Basel), 2020. **5**(4).
418. Chahal, S., S.J. Fathima, and M.B. Yusoff, *Biomimetic growth of bone-like apatite via simulated body fluid on hydroxyethyl cellulose/polyvinyl alcohol electrospun nanofibers.* Biomed Mater Eng, 2014. **24**(1): p. 799-806.
419. Ghorbani, F., et al., *Microwave-induced rapid formation of biomimetic hydroxyapatite coating on gelatin-siloxane hybrid microspheres in 10X-SBF solution.* e-Polymers, 2018. **18**(3): p. 247-255.
420. Chen, X., et al., *Microstructures and bond strengths of the calcium phosphate coatings formed on titanium from different simulated body fluids.* Materials Science and Engineering: C, 2009. **29**(1): p. 165-171.
421. Navarro-Requena, C., et al., *Wound healing-promoting effects stimulated by extracellular calcium and calcium-releasing nanoparticles on dermal fibroblasts.* Nanotechnology, 2018. **29**(39): p. 395102.
422. Kim, S., et al., *Toxicity of Povidone-iodine to the ocular surface of rabbits.* BMC Ophthalmol, 2020. **20**(1): p. 359.
423. Florencio-Silva, R., et al., *Biology of Bone Tissue: Structure, Function, and Factors That Influence Bone Cells.* Biomed Res Int, 2015. **2015**: p. 421746.
424. Momeni, A. and M.J. Filiaggi, *Synthesis and characterization of different chain length sodium polyphosphates.* Journal of Non-Crystalline Solids, 2013. **382**: p. 11-17.
425. Alvarez, M.M., et al., *Delivery strategies to control inflammatory response: Modulating M1-M2 polarization in tissue engineering applications.* J Control Release, 2016. **240**: p. 349-363.
426. Stefanescu, C., W.H. Daly, and I.I. Negulescu, *Biocomposite films prepared from ionic liquid solutions of chitosan and cellulose.* Carbohydrate Polymers, 2012. **87**(1): p. 435-443.

427. Costa, J., et al., *A comparative study of Bowman's layer in some mammals: Relationships with other constituent corneal structures.* European Journal of anatomy, ISSN 1136-4890, Vol. 6, Nº. 3, 2002, pags. 133-140, 2002. **6**.
428. Kammergruber, E., et al., *Morphological and immunohistochemical characteristics of the equine corneal epithelium.* Vet Ophthalmol, 2019. **22**(6): p. 778-790.
429. Hammond, G., et al., *The microanatomy of Bowman's layer in the cornea of the pig: Changes in collagen fibril architecture at the corneoscleral limbus.* European Journal of Anatomy, 2020. **24**: p. 399-406.
430. Shiju, T.M., R. Carlos de Oliveira, and S.E. Wilson, *3D in vitro corneal models: A review of current technologies.* Exp Eye Res, 2020. **200**: p. 108213.
431. Koehn, D., et al., *Ketamine/Xylazine-Induced Corneal Damage in Mice.* PLoS One, 2015. **10**(7): p. e0132804.

ADVANCED FUNCTIONAL MATERIALS
www.afm-journal.de

Material, Immunological, and Practical Perspectives on Eye Drop Formulation

*Naomi H. Bennett, Holly R. Chinnery, Laura E. Downie, Lisa J. Hill, and Liam M. Grover**

Eye drops are the most common and inexpensive approach to topical ocular drug delivery. Eye drops offer a noninvasive treatment strategy; however, this can be detrimental to therapeutic efficacy when compared to invasive methods such as surgeries, implants, and injections. Improvements to the efficacy of the topical delivery of drugs to ocular tissues are currently being explored and much of this work centers on adjusting the formulation of the eye drops and prolonging the bioavailability of the therapeutic agent. This is often in preference to improving other patient-focused or clinical factors. In this progress report, conventional, commercially available polymer eye drops are explored and the ability for current and future innovations to maintain the existing benefits of eye drops to the patient is assessed. The final materials and form of the drops (liquid, gel, or other) and the immunological implications for the user are explored. There is currently no consensus for how to most effectively improve the ocular retention and drug delivery capabilities of eye drops, but key issues are highlighted in the context of current methods under development, and potential questions and considerations for future innovations are raised.

1. Introduction: The Barriers to Topical Ocular Drug Delivery

Ocular drug delivery is a challenging but rapidly evolving area of research. It is well documented that biological systems that keep the eye free of debris and pathogens and protect the vital posterior structures, present a barrier to topical drug delivery.[1] Usual treatments for ocular diseases include intraocular injections, surgical interventions, and/or eye drops.[2] Eye drops are most commonly used for treating conditions affecting the anterior structures of the eye (**Figure 1**)—the cornea, conjunctiva, sclera, and trabecular meshwork—as passage through these structures to the posterior segment of the eye is relatively restricted.[3] The cornea comprises sublayers with different properties; the epithelial and endothelial layers are lipophilic, and the stroma is hydrophilic.[3b,4] These properties heavily influence which drugs and carriers are effective in passing across the cornea, with positively charged carriers showing higher penetration than neutral or negatively charged carriers.[5] Drugs that are both lipid- and water-soluble (amphiphilic) also show improved penetration.[4,6]

1.1. The Anterior Ocular Immune System

The anterior segment of the eye is considered "immune privileged," with a higher level of immunological regulation of some immune responses occurring within the cornea and anterior chamber, to limit inflammation that can threaten tissue integrity, and thus compromise vision.[7] So-called "immune privilege" applies to intraocular tissues that are protected by a blood-ocular-barrier, developing tolerance to certain stimuli on exposure, rather than inducing the expected inflammatory response that would occur in other peripheral tissue sites such as the skin.[8,9] Mechanisms of immune privilege of the anterior segment have been widely reported, and are largely explained by three major components including formidable physical and cellular barriers, immunological tolerance, and a local immunosuppressive microenvironment.[7b] This allows for some degree of protection against infection, while protecting the delicate, nonregenerative intraocular cells and tissues against the ramifications of repeated inflammatory responses, which can result in the loss of transparency of key tissues and ultimately blindness.[3b,10] The bias toward tolerance is maintained through the presence of immuno-suppressive factors, such as transforming growth factor-β-2 (TGF-b2)[11] and α-melatonin stimulating hormone,[12] which limit or direct the activity of both the resident and infiltrating leukocytes in the cornea and anterior segment. In addition to mechanisms that regulate the nature of the adaptive immune responses, the resilience of the ocular surface in avoiding infection—despite its exposed location—is due to a robust repertoire of anatomical features (including stratified epithelium, apical epithelial tight junctions) and innate immune components such as tear lysozyme, antimicrobial defensins, and secretory immunoglobulin A (sIgA).

N. H. Bennett, Prof. L. M. Grover
Healthcare Technologies Institute, School of Chemical Engineering
University of Birmingham
Birmingham B15 2TT, UK
E-mail:
Dr. H. R Chinnery, Dr. L. E. Downie
Department of Optometry and Vision Sciences
The University of Melbourne
Parkville, VIC 3010, Australia
Dr. L. J. Hill
School of Biomedical Sciences
Institute of Clinical Sciences
University of Birmingham
Edgbaston, Birmingham B15 2TT, UK
The ORCID identification number(s) for the author(s) of this article can be found under https://doi.org/10.1002/adfm.201908476.

DOI: 10.1002/adfm.201908476

Most nonviral infections that occur in the cornea are usually secondary to mechanical damage to the ocular surface, from injury or contact lens wear,[13] or impaired barrier integrity, which compromises the innate ocular defense mechanisms.[10a,14]

When considering the immunological implications of eye drops, it is the anterior tissues that are of particular interest (the conjunctiva, cornea, and sclera), as these tissues are both in contact with and treated directly by these topical therapies. The immune cells naturally present in the anterior tissues of the eye can change their phenotype and function depending on the inflammatory environment and the disease state.[15] It is also important to recognize the diverse functions of the tear film, especially if an eye drop is to be designed to aid/replicate those functions.

1.1.1. The Tear Film

Tears lubricate and smooth the ocular surface and the components of the tear film work to trap debris (mucins), kill pathogens (lysozymes, phospholipase, etc.), facilitate the aggregation of the neutralized foreign bodies (sIgA), and assist with the removal of said bodies through blinking.[16]

The aqueous content of eye drops plays an important role in lubricating the ocular surface and the osmolarity of the tear film is key to preserving the integrity of the ocular surface barrier. Tear hyperosmolarity is regarded as both one of the most important indicators and primary causes of dry eye disease.[17] Tear hyperosmolarity, and as a result tear film instability, can lead to the onset of inflammation of the corneal epithelial layer.[18]

Mucins act to promote an optimally lubricated ocular surface by supporting the spreading of the bulk of the tear film over the corneal and conjunctival tissues. In particular, secreted, gel-forming MUC5AC and cell adhesive MUC1 facilitate pathogen removal by trapping the pathogen and preventing its adhesion to the underlying epithelial tissue.[16b,19] The longer, surface adhesive mucins also allow for the formation of reservoirs of oxidative enzymes, defensins, lysozymes, and lactoferrin—proteins produced by scavenger cells, neutrophilic granulocytes, that are attracted to inflammation—which work to reduce the adhesion of bacteria and remove damaged host tissue.[16b,20] Certain molecules are bactericidal: Gram-negative bacteria are killed by lysozymes which split their muramic acid linkages,[16a,21] whereas secretory phospholipase A2 acts against Gram-positive bacteria,[16] as do lactoferrin and transferrin which—as the names indicate—bind iron.[16a,20] Psoriasin, an antimicrobial agent found on the skin, has also been detected at the ocular surface.[22] These mucins can also interact with polymers to facilitate the beneficial mucoadhesive properties of some eye drops.[23] In order to stabilize the tear film, these mucins are hydrophilic, and the longest (MUC16) have a MW of around 2.5 million D. Polymers exhibit mucoadhesion through a number of possible mucin–polymer interactions which can be electrostatic (hydrogen bonding or electrostatic binding) or through physical entanglement (**Figure 2**).[19c,24] As mucoadhesion therefore requires direct contact between the polymer and the mucosal layer, the wettability of the polymer matrix and the contact angle between the two layers are vitally important.[25]

The primary antibody present in tears is sIgA, which is produced in the lacrimal gland and works to prevent bacterial adhesion, aggregate neutralized pathogens, and allow clearance of the pathogens from the ocular surface.[16b,26] It has also been associated with the increased chemotaxis of neutrophils and other immune cells during the prolonged period of eyelid closure during sleep.[27] Tear lipids can also augment the bactericidal properties of tears, as short-chain lipids affect the surface properties of the bacterial cell membrane, and long-chain lipids have a direct effect on bacterial metabolism.[20,28] It has been shown that tear film lipids can induce cell lysis, distortion, and cell wall damage in both Gram-negative and Gram-positive bacteria.[28] These processes all act as part of a wider complex mechanism of ocular surface protection. This system remains

Naomi H. Bennett is currently a Ph.D. student within the School of Chemical Engineering TRAILab at the University of Birmingham. She is investigating novel topical treatments for corneal mineralization and is supervised by Dr. Lisa Hill and Professor Liam Grover. She received her undergraduate degree in Sport and Materials Science (Joint Honors) B.Sc. from the University of Birmingham in 2018.

Lisa J. Hill is a Lecturer in the Institute of Clinical Sciences at the University of Birmingham. She specializes in the development and translation of new treatments for degenerative ocular diseases, including age-related macular degeneration and glaucoma. Lisa has a keen interest in developing novel methods for drug delivery into the eye.

Liam M. Grover is a materials scientist and Director of the Healthcare Technologies Institute at the University of Birmingham. His research focuses on the investigation of the interactions between materials and biological systems. Enhanced understanding of these interactions has enabled him to develop a range of materials capable of enhancing tissue regeneration. He currently has a portfolio of research focused on the prevention of scarring in tissues throughout the body.

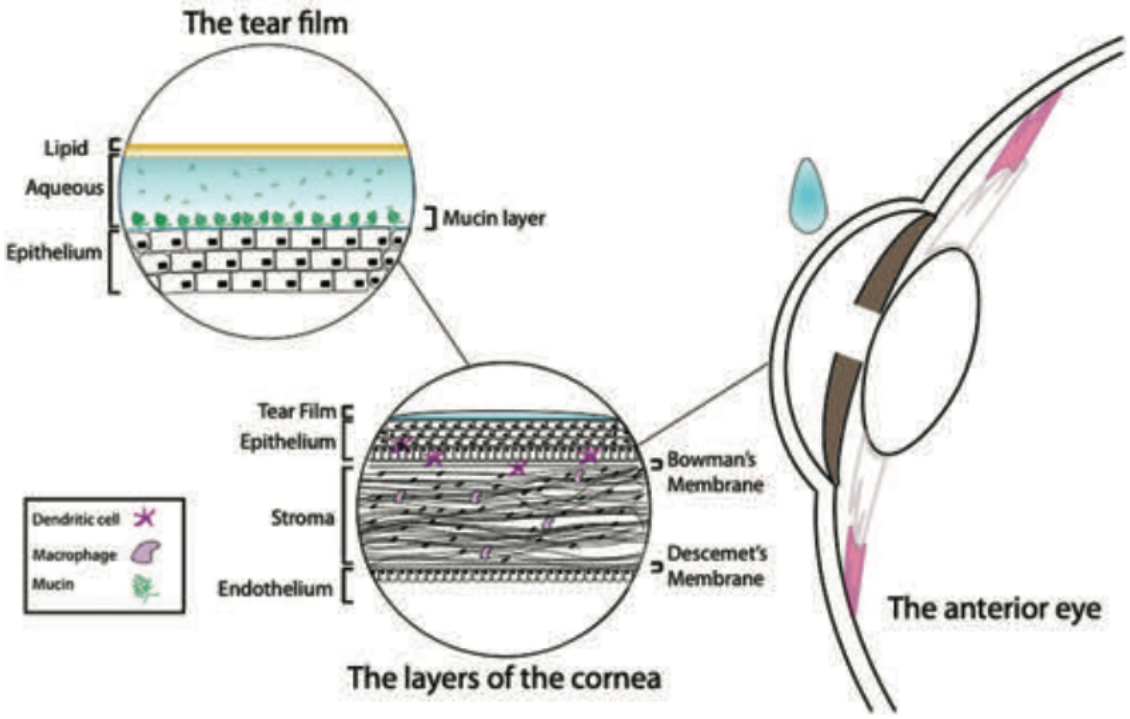

Figure 1. The structure of the cornea and the tear film.

virtually impenetrable to pathogens unless there is a physical disruption to the barrier or injury to the tissue.

1.1.2. The Cornea, Sclera, and Conjunctiva

Research in both human and murine models has demonstrated, after substantial debate, that bone marrow-derived macrophages ($CD45^+$, $CD11b^+$, $CD11c^-$) and dendritic cells ($CD45^+$, $CD11b^+$, $CD11c^+$) reside in the healthy cornea, more specifically in the stroma (Figure 1).[29] It has also been widely reported that dendritic cells and macrophages become more abundant in ocular tissues as disease severity and inflammation progress, as with elsewhere in the body.[29a,30] It has been suggested that dendritic cells, in particular, are recruited to the cornea from the limbus.[20,31] Not all macrophages and dendritic cells in the

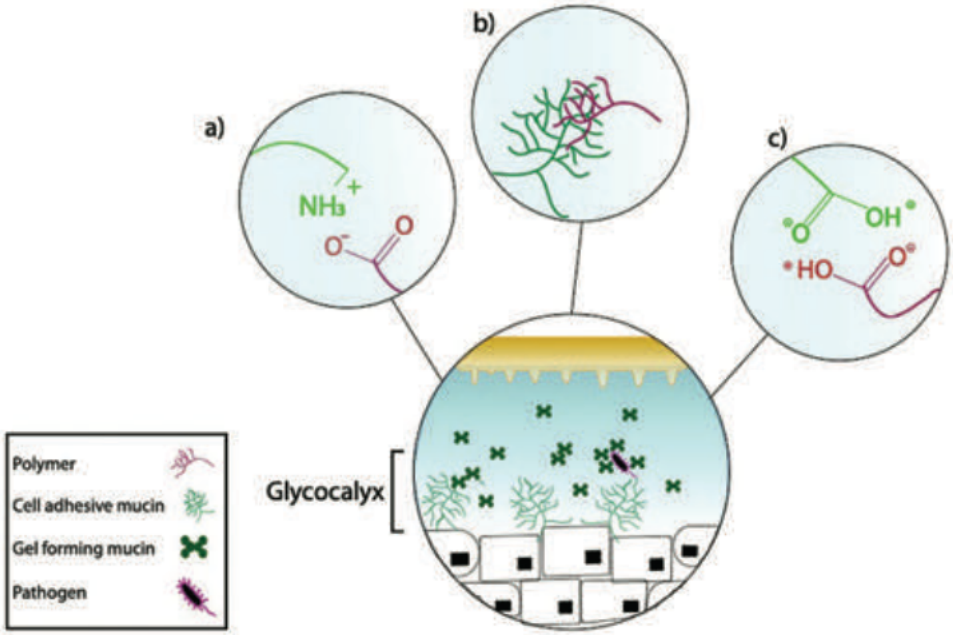

Figure 2. The anatomical elements of mucoadhesion and the mechanisms of adhesion including a) strong electrostatic attraction, b) physical entanglement, and c) hydrostatic bonding.

cornea are mature and ready to act as antigen presenting cells, as ≈70% of resident tissue macrophages are negative for the MHC class II complex, which is a molecule critical for activation of T lymphocytes.[31,32] Epithelial tissues elsewhere in the body are associated with a much wider variety of leukocyte subsets, so it is suggested that resident corneal macrophages have the ability to adapt after exposure to certain stimuli (such as trauma) to impart wound-healing functions.[29a,30d,33] Previously, the idea was upheld that macrophages act as part of the innate immune system and dendritic cells as part of the adaptive immune system, however in the eye these lines are blurred due to the adaptability of both cell types, and their role in the tolerance and wound healing responses.[30d,34] Cytokines regulate the recruitment and function of inflammatory cells that play critical roles in epithelial cell regeneration and stromal remodeling.[29a,31]

The limbus, which defines the border between the transparent cornea and the nontransparent sclera, is home to the blood and lymphatic vessels that provide a pathway for the antigen presenting macrophages and dendritic cells to engage with T-lymphocytes.[31] Gamma-delta ($\gamma\delta$) T-cells, which primarily reside in the limbus, have been shown to be pivotal in the regeneration of corneal epithelial tissue after injury.[35] In mice, specific T-helper cells have been shown to gather in the limbus and then spill into the conjunctiva during an inflammatory response, leading to conjunctiva-related allergy symptoms.[36]

The activities of the immune cells and the limbal vasculature are influenced by the release of histamines and prostaglandins by immunocompetent cells residing in the conjunctival epithelium.[29b] The conjunctiva is home to the same immune cell types that reside in the cornea (i.e., dendritic cells and macrophages)[20] but also has its own lymphatic drainage, allowing rapid trafficking by the antigen presenting cells and the induction of a rapid response to pathogens and/or injury.[26] The conjunctiva also contains its own collection of immune cells such as T-cells, antibody-secreting B-cells, and histamine-producing mast cells, which are arranged as so-called conjunctiva associated lymphoid tissue.[37] As a result, the conjunctiva is far more prone to inflammatory and allergic responses than tolerance responses compared with the cornea.[20]

2. Topical Ocular Drug Delivery: Eye Drops

Eye drops are applied directly to the cornea or into the conjunctival sac. Eye drops can be used for therapeutic drug delivery (e.g., corticosteroids, antibiotics, etc.), or for symptom management (e.g., artificial tears for dry eye disease). Eye drops typically include a solvent, electrolytes, a thickening agent (see **Table 1**), an active agent/drug (see **Table 2**), and in some cases a preservative (e.g., benzalkonium chloride). In addition, with the intent of mirroring natural tears, eye drops have an optimum pH of ≈7.4 and are osmoregulated.[7a]

Polymers were first used within eye drops to take advantage of their mucoadhesive properties and improve the residence time and resistance to lacrimal clearance of the drops.[3a] Conventional aqueous eye drops are rapidly cleared by blinking and lacrimal drainage, which creates severe limitations to the bioavailability of any therapeutic agent being delivered. Eye drops are said to provide a bioavailability of around 5% of the delivered drug.[38] Predictions of the average residence time of eye drops on the ocular surface vary greatly, with there being multiple methods of assessing this in both clinical and research settings. Optical coherence tomography can be used for in vivo assessments in clinical settings, and has shown retention times of up to 60 min with gel eye drops, and significant differences in the clearance rates for gel and aqueous drop formulations.[39] It is more common for residence time to be measured as a function of tear film break up time using fluorescein, which provides values ranging from 10 to 90 min.[40] The nature of the drug being delivered, the polymer additive, its concentration, and the use of preservative can be adapted to create the best possible combination of properties for the desired treatment effect. These changes only have minimal impact on the objectively low efficacy of eye drops compared to more invasive treatments (e.g., such as intraocular injections) for certain diseases.[2] Despite this, eye drops still offer an attractive treatment option, due to their ease of administration, versatility, and low cost.

Formulation decisions made purely on the potential therapeutic efficacy can disregard factors such as patient comfort, cost, and the ease of manufacture. In order to continue to pursue improvements in topical ocular drug delivery, it is important to understand the reasoning behind the use of eye drops as a treatment, and the choices behind currently available formulations.

2.1. Conventional Polymer Additives for Eye Drop Formulations

Eye drops formulated for the management of dry eye disease, which involves chronic damage to the ocular surface and leads to eye discomfort and inflammation (particularly in the advanced stages of the disease[17]) typically use polymeric agents to provide ocular lubrication and/or stabilize the tear film.[17,41] Polymers also increase the ocular retention time of the drops compared to purely aqueous solutions. Certain charged polymers (of which many are listed below) offer the advantage of mucoadhesion–adherence to the mucosal layer of the tear film, which further increases the residence time of the drops on the ocular surface.[6,42] Currently, commercially available eye drop products will often include one, or more, of the following biocompatible polymeric agents.

2.1.1. Natural Polymers

Various ethers of different viscosities and solubilities can be harvested from cellulose, including carboxymethylcellulose (CMC) (**Figure 3**) and hydroxypropylmethylcellulose (HPMC) (**Figure 4**).[43] These inexpensive polymers are found in many commercial eye drops (see Tables 1 and 2) as mucoadhesive thickening agents. Cellulose alone is poorly soluble, however CMC, as a cellulose ether, overcomes this drawback.[44] Their renewable source qualifies them as sustainable polymers.[43]

The viscosities of eye drops created with CMC are directly proportional to the molecular weight of the CMC chains, and CMC solutions can reach high viscosities without the presence

Table 1. Examples of over-the-counter (United Kingdom) nonmedicated artificial tear eye drops and their thickening agents.

Type	Product name/*Brand*	Thickening agent	Concentration [%]
Artificial tears	Carmize 0.5% *Aspire Pharma* (PF), Cellusan 1% *Farmigea* (PF), Evolve Carmellose *Lumecare* 0.5% (PF), Melopthal, PF Drops Carmellose *Martindale*, Xailin Fresh *Nicox*	Carboxymethycellulose	0.5–1.0%
	Optive *Allergan*	Carboxymethycellulose	0.5%
	Optive Plus *Allergan*	Carboxymethycellulose	0.5%
		Castor oil	0.25%
	Systane, Systane Gel Drops, Systane Ultra *Alcon (Novartis)*	Polypropylene glycol	0.3%
		PEG 400	0.4%
	Systane Balance *Alcon (Novartis)*	Polypropylene glycol	0.6%
	Evolve Hypromellose *Lumecare*, Hydromoor *Rayner*, Hypromellose *FDC*, Hypromol *Ennogen*, Lumecare Hypromellose, Lumecare Tear drops, Ocu-lube Sai-Med, PF Drops Hypromellose *Moorfields*, SoftDrops eye drops *Ajanta*, Vizulize Hypromellose, Xailin Hydrate *Nicox*	Hydroxypropylmethylcellulose	0.3–0.5%
	Liquifilm Tears *Allergan*, Sno tears *Chavvin*	Polyvinyl alcohol	1.4%
	Refresh Opthalmic *Allergan*	Polyvinyl alcohol	1.4%
		Povidone	0.6%
	Artelac Rebalance *Bausch + Lomb*, Clinitas, Evolve HA *Lumecare*, Hy-Opti *Alissa*, Hyabak *Thea pharmaceuticals*, Hylo-fresh *URSAPHARM*, Hylo-forte *URSAPHARM*	Sodium hyaluronate	0.1–0.4%
	Blink Intensive Tears *Abbot*	Sodium hyaluronate	0.2%
		PEG	0.25%
	HydraMed *Farmigea*	Sodium hyaluronate	0.2%
		Tamarind seed polysaccharide	0.2%
	Hylo-care *URSAPHARM*	Sodium hyaluronate	0.1%
		Dexpanthanol	2%
	Hylo-Dual *URSAPHARM*	Sodium hyaluronate	0.05%
		Ectoin	2%
	Lubristil Gel *Moorfields*	Sodium hyaluronate	0.15%
		Xanthan gum	1%
	Optive Fusion *Allergan*	Sodium hyaluronate	0.1%
		Carboxymethylcellulose	0.5%
		Glycerol	0.9%
	Thealoz Duo *Thea*	Sodium hyaluronate	0.15%
		Trehalose	3%
	Thealoz Duo Gel Thea	Sodium hyaluronate	0.15%
		Trehalose	3%
		Carbomer	0.25%
	Emustil *Rayner*	Soy bean oil	7%
		Natural phospholipids	3%
	Artelac Nighttime gel *Bausch + Lomb*, Clinitas Carbomer gel *Altacor*, Evolve carbomer 980 eyegel *Lumecare*, Lumecare carbomer eye gel, Xailin gel *VISU pharma*	Carbomer (polyacrylic acid)	0.2%

of crosslinks.[45] Viscosity is also influenced by the pH and ions in the solvent/solution as this alters the conformation of the polymer chains.[46] CMC is polyanionic and the presence of multiple hydroxy groups provides CMC with mucoadhesive, hydrophilic properties.[6,47] This also enhances swelling in CMC gels, branding them "superabsorbent," and allows CMC to be pH responsive.[43] The mucoadhesive properties of CMC (and other polymers) are advantageous for drug delivery using eye drops. Compared to medicated nonpolymeric (nonviscous) drops, medicated CMC drops have been shown to improve the ocular concentration of the glaucoma drug timolol by 300–900%.[48] CMC is, however, most commonly used in artificial tear eye drops, which are used to provide supportive relief of dry eye symptoms, rather than in other therapeutic drops. Although CMC is efficacious for the symptomatic treatment of dry eye disease, there are now artificial tear formulations with more advanced and properties, such as sodium hyaluronate.[45]

HPMC (Figure 4) is less viscous than CMC but shows superior properties as an emollient—an important factor for treating

Table 2. Active ingredients and main thickening agents of different types of medicated eye drops (United Kingdom).

Purpose	Product name/*Brand*	Active ingredient	Thickening agent
Artificial tear	Ilube *Rayner*	Acetylcysteine 5%	Hydroxypropylmethylcellulose
Antiviral treatment	Virgan *Thea pharmaceuticals*	Ganciclovir 0.15%	Carbomer 974P
Allergy relief	Otrivine-Antistin *Thea pharmaceuticals*	Xylometazoline 0.05% Antazoline 0.5%	–
	Optilast *Mylan*	Azelastine hydrochloride 0.05%	Hydroxypropylmethylcellulose
	Emadine *Alcon*	Emedastine 0.5 mg mL^{-1}	Hydroxypropylmethylcellulose
	Relestat *Allergan*	0.5 mg mL^{-1} epinastine hydrochloride	–
	Zaditen *Thea Pharmaceuticals*	0.345 mg mL^{-1} ketotifen fumarate	Glycerol
	Alomide *Novartis*	Lodoxamide 0.1%	Hydroxypropylmethylcellulose
Glaucoma treatment	Iopidine *Novartis*	Apraclonidine 5 mg mL^{-1}	–
	Lumigan *Allergan*	0.3 mg mL^{-1} bimatoprost	–
	Alphagan/ Brymont *Allergan*	2 mg mL^{-1} Brimonidine	Polyvinyl alcohol
	Azopt *Novartis*	10 mg mL^{-1} brinzolamide	Carbomer 974P
	Trusopt *Santen*	22.26 mg mL^{-1} dorzolamide hydrochloride	Hydroxyethyl cellulose
	Monopost *Thea Pharmaceuticals*	50 µg mL^{-1} latanoprost	Carbomer 974P PEG (macrogol 4000)
	Betagan *Allergan*	Levobunolol hydrochloride 0.5%	Polyvinyl alcohol
	Oftaquix *Santen*	5.12 mg mL^{-1} levofloxacin hemihydrate	–
	Saflutan *Santen*	15 µg mL^{-1} tafluprost	Glycerol
	Travatan *Novartis*	40 µg mL^{-1} travoprost	Polypropylene glycol
	Betoptic *Novartis*	Betaxolol 0.5%	Carbomer 974P
	Tiopex gel *Thea Pharmaceuticals*	1 mg g^{-1} timolol	Polyvinyl alcohol
Bacterial eye infections	Azyter *Thea*	Azithromycin dihydrate 15 mg g^{-1}	Medium chain triglycerides
	Golden Eye	Chloramphenicol 0.5%	–
	Fucithalmic Viscous eye drops *Advanz pharma*	10 mg g^{-1} fusidic acid	Carbomer
	Gentamicin eye/ear *FDC International*	0.3% gentamicin	–
	Ciloxan *Novartis*	Ciprofloxacin 0.3%	–
Eye inflammation (e.g., post-cataract surgery)	Betnesol *RPH Pharmaceuticals AB*	Betamethasone 0.1% Neomycin 0.385%	PEG 300
	Vistamethasone *Martindale Pharma*	Betamethasone sodium phosphate 0.1%	–
	Yellox *Bausch + Lomb*	0.9 mg mL^{-1} sodium sesquihydrate/Bromfenac	–
	Maxidex *Novartis*	Dexamethasone 0.1%	Hydroxypropylmethylcellulose
	FML *Allergan*	1 mg mL^{-1} fluorometholone	Polyvinyl alcohol
	Ocufen *Allergan*	Flurbiprofen sodium 0.03%	Polyvinyl alcohol
	Acular *Allergan*	Ketorolac trometamol 5 mg mL^{-1}	–
	Lotemax *Bausch + Lomb*	0.5%, w/v loteprednol etabonate	Glycerol
	Nevanac *Novartis*	3 mg mL^{-1} nepafenac	Polypropylene glycol Carbomer Carboxymethylcellulose galactomannan polysaccharide
	Pred forte *Allergan*	1% prednisolone acetate	hydroxypropylmethylcellulose
	Vexol *Alcon*	1% Rimexolone	Carbomer
	Tobradex *Novartis*	Tobramycin 3 mg mL^{-1} Dexamethasone 1 mg mL^{-1}	Hydroxyethylcellulose
	Voltarol Optha *Thea Pharmaceuticals*	Diclofenac sodium 1 mg mL^{-1}	Polypropylene glycol

dry eye disease and promoting epithelial health.[45] HPMC is used both as a thickening agent in medicated drops, and as a mucoadhesive and treating agent in artificial tear drops. HPMC and HPMC-composite microspheres have also been created and tested for drug delivery applications and shown favorable drug delivery profiles in the gut.[49]

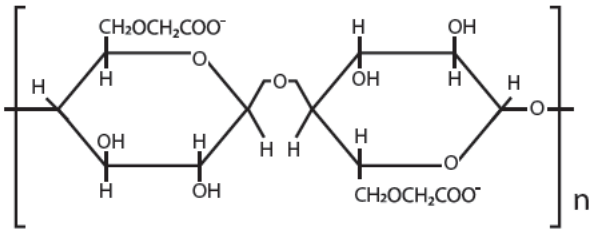

Figure 3. Carboxymethylcellulose structure.

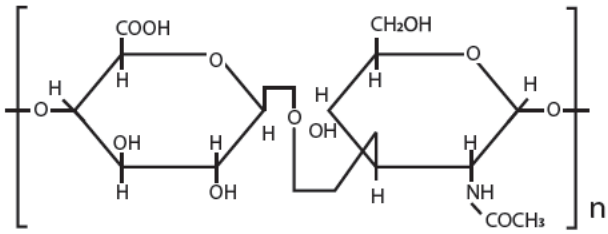

Figure 5. Structure of hyaluronic acid.

Hyaluronic acid (HA; **Figure 5**) is a naturally occurring polymer formed of linear polysaccharide chains, with subunits of d-glucuronic acid and N-acetyl-d-glucosamine. These polysaccharide chains form with multiple hydrophilic anionic sites, which attract water molecules and allow HA solutions to become viscous and show beneficial rheological properties.[44] The molecular weight of the HA naturally present in the body elicits different immunological and cellular responses, with shorter chains appearing more conducive to cell growth and repair than long chain forms.[44,50] This has potential repercussions for the systemic effects of HA use. Chain length has also been found to have a direct influence on the appropriate concentration of HA that should be incorporated into eye drops to allow for improved ocular retention and viscoelasticity. For a given concentration, it was found that, in most cases, commercially available eye drops only reach one third of the optimum chain length value.[51]

HA is incorporated into eye drops to manage dry eye in artificial tears but is not commonly used in medicated drops. HA has a higher ocular retention compared to CMC or HPMC, and has also been shown to have effects on corneal epithelial cell healing in animal models[45] and to improve corneal recovery in patients with superficial punctate keratitis compared to CMC.[52] Larger studies have shown comparable results between CMC and HA with respect to the stabilization of the tear film after cataract surgery,[53] and clinical trials using HA eye drops demonstrate the efficacy of this therapy for improving symptoms and clinical signs in moderate-to-severe dry eye disease over 3 months.[54] Although HA shows the same, if not improved, benefits with respect to on-eye retention and epithelial health compared to CMC and HPMC in the treatment of dry eye disease, it is infrequently used in medicated drops for other eye conditions. HA does not show a significant detrimental drug binding effect.[55] The exclusion of HA from medicated drops could be due to cellulose-based polymers being of lower cost and simpler synthesis.

2.1.2. Synthetic Polymers

Polyethylene glycol (PEG) (**Figure 6**) and polypropylene glycol (PPG) are biocompatible synthetic polymers.[56] PEG and PPG are usually used as a backbone and then modified in various ways to create the desired properties. In comparison to CMC, PPG/PEG eye drops maintain a higher optical clarity after use, which can improve the patient experience and subsequently could improve compliance with treatment regimens.[57] When chain length exceeds a threshold of 200 kDA, PEG exhibits mucoadhesive properties, but still shows limited adhesion in comparison to CMC.[23f] Used either separately, or in conjunction as a mixture or co-block polymer, PEG and PPG polymers are relevant to a spectrum of medical and industrial applications. PPG and PEG have been used alongside hydroxymethyl-guar (a naturally occurring gelling agent) to increase the viscosity of eye drops.[57,58] This combination has been shown to be effective as a therapy for dry eye disease.[58,59]

PEG is amphiphilic and therefore very versatile and modifiable. These properties render PEG a common choice for testing hybrid lipid–polymer systems and for modifying the surface of difference carriers.[60] PEGylation is the name given to this process. As PEG does not illicit an immune response, it is used to dampen the potential response to an otherwise immunogenic carrier by modifying the surface charge or acting as a bridge for other molecules which illicit the desired immune response.[60b] PEGylation can also modify the solubility of proteins—such modifications could make a vital difference to the penetrability of a carrier through the corneal barrier, for which charge is a vital factor.

Polyacrylic acid (PAA; **Figure 7**) is another synthetic hydrophilic polymer used to create superabsorbent gels for nappies and cosmetics under the commercial name "carbomer."[61] Carbomers are traditionally synthesized in a benzene solvent, raising issues for medical applications. Other solvents, such as ethyl acetate and cyclohexane,[62] can be used as an alternative. Most commercial drops that describe themselves as "gel" drops use carbomers. Carbomers do gel, however the properties

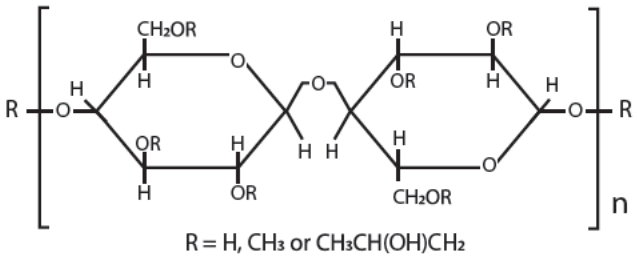

Figure 4. Hydroxypropylmethylcellulose structure.

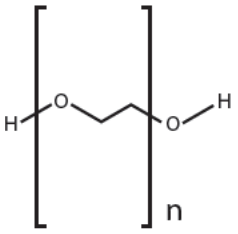

Figure 6. Polyethylene glycol structure.

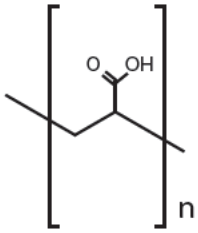

Figure 7. Polyacrylic acid monomer structure.

of these gels are heavily influenced by pH, solvents, and surfactants; their rheological properties become less favorable and more unpredictable with variations in these factors (pH, solvents, and surfactants) in the formulation conditions.[63]

Polyvinyl alcohol (PVA; **Figure 8**) is a common synthetic polymer used to enhance the viscosity of eye drops. Synthesis of PVA involves hydrolyzing polyvinyl acetate.[64] Thiolated PVA is mucoadhesive, and even short chain PVA could enhance the viscosity of eye drops beyond the threshold to achieve greater corneal retention.[64,65] It is much more common for PVA to be used in gel form. PVA gels can be formed through physical crosslinking or irradiation, and show favorable degradation profiles for drug delivery.[66]

3. Innovations in Topical Ocular Drug Delivery

The drawbacks of currently available eye drops are well documented and it is worth noting that alternative forms of topical treatment are being investigated, including ocular devices such as contact lenses and inserts.[10b,38,67] However, eye drops remain a noninvasive and patient friendly approach to ocular disease management and treatment.

Patients have previously reported limitations to their daily activities when eye drop application frequency is increased, as they must accommodate more applications and may not feel comfortable using eye drops outside of their house or a bathroom.[68] The simplest treatment regimens are shown to have better adherence and persistence from patients.[68] The increase in efficacy of drops with higher bioavailability may reduce the necessary frequency of administration and increase patient adherence to the regimes.

A number of reviews have explored the cutting-edge ways in which eye drops are being adapted to overcome their current limitations of bioavailability.[1b,6,7,23a,56,67b,69] Each of these routes for innovation either show promising improvements to the bioavailability of the delivered drug or with artificial tears—the symptoms of dry eye disease. They do, however, each come

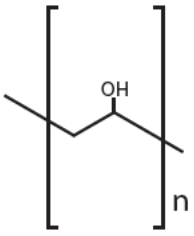

Figure 8. Polyvinyl alcohol monomer structure.

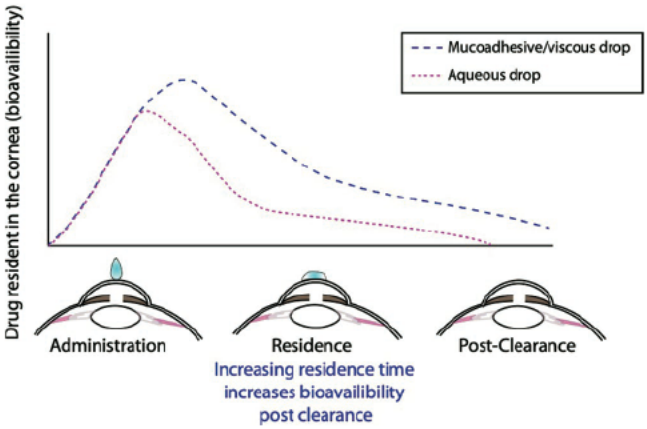

Figure 9. Schematic representation of the effects of increased residence on bioavailibility.

with their own limitations, both in terms of immunological considerations and also practical, patient-focused considerations.

Bioavailability considers the therapeutic efficacy of a treatment in terms of the amount of drug that becomes available to the tissue over the treatment window. When formulating an eye drop with greater bioavailability, there are multiple approaches to consider: i) Ensuring the residence time of the drop is extended to create a larger delivery window (**Figure 9**), ii) ensuring the release profile of the delivery vehicle and the dose of the drug being carried allows for the optimum dose to be delivered across that window, and iii) enhancing the permeation of the drug through the tissue.

3.1. Bioavailability

3.1.1. Improving the Residence Time of Eye Drops

The residence time of eye drops is increased when the drops can overcome the ocular surface's natural clearance mechanisms. Two particular properties that assist in this are mucoadhesion and increased viscosity. It is important to note that these two properties influence each other, and must be balanced for an optimal formulation.

Predictions of eye drop residence time are commonly calculated based on a combination of rheological testing and estimations of tear turnover rate and blinking mechanics. However, blinking mechanics and the rheological properties of the natural tear film are complex and are still being investigated.[70] It generally understood that the natural tear film is shear thinning, a property which could be relatively easily emulated in polymeric eye drops.[71] Assessment of tear film turnover is commonplace in clinical settings in the form of simple fluorescein clearance tests. In order to assess the residence of eye drops in vivo, this same test can be replicated with the fluorescein dye incorporated into the eye drop.[72] This assessment is dependent on the affinity of the eye drop formulation to fluorescein, as a drop that carried fluorescein poorly would appear to remain resident for a shorter time. A number of more sophisticated in vivo imaging techniques also rely on the tracking of fluorescent or radio-traceable molecules, which are again dependent on the

nature of the carrier as the release profile and residence profiles may not match up for different carrier chemistries.[73]

3.1.2. Mucoadhesion

The mucosa of the ocular surface plays an important role in the protection and function of the eye. Mucins on the ocular surface originate from the conjunctival goblet cells. The glands that produce the aqueous and lipid components of the tear film are also based in the surrounding mucosal tissue. Changes in the amount and the consistency of the ocular mucins can be indicative of inflammation, or in the case of a reduction, can lead to epithelial damage and dry eye disease.[24,74] Most of the ocular mucin is held to the surface of the eye in a glycocalyx layer, however some secreted mucins float freely in the aqueous portion of the tear film.[19c,74,75] The glycocalyx forms a protective barrier and an additional layer to penetrate for drug delivery purposes. However, from the perspective of designing artificial tears for the alleviation of dry eye symptoms, the potential for mucosal–polymer interactions may assist in stabilizing the tear film and lubricating the ocular surface. Mucoadhesion also creates the possibility of extending the residence time of an eye drop if the correct properties are enhanced. The mucins responsible for the improvement in retention time of mucoadhesive vehicles are the surface adhesive mucins in the glycocalyx.[19a,c] For microspheres and nanoparticles, their mucoadhesion depends on surface charge.

A number of tests can be deployed to assess the level of mucoadhesion of a polymeric drug delivery vehicle. Depending on the desired application, different tests can be chosen to replicate more realistically the environment in vivo.[60a,76] Similarly, attempts to artificially recreate realistic mucosal tissue have yielded positive results.[77] Different compositions of mucins can be used for testing, either fully or partially hydrated and of different film thickness.[78]

Tensile mucoadhesion tests can be done both in vitro and ex vivo to provide a comparative value of mucoadhesion between materials or a value of mucoadhesive force.[25] They rely on creating contact between two surfaces and measuring the force necessary to separate them.[25] One of the most common methods of tensile mucoadhesion analysis is to use a texture analyzer and coat the probe in an appropriate mucin.[23d,77,79] Alternative tests can also involve peeling one layer away, a vertical gravity resistance test, or a shear resistance test.[25]

A different approach to investigating mucoadhesion can focus more closely on the nature of the polymer–mucin interactions—e.g., through surface plasmon resonance.[80] This technique can quantify the strength of molecular interactions between two films by measuring the change in the refractive index.[81] This provides a much more in-depth analysis and predication of the level of mucoadhesion that may be expected in vivo.

3.1.3. Viscosity

Another innovation investigated for overcoming the eye's natural barriers to drug delivery and improving the bioavailability of the carried drug is to increase the viscosity of the eye drop.[7a,69b,82] Tests have shown that more viscous drops show a higher resistance to lacrimal clearance and stay resident on the surface of the eye longer.[2,10b,38,51,61,76,83] As with mucoadhesion, this increases the window available for drug delivery. Rheological assessments that determine viscosity are also frequently used to test the mucoadhesive properties of a polymer solution or gel.[76,79,84] This links properties like viscosity and elastic strength to mucoadhesion. However, both cannot be increased indefinitely; as viscosity increases so does the surface tension of the drop. Various studies have examined the contact angle of drops in vivo and in vitro to assess how changes in viscosity, surface tension, and surface chemistry effect the "wetting" of the drop.[85] Viscosity appears to limit the spreadability of the drop which in turn limits mucoadhesion.[25] This is not necessarily a linear relationship, as, e.g., in viscous hydrogel drops, the crosslinking mechanism in the gel may change the surface chemistry, which can also influence mucoadhesion either positively or negatively.[76]

The surface tension of an eye drop formulation has also been highlighted to have an important relationship with the drop size, and its consistency over multiple applications.[86] It was also shown that drop bottle applications produce highly variable results among patients, with drug type (flow characteristics), concentration, and drop viscosity affecting drop size.[86a] These factors need to be considered when evaluating the efficacy of eye drops, as if the drop size is not controlled then different dosages of the drug will be administered and the therapeutic efficacy will become variable.[86b]

Rheological assessments provide an idea of the theoretically expected residence time for an eye drop.[87] Although most preparations undergo some form of rheological testing in vitro as an assessment of properties, this often does not take into account the complexity of blinking conditions. The natural curvature of the eye, and where the drop sits in relation to the eyelids must be considered and assessed when examining the behavior of the drops and their efficacy as a treatment.[23d,50b,63a,83b,87,88]

3.1.4. Controlled Release

Therapeutic drugs have an upper and lower limit of efficacy—a therapeutic threshold—which is associated with the concentration present in the target tissue. Drug delivery systems need to release their load at a suitable rate to maintain a therapeutically effective dose across the treatment time window, otherwise any improvements in residence time will not translate to improvements in treatment efficacy.[83a] Different drug delivery vehicles offer different levels of tunability of the drug release profile.[10b,56,82a,89] Where the drug delivery relies on the disintegration of the carrier, highly structured vehicles may limit drug release by disintegrating slowly, and diffusion models are influenced by the drug–polymer interactions. Relevant tests which take into account the temperature and pH of the destination tissue can give an idea of the expected in vivo delivery profile.

The release of a drug can also be inhibited by interactions between the drug and the carrier. Many hydrogels are

responsive to ionic and pH changes.[69p,82a,90] A strong interaction between the drug and the carrier may change the release profile of the delivery device, hindering delivery, and preventing the drug from reaching or sustaining the therapeutic threshold.[91] The mechanism of drug loading is also important, as different methods create different release profiles but also involve different solvents.[92] The loading of nanoparticles is also limited by the fact that the encapsulated phase makes up a very small fraction of the overall mixture, and the loading is limited to the equilibrium point between the phases.[93] Encapsulated delivery systems also pose the risk of premature release in storage which can decrease the possible dosage in vivo.

One way to circumvent problems arising from unwanted drug/carrier interactions is to take a prodrug approach and specifically design drugs that work with carriers that have shown promising results. Prodrugs are modified versions of existing drugs, which as a result can carry a different charge or can be nonreactive. Once they reach the host tissue, the environment in that tissue is normally home to an enzyme or other trigger compound, which alters the pro-drug back into its active, therapeutic state.[94] This approach can allow drugs which are not normally penetrative or carriable in certain devices to be delivered successfully, but depends heavily on the nature of the tissue being delivered to and the disease state of that tissue. There is also a risk that the full dose may not be released and the therapeutic threshold may not be reached or maintained for a period long enough to see adequate therapeutic effects.

3.1.5. Mechanisms of Penetration

Formulating eye drops that overcome the ocular barriers to drug delivery can involve improving resistance to lacrimal clearance through increasing mucoadhesion or viscosity but can also involve facilitating easier passage of the drug through the ocular tissue. The main barrier to transcorneal drug delivery is the epithelial layer, within which there are inter-cellular tight junctions and protein binding sites that work to prevent penetration through the multiple cellular layers (**Figure 10**). Lipophilic drugs travel through the cornea by passing through the lipid bilayer of the cells themselves. Transport through the stroma is restricted to diffusion, so this is the rate-limiting step of the process.[38] For hydrophilic drugs, they must pass through the cellular tight junctions, which present the most significant barrier. It is also common for hydrophilic drugs to accumulate in the stroma, which may limit passage to posterior tissues.[38]

The first attempts at improving penetration of drugs through the cornea involved incorporating pharmaceutical permeation enhancers such as ethylenediaminetetraacetic acid (EDTA) to interfere with the epithelial tight junctions to allow for the passage of drugs into the stroma. Both benzalkonium chloride (BAK)—a common preservative used in multi-dosage drops—and EDTA have been shown to improve the penetration of drugs through the cornea in vitro.[6,95] EDTA and similar compounds sequester calcium ions from the epithelial layer, impacting the function of the tight junctions and allowing for the delivery of molecules through the epithelial layer.[96] Although this may appear positive for the treatment of the primary condition, both types of preservatives can affect the health of the corneal epithelium, which can lead to additional discomfort and secondary ocular damage, such as superficial punctate keratitis and lower sensory nerve density.[97] BAK is even used experimentally to replicate the effects of dry eye disease, as it can cause cell lysis and can be cytotoxic to corneal epithelial cells.[99] The enhanced ocular penetrative effect has also not been replicated in in vivo

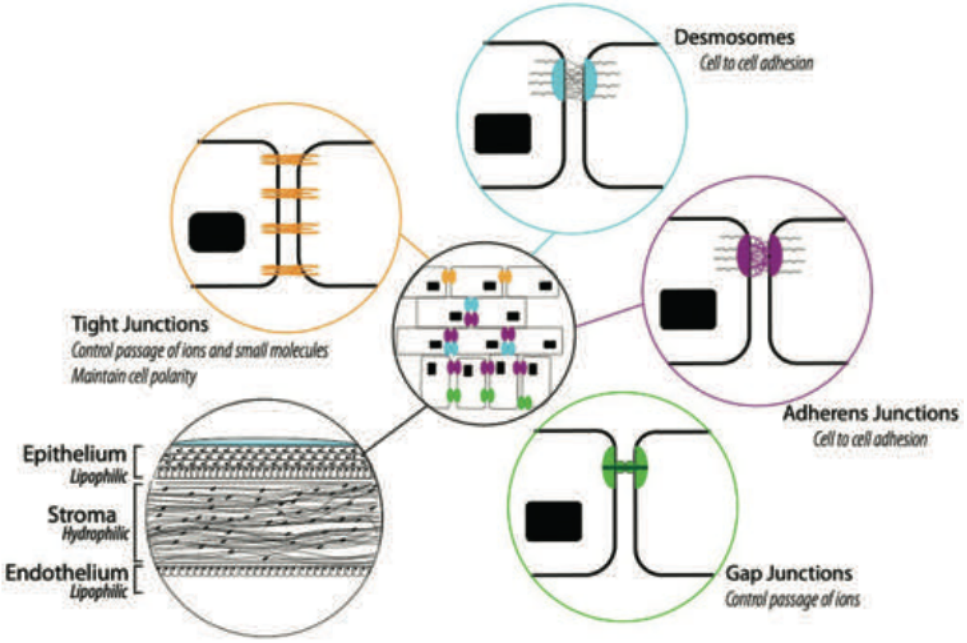

Figure 10. The wider structural and epithelial intracellular barriers to drug penetration in the cornea.[98]

studies, where the contact time of the eye drop preparation is much shorter.[100]

There is also evidence to suggest that in drops that use a combination approach of pharmaceutical permeation enhancer and residence prolonging polymers in solution, the polymer/drug/permeation enhancer interactions overall limit the bioavailability of the drug.[101] When this approach was taken with nanoparticles, the effects were much more positive, with the permeation enhancers effectively working to enhance the penetration of polymer-coated nanoparticles.[102] The surface chemistry of the nanoparticles was found to be the deciding factor in the efficacy of the combination approach, which raises an important formulation consideration for permeation enhancing micro and nanoparticles.[102] An additional study found again that adjustments to the particles size and charge influenced penetration.[9]

In recent years, the focus has shifted away from modifying the tissue and toward engineering carriers that can circumvent the eye's natural barriers. One promising innovation has been the development of cell penetrating peptides (CPPs). CPPs are amino-acids containing 5–40 peptides which can pass through cells in a receptor-independent manner.[103] They can be easily specialized and are incredibly versatile, capitalizing on their polyanionic nature to navigate a variety of cellular and tissue barriers.[103,104] A variety of CPPs has been developed for topical ocular drug delivery. CPPs can be modified with fluorescent binding agents which allow them to be tracked through the cornea, and through these studies are gaining understanding of how the constituent peptide make-up of the CPPs influences their ability to penetrate the different corneal layers.[104] A recent study found that CPP-containing drops could deliver therapeutically effective doses of anti-VEGF drugs to the choroid, potentially allowing an alternative treatment to the current invasive ocular injections.[105] CPPs can also be used to modify polymeric nanocarriers and improve their ocular penetration.[104]

3.2. Novel Materials Approaches

3.2.1. Hydrogels and Fluid Gels

Hydrogels are now increasingly being investigated for use as biological scaffolds, drug delivery devices, and as alternatives to plasters and sutures. Hydrogels show tuneable mechanical properties, drug-release profiles, and degradation rates. Natural polymers are generally nontoxic and biodegradable and have the added advantage of binding with cells and proteins. However, natural polymer-based hydrogels can have poor mechanical strength, high variability, and can still provoke an immune response despite being nontoxic. Synthetic polymers are more consistent and tuneable in their properties, but do not inherently interact with proteins or cells.[69g]

Recently, research efforts have focused on improving the penetrative ability and residence time of eye drops. Much of this research has been directed toward investigating the use of more viscous-based materials, primarily hydrogels, for eye drop formulations and several manufacturers advertise commercially available "gel" eye drops. However, there is a disparity between commercial and academic interpretation of what constitutes a "gel," with many "gel" drops simply incorporating viscous polymers to improve the rheological properties instead of creating a true hydrogel. True hydrogels, crosslinked polymer networks that entrap and hold water (**Figure 11**),[69i] are yet to fully translate into commercial use. This is due to a number of practical factors, including the toxicity of some crosslinking agents to the ocular surface, the rate of lacrimal clearance limiting in situ gelling, preformed gels being harder to administer, limitations

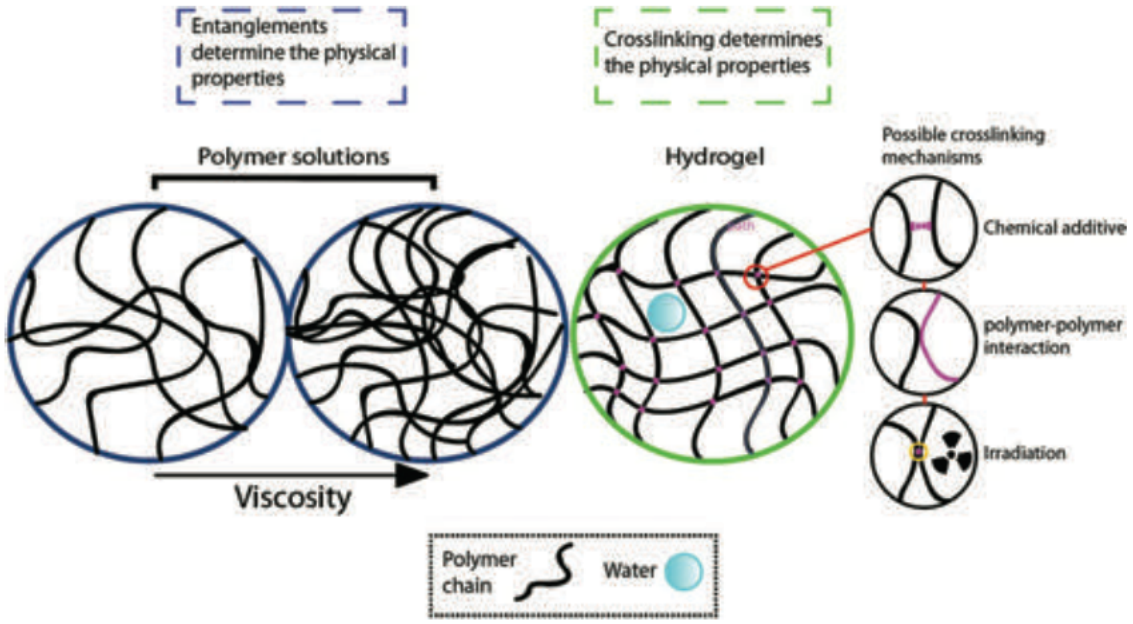

Figure 11. A comparison of the structure of polymer solutions and hydrogels.

in pH and temperature sensitivity, and patient-focused outcomes (such as comfort and clarity of vision).

As an alternative to preformed gels, in situ gels have been tested to allow for simple ocular administration.[7a,69g,p,106] Harsh chemical gelating agents would be inappropriate for ocular use, so natural variables should be exploited, such as temperature, pH, and the presence of electrolytes or proteins.[69d] Carbomer and carbomer/HPMC gels can form spontaneously at a suitable pH when used in combination.[69d] There are gels which can form at certain temperatures such as HPMC,[43,107] however the gelling temperature would need to match the ocular surface temperature closely enough to be effective. The gelling process would also need to occur almost instantaneously in order to take full advantage of the desired effect, or much of the liquid base-material will be lost through lacrimal flow before gelling occurs.[19c,26] The formed gel then needs to show the appropriate rheological, mucoadhesive, and drug-release characteristics.

Other considerations for formulations include that the solvent and cross-linking agents that form the gel structure must not have a toxic or damaging effect on ocular cells and tissues. They must also be compatible with the drug being carried.[108] That said, they impact the final structure of the gel and therefore must also produce the desired characteristics in the gel.[88a] Aqueous versus anhydrous (alcohol) gel formation provides different structures and properties of gel, and these structural changes can inhibit the ability of certain polymer structures to deliver drugs effectively.[108,109] The radiation-initiated cross-linking of some gels has the added benefit of sterilizing the gel,[43] however preformed gels pose a challenge for topical application.

Fluid gels may circumvent issues with administration, allowing for better control of rheological properties and the ability to administer consistent drops.[61,110] Fluid gels have been explored as a versatile deviation from the traditional hydrogel structure and are formed by shearing hydrogel to produce a complex hydrogel microstructure as opposed to a macrostructure.[61] Fluid gels therefore retain the viscosity and favorable drug delivery profile of a gel, while allowing for the necessary flow characteristics for spraying, pouring, and drop formation, and they present as a promising medium for eye drops.[61,110,111] The level of shearing the 'gel' is exposed to also 'controls' the microstructure, which in turn can control the spreadability of the drop. The use of mucoadhesive gels which have been sheared to provide a fluid gel with the optimum balance of viscosity and wettability may circumvent some of these issues.

3.2.2. Polymeric Microspheres and Nanocarriers

Microspheres have also been investigated in the context of ocular drug delivery, with respect to resolving potential problems associated with poorly soluble drugs and poor bioavailability, with some showing marked improvements compared to aqueous drops.[23b,69o] They can increase the penetration of the delivered drug, with some models showing successful delivery to posterior tissues such as the retina and choroid.[69n,106c,112] Microspheres show controllable degradation rates, with synthetic polymer composite—PEG/PPG/PAA—microspheres, as with hydrogels, showing much more controllable degradation properties than those made with natural polymers.[60c,113]

On a much smaller scale, nanocarriers have also shown promise for improving the permeability of treatments.[1b,5,9,69o,112,114] With regards to the incorporation of microspheres and nanocarriers into eye drops, the potential for phagocytosis by resident corneal and conjunctival immune cells and an associated inflammatory response needs to be considered—both as a drawback and as a potential for immunomodulation.[115] Different shapes, charges, and functional groups can influence the immunological response to nanocarriers and the response in inflamed tissue can vary from the response in noninflamed tissues—an important consideration for treating different pathologies.[116]

3.2.3. Lipid-Based Drug Delivery Systems

Although tailoring mucoadhesive polymers presents one option for improving the efficacy of eye drops, other avenues are also being explored, including emulsions and microemulsions, lipid-based carriers, and permeation enhancers.[63c,111b,117] Lipid or emulsion-based eye drops show comparable results to conventional polymer-based drops.[117,118] Emulsions also offer the added benefit of being able to carry hydrophobic/poorly soluble drugs,[119] however there are concerns with regards to the methods of synthesis relying on a high proportion of surfactants (<10%) which interact with the ocular surface and increase the residence time of the drops, but can be cytotoxic to the corneal cells.[120] There are also concerns as to how well emulsions will last in prolonged storage—if the dispersion of the emulsion becomes uneven and separation occurs, the dosage of each eye drop will become uneven and the therapeutic threshold may not be reached.[120b]

As with simple polymeric drugs for dry eye disease, eye drops do not necessarily have to carry a drug to have a beneficial clinical effect. The lipid components of eye drops can assist with supplementing the tear lipid layer, which is often deficient in conditions such as dry eye disease and meibomian gland dysfunction.[117,118b,121] The addition of topical lipids or fatty acids can help rebuild the natural lipid film, thus replenishing the protective function of the lipid components of the tears.[121a] Such as with the polymer choice in polymeric drops, the choice of oil-in-emulsion-based drops significantly changes the properties of the drop. Long chain oils do not interact with the surfactants and emulsify as easily as short chain oils, but show a higher drug solubility.[122] This means that there needs to be a balance between drug compatibility and emulsion compatibility. The proportion of oil in the eye drop is also dependent on the dose of drug that needs to be carried.[120b] This means the properties of the resulting emulsion are largely dictated by the nature of the drug being delivered.

Liposomes—nanospheres with one or more phospholipid bi-layers—have also been investigated for use in eye drops to increase corneal penetration, with considerable success.[115c,122,123] However, the use of liposomes elsewhere in the body has been shown to illicit an inflammatory immune response—this has even been harnessed to improve the response to vaccines.[123,124]

This raises questions for long-term ocular use, as prolonged inflammation can be detrimental to ocular surface health.

Solid lipid nanoparticles (SLNs) offer similar advantages to polymeric nanoparticles in terms of permeation of the natural barriers of the eye, while also presenting the option to carry drugs that may not be transportable in a polymeric system. SLNs can be optimized to target specific pathologies as different combinations of lipid structures (triglycerides, fatty acids, waxes, etc.) can be used.[125] Solid lipid nanoparticles are less likely to be made with harsh solvents, which may be beneficial for conditions where the ocular surface is already damaged or inflamed. However, they do normally incorporate surfactants to stabilize the emulsion, and despite these measures can still carry a lot of water and undergo structure changes during storage which can lead to a reduced drug carrying capacity.[125] SLN drops do however typically contain less surfactant than emulsion drops.[119] Similarly, smaller liposomes can be designed and optimized to carry and deliver both hydrophilic and hydrophobic drugs by adjusting the lamellar structure.[126] Both SLNs and liposomes can be designed as polymer–lipid composites to draw on the advantageous properties of both and allow for various synthesis methods.[126b]

3.2.4. Hybrid Approaches

There is no single simple or ideal answer to how to most effectively improve the formulation of topical eye drops. A combination of approaches can benefit from a multitude of advantages, e.g., microspheres incorporated into gels to allow for a much more consistent and controllable drug delivery profile.[127] The question of which material or structure will be most effective ultimately depends on the nature of the disease being treated and its influence on the physiology and function of the eye's anterior tissues.

Emulsion-based eye drops can incorporate polymers to allow for mucoadhesion, while using lipids to transport the hydrophobic drug.[128] This approach can be carried across into nanocarriers, with the synthesis of lipid–polymer hybrid nanoparticles. These nanocarriers can deliver a hydrophobic drug in a polymer core, which is surrounded by a lipid layer. This lipid layer acts to ensure the hydrophobic drug remains encapsulated while also enhancing permeability through lipophilic tissues.[126b]

3.3. Preservatives, Surfactants, Ease of Sterilization, and Storage

Eye drops designed for multiple usages contain preservatives to maintain the sterility of the product. Phosphate-based preservatives have been found to induce rapid corneal calcification and temporary loss of sight when applied to an already injured ocular surface, which has ultimately led them to be phased out of use.[129] BAK is a common preservative, but has also been found to interact with carbomers and influence their viscosity, to the detriment of the desired improvement in bioavailability.[88a,130] Due to the interference of preservatives with gel structures [63a,87,88,109] and also the potential side-effects of common preservatives,[100,130,131] the manufacture of eye drops (especially multi-dose formulations and gels) must be performed under sterile conditions to prevent the entrapment of pathogens in the drops that could be later released in vivo. Many preservatives, although useful for maintaining sterility, interact with the polymers and influence the structure of the gel.[88a,114] When incorporating preservatives or other additives, it must be prioritized that the structure and function of the eye drops are maintained over a reasonable window of storage (≈12 months). Multiuse drops in particular need to remain sterile over a window of use which may span a number of weeks. If this cannot be achieved, then a simple process for creating an appropriate, sterile formulation at the point of use needs to be considered. Alternative preservatives and preservative-free options have therefore been explored as a result.

The storage temperature of different polymer solutions can impact their osmolarity over time.[133] Osmolarity is a key formulation criterion for eye drops, and thus needs to be measured accurately and maintained well over the storage period. Modeling and in vitro testing are needed to predict the "worst-case storage scenario" and allow for the formulation to accommodate any associated osmolarity changes. This is critical, as a large difference from the natural tear osmolarity will affect the integrity of the tear film.[133]

3.4. Novel Polymers and Polymer Combinations

There are hundreds of possible polymer combinations that could be used to formulate hydrogels, with each different pairing creating different properties and advantages.[43,56,61,69b,c,f,g,j,90,134] Novel processing and characterization techniques have highlighted a number of new synthetic, naturally occurring, and hybrid polymers which show advantageous properties for ocular drug delivery (**Table 3**).

4. The Immunological Response to Polymeric Materials

The relationship between the immune system and several classes of medical materials are well established. Implantation in the body can induce a foreign body response, with the severity of the response dependent partly on the material properties of the implant. Materials are generally classed as toxic/harmful, bio-inert, or bio-compatible. The first stage of an immune response to implantation of an exogenous component results in neutrophil migration to the site and subsequently, macrophage recruitment. Implantation may result in chronic inflammation and fibrous encapsulation rather than integration into the tissue, which can cause the implant to fail.[30c]

Synthetic and natural polymers are well established in the field of medical devices and are used in implants and drug delivery devices.[67b] More recently, hydrogels have been investigated as a means of delivering or attracting immune cells for immunotherapy. They have successfully been used for the delivery of dendritic cells[135] or agents to improve the chemotaxis of dendritic cells, such as granulocyte-macrophage colony-stimulating factor[136] and MIP3-beta[137] for the treatment of or vaccination against cancer. Also, to deliver antigens to induce tolerance in T-cells[141] and prevent autoimmunity. The optimal combination of base-polymers to

Table 3. A brief overview of polymers showing promising results in research, which are not yet available in over-the-counter eye drop formulations.

Name	Structure	Natural/synthetic	Charge	Properties
Sodium Alginate	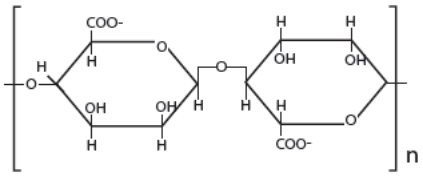	Natural	Anionic (Hydrophilic)	Mucoadhesive[25,42] Gels in the presence of Ca^{2+}[69h]
Gellan	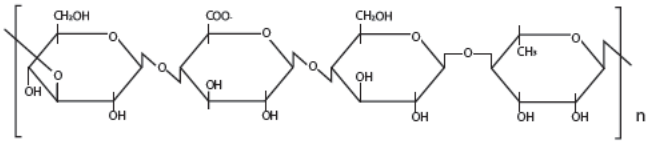	Natural	Anionic (Hydrophilic)	Gels in the presence of Na^+, Ca^{2+}, or Mg^{2+} ions[69p] Mucoadhesion[25] Property enhancement through shearing[61]
Poloxamer	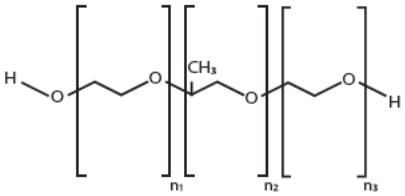	Synthetic	Amphiphilic	Thermal gelation[82b,83c,138]
Poly-NIPAAM	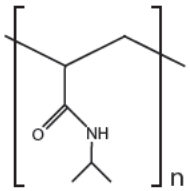	Synthetic	Amphiphilic	Thermal responsiveness[139]
PLGA	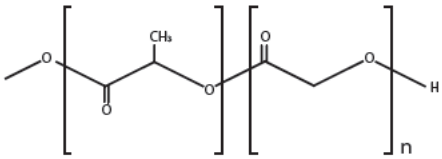	Synthetic (natural co-polymers)	Hydrophilic	Tunable biodegradation into metabolizable by-products[140]

form the gel, as well as the desired final properties of the gel, depends on the types of cells and chemokines being delivered.[142]

It has also been shown that the properties of the materials used in biomedical applications themselves, rather than the drugs or cells they carry, can regulate immune responses.[143] The innate immunogenic properties of HA have been harnessed to target specific tumor cells. Specific chain lengths of the HA on a coating of nanoparticles were found to have an affinity for CD44+ cells, opening up opportunities for targeted drug delivery and immune activation.[144]

Macrophages switch polarization depending on their environment.[30c,35,115b,c,136,145] Hydrophilic versus hydrophobic surfaces produce different macrophage profiles in culture, with hydrophilic surfaces inducing the M1 (proinflammatory) phenotype and hydrophobic surfaces eliciting an anti-inflammatory M2 phenotype that encourages wound healing and tissue remodeling.[145f,146] It was found that different processing methods during manufacturing of the same implant induced different macrophage responses in rodents.[145c] It has also been shown that a surface topography that encourages cellular elongation may facilitate M2 polarization and therefore wound remodeling.[30b]

With regard to microspheres and nanoparticles for general drug delivery, the likelihood and consequences of phagocytosis need to be considered.[115c,145e,146,147] Immunomodulatory effects are achievable through either releasing immunomodulatory drugs or inducing macrophage polarization by targeting phagocytotic activity or surface adhesion. Again, surface chemistry is important for modulating the immune response, with hydrophobic microspheres phagocytosed by macrophages to a greater degree than their hydrophilic counterparts.[145f] This may be due to differing protein adsorption on the surface, which is the primary cue for macrophage activity.[147] Surface modification of synthetic polymer microspheres may be advisable to allow for mucoadhesion and better tissue retention[112,145e] however the influence on the subsequent phagocytosis or inflammatory response would need to be monitored. The response is also likely to differ depending on the existing level of inflammation in the target tissue.

4.1. Biomaterials in the Eye

The response of immune cells to the presence of biomaterials on the ocular surface will likely differ from examples of implantation elsewhere in the body, due to the plasticity and

tolerance of ocular immune cells, and the consistent exposure of the ocular surface to the external environment. One example of regular, prolonged contact of polymers to the ocular surface (as opposed to the current minimal contact of aqueous eye drops) is with contact lenses. An increase in dendritic cell numbers in the central cornea has been observed to occur in silicone-hydrogel contact lens wear,[148] as has an increase in tear inflammatory markers.[149] Contact lens wearers can also experience a range of conditions linked to ocular surface inflammation, including dry eye disease,[150] contact lens associated red eye,[151] and contact lens intolerance.[152] The use of nonaqueous eye drops is unlikely to illicit a similar response, as even with a prolonged residence time, overall the contact with the ocular surface and any mechanical disruption will be minimal in comparison.

There may be potential to harness the properties of the polymers used to induce biomaterials-based immunomodulation in relation to ocular surface diseases. This is particularly worth exploring in dry eye disease, which is often associated with ocular surface inflammation and is one of the conditions for which eye drops are currently most commonly prescribed.

Many current topical therapies for dry eye disease, which often incorporate the polymers listed in Table 1, provide some relief of dry eye symptoms but generally do not treat the underlying etiology of the condition. The use of pharmaceutical components that promote the production of mucins and lipids are being investigated,[17] as are components targeting lymphocytes to reduce the inflammatory response that triggers epithelial damage.[18a,153] For example, by interfering with the antigen receptors on T-cells, Lifitegrast attenuates the immune response by reducing the secretion of proinflammatory cytokines.[154] Immunomodulation, both intentional and unintentional (as a result of interaction between immune cells and drug delivery devices), needs to be considered when formulating eye drops.

Concerns for the use of materials with longer residence times in the eye have arisen around the potential for incomplete breakdown of devices designed to biodegrade in order to release their drug load, and the uncertainty of responses to the by-products of different materials' decomposition. In a repeated dosing situation, such as with eye drops there is a risk of material build up and an associated inflammatory response.[116] Material may build in the conjunctival sac, which poses a potential risk as the conjunctiva is more prone to inflammatory responses than the cornea.[20] This could also lead to a foreign body response and a feeling of discomfort, which will not aid adherence to a treatment regime.

5. Patient-Focused Considerations for Eye Drop Formulations

In order to design an optimized eye drop that can make the full transition from benchtop to effective clinical use, considerations beyond just the achievable bioavailibility in controlled conditions need to be made. Like any biomedical device, the interaction between the patient and their eye drops—practically, physiologically, and psychologically—needs to be assessed to achieve the optimum outcome, and each decision influences another (**Figure 12**). There are also formulation considerations that influence each other, and in turn influence the experience of use for the patient.

5.1. Comfort

The performance of an eye drop after instillation is only one of the important clinical factors to consider. Eye drops can be administered at home and with minimal discomfort and relative ease. With a trend for eye drops to have increased viscosity, the eye drop still needs to be dispensable from a bottle and produce drops of the desired size and drug concentration. The surface tension and viscosity of a drop also has important implications for the sensation of the drop on the cornea.[155]

A shift toward more viscous eye drops, which are more resistant to lacrimal clearance and blinking may increase bioavailability in theory, however in practice they will be more uncomfortable for the patient, increasing blinking and clearance, and creating blurred vision.[155] The potential for longer residence times also raises questions around the use of other ocular devices, such as contact lenses.

Depending on the longevity and severity of the eye condition being treated, patients may inappropriately stop using their eye drops if they find the formulation uncomfortable or hard to administer, or if their symptoms subside too rapidly or insufficiently. Some researchers suggest semipermanent devices would be a preferable alternative, as they do not rely on adherence from the patient.[67a,b] However, eye drops are still preferable for conditions where the anterior tissues are damaged or inflamed, as semipermanent devices can aggravate these conditions. Where more viscous drops may also be an advantage is in reducing the administration frequency, which may balance out the unpleasant patient experience.

5.2. Personalization of Treatment Regimes

Dry eye disease is one of the most common conditions for which eye drops are used. Patients who present with symptoms of dry eye often purchase over-the-counter artificial tears (see Table 1) with the intent of reducing ocular surface irritation. With this method of self-selection, there is no assurance that the formulation they choose will be the most effective for their particular manifestation of the condition.[18a,41a,59,118a,156] A key feature of dry eye disease is the presence of elevated tear film osmolarity (i.e., tear hyperosmolarity), which occurs ubiquitously in all subtypes of the disease.[157] There are two primary forms of dry eye disease, characterized by either insufficient lacrimal secretion (aqueous-deficient dry eye) or lipid layer deficiency (evaporative dry eye).[17,156a] Although patient symptoms for each disease subtype are similar, different subtypes may respond better to different formulations of eye drops.[118a,158] There is also large within-patient variability in the rate of lacrimal flow and clearance of an eye drop from the target tissues. Patients with a high lacrimal flow will potentially dilute the drug and clear it faster than those with a low or inhibited lacrimal flow, and thus may have a poorer treatment outcome with the same concentration of drug.[6] There are also different lifestyle factors that can affect the expression of dry eye disease, and which will affect the treatment regime, e.g., prolonged computer use reduces the blink rate and can exacerbate the dry eye.[159]

As well as individual differences in lacrimal flow and tear osmolarity, the health and thickness of the mucin layer on the

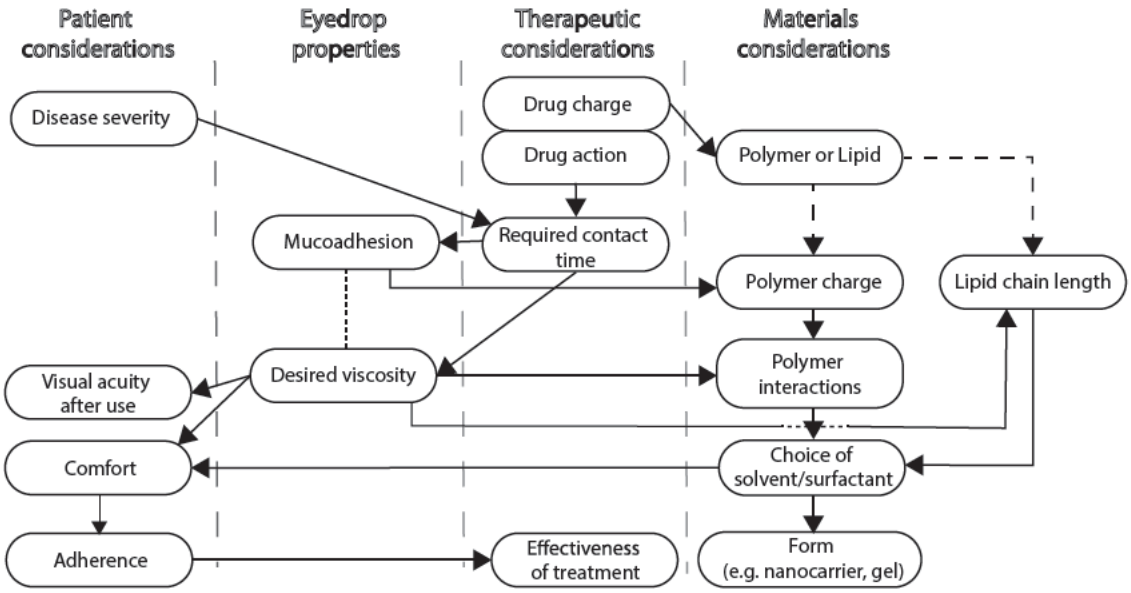

Figure 12. The relationship between various formulation decisions.

ocular surface may also play a key role in influencing how well mucoadhesive polymers and gels work to improve the bioavailability of a therapeutic agent. An investigation into the mucoadhesive capacity of carbomer gels found that it was the concentration of mucins naturally available on the ocular surface that was the major determining factor, rather than factors related to the gel itself.[88b] These differences in tear composition can also be exaggerated by diurnal patterns and environmental cues, and an approach which incorporates multiple drop types is advocated for by some clinicians.[160]

5.3. Patient Adherence

Investigations into methods of improving the efficacy of eye drops often rely on the assumption that there is already good adherence to treatment regimes in the patient population, which unfortunately is not necessarily the case. Studies in clinical populations have reported nonadherence rates between 27% and 80%.[161]

Self-efficacy and difficulty administering eye drops are two of the most important barriers to adherence to glaucoma medications.[161a] A study in elderly patients showed that 56% of patients required two or more attempts to accurately administer an eye drop, and 28% of attempts missed the eye completely.[162] It has also been shown that even after education, patients can still unknowingly administer eye drops incorrectly.[163]

However, there are practical methods which can be enlisted to improve technique, efficacy, and as a result—adherence. Aids have been shown to be effective in improving eye drop administration in some cases,[86b,164] however the instructions for the guide must be clear also.[165] Where consistent positive communication is combined with reminders and education, significant improvements to adherence have been shown.[166] Where access is a barrier or where patients have negative connotations with clinical settings, education can take place in a more relaxed environment or at home through short educational videos.[167]

6. General Discussion

Polymers were originally incorporated into eye drops to improve the residence time and bioavailability of a carried drug. They achieve this through mucoadhesion and small increases in viscosity, which allow for better resistance of the drop to the clearance mechanisms of the ocular surface. There still may be benefits to be had from optimizing the formulations of these eye drops, e.g., ensuring the optimum chain length and viscosity is reached.

Innovations in eye drop formulations are moving toward creating highly viscous hydrogels or micro/nanoencapsulated drug delivery systems, with the ability to provide controlled release of the required drug. Although this may in theory provide greater bioavailability and improve treatment outcomes, patient comfort and its implication on the adherence to treatment regimens need to be considered.

The response of the ocular immune systems to long-term use of these carriers is not well understood and needs to be further investigated, as it will likely differ from the response to polymeric materials elsewhere in the body. Although the response to contact lenses can be used as a point of comparison, it cannot be assumed that the responses would be the same at such low contact times. A particular point of interest would be the risk of immune cells engulfing nanocarriers and the associated risks of increased inflammation or the opportunity to use this process for immunomodulatory purposes. The potential for a build-up of "waste" material needs to be investigated, as does a systemic absorption of micro/nanocarriers.

Mucoadhesion plays an important role in increasing in the resistance of the drops to the eye's natural clearing mechanisms. The polymers investigated show a range of tuneable

properties, and versatility and adaptability are clearly important properties to look for in choosing the polymers for eye drop formulation. This should come alongside testing that replicates the application scenario, with the drop size and application ease given due consideration.

The impact of the disease on the ocular environment needs to also be considered, as tear formulation, glycocalyx health, and pre-existing inflammation may influence the efficacy of the treatment. Particularly for dry eye, but also for carrying non-charged drugs for other conditions, lipid and hybrid drops offer similar benefits to polymeric drops.

Where the material properties of the delivery vehicle can create increases in mucoadhesion and viscosity and in theory increase the bioavailability of the delivered drug, these advances can be compromised by interference of the drug with the carrier if not selected with this in mind. The delivery mechanism therefore becomes important to consider in light of the nature of the drug to be delivered.

Conflict of Interest

The authors declare no conflict of interest.

Keywords

drug delivery, eye drops, hydrogels, polymers

Received: October 15, 2019
Revised: December 15, 2019
Published online:

[1] a) J. Cunha-Vaz, R. Bernardes, C. Lobo, *Eur. J. Ophthalmol.* **2011**, *21*, 3; b) D. R. Janagam, L. Wu, T. L. Lowe, *Adv. Drug Delivery Rev.* **2017**, *122*, 31.
[2] A. Subrizi, E. M. Del Amo, V. Korzhikov-Vlakh, T. Tennikova, M. Ruponen, A. Urtti, *Drug Discovery Today* **2019**, *24*, 1446.
[3] a) J. A. Calles, J. Bermúdez, E. Vallés, D. Allemandi, S. Palma, in *Advanced Polymers in Medicine* (Ed: F. Puoci), Springer, Cham **2015**, Ch. 6, p. 147; b) A. O. Eghrari, S. A. Riazuddin, J. D. Gottsch, *Prog. Mol. Biol. Transl. Sci.* **2015**, *134*, 7.
[4] I. Pepic, J. Lovric, B. Cetina-Cizmek, S. Reichl, J. Filipovic-Grcic, *Drug Discovery Today* **2014**, *19*, 31.
[5] J. C. Imperiale, G. B. Acosta, A. Sosnik, *J. Controlled Release* **2018**, *285*, 106.
[6] I. P. Kaur, R. Smitha, *Drug Dev. Ind. Pharm.* **2002**, *28*, 353.
[7] a) P. Baranowski, B. Karolewicz, M. Gajda, J. Pluta, *Sci. World J.* **2014**, *2014*, 861904; b) J. Hori, T. Yamaguchi, H. Keino, P. Hamrah, K. Maruyama, *Prog. Retinal Eye Res.* **2019**, *72*, 100758.
[8] J. Y. Niederkorn, *Nat. Immunol.* **2006**, *7*, 354.
[9] K. Baba, Y. Tanaka, A. Kubota, H. Kasai, S. Yokokura, H. Nakanishi, K. Nishida, *J. Controlled Release* **2011**, *153*, 278.
[10] a) G. Di Colo, Y. Zambito, C. Zaino, M. Sanso, *Drug Dev. Ind. Pharm.* **2009**, *35*, 941; b) V. Singh, S. S. Bushetti, S. A. Raju, R. Ahmad, M. Singh, M. Ajmal, *J. Pharm. BioAllied Sci.* **2011**, *3*, 280.
[11] S. W. Cousins, M. M. McCabe, D. Danielpour, J. W. Streilein, *Invest. Ophthalmol. Visual Sci.* **1991**, *32*, 2201.
[12] A. W. Taylor, J. W. Streilein, S. W. Cousins, *Curr. Eye Res.* **1992**, *11*, 1199.
[13] P. A. Thomas, J. Kaliamurthy, *Clin. Microbiol. Infect.* **2013**, *19*, 210.
[14] D. J. Evans, S. M. J. Fleiszig, *Am. J. Ophthalmol.* **2013**, *155*, 961.
[15] I. Bravo-Osuna, V. Andres-Guerrero, A. Arranz-Romera, S. Esteban-Perez, I. T. Molina-Martinez, R. Herrero-Vanrell, *Adv. Drug Delivery Rev.* **2018**, *126*, 127.
[16] a) P. Skopiński, P. Krawczyk, A. M. Ambroziak, *Cent. Eur. J. Immunol.* **2013**, *2*, 254; b) A. M. McDermott, *Exp. Eye Res.* **2013**, *117*, 53.
[17] J. P. Craig, K. K. Nichols, E. K. Akpek, B. Caffery, H. S. Dua, C. K. Joo, Z. Liu, J. D. Nelson, J. J. Nichols, K. Tsubota, F. Stapleton, *Ocul. Surf.* **2017**, *15*, 276.
[18] a) M. Markoulli, A. Hui, *Drug Discovery Today* **2019**, *24*, 1427; b) H. Liu, C. Begley, M. Chen, A. Bradley, J. Bonanno, N. A. McNamara, J. D. Nelson, T. Simpson, *Invest. Ophthalmol. Visual Sci.* **2009**, *50*, 3671; c) V. Y. Bunya, N. M. Fuerst, M. Pistilli, B. E. McCabe, R. Salvo, I. Macchi, G. S. Ying, M. Massaro-Giordano, *JAMA Ophthalmol.* **2015**, *133*, 662.
[19] a) I. K. Gipson, P. Argüeso, in *International Review of Cytology*, Vol. *231* (Ed: K. Jeon), Academic Press, San Diego, CA **2003**, p. 1; b) R. R. Hodges, D. A. Dartt, *Exp. Eye Res.* **2013**, *117*, 62; c) M. Ruponen, A. Urtti, *Eur. J. Pharm. Biopharm.* **2015**, *96*, 442.
[20] J. V. Forrester, A. D. Dick, P. G. McMenamin, F. Roberts, E. Pearlman, in *The Eye* (Ed: W. B. Saunders), Elsevier, Edinburg **2016**, p. 370.
[21] M. C. Schechter, S. W. Satola, D. S. Stephens, in *Clinical Immunology*, 5th ed. (Eds: R. R. Rich, T. A. Fleisher, W. T. Shearer, H. W. Schroeder, A. J. Frew, C. M. Weyand), Content Repository Only!, London **2019**, p. 391.
[22] F. Garreis, M. Gottschalt, T. Schlorf, R. Gläser, J. Harder, D. Worlitzsch, F. P. Paulsen, *Invest. Ophthalmol. Visual Sci.* **2011**, *52*, 4914.
[23] a) Y.-C. Nho, J.-S. Park, Y.-M. Lim, *Polymers* **2014**, *6*, 890; b) C. G. Park, Y. K. Kim, M. J. Kim, M. Park, M. H. Kim, S. H. Lee, S. Y. Choi, W. S. Lee, Y. J. Chung, Y. E. Jung, K. H. Park, Y. B. Choy, *J. Controlled Release* **2015**, *220*, 180; c) H. Takeuchi, J. Thongborisute, Y. Matsui, H. Sugihara, H. Yamamoto, Y. Kawashima, *Adv. Drug Delivery Rev.* **2005**, *57*, 1583; d) C. Woertz, M. Preis, J. Breitkreutz, P. Kleinebudde, *Eur. J. Pharm. Biopharm.* **2013**, *85*, 843; e) J. Yan, X. Chen, S. Yu, H. Zhou, *J. Drug Delivery Sci. Technol.* **2017**, *40*, 157; f) T. Yu, G. P. Andrews, D. S. Jones, in *Mucosal Delivery of Biopharmaceuticals* (Eds: J. das Neves, B. Sarmento), Springer, Boston, MA **2014**, Ch. 2, p. 35.
[24] Y. Uchino, *Invest. Ophthalmol. Visual Sci.* **2018**, *59*, DES157.
[25] S. Mansuri, P. Kesharwani, K. Jain, R. K. Tekade, N. K. Jain, *React. Funct. Polym.* **2016**, *100*, 151.
[26] M. Zierhut, M. R. Dana, M. E. Stern, D. A. Sullivan, *Trends Immunol.* **2002**, *23*, 333.
[27] J. X. Lan, M. D. P. Willcox, G. D. F. Jackson, A. Thakur, *Aust. J. Ophthalmol.* **1998**, *26*, S36.
[28] P. Mudgil, *Invest. Ophthalmol. Visual Sci.* **2014**, *55*, 7272.
[29] a) H. R. Chinnery, P. G. McMenamin, S. J. Dando, *Pfluegers Arch.* **2017**, *469*, 501; b) J. V. Forrester, A. D. Dick, P. G. McMenamin, F. Roberts, E. Pearlman, in *The Eye* (Ed: W. B. Saunders), Elsevier, Edinburgh **2016**, p. 1.
[30] a) P. Hamrah, Q. Zhang, Y. Liu, M. R. Dana, *Invest. Ophthalmol. Visual Sci.* **2002**, *43*, 639; b) F. Y. McWhorter, T. Wang, P. Nguyen, T. Chung, W. F. Liu, *Proc. Natl. Acad. Sci. U. S. A.* **2013**, *110*, 17253; c) K. Sadtler, M. T. Wolf, S. Ganguly, C. A. Moad, L. Chung, S. Majumdar, F. Housseau, D. M. Pardoll, J. H. Elisseeff, *Biomaterials* **2019**, *192*, 405; d) T. A. Wynn, K. M. Vannella, *Immunity* **2016**, *44*, 450.
[31] M. R. Dana, *Invest. Ophthalmol. Visual Sci.* **2004**, *45*, 722.
[32] H. R. Chinnery, T. Humphries, A. Clare, A. E. Dixon, K. Howes, C. B. Moran, D. Scott, M. Zakrzewski, E. Pearlman, P. G. McMenamin, *Immunology* **2008**, *125*, 541.
[33] M. Thill, K. Schlagner, S. Altenähr, S. Ergün, R. G. A. Faragher, N. Kilic, J. Bednarz, G. Vohwinkel, X. Rogiers, D. K. Hossfeld, G. Richard, U. M. Gehling, *Stem Cells Dev.* **2007**, *16*, 733.

[34] D. Ferenbach, J. Hughes, *Kidney Int.* **2008**, *74*, 5.
[35] L. Chung, D. R. Maestas, Jr., F. Housseau, J. H. Elisseeff, *Adv. Drug Delivery Rev.* **2017**, *114*, 184.
[36] C. Tan, W. S. Wandu, A. St Leger, J. Kielczewski, E. F. Wawrousek, C.-C. Chan, I. Gery, *Exp. Eye Res.* **2018**, *166*, 116.
[37] a) N. Knop, E. Knop, *Acta Ophthalmol.* **2008**, *86*, 0; b) N. Knop, E. Knop, *J. Anat.* **2005**, *207*, 409.
[38] S. Gause, K. H. Hsu, C. Shafor, P. Dixon, K. C. Powell, A. Chauhan, *Adv. Colloid Interface Sci.* **2016**, *233*, 139.
[39] a) C. Gagliano, V. Papa, R. Amato, G. Malaguarnera, T. Avitabile, *Curr. Eye Res.* **2018**, *43*, 499; b) H. Jiao, L. J. Hill, L. E. Downie, H. R. Chinnery, *Clin. Exp. Optom.* **2019**, *102*, 208.
[40] a) M. Ipinazar Undurraga, G. OuslerIII, M. Schindelar, J. Paugh, *Acta Ophthalmol. Scand.* **2007**, *85*, 0; b) H. Mochizuki, M. Yamada, S. Hato, T. Nishida, *Brit. J. Ophthalmol.* **2008**, *92*, 108; c) J. R. Paugh, A. L. Nguyen, H. A. Ketelson, M. T. Christensen, D. L. Meadows, *Optom. Visual Sci.* **2008**, *85*, 725.
[41] a) D. T. Bulletin, *BMJ* **2016**, *353*, i2333; b) L. E. Downie, P. R. Keller, *Optom. Visual Sci.* **2015**, *92*, 957.
[42] K. Kumar, N. Dhawan, H. Sharma, S. Vaidya, B. Vaidya, *Artif. Cells, Nanomed., Biotechnol.* **2014**, *42*, 274.
[43] A. Sannino, C. Demitri, M. Madaghiele, *Materials* **2009**, *2*, 353.
[44] A. Aravamudhan, D. M. Ramos, A. A. Nada, S. G. Kumbar, in *Natural and Synthetic Biomedical Polymers* (Eds: S. G. Kumbar, C. T. Laurencin, M. Deng), Elsevier, New York **2014**, p. 67.
[45] X. Zheng, T. Goto, Y. Ohashi, *Invest. Ophthalmol. Visual Sci.* **2014**, *55*, 3454.
[46] L. Y. C. Madruga, P. C. F. da Câmara, N. D. N. Marques, R. D. C. Balaban, *J. Mol. Liq.* **2018**, *266*, 870.
[47] T. Fekete, J. Borsa, E. Takács, L. Wojnárovits, *Radiat. Phys. Chem.* **2016**, *124*, 135.
[48] K. Kyyronen, A. Urtti, *Invest. Ophthalmol. Visual Sci.* **1990**, *31*, 1827.
[49] a) M. Sharma, S. Kohli, A. Dinda, *Saudi Pharm. J.* **2015**, *23*, 675; b) S. Arthanari, P. Renukadevi, V. Saravanakumar, *J. Ind. Eng. Chem.* **2014**, *20*, 2018; c) E. Reverchon, G. Lamberti, A. Antonacci, *J. Supercrit. Fluids* **2008**, *46*, 185.
[50] a) D. C. West, S. Kumar, *Ciba Found. Symp.* **1989**, *143*, 187; b) W. E. Krause, E. G. Bellomo, R. H. Colby, *Biomacromolecules* **2001**, *2*, 65.
[51] R. Salzillo, C. Schiraldi, L. Corsuto, A. D'Agostino, R. Filosa, M. De Rosa, A. La Gatta, *Carbohydr. Polym.* **2016**, *153*, 275.
[52] F. Brignole, P. J. Pisella, B. Dupas, V. Baeyens, C. Baudouin, *Graefe's Arch. Clin. Exp. Ophthalmol.* **2005**, *243*, 531.
[53] R. C. B. Mencucci, R. Caputo, E. Favuzza, *J. Cataract Refractive Surg.* **2015**, *41*, 1699.
[54] P. Aragona, V. Papa, Micali, A. , Santocono, M. , G. Milazzo, *Brit. J. Ophthalmol.* **2002**, *86*, 181.
[55] M. L. McDermott, H. F. Edelhauser, *Arch. Ophthalmol.* **1989**, *107*, 261.
[56] C. C. Lin, K. S. Anseth, *Pharm. Res.* **2009**, *26*, 631.
[57] T. G. , *Clin. Ophthalmol.* **2009**, *3*, 501.
[58] A. Aguilar, M. Berra, J. Tredicce, A. Berra, *Clin. Ophthalmol.* **2018**, *12*, 1237.
[59] P. Asbell, A. J. Vingrys, J. Tan, A. Ogundele, L. E. Downie, G. Jerkins, L. Shettle, *Invest. Ophthalmol. Visual Sci.* **2018**, *59*, 2275.
[60] a) Y. Shtenberg, M. Goldfeder, A. Schroeder, H. Bianco-Peled, *Carbohydr. Polym.* **2017**, *175*, 337; b) F. M. Veronese, A. Mero, *BioDrugs* **2008**, *22*, 315; c) J. Buske, C. Konig, S. Bassarab, A. Lamprecht, S. Muhlau, K. G. Wagner, *Eur. J. Pharm. Biopharm.* **2012**, *81*, 57; d) H. J. Jang, C. Y. Shin, K. B. Kim, *Toxicol. Res.* **2015**, *31*, 105.
[61] M. E. Cooke, S. W. Jones, B. Ter Horst, N. Moiemen, M. Snow, G. Chouhan, L. J. Hill, M. Esmaeli, R. J. A. Moakes, J. Holton, R. Nandra, R. L. Williams, A. M. Smith, L. M. Grover, *Adv. Mater.* **2018**, *30*, 1705013.
[62] S. M. Mammadova, S. Tapdiqov, S. F. Humbatova, S. A. Aliyeva, N. A. Zeynalov, C. A. Soltanov, A. A. Cavadzadeh, *Asian J. Chem.* **2017**, *29*, 576.
[63] a) M. T. Islam, N. Rodriguez-Hornedo, S. Ciotti, C. Ackermann, *Pharm. Res.* **2004**, *21*, 1192; b) A. N. Lyapunov, E. P. Bezuglaya, N. A. Lyapunov, I. A. Kirilyuk, *Pharm. Chem. J.* **2015**, *49*, 639; c) A. Ochoa-Andrade, M. E. Parente, A. Jimenez-Kairuz, L. Boinbaser, A. Torregrosa, *AAPS PharmSciTech* **2017**, *18*, 2269.
[64] W. Suchaoin, I. Pereira de Sousa, K. Netsomboon, J. Rohrer, P. Hoffmann Abad, F. Laffleur, B. Matuszczak, A. Bernkop-Schnurch, *Int. J. Pharm.* **2016**, *503*, 141.
[65] G. Leone, M. Consumi, S. Pepi, A. Pardini, C. Bonechi, G. Tamasi, A. Donati, C. Rossi, A. Magnani, *Mater. Today Commun.* **2019**, 21, 100634.
[66] N. A. Peppas, J. Z. Hilt, A. Khademhosseini, R. Langer, *Adv. Mater.* **2006**, *18*, 1345.
[67] a) I. D. Rupenthal, *Curr. Opin. Pharmacol.* **2017**, *36*, 44; b) C. J. F. Bertens, M. Gijs, F. van den Biggelaar, R. Nuijts, *Exp. Eye Res.* **2018**, *168*, 149; c) A. Chauhan, *Delhi J. Ophthalmol.* **2015**, *26*, 131; d) M. N. Yasin, D. Svirskis, A. Seyfoddin, I. D. Rupenthal, *J. Controlled Release* **2014**, *196*, 208; e) A. E. Ross, L. C. Bengani, R. Tulsan, D. E. Maidana, B. Salvador-Culla, H. Kobashi, P. E. Kolovou, H. Zhai, K. Taghizadeh, L. Kuang, M. Mehta, D. G. Vavvas, D. S. Kohane, J. B. Ciolino, *Biomaterials* **2019**, *217*, 119285; f) U. Ubani-Ukoma, D. Gibson, G. Schultz, B. O. Silva, A. Chauhan, *Int. J. Pharm.* **2019**, *565*, 499.
[68] H. Waterman, J. R. Evans, T. A. Gray, D. Henson, R. Harper, *Cochrane Database Syst. Rev.* **2013**, CD006132.
[69] a) E. M. Ahmed, *J. Adv. Res.* **2015**, *6*, 105; b) A. Al-shohani, *Doctoral Thesis*, University College London **2017**; c) E. Caló, V. V. Khutoryanskiy, *Eur. Polym. J.* **2015**, *65*, 252; d) F. J. Otero-Espinar, A. Fernández-Ferreiro, M. González-Barcia, J. Blanco-Méndez, A. Luzardo, *Drug Targeting and Stimuli Sensitive Drug Delivery Systems* (Ed: A. M. Grumezescu), William Andrew Publishing **2018**, pp. 211–270; e) C. B. Highley, G. D. Prestwich, J. A. Burdick, *Curr. Opin. Biotechnol.* **2016**, *40*, 35; f) T. R. Hoare, D. S. Kohane, *Polymer* **2008**, *49*, 1993; g) S. Kirchhof, A. M. Goepferich, F. P. Brandl, *Eur. J. Pharm. Biopharm.* **2015**, *95*, 227; h) K. Y. Lee, D. J. Mooney, *Prog. Polym. Sci.* **2012**, *37*, 106; i) P. F. van der Meer, J. Seghatchian, D. C. Marks, *Transfus. Apheresis Sci.* **2016**, *54*, 164; j) N. A. Peppas, P. Bures, W. Leobandung, H. Ichikawa, *Eur. J. Pharm. Biopharm.* **2000**, *50*, 27; k) I. L. Tsai, C. C. Hsu, K. H. Hung, C. W. Chang, Y. H. Cheng, *J. Chin. Med. Assoc.* **2015**, *78*, 212; l) R. Gaudana, H. K. Ananthula, A. Parenky, A. K. Mitra, *AAPS J.* **2010**, *12*, 348; m) V. D. Wagh, B. Inamdar, Samanta, M. K. , *Asian J. Pharm.* **2008**, *2*, 12; n) Y. Weng, J. Liu, S. Jin, W. Guo, X. Liang, Z. Hu, *Acta Pharm. Sin. B* **2017**, *7*, 281; o) A. Zimmer, J. Kreuter, *Adv. Drug Delivery Rev.* **1995**, *16*, 61; p) Y. Wu, Y. Liu, X. Li, D. Kebebe, B. Zhang, J. Ren, J. Lu, J. Li, S. Du, Z. Liu, *Asian J. Pharm. Sci.* **2019**, *14*, 1.
[70] A. McDonnell, J.-H. Lee, E. Makrai, L. Y. Yeo, L. E. Downie, *Ophthalmology* **2019**, *126*, 1196.
[71] B. J. Chung, D. Platt, A. Vaidya, *Int. J. Non-linear Mech.* **2016**, *86*, 133.
[72] A. Tomlinson, S. Khanal, *Ocul. Surf.* **2005**, *3*, 81.
[73] A. Fernandez-Ferreiro, J. Silva-Rodriguez, F. J. Otero-Espinar, M. Gonzalez-Barcia, M. J. Lamas, A. Ruibal, A. Luaces-Rodriguez, A. Vieites-Prado, I. Lema, M. Herranz, N. Gomez-Lado, J. Blanco-Mendez, M. Gil-Martinez, M. Pardo, A. Moscoso, J. Cortes, M. Sanchez-Martinez, J. Pardo-Montero, P. Aguiar, *Eur. J. Pharm. Biopharm.* **2017**, *114*, 317.
[74] N. Washington, C. Washington, C. Wilson, *Physiological Pharmaceutics—Barriers to Drug Absorption*, CRC, Boca raton, FL **2001**.
[75] V. V. Khutoryanskiy, *Mucoadhesive Materials and Drug Delivery Systems*, John Wiley & Sons, Incorporated, New York **2014**.

[76] S. B. De Souza Ferreira, J. B. Da Silva, F. B. Borghi-Pangoni, M. V. Junqueira, M. L. Bruschi, *J. Mech. Behav. Biomed. Mater.* **2017**, *68*, 265.
[77] J. B. da Silva, V. V. Khutoryanskiy, M. L. Bruschi, M. T. Cook, *Int. J. Pharm.* **2017**, *528*, 586.
[78] A. Tachaprutinun, P. Pan-In, S. Wanichwecharungruang, *Int. J. Pharm.* **2013**, *441*, 801.
[79] a) S. Tamburic, D. Q. M. Craig, *Eur. J. Pharm. Biopharm.* **1997**, *44*, 159; b) D. S. Jones, T. P. Laverty, C. Morris, G. P. Andrews, *Colloids Surf., B* **2016**, *144*, 125.
[80] a) W. Zeng, Q. Li, T. Wan, C. Liu, W. Pan, Z. Wu, G. Zhang, J. Pan, M. Qin, Y. Lin, C. Wu, Y. Xu, *Colloids Surf., B* **2016**, *141*, 28; b) D. G. Drescher, N. A. Ramakrishnan, M. J. Drescher, *Methods Mol. Biol.* **2009**, *493*, 323.
[81] P. Schuck, *Annu. Rev. Biophys. Biomol. Struct.* **1997**, *26*, 541.
[82] a) X. Xu, Y. Weng, L. Xu, H. Chen, *Int. J. Biol. Macromol.* **2013**, *60*, 272; b) S. Deepthi, J. Jose, *Int. Ophthalmol.* **2018**, *39*, 1355.
[83] a) L. M. Grover, A. M. Smith, in *Handbook of Biopolymers and Biodegradable Plastics* (Ed: S. Ebnesajjad), Elsevier, New York **2013**, p. 365.; b) M. Q. Rahman, K. S. Chuah, E. C. Macdonald, J. P. Trusler, K. Ramaesh, *Eye* **2012**, *26*, 1579; c) M. Mansour, S. Mansour, N. D. Mortada, S. S. Abd Elhady, *Drug Dev. Ind. Pharm.* **2008**, *34*, 744.
[84] a) F. Laffleur, K. Netsomboon, L. Erman, A. Partenhauser, *Int. J. Biol. Macromol.* **2019**, *123*, 1204; b) S. Rossi, B. Vigani, M. C. Bonferoni, G. Sandri, C. Caramella, F. Ferrari, *J. Pharm. Biomed. Anal.* **2018**, *156*, 232.
[85] a) M. Abdulrazik, S. Benita, *Invest. Ophthalmol. Visual Sci.* **2012**, *53*, 6111; b) R. M. Shanker, I. Ahmed, P. A. Bourassa, K. V. Carola, *Int. J. Pharm.* **1995**, *119*, 149; c) C. Purslow, R. Wilcox, F. Drijfhout, *Contact Lens Anterior Eye* **2018**, *41*, S72.
[86] a) E. H. German, M. A. Hurst, D. Wood, *Eye* **1999**, *13*, 93; b) L. Van Santvliet, A. Ludwig, *Surv. Ophthalmol.* **2004**, *49*, 197.
[87] K. Edsman, J. Carlfors, K. Harju, *Int. J. Pharm.* **1996**, *137*, 233.
[88] a) R. Barreiro-Iglesias, C. Alvarez-Lorenzo, A. Concheiro, *J. Controlled Release* **2001**, *77*, 59; b) J. Ceulemans, A. Ludwig, *Eur. J. Pharm. Biopharm.* **2002**, *54*, 41; c) A. Kate Gurnon, N. J. Wagner, *J. Rheol.* **2012**, *56*, 333.
[89] a) N. Bhattarai, J. Gunn, M. Zhang, *Adv. Drug Delivery Rev.* **2010**, *62*, 83; b) K. Wang, Z. Han, *J. Controlled Release* **2017**, *268*, 212.
[90] G. Kaklamani, D. Cheneler, L. M. Grover, M. J. Adams, J. Bowen, *J. Mech. Behav. Biomed. Mater.* **2014**, *36*, 135.
[91] R. C. Cooper, H. Yang, *J. Controlled Release* **2019**, *306*, 29.
[92] A. George, P. A. Shah, P. S. Shrivastav, *Int. J. Pharm.* **2019**, *561*, 244.
[93] A. Subrizi, E. M. Del Amo, V. Korzhikov-Vlakh, T. Tennikova, M. Ruponen, A. Urtti, *Drug Discovery Today* **2019**, *24*, 1446.
[94] T. Ye, K. Yuan, W. Zhang, S. Song, F. Chen, X. Yang, S. Wang, J. Bi, W. Pan, *Asian J. Pharm. Sci.* **2013**, *8*, 207.
[95] P. C. M. Fabrizio Saettonea, R Cerbaia, G Mazzantib, L Braghirolib, *Int. J. Pharm.* **1996**, *142*, 103.
[96] P. W. Morrison, V. V. Khutoryanskiy, *Int. J. Pharm.* **2014**, *472*, 56.
[97] E. Villani, M. Sacchi, F. Magnani, A. Nicodemo, S. E. Williams, A. Rossi, R. Ratiglia, S. De Cilla, P. Nucci, *Invest. Ophthalmol. Visual Sci.* **2016**, *57*, 1003.
[98] F. Mantelli, J. Mauris, P. Argueso, *Curr. Opin. Allergy Clin. Immunol.* **2013**, *13*, 563.
[99] a) M. T. Droy-Lefaix, L. Bueno, P. Caron, E. Belot, O. Roche, *Invest. Ophthalmol. Visual Sci.* **2013**, *54*, 2705; b) P. R. Ingram, A. R. Pitt, C. G. Wilson, O. Olejnik, C. M. Spickett, *Free Radical Res.* **2004**, *38*, 739.
[100] S. Johannsdottir, P. Jansook, E. Stefansson, I. M. Kristinsdottir, G. M. Asgrimsdottir, T. Loftsson, *J. Drug Delivery Sci. Technol.* **2018**, *48*, 125.
[101] I. Rodriguez, J. A. Vazquez, L. Pastrana, V. V. Khutoryanskiy, *Int. J. Pharm.* **2017**, *529*, 168.
[102] B. Mahaling, D. S. Katti, *Int. J. Pharm.* **2016**, *501*, 1.
[103] W. B. Kauffman, T. Fuselier, J. He, W. C. Wimley, *Trends Biochem. Sci.* **2015**, *40*, 749.
[104] S. Pescina, C. Ostacolo, I. M. Gomez-Monterrey, M. Sala, A. Bertamino, F. Sonvico, C. Padula, P. Santi, A. Bianchera, S. Nicoli, *J. Controlled Release* **2018**, *284*, 84.
[105] F. de Cogan, L. J. Hill, A. Lynch, P. J. Morgan-Warren, J. Lechner, M. R. Berwick, A. F. A. Peacock, M. Chen, R. A. H. Scott, H. Xu, A. Logan, *Invest. Ophthalmol. Visual Sci.* **2017**, *58*, 2578.
[106] a) A. A. Al-Kinani, G. Zidan, N. Elsaid, A. Seyfoddin, A. W. G. Alani, R. G. Alany, *Adv. Drug Delivery Rev.* **2018**, *126*, 113; b) H. Shelley, R. M. Rodriguez-Galarza, S. H. Duran, E. M. Abarca, R. J. Babu, *J. Pharm. Sci.* **2018**, *107*, 3089; c) A. Madni, M. A. Rahem, N. Tahir, M. Sarfraz, A. Jabar, M. Rehman, P. M. Kashif, S. F. Badshah, K. U. Khan, H. A. Santos, *Int. J. Pharm.* **2017**, *530*, 326.
[107] C. Demitri, R. Del Sole, F. Scalera, A. Sannino, G. Vasapollo, A. Maffezzoli, L. Ambrosio, L. Nicolais, *J. Appl. Polym. Sci.* **2008**, *110*, 2453.
[108] T. Mills, A. Koay, I. T. Norton, *Food Hydrocolloids* **2013**, *32*, 172.
[109] M. T. Islam, N. Rodriguez-Hornedo, S. Ciotti, C. Ackermann, *AAPS J.* **2004**, *6*, 61.
[110] a) M. H. Mahdi, B. R. Conway, A. M. Smith, *Int. J. Pharm.* **2014**, *475*, 335; b) I. Fernández Farrés, I. T. Norton, *Food Hydrocolloids* **2014**, *40*, 76.
[111] a) G. Chouhan, R. J. A. Moakes, M. Esmaeili, L. J. Hill, F. deCogan, J. Hardwicke, S. Rauz, A. Logan, L. M. Grover, *Biomaterials* **2019**, *210*, 41; b) M. D. Moya-Ortega, T. F. Alves, C. Alvarez-Lorenzo, A. Concheiro, E. Stefansson, M. Thorsteinsdottir, T. Loftsson, *Int. J. Pharm.* **2013**, *441*, 507; c) B. Ter Horst, R. J. A. Moakes, G. Chouhan, R. L. Williams, N. S. Moiemen, L. M. Grover, *Acta Biomater.* **2019**, *89*, 166; d) J. F. Bradbeer, R. Hancocks, F. Spyropoulos, I. T. Norton, *Food Hydrocolloids* **2015**, *43*, 501; e) I. Fernández Farrés, R. J. A. Moakes, I. T. Norton, *Food Hydrocolloids* **2014**, *42*, 362; f) M. H. Mahdi, B. R. Conway, T. Mills, A. M. Smith, *Int. J. Pharm.* **2016**, *515*, 535; g) M. H. Mahdi, B. R. Conway, A. M. Smith, *Int. J. Pharm.* **2015**, *488*, 12.
[112] K. Tahara, K. Karasawa, R. Onodera, H. Takeuchi, *Asian J. Pharm. Sci.* **2017**, *12*, 394.
[113] a) M. Parlato, A. Johnson, G. A. Hudalla, W. L. Murphy, *Acta Biomater.* **2013**, *9*, 9270; b) D. C. Cui, W. L. Lu, E. A. Sa, M. J. Gu, X. J. Lu, T. Y. Fan, *Int. J. Pharm.* **2012**, *436*, 527; c) E. Jain, K. M. Scott, S. P. Zustiak, S. A. Sell, *Macromol. Mater. Eng.* **2015**, *300*, 823; d) Q. Zhang, J. Hubenak, T. Iyyanki, E. Alred, K. C. Turza, G. Davis, E. I. Chang, C. D. Branch-Brooks, E. K. Beahm, C. E. Butler, *Biomaterials* **2015**, *73*, 198.
[114] G. Abrego, H. Alvarado, E. B. Souto, B. Guevara, L. H. Bellowa, A. Parra, A. Calpena, M. L. Garcia, *Eur. J. Pharm. Biopharm.* **2015**, *95*, 261.
[115] a) T. Brunner, S. Cohen, A. Monsonego, *Biomaterials* **2010**, *31*, 2627; b) S. A. Im, S. T. Oh, S. Song, M. R. Kim, D. S. Kim, S. S. Woo, T. H. Jo, Y. I. Park, C. K. Lee, *Int. Immunopharmacol.* **2005**, *5*, 271; c) F. Ahsan, I. P. Rivas, M. A. Khan, A. I. Torres Suárez, *J. Controlled Release* **2002**, *79*, 29.
[116] T. Meng, V. Kulkarni, R. Simmers, V. Brar, Q. Xu, *Drug Discovery Today* **2019**, *24*, 1524.
[117] P. A. Simmons, C. Carlisle-Wilcox, J. G. Vehige, *Clin. Ophthalmol.* **2015**, *9*, 657.
[118] a) L. Essa, D. Laughton, J. S. Wolffsohn, *Contact Lens Anterior Eye* **2018**, *41*, 60; b) P. A. Simmons, C. Carlisle-Wilcox, R. Chen, H. Liu, J. G. Vehige, *Clin. Ther.* **2015**, *37*, 858; c) K. Suda, T. Murakami, N. Gotoh, R. Fukuda, Y. Hashida, M. Hashida, A. Tsujikawa, N. Yoshimura, *J. Controlled Release* **2017**, *266*, 301.
[119] J. Alvarez-Trabado, Y. Diebold, A. Sanchez, *Int. J. Pharm.* **2017**, *532*, 204.

[120] a) J. Ye, H. Wu, Y. Wu, C. Wang, H. Zhang, X. Shi, J. Yang, *Eye* **2012**, *26*, 1012; b) C. C. Peng, L. C. Bengani, H. J. Jung, J. Leclerc, C. Gupta, A. Chauhan, *J. Drug Delivery Sci. Technol.* **2011**, *21*, 111.
[121] a) M. A. Di Pascuale, E. Goto, S. C. Tseng, *Ophthalmology* **2004**, *111*, 783; b) J. Qiao, X. Yan, *Clin. Ophthalmol.* **2013**, *7*, 1797.
[122] P. Jaiswal, B. Gidwani, A. Vyas, *Artif. Cells, Nanomed., Biotechnol.* **2016**, *44*, 27.
[123] A. Akbarzadeh, R. Rezaei-Sadabady, S. Davaran, S. W. Joo, N. Zarghami, Y. Hanifehpour, M. Samiei, M. Kouhi, K. Nejati-Koshki, *Nanoscale Res. Lett.* **2013**, *8*, 102.
[124] J. Szebeni, S. M. Moghimi, *J. Liposome Res.* **2009**, *19*, 85.
[125] S. Samimi, N. Maghsoudnia, R. B. Eftekhari, F. Dorkoosh, in *Micro and Nano Technologies, Characterization and Biology of Nanomaterials for Drug Delivery* (Eds: S. S. Mohapatra, S. Ranjan, N. Dasgupta, R. K. Mishra, S. Thomas), Elsevier **2019**, pp. 47–76.
[126] a) A. Lim, M. R. Wenk, L. Tong, *Trends Mol. Med.* **2015**, *21*, 736; b) V. Dave, K. Tak, A. Sohgaura, A. Gupta, V. Sadhu, K. R. Reddy, *J. Microbiol. Methods* **2019**, *160*, 130.
[127] M. V. Fedorchak, I. P. Conner, J. S. Schuman, A. Cugini, S. R. Little, *Sci. Rep.* **2017**, *7*, 8639.
[128] L. Ying, K. Tahara, H. Takeuchi, *Int. J. Pharm.* **2013**, *453*, 329.
[129] a) A. S. Nevyas, I. M. Raber, R. C. Eagle Jr., I. B. Wallace, H. J. Nevyas, *Arch. Ophthalmol.* **1987**, *105*, 958; b) G. Prasad Rao, C. O'Brien, M. Hicky-Dwyer, A. Patterson, *Eur. J. Implant Refractive Surg.* **1995**, *7*, 251.
[130] R. Noecker, K. V. Miller, *Ocul. Surf.* **2011**, *9*, 159.
[131] R. M. Dutescu, C. Panfil, N. Schrage, *Exp. Toxicol. Pathol.* **2017**, *69*, 123.
[132] a) C. Coquelet, N. Lakhchaf, B. Pages, M. Persin, L. S. Rao, J. Sarrazin, G. Tarrago, *J. Membr. Sci.* **1996**, *120*, 287; b) Y.-Q. Wang, X. Wang, P. Liu, *Asian Pac. J. Trop. Med.* **2013**, *6*, 1004.
[133] D. Arbelaez-Camargo, M. Roig-Carreras, E. Garcia-Montoya, P. Perez-Lozano, M. Minarro-Carmona, J. R. Tico-Grau, J. M. Sune-Negre, *Int. J. Pharm.* **2018**, *543*, 190.
[134] a) E. Akar, A. Altinisik, Y. Seki, *Carbohydr. Polym.* **2012**, *90*, 1634; b) M. F. Akhtar, M. Hanif, N. M. Ranjha, *Saudi Pharm. J.* **2016**, *24*, 554; c) G. Yang, L. Espandar, N. Mamalis, G. D. Prestwich, *Vet. Ophthalmol.* **2010**, *13*, 144; d) S. H. Jahromi, L. M. Grover, J. Z. Paxton, A. M. Smith, *J. Mech. Behav. Biomed. Mater.* **2011**, *4*, 1157; e) F. Ullah, M. B. Othman, F. Javed, Z. Ahmad, H. Md Akil, *Mater. Sci. Eng., C* **2015**, *57*, 414.
[135] Y. Hori, A. M. Winans, C. C. Huang, E. M. Horrigan, D. J. Irvine, *Biomaterials* **2008**, *29*, 3671.
[136] Y. Liu, L. Xiao, K. I. Joo, B. Hu, J. Fang, P. Wang, *Biomacromolecules* **2014**, *15*, 3836.
[137] A. Singh, H. Qin, I. Fernandez, J. Wei, J. Lin, L. W. Kwak, K. Roy, *J. Controlled Release* **2011**, *155*, 184.
[138] K. A. Soliman, K. Ullah, A. Shah, D. S. Jones, T. R. R. Singh, *Drug Discovery Today* **2019**, *24*, 1575.
[139] M. Zhang, Y. Li, Q. Yang, L. Huang, L. Chen, Y. Ni, H. Xiao, *Carbohydr. Polym.* **2018**, *195*, 495.
[140] H. K. Makadia, S. J. Siegel, *Polymers* **2011**, *3*, 1377.
[141] C. S. Verbeke, S. Gordo, D. A. Schubert, S. A. Lewin, R. M. Desai, J. Dobbins, K. W. Wucherpfennig, D. J. Mooney, *Adv. Healthcare Mater.* **2017**, *6*, 1600773.
[142] A. N. Stachowiak, D. J. Irvine, *J. Biomed. Mater. Res., Part A* **2008**, *85A*, 815.
[143] S. Féréol, R. Fodil, B. Labat, S. Galiacy, V. M. Laurent, B. Louis, D. Isabey, E. Planus, *Cell Motil. Cytoskeleton* **2006**, *63*, 321.
[144] S. Mizrahy, S. R. Raz, M. Hasgaard, H. Liu, N. Soffer-Tsur, K. Cohen, R. Dvash, D. Landsman-Milo, M. G. Bremer, S. M. Moghimi, D. Peer, *J. Controlled Release* **2011**, *156*, 231.
[145] a) R. Sridharan, A. R. Cameron, D. J. Kelly, C. J. Kearney, F. J. O'Brien, *Mater. Today* **2015**, *18*, 313; b) M. M. Alvarez, J. C. Liu, G. Trujillo-de Santiago, B. H. Cha, A. Vishwakarma, A. M. Ghaemmaghami, A. Khademhosseini, *J. Controlled Release* **2016**, *240*, 349; c) S. F. Badylak, J. E. Valentin, A. K. Ravindra, G. P. McCabe, A. M. Stewart-Akers, *Tissue Eng., Part A* **2008**, *14*, 1835; d) B. N. Brown, B. D. Ratner, S. B. Goodman, S. Amar, S. F. Badylak, *Biomaterials* **2012**, *33*, 3792; e) R. Rattan, S. Bhattacharjee, H. Zong, C. Swain, M. A. Siddiqui, S. H. Visovatti, Y. Kanthi, S. Desai, D. J. Pinsky, S. N. Goonewardena, *Bioorg. Med. Chem.* **2017**, *25*, 4487; f) Y. Tabata, Y. Ikada, *Biomaterials* **1988**, *9*, 356; g) X. F. Zhang, W. Shen, S. Gurunathan, *Int. J. Mol. Sci.* **2016**, *17*, E1534.
[146] H. M. Rostam, S. Singh, F. Salazar, P. Magennis, A. Hook, T. Singh, N. E. Vrana, M. R. Alexander, A. M. Ghaemmaghami, *Immunobiology* **2016**, *221*, 1237.
[147] H. H. Gustafson, D. Holt-Casper, D. W. Grainger, H. Ghandehari, *Nano Today* **2015**, *10*, 487.
[148] a) C. W. Sindt, T. K. Grout, D. B. Critser, J. R. Kern, D. L. Meadows, *Clin. Ophthalmol.* **2012**, *6*, 511; b) Y Qazi, A. Cruzat, N. Baniasadi, L. Zheng, D. Witkin, D. B. Critser, A. Watts, J. Beyer, C. W. Sindt, P. Hamrah, *Invest. Ophthalmol. Vis. Sci.* **2011**, *52*, 6551.
[149] a) C. Chao, K. Richdale, I. Jalbert, K. Doung, M. Gokhale, *Contact Lens Anterior Eye* **2017**, *40*, 273; b) A. Gad, A. J. Vingrys, C. Y. Wong, D. C. Jackson, L. E. Downie, *Ocul. Surf.* **2019**, *17*, 89.
[150] a) K. Pili, S. Kastelan, M. Karabatic, B. Kasun, B. Culig, *Psychiatr. Danubina* **2014**, *26*, 528; b) K. L. Greiner, J. J. Walline, *Eye Contact Lens* **2010**, *36*, 352.
[151] D. Sweeney, I. Jalbert, M. Covey, P. Sankaridurg, C. Vajdic, B. Holden, S. Sharma, L. Ramachandran, M. D.P. Willcox, G. Rao, *Cornea* **2003**, *22*, 435.
[152] E. M. Espana, S. C. G. Tseng, *Contact Lens Anterior Eye* **2003**, *26*, 131.
[153] R. Hemady, J. Tauber, C. S. Foster, *Surv. Ophthalmol.* **1991**, *35*, 369.
[154] G. M. Keating, *Drugs* **2017**, *77*, 201.
[155] M. Hotujac Grgurevic, M. Juretic, A. Hafner, J. Lovric, I. Pepic, *Drug Dev. Ind. Pharm.* **2017**, *43*, 275.
[156] a) J. A. P. Gomes, R. M. Santo, *Ocul. Surf.* **2018**, *17*, 9; b) E. Martin, K. M. Oliver, E. I. Pearce, A. Tomlinson, P. Simmons, S. Hagan, *Cytokine* **2018**, *105*, 37.
[157] B. D. Sullivan, D. Whitmer, K. K. Nichols, A. Tomlinson, G. N. Foulks, G. Geerling, J. S. Pepose, V. Kosheleff, A. Porreco, M. A. Lemp, *Invest. Ophthalmol. Visual Sci.* **2010**, *51*, 6125.
[158] L. Jones, L. E. Downie, D. Korb, J. M. Benitez-Del-Castillo, R. Dana, S. X. Deng, P. N. Dong, G. Geerling, R. Y. Hida, Y. Liu, K. Y. Seo, J. Tauber, T. H. Wakamatsu, J. Xu, J. S. Wolffsohn, J. P. Craig, *Ocul. Surf.* **2017**, *15*, 575.
[159] C. Blehm, S. Vishnu, A. Khattak, S. Mitra, R. W. Yee, *Surv. Ophthalmol.* **2005**, *50*, 253.
[160] M. Guillon, S. Shah, *Contact Lens Anterior Eye* **2019**, *42*, 147.
[161] a) P. A. Newman-Casey, A. L. Robin, T. Blachley, K. Farris, M. Heisler, K. Resnicow, P. P. Lee, *Ophthalmology* **2015**, *122*, 1308; b) C. M. G. Olthoff, J. S. A. G. Schouten, B. W. van de Borne, C. A. B. Webers, *Ophthalmology* **2005**, *112*, 953.
[162] J. Colomé-Campos, I. Martínez-Salcedo, M. C. Martorell-Hallado, P. Romero-Aroca, *Arch. Soc. Esp. Oftalmol.* **2014**, *89*, 177.
[163] A. Al-Busaidi, D. A. Samek, O. Kasner, *Oman J. Ophthalmol.* **2016**, *9*, 11.
[164] I. Davies, A. M. Williams, K. W. Muir, *Surv. Ophthalmol.* **2017**, *62*, 332.
[165] A. Salyani, C. Birt, *Can. J. Ophthalmol.* **2005**, *40*, 170.
[166] C. O. Okeke, H. A. Quigley, H. D. Jampel, G. S. Ying, R. J. Plyler, Y. Jiang, D. S. Friedman, *Ophthalmology* **2009**, *116*, 2286.
[167] a) S. A. Davis, D. M. Carpenter, S. J. Blalock, D. L. Budenz, C. Lee, K. W. Muir, A. L. Robin, B. Sleath, *Patient Educ. Couns.* **2019**, *102*, 937; b) S. Sapru, J. Berktold, J. E. Crews, L. J. Katz, L. Hark, C. A. Girkin, C. Owsley, B. Francis, J. B. Saaddine, *Eval. Program Plann.* **2017**, *65*, 40.